Molecular and genetic mechanisms regulating sperm cell development in *Arabidopsis thaliana*

Thesis submitted for the degree of

Doctor of Philosophy

Hoda Khatab

Department of Biology

University of Leicester

September 2011

This thesis is dedicated to my parents.

For their love, endless support and encouragement

Abstract

Molecular and genetic mechanisms regulating sperm cell development in *Arabidopsis thaliana*

Hoda Khatab

Sexual reproduction in flowering plants involves the production of male and female gametes crucial for successful fertilisation, yet molecular mechanisms in these processes are largely unknown. The goal of the research presented in this thesis is to understand more about these mechanisms. A novel pollen division mutant, *duo pollen 4* (*duo4*), that fails to produce twin sperm cells was investigated. Genetic analyses revealed that *duo4* acts post-meiotically and does not affect female gametophyte development. The majority of *duo4* germ cells complete DNA replication and fail to enter mitosis, but mutant germ cell appears to differentiate normally when crossed to different cell fate markers. Map-based cloning defined the *DUO4* locus to a 14.5 kb region containing the Cdh1/Fzr/Ste9- related, APC activator gene, *CCS52A1*. Molecular genetic approaches were combined to identify the cause of the germline defects in *duo4*. Gene expression analysis, misexpression and RNA interference (RNAi) experiments indicate that the *duo4* phenotype results from misexpression of CCS52A1 in the male germline. This is persuasive evidence that CCS52 activity is subject to tight control during male germ cell cycle progression. *DUO1* is a major transcription regulator of germ cell division and differentiation and the second major objective describes the validation of four native target genes in the *DUO1* regulatory network. These target genes encode metabolic and transport-related proteins. The activity of these promoters was shown to be DUO1-dependent in the male gametophyte or the male germline, highlighting the importance of the DUO1 regulon in a range of functions required for sperm cell development. Collectively, these results advance understanding of how the male gametes are produced, and provide an improved molecular understanding of reproduction in higher plants.

Acknowledgements

It is a pleasure to thank those who made this thesis possible. First and foremost, I would like to thank Allah; our Lord, the All-Knowing, the Almighty, the most Merciful and the most Compassionate. Prayers and peace be upon His prophet Mohammed, the last messenger for all humankind.

I would also like to thank my supervisor Prof David Twell. I deeply appreciate David for his excellent supervision, consistent encouragement, great support and help. Especially throughout the difficult time course of the fighting in my country, Libya, when I had no contact with my family.

I am also very thankful to my friends in the lab Michael for his suggestions and lively discussion about anything. Nadia for her support and close friendship. Tony, Mihai, Ugur, and, the newest member of the lab Nicholas for sharing many good moments in these four years. Their assistance and friendship have made my experience in the lab a happy one.

My special thanks go to the past members of Twell lab. Said, even now he is always ready to help in times of needs. Gael Le Trionnaire, Trude Allen and Anna Sidorova who helped me to overcome many troubles and supported me during my research. A warm thanks goes to Sofia for her valuable suggestions during the course of the writing of my thesis.

My sincere thanks go to the members of the Biology Department specially Sue Ogden, Judy Horner, Penny Butler, Ramesh Patel, Steve Ison for their support during the course of this project. My special thanks go to Lesley Barnett for always giving me a spare room to pray in.

I am very grateful to my dear family, my father and my mother for their daily phone call, my sisters and my brothers for their help and continuing support and understanding. My love to my sister, Jameela for all her love and keeping me up-dated every Friday.

I take the chance to thank and express my gratitude to all my friends for their encouragement, advice and understanding.

I must also acknowledge and thank the Libyan Government for the financial support provided to me during my PhD studies.

Finally, I would like to thank everybody who was involved in this work as well as expressing my apology to those I did not mention in this acknowledgment.

Hoda

Contents

Chapter 3

Characterization of the *duo4* mutant

Introduction

Chapter 5

Identification of novel *DUO1* target genes

List of figure

List of tables

Abbreviations

APC	Anaphase promoting complex
BAP	6-benzylaminopurine
bp	base pair
BSA	bovine serum albumin
C	cytosine
ºC	degrees centigrade
CAK	CDK-activating kinase
CDKA;1	Cyclin-dependent kinase A;1
cDNA	complementary DNA
chi	Chi-square statistic
cm	centimetre
CoA	coenzyme A
CCS52	cell cycle switch 52
CDK	Cyclin-dependent kinase
Cdc	cell division control
Cdh1	Cdc20 homologue 1
D-box	destruction box
CDS	coding sequence
DIC	Differential interference contrast
CKI	CDK inhibitory subunit
CSM	Cdc20-specific motif
CYC	Cyclin
DAA1	DUO1 activate ATPase
DAP	days after pollination
DAPI	4',6-diamidino-2 phenylindole dihydrochloride
DAT	DUO1-activated target
DEL	DP-E2F Like

DEPC	diethyl pyrocarbonate
DNA	deoxyribonucleic acid
dNTP	deoxynucleotide triphosphate
DUO1	Duo Pollen-1
DUO2	Duo Pollen-2
DUO3	Duo Pollen-3
DUO4	Duo Pollen-4
E1	Ubiquitin-activating enzyme
E2	Ubiquitin-conjugaing enzyme
E2F	Adenovirus E2 promotor binding factor
E3	Ubiquitin-ligase
EDTA	ethylenediaminetetraacetic acid
F1,F2,F3	first, second, third generation after a cross
FBL17	F-box-Like 17
FDA	fluorescein diacetate
FZR	FIZZY-related
FZY	FIZZY
fm	fentamole
g	gram
g	*gravity*
G	guanine
GCS1 / HAP2	Generative cell-specific-1 / hapless-2
gDNA	genomic DNA
GEX2	Gamete expressed-2
GFP	green fluorescent protein
GRSF	germline-restrictive silencing factor
GUS	beta-glucuronidase
H2B	histone H2B
IC	information content

kb	kilobase pair
kDa	kilodalton
KRP	Kip-related protein
IMPa-8	importin alpha
l	litre
LB media	Luria Bertani media
LBC	late bicellular
M	molar
MBC	mid bicellular
MES	2-(N-Morpholino)ethanesulfonic acid
mg	milligram
MGH3	male gamete-specific histone-3
ml	millilitre
mM	millimolar
mRFP	monomeric red fluorescent protein 1
mRNA	messenger RNA
MS	Murashige and Skoog
MSA	M-phase specific activator
MT	microtubules
ng	nanogram
NLS	nuclear localisation signal
OD	optical density
p	plasmid
PPB	Pre-prophase band
PCR	polymerase chain reaction
PCR11	*PLANT CADMIUM RESISTANCE*
pg	picogram
prom	promoter
qRT-PCR	quantitative RT-PCR

RBR	Retinoblastoma-related
RNA	ribonucleic acid
RNAi	RNA interference
ROI	region of interest
rpm	revolutions per minute
RSAT	regulatory sequence analysis tools
RT	room temperature
SCF	Skp, Cullin, F-box containing E3 ligase complex
RT-PCR	reverse transcriptase-PCR
SEM	standard error of the mean
SSLP	Single Sequence Length Polymorphism
T	thymine
T1	first generation of transformed Arabidopsis plants
TAE	tris-acetate EDTA
TAIR	The Arabidopsis Information Resource
T-DNA	transfer DNA
TEM	Transmission electron microscopy
TEMED	N,N,N',N'-tetramethylethylenediamine
TIO	Two-in-one
TIP5;1	Tonoplast intrinsic protein-5;1
Tris	tris(hydroxymethyl)aminomethane
Triton X-100	(t-Octylphenoxypolyethoxyethanol)
U	enzyme units
mg	microgram
ml	microlitre
mM	micromolar
UTR	untranslated region
V	volts
VCK	Vegetative cell kinase

v/v	volume per volume
w/v	weight per volume
WT	wild type

Chapter One

Introduction

1.1 The plant life cycle

Flowering plants have a complex life cycle characterized by alternating generations of diploid sporophytes and haploid gametophytes. Gametophytes and sporophytes differ morphologically and functionally, both of which express a large number of genes. The sporophyte is the predominant generation that ends in meiosis to produce the haploid gametophytes, while the haploid gametophyte has a relatively short phase. The sporophyte phase constructs the main plant body with roots, shoots, leaves and flowers, without going through sexual reproduction. Instead, meiotic divisions in specialized floral tissues leads to the formation of haploid microspores and megaspores. These spores represent the starting point of the haploid gametophyte phase, which gives rise to the male and female gametes. The fusion of the gametes gives rise to the zygote and the seeds consisting of distinct embryo and endosperm structures that arise from the double fertilisation of the egg and central cell respectively, which initiates a new diploid sporophyte generation, thereby completing the plant life cycle (Figure1.1).

1.1.2 Development of the plant gametophyte

In animals, the germline is established early in embryogenesis and remains as a separate stem-cell population throughout life. These are the only cells that undergo meiosis to produce the gametes. In contrast, flowering plants do not have a distinct germline in the sporophyte but maintain stem cell populations located in the shoot apical meristems (SAMs) that direct the growth of the flowering plant shoot. The SAM shifts from producing vegetative structures to reproductive organs containing diploid sporogenous cells. The sporophyte produces two types of spores, microspores and megaspores that give rise to male gametophytes and female gametophytes, respectively. The angiosperm gametophytes develop within sporophytic tissues that constitute the sexual organs of the flower. The development of female gametophyte (the embryo sac or megagametophyte) takes place within the ovule, which is located inside the carpel of the flower. Within the ovule, diploid mother cells undergo three rounds of division. Thus, these subsequent divisions give rise to seven cells: three antipodal cells, two synergid cells, one egg cell, and one central cell. After fertilisation the egg cell and central cell develop into embryo

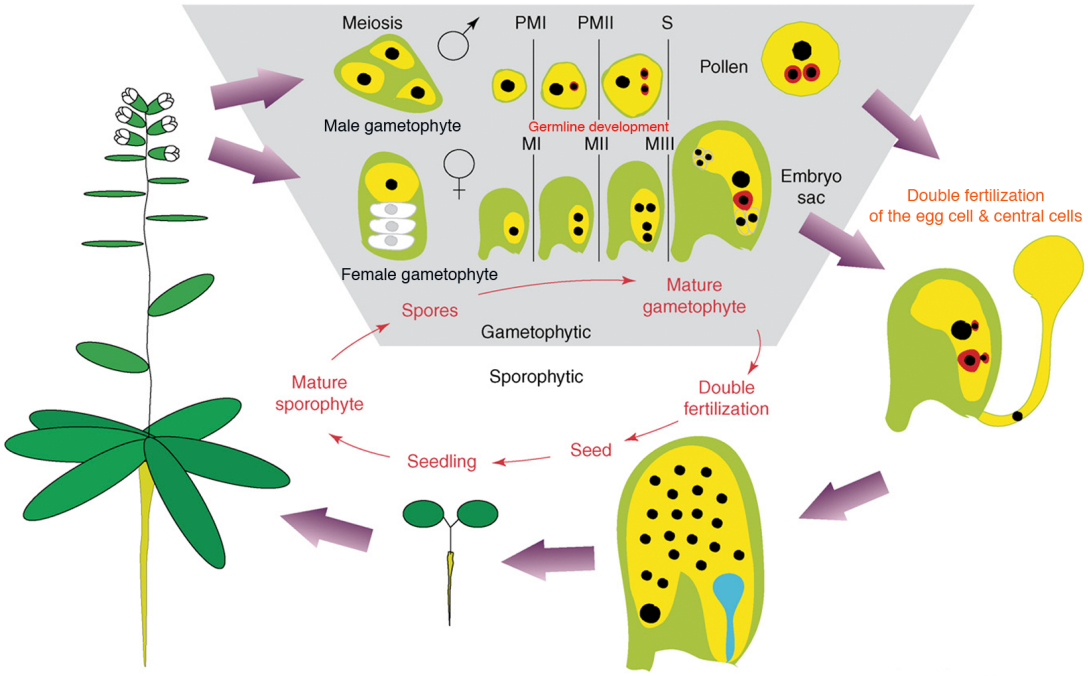

Figure 1.1 The life cycle of *Arabidopsis thaliana* alternates between sporophyte and gametophyte phases. The diploid sporophyte undergoes meiosis to produce haploid gametophytes. Microspores undergo two mitotic division to produce twin sperm cells (marked red). Haploid megaspores produce seven-celled female gametophyte by undergoing three mitotic division. The female gametophyte consists of the egg cell (red), two synergid cells and the central cell (black). The two sperm cells have transported to the embryo sac through the pollen tube, which results in double fertilisation. During double fertilisation , one sperm cell fertilise the egg to form the embryo, while the second sperm cell fuse with the central cell to form the triploid endosperm. After completion of embryo development, the seedling is released from the seed and develops into the new sporophyte (Adapted from Berger *et al.*, 2006).

and endosperm, respectively (Drews and Goldberg, 1989; Drews and Yadegari, 2002)(Figure1.1).

The haploid male gametophyte (pollen grain) is a highly reduced haploid structure that is responsible for the production of twin sperm cells. The development of the male gametophyte takes place within the anther of the flower when the sporogenous cells undergo a mitotic division to produce diploid meiocytes, also referred to as pollen mother cells. The progression of male gametophyte development from the pollen mother consists of two sequential phases, microsporogenesis and microgametogenesis (Figure1.2). During microsporogenesis, the diploid microsporocytes undergo meiosis to produce a tetrad of four haploid microspores enclosed in a callose wall. This stage is completed by the release of unicellular microspores from the tetrad by the action of hydrolytic callase enzymes secreted by the inner layer of the tapetum (Scott *et al.*, 2004). During microgametogenesis, haploid microspores enlarge due to an increase in vacuole size and number. This is accompanied by the fusion of smaller vacuoles to generate a large single vacuole that is associated with the migration of the microspore nucleus to a peripheral position against the cell wall (Owen and Makaroff, 1995; reviewed by Malhó *et al.*, 2006) . The polarised microspore undergoes two successive mitotic divisions to produce a mature pollen grain. Microspore mitosis (PMI) results in the formation of cell-within-a-cell structure with distinct cell structures and fates. A small generative or germ cell, representing the male germline, is contained within the cytoplasm of the large vegetative cell. This is a unique feature of male gametophyte development and has raised stimulating questions about the factors that determine the separate cell fates of the vegetative and germ cells that arise from the same division. Undoubtedly, the asymmetric division of the haploid microspore is known to be important for the correct germ cell fate specification, and fate is a default developmental pathway (Eady *et al.*, 1995). After PMI, the vegetative cell exits the cell cycle and remains in G1 phase (Žárský *et al.*, 1992). The vegetative cells accumulate stored metabolites that are required for germ cell development and most importantly for delivery of the sperm cells to the embryo sac (Twell, 1995).

The germ cell with condensed nuclear chromatin migrates to the centre of the pollen grain and elongates to form a spindle shaped cell prior to entry into mitosis. This structure is maintained by a cortical cage of microtubules aligned longitudinally to the long axis (Cresti *et al.*, 1990; Palevitz and Cresti, 1989). The germ cell undergoes a second mitotic division termed germ cell mitosis (PMII) to produce two genetically identical daughter sperm cells. Thus, mature pollen contains two sperm cells that remain associated with the vegetative cell nucleus that is termed the male germ unit (Dumas *et al.*, 1998*;* Lalanne and Twell, 2002) (Figure 1. 2). In approximately 70 % of plant families the second mitotic division occurs while the pollen tube grows in the style. Therefore, bicellular pollen grains are shed from the anther before the germ cell divides to give rise to the two sperm cells. In other plant families, such as Brassicacae to which Arabidopsis belongs, the second mitotic division takes place before pollen is shed. More detailed studies have revealed heterochrony or variability in the timing of the cell cycle associated with sperm cell development and fertiliseation among higher plants (Friedman, 1999).

The distinct stages of development and simple cell lineage of pollen grains makes them an excellent system for studying cell fate determination, cytoskeleton organisation and gene expression (Twell, 1998; Friedman, 1999). The majority of genes that are expressed during Arabidopsis male gametophyte development have been identified based on transcriptome analysis of developing pollen using microarray technology and more recently from isolated sperm cells (Borges *et al.*, 2008; Honys and Twell, 2004; Pina *et al.*, 2005). In addition, identification of several gametophytic mutants has lifted the boundaries that had previously hindered progress in understanding molecular mechanisms that govern male gametophyte development (Twell, 2011).

1.1.2.1 Mutants defective at PMI lack germ cell fate characteristics

The asymmetry of division at PMI is a key process in the formation of the male germline. Following division, two daughter cells are generated that are distinct from each other. Genetic screens, in Arabidopsis, have led to the identification of several mutants that are involved in particular in asymmetric cell division and cell fate determination. Interestingly, these mutants disturb both asymmetric division and

subsequent cell fate determination, suggesting that these processes are tightly linked. *Sidecar pollen* (*scp*) was identified as a gametophytic mutant that affects microspore division symmetry (Chen and McCormick, 1996). Released microspores undergo normal nuclear migration, but show a significant delayed entry into microspores mitosis to produce two equal-sized cells, one of the daughter cells with a vegetative cell fate (Oh *et al*., 2010a). The other daughter cell undergoes a asymmetric division to produce the germ line and then twin sperm cells. Eventually, *scp* mature pollen possess an extra vegetative cell. This gene responsible for the *scp* phenotype encodes LATERAL ORGAN BOUNDARIES DOMAIN/ASYMMETRIC LEAVES2-like (LBD27/ASL29), a member of the plant-specific LBD/ASL family that is essential for microspore development (Oh *et al*., 2010a).

Similarly, the *gemini pollen 1* (*gem1*) mutant was also shown to affect microspore polarity, resulting in microspores that divide less asymmetrically than wild type (Park *et al*., 1998). *GEM1* is identical to *MOR1* (Whittington *et al*., 2001) and belongs to MAP215 family of microtubule binding proteins, and was essential in stimulating growth of interphase, spindle and phragmoplast microtubule arrays (Twell *et al*., 2002). RNAi mediated suppression a homologue of *MOR1*/*GEM1*, *TMBP200*, in tobacco induced similar division defects to those in *gem1* that were associated with altered organization of microtubules (Oh *et al*., 2010b). A similar altered division phenotype has been described in *gem2* (Park *et al*., 2004), however, the gene identity remains unknown (Figure1. 2).

In contrast, several other mutants that fail to establish and to maintain the germline do not disturb polarity, but show specific defects in cytokinesis (Lee *et al*., 2007; Oh *et al*., 2008; Oh *et al*., 2005). The *TWO-IN-ONE* (*TIO)* is a plant homologue of the Ser/Thr protein kinase FUSED that is involved in centrifugal plate expansion (Oh *et al*., 2005). *tio* microspores fail to complete cytokinesis, resulting in binuclear pollen grains at anthesis with a vegetative cell fate. This confirms that the vegetative cell fate is the default program and that germ cell fate must be established gametophytically (Twell *et al*., 1998). PAKRP1/Kinesin-12A and PAKRP1L/Kinesin-12B represent two functionally redundant microtubule motor kinesins that also localize to the middle region of the phragmoplast to organize microtubules. The *kinesin-12A kinesin-12B*

double mutant shows failure of cell plate formation as a result of microtubule disorganisation (Lee *et al.*, 2007). HINKEL (HIK) and TETRASPORE (TES), the Arabidopsis orthologues of NACK1 and NACK2 kinesin-related proteins, are essential for somatic cell cytokinesis in tobacco. The *hik-1 tes-1* double mutant shows cell plate expansion defects and fails to form antiparallel microtubule array between reformed nuclei during PMI (Oh *et al.*, 2008).

Thus, it is clear that defects in PMI progression can have adverse consequences on the subsequent division (PMII) and cell fate specification, and correct polarization of the microspore nuclei is a pre-requisite to establish germ cell fate. These observations support the hypothesis that correct differentiation of the germ cell lineage depends on persistent cell fate determinants being correctly segregated between the unique daughter cells during the course of microspore mitosis (Berger and Twell, 2010; Borg *et al.*, 2009; Twell, 2011), and it will thus be interesting to discover the linked cell fate determinants responsible for specifying the differing fates of the vegetative and germ cells.

1.1.2.2 Regulators of germ cell division

Following asymmetric division at microspore mitosis (PMI), the vegetative cell remains in G1 phase of cell cycle. In contrast, the germ cell further divides symmetrically, giving rise to the twin sperm cells that are required for double fertilisation. The timing of germ cell mitosis is regulated differently among species. Arabidopsis, rice and maize shed tricellular pollen, as PMII occurs within the pollen grain prior to anthesis. Unlike the case in rice and maize, lily and tobacco shed bicellular pollen, and germ cell mitosis (PMII) take places during pollen tube growth. In Arabidopsis upon twin sperm cell formation a new S phase is initiated during pollen maturation and is completed at the end of pollen tube growth (Durbarry *et al.*, 2005; Friedman, 1999).

Thus far, no mechanisms have been verified at the molecular level that specifies the fate of the germ cell from the default vegetative cell fate. However several models have been proposed based on the significance of asymmetric division, which implicate unequal partitioning of the cell fate determinants that repress the germ cell fate in the

vegetative cell and allow expression of germ cell-specific genes (Eady *et al.*, 1995). Recent transcriptomic studies of germ cell-specific expressed transcripts generated from isolated germ cells of *Lilium longiflorum* (lily), led to the identification of a ubiquitous non-germ cell repressor protein, Germline Restrictive Silencing Factor (GRSF) that has been proposed to repress male germline specific gene expression in non-germ cells (Haerizadeh *et al.*, 2006). GRSF is present in microspores in lily but is absent in the germ cell after PMI, parallel to the activation of the male germline–specific transcriptional program.

Development of new techniques that allowed isolation of the male germ cell has led to a growing number of studies focused on understanding the transcriptomic profile of the male germline. As such, there is now evidence for extensive male germline gene expression in maize (Engel *et al.*, 2003), lily (Okada *et al.*, 2006), male germline specific expressed genes in Arabidopsis (Twell, 2011) and recently a near complete transcriptome from Arabidopsis sperm cells (Borges *et al.*, 2008). These findings implicate the presence of regulatory networks that govern this specific pattern of germ cell development and gene expression (Figure1.2).

A number of mutations have been described in Arabidopsis, which lead to delay or blocked germ cell division at PMII, producing bicellular pollen grains with a single germ cell and vegetative cell nucleus. Most of the genes affecting germ cell division that have been described to date are essential components of the cell cycle machinery, reflecting the dominant cellular process undertaken by the germ cell in the production of two sperm cells. Cyclin dependent kinase of the A type family (*CDKA*;*1*) is a key regulator of the cell cycle machinery that operates from licensing DNA replication to entry and progression through mitosis. Analysis of T-DNA insertions in *CDKA*;*1* gene result in a pollen with a single germ cell in mature pollen, with a significant delay of S-phase of the cell cycle (Iwakawa *et al.*, 2006; Nowack *et al.*, 2006). Despite the lack of division, the *cdka*;*1* germ cell is capable of growing a pollen tube and subsequently to fertilise either the egg or central cells (Awe *et al.*, 2010). In addition in about 70 % of *cdka;1* germ cells undergo mitotic division during pollen tube growth, and subsequently, perform double fertilisation (Aw *et al.*, 2010; Nowack *et al.*, 2006), demonstrating that germ cell differentiation can be uncoupled from cell division.

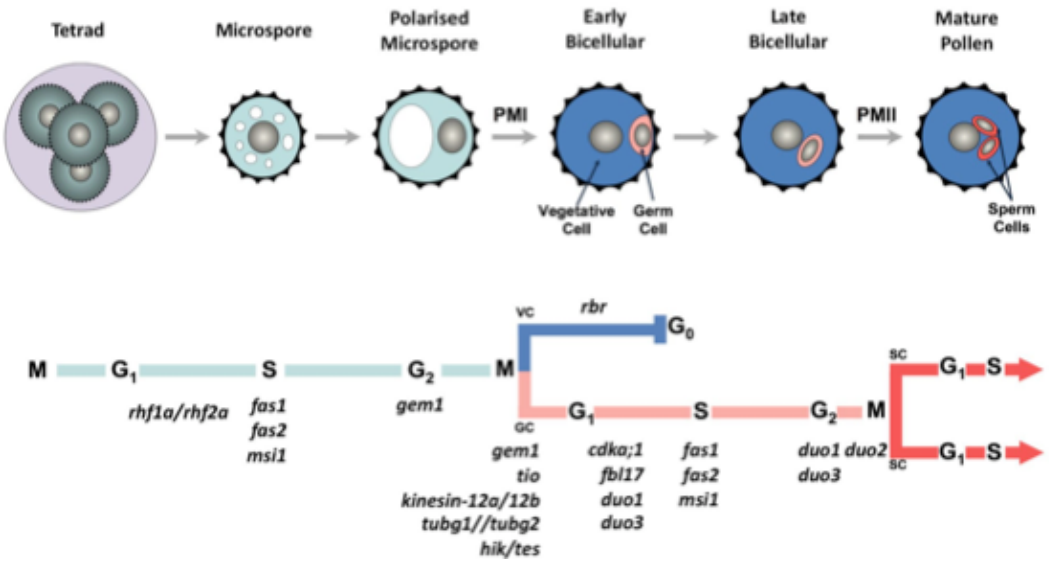

Figure 1.2: Schematic representing male gametophyte development and mutants affecting cell division in *Arabidopsis*. Diploid pollen mother cells undergo meiotic division to produce a tetrad of haploid microspores. Each microspore undergoes a highly asymmetric division to produce a large vegetative cell and small germ cell. At G2, the germ cell elongates and undergoes further division to form two sperm cells. The sperm cells then continue through cell cycle to reach G2 before double fertilisation. The lower panel illustrates the known mutants that disturb patterning and development of the male gametophyte (adapted from Twell, D 2011).

Knockout of the *F-box-Like 17* (*FBL17*) gene in male germ cells was shown to phenocopy the *cdka;1* germ cell defects (Gusti *et al*., 2009; Kim *et al*., 2008). The F-box is a protein motif of approximately 50 amino acids that mediates protein-protein interaction and is one of the components of the SCF ubiquitin-ligase complexes that consists of Skp1 and CUL1 that form the SKP1-CUL1-F-box (SCF) E3-ubiquitin protein ligase complex (Kipreos and Pagano, 2000). These SCF complexes have critical role in the ubiquitination of substrates for 26S proteosome mediated proteolysis. F-box-like proteins regulate CDKA activities through degradation of *CDKA* inhibitory proteins (Kip related proteins, KRPs). It has been shown that expression of *FBL17* during male gametophyte development is excluded from the vegetative cell and is only transiently expressed in the male germ cell, targeting KRP6 and KRP7 proteins for degradation and allow the germ cell to proceed through S-phase (Kim *et al*., 2008). In the absence of *FBL17*, the degradation of *KRP6* fails in germ cell, which result in persistence KRP6 leading to a slower S-phase and delay in a mitotic entry at PMII. Thus, *FBL17* provides a differential cell cycle switch that defines germ cell division competence and potentially the quiescent state of the vegetative cell.

A recent report has shown that disruption of the retinoblastoma-related (RBR) protein results in hyperproliferation of the vegetative cell and to a lesser extent the germline, leading to pollen with four sperm cells (Chen *et al*., 2009). The hyperproliferation that results from lack of *RBR* activity is dependent on *CDKA;1* activity since its proliferation phenotype were rescued by introduction of *cdka;1* mutant allele in hypomorphic *rbr* pollen. Clearly, cell fate is also incorrectly specified in a proportion of *rbr* vegetative cells. These cells appear to behave like a microspore attempting imperfectly to reiterate an unequal division to produce an additional cell with a range of fate identities (Chen *et al*., 2009). This places RBR repression of the E2F-DP pathway downstream of KRP-dependent CDKA;1 inhibition, so that both mechanisms are combined to determine cell cycle exit that is associated with commitment to vegetative cell fate.

Another sets mutants that also disturb male gametophyte development are mutations in the *Chromatin Assembly Factor-1* (*CAF-1*) components. Analysis of CAF-1 pathway

mutants (*fas1, fas2, msi1*) show that *caf-1* mutants display a range of phenotypes with some pollen that fail to divide either at PMI or at PMII, while the rest of the population succeed to produce two functional sperm cells (Chen *et al.*, 2008). This result indicates that the *CAF*-1 pathway has a wide role in male gametophyte cell division that could be required to direct epigenetic regulation (Chen *et al.*, 2009). Mutant bicellular *CAF*-1 deficient pollen grains correctly express germ cell fate markers and are able to equally fertilise the egg cell or the central cell (Chen *et al.*, 2008). Thus, *CAF-1* has an essential role during pollen development and loss of its activity (*caf-1*), indicates that correct chromatin assembly is important for germline and sperm cell formation.

1.1.2.2.1 *duo pollen* mutants: a novel class of male germ cell division mutants

Single germ cell phenotypes are also observed in the *duo pollen* (*duo*) mutants. Asymmetric microspore division is normally completed in these mutants, however, the resulting germ cell fails to divide (Durbarry *et al.*, 2005). Heterozygous *duo1* and *duo2* mutants produce approximately 50 % bicellular pollen containing a single germ cell, demonstrating complete penetrance of the mutations (Figure 1.4). *duo2* mutant germ cells enter mitosis but arrest at prometaphase, highlighting the role for *DUO2* in mitotic progression (Durbarry *et al.*, 2005). In contrast, mutant germ cells in *duo1* complete S-phase but fail to enter mitosis (Durbarry *et al.*, 2005).

1.1.2.2.1.1 *DUO1* a unique male germline R2R3 MYB transcription factor

One gene identified from these mutants is *DUO1*, which encodes a unique R2R3 MYB transcription factor in Arabidopsis that is specifically expressed in the male germline (Rotman *et al.*, 2005). A 1.2kb fragment upstream of the *DUO1* start codon has been shown to direct expression of a fluorescent reporter protein specifically to the germ and sperm cells (Rotman *et al.*, 2005). Monitoring the DNA content of germ and sperm cell nuclei during pollen development has revealed that *DUO1* expression is vital for the G2/M transition in the germ cell cycle (Durbarry *et al.*, 2005). Moreover, RT-PCR analysis showed that *DUO1* transcripts peak at the bicellular pollen stage during male gametogenesis prior to germ cell mitosis (Brownfield *et al.*, 2009a). This data collectively suggests that *DUO1* is a key germline-specific transcription factor that

controls germ cell cycle progression during male germline development.

DUO1 belongs to one of the largest transcription factor gene families in plants, with 130 MYB genes identified in the Arabidopsis genome (Jiang *et al*., 2004). The first MYB gene to be identified was the avian myeloblastosis virus oncogene v-MYB (Klempnauer *et al*., 1982). Many vertebrates are known to have three genes related to v-MYB, a-MYB, b-MYB and c-MYB (Weston, 1998), and similar MYB genes have been identified in plants, fungi, slime moulds, and insects (Ito, 2005). Non-plant MYB genes have been shown to play essential roles in the control of cellular proliferation and differentiation, and all share a conserved MYB DNA-binding motif. They all posses a MYB domain composed of up to three imperfect tandem repeats (R1, R2 and R3) each about 50 amino acids long. Contrary to the situation in other kingdoms, MYB proteins with two repeats (R2R3 Mybs) have been preferentially amplified in the plant kingdom (Romero *et al*., 1998). The MYB domain binds to DNA in a sequence-specific manner, where its predicted helix-turn-helix structure interacts with bases and phosphates in the major groove.

DUO1, the major regulator of germ cell division has been identified to regulate important genes that are specifically expressed in the germline (Brownfield *et al*., 2009a). Three of these regulated targets genes have been show to be specifically expressed in the male germline, and include a *MALE-GAMETE-SPECIFIC HISTONE H3* (*MGH3*) (Okada *et al*., 2005), *GAMETE EXPRESSED 2* (*GEX2*) (Engel *et al*., 2005) and *GENERATIVE CELL SPECIFIC 1* (*AtGCS1*) (Mori *et al*., 2006). The latter two target genes encode plasma membrane-bound proteins, with GCS1/HAP2 shown to be essential for normal pollen tube guidance and fertilisation (Mori *et al*., 2006; von Besser *et al*., 2006). The absence of GCS1 expression in *duo1* germ cells provides a likely explanation for the infertility of *duo1* pollen. RT-PCR analysis has shown that *DUO1* target gene transcripts accumulate significantly at the tricellular pollen stage that follows the bicellular pollen stage where the *DUO1* transcripts peak (Brownfield *et al*., 2009a). Introduction of the GFP marker driven by the three native target promoters into the *duo1* mutants has shown no expression or a weak GFP signal in *duo1* mutant germ cells. In contrast, when these markers were introduced to a *cdka;1* mutant background, normal specification of sperm cell fate has been observed. In *cdka;1* mutant cells

regulation of these target genes, particularly GCS1 indicate that DUO1 is expressed normally in *cdka;1* mutant pollen (Brownfield *et al.*, 2009a) (Figure1. 2).

Further work has revealed that *DUO1* controls an essential regulator of the cell cycle, the CYCLINB1;1 (CYCB1;1) (Brownfield *et al.*, 2009a). Together with cyclin-dependent kinase A (CDKA;1), *CYCB1;1* forms a complex that is essential for G2/M transition in the cell cycle (Mironov *et al.*, 1997). A CYCB1;1:GUS fusion containing the native CYCB1;1 mitotic destruction box is targeted for degradation at anaphase and is thus able to act as a G2/M phase-specific marker (Colón-Carmona *et al.*, 1999). This marker was used to examine the dynamic expression of CYCB1;1 during pollen development and it was shown to exhibit GUS activity in both microspores and germ cells, consistent with them entering microspore mitosis and germ cell mitosis, respectively (Brownfield *et al.,* 2009a). Furthermore, this G2/M phase-specific marker is suppressed in undivided germ cells in the *duo1* background (Brownfield *et al.*, 2009a). Activation of CYCB1; 1 by *DUO1* is a required for germ division at germ cell mitosis, explaining the bicellular pollen phenotype observed in the *duo1* mutant. Hence, by regulating these two independent pathways, *DUO1* provides the link between cell cycle progression and germline specification. The incorporation of these pathways ensures a pair of gametes that are able to carry out successful double fertilisation and contribute to the next generation (Figure1.2).

1.1.2.2.1.2 *DUO3* is required for progression through germ cell mitosis

DUO3 is another regulatory protein that also required for germ cell division and correct specification (Brownfield *et al.*, 2009b; Brownfield and Twell, 2009). DUO3 is a conserved nuclear protein in land plants and contains domains related to GON-4, a cell lineage regulator of gonadogenesis in *Caenorhabditis elegans* and hematopoeisis in zebrafish (Friedman *et al.*, 2000; Liu *et al.*, 2007). Similar to *DUO1*, *DUO3* is a key regulatory protein that is required for germ cell division and correct gamete specification (Brownfield *et al.*, 2009b). However, unlike the case in *duo1*, *duo3* mutant germ cell fail to proceed into mitosis independent of *CYCB1;1*. A proportion of *duo3* germ cells show persistent expression of *CYCB1;1*, indicating that failure of division in

duo3 could be due to incomplete activation of the anaphase promoting complex (APC), which normally targets CYCB1;1 for degradation to promote exit from mitosis (Peters, 2006). In addition, *duo3* germ cells either fail to divide or show a delay in division. Previous studies showed that *MGH3*, *GEX2* and *GCS1* are suppressed in the *duo1* mutant (Brownfield *et al*., 2009b), however, when the same markers were analysed in *duo3* germ cell the result showed that normal expression of *GCS1* and *GEX2* also requires DUO3. Whilst expression of *MGH3* depends exclusively upon DUO1, the mechanism by which DUO1 and DUO3 activate the expression of common targets remains unidentified (Brownfield *et al*., 2009b). It has been proposed that both *DUO1* and *DUO3* might cooperate in a transcriptional complex or that they may interact through a DUO3- dependent chromatin remodeling pathway (Brownfield *et al*., 2009b).

DUO3 shows expression beyond the gametophyte. For example in sporophytic plant tissues, DUO3 is expressed in regions that show cell division activity. Consistent with this, *duo3* embryos revealed defects in both morphogenesis and patterning. As *duo3* embryos show reduced rate and loss of coordination of cell division compared to wild germline type embryos, this suggests that *DUO3* may also regulate a number of different cell cycle targets in sporophytic tissues (Brownfield *et al*., 2009b).

1.2 The cell-cycle engine and its control

The major mechanisms of eukaryotic cell cycle are typically defined on the basis of chromosomal events, ensuring correct cell division. In the early events of the cell cycle, genomic DNA is replicated and chromosomes are duplicated in S-phase. The second major stage of the cell cycle is the mitosis that is typically composed of two consecutive processes: nuclear division (mitosis) and cell division (cytokinesis). Replication of DNA occurs in a specific part of interphase called S phase, which occurs between two gap phases (G1 and G2). G1 phase during which the cell is preparing for DNA synthesis followed by G2, which provides additional time for entry into the next cell cycle phase (mitosis) and the starting point for the reorganization of the cytoskeleton prior to M-phase (Elledge, 1996). M-phase (mitosis), the only microscopically visible stage, consists of four consecutive phases, pro-, meta-, ana- and telophases preceding

cytokinesis (Figure1.3). At the onset of mitosis, interphase arrays of cortical microtubules arranged transversely with regard to the main axis of growth are reorganized into a narrow cortical ring, called the preprophase band (PPB). This is unique to plants and consists of a belt-like arrangement of microtubules and actin filaments that forecasts the division plane. The preprophase band dissolves as the spindle array is built, which segregates the duplicated chromosomes during anaphase. The microtubules then rearrange again to form the phragmoplast, which control the expansion of the new cell wall required between the newly formed cells. Phragmoplast assembly starts centrally and expands with the growing cell wall toward the exterior of the cell (Kost *et al*., 2002; Lucas *et al*., 2006).

The progression of the cell cycle is regulated at multiple points by the activity of highly conserved heterodimeric cyclin– dependent-kinase/cyclin complexes (reviewed by Morgan, 1997). The different cyclin partners of the CDK/cyclin complexes mediate the substrate specificity of the complex in a spatial and temporal manner. The cell cycle machinery acts through transcriptional regulation of genes that mediate the mechanical processes, such as DNA replication (Amon *et al*., 1993). Therefore, the main role of the cell cycle regulatory proteins is to act as direct or indirect transcriptional regulators. In addition, proteins that directly regulate cell cycle are also periodically expressed at appropriate times to allow phase-specific functions during the cell cycle (Dynlacht, 1997).

1.3 Regulation of the plant cell cycle

Plant growth and development are driven by the continuous generation of new cells. Although the plant cell cycle is one of the most comprehensively studied processes, little is known about the molecular mechanisms that regulate progression through the different cell cycle phases and how the cell cycle is linked with cell differentiation and the ability to produce new daughter cells over very long periods. The sequencing of the complete rice and Arabidopsis genomes and the molecular studies of plant genes involved in cell cycle regulation suggests that many of the fundamental control mechanisms that govern cell division are conserved in other eukaryotes (Dewitte *et al*., 2003). Progression of the cell cycle requires many regulatory proteins, which include cyclin-dependent kinases

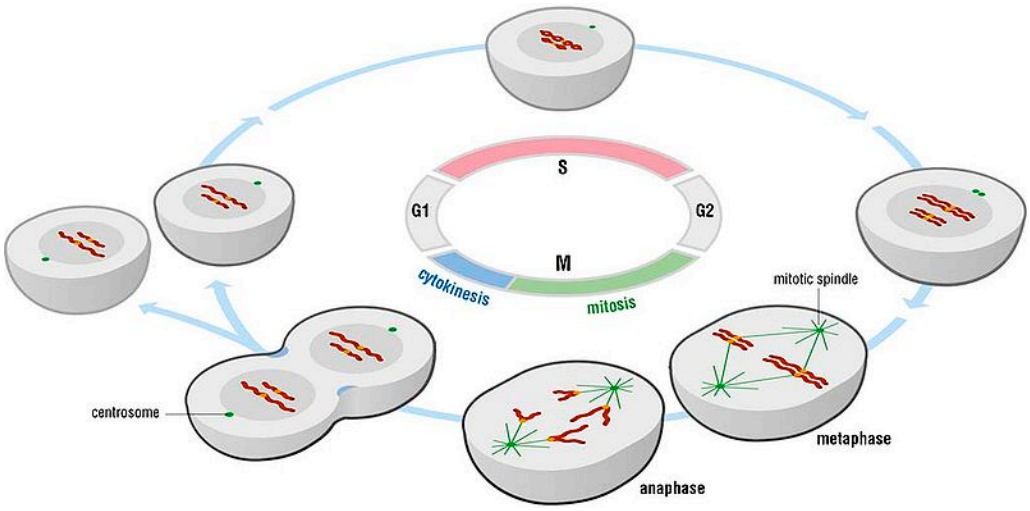

Figure1-3 Layout of the cell cycle progression showing cell in G1 (first gap), cell undergoes DNA synthesis in S-phase, cell prepares for mitosis in G2 (second gap) and finally M phase (mitosis) (taken from Morgen, 2006).

(CDKs), cyclins, cyclin-dependent kinase inhibitors (CKIs), and retinoblastoma protein (RBR) (Stals and Inze, 2001). As in other eukaryotic organisms, different cyclin-dependent kinase complexes phosphorylate many proteins at the G/S and G2/M transition points. These catalytic CDKs are dependent on non catalytic regulatory partners cyclins, resulting in different complexes at specific phases of the cell cycle to drive one stage of the cycle to another (Dewitte and Murray, 2003).

1.3.1 Cyclin-Dependent Protein Kinases

Cyclin-dependent kinases (CDKs) are a family of well conserved serine/threonine kinases. The universal PSTAIRE motif is the main feature in the CDKs protein, and plant CDKs with the PSTAIRE motif are able to complement CDK deficient mutants in yeasts (Ferreira *et al.*, 1991; Hirayama *et al.*, 1991). Seven classes (A-F) of plant CDK-related genes have shown to be involved in the regulatory mechanisms of the plant cell cycle (Dewitte and Murray, 2003; Doonan and Kitsios, 2009; Inze and De Veylder, 2006). However, the F-type CDK does not show typical cell cycle CDK features, such as the PSTAIRE motif of CDKA;1. In plants, two of the CDK classes, A-type CDK and B-type CDKs are best characterized so far (Boudolf *et al.*, 2001; Ferreira *et al.*, 1991; Hirayama *et al.*, 1991; Mironov *et al.*, 1999; Porceddu *et al.*, 2001) (Figure1-4).

Plants posses only one gene that encodes the A-type CDK with the PSTAIRE hallmark, is most closely related to animal CDK1 and CDK2 (Joubes *et al.*, 2000). The expression of CDKA is restricted to competent dividing tissues and is constitutively expressed throughout the cell cycle (Fobert *et al.*, 1996; Menges and Murray, 2002). At the transcript and proteins levels, CDKA;1, accumulate in a cell cycle phase independent manner, while Histone H1 kinase activity associated with A- type CDKs is high during G1/S, G2 and M phases (Mironov *et al.*, 1999; Sorrell *et al.*, 2002). In Arabidopsis, maize and tobacco different studies with dominant negative variants demonstrated that CDKA activity can be detected at both G1/S and G2/M check points. This highlights the activity of CDKA;1 in both mitosis and DNA synthesis phase, indicating that the CDKA;1 is likely to be an important cell cycle regulator (Hemerly *et al.*, 1995; Joubes *et al.*, 2004; Porceddu *et al.*, 2001). In Arabidopsis, CDKA;1 plays an important role through the early developmental stages of gametogenesis and embryogenesis. Analysis of the heterozygous *cdka;1* mutant

showed a normal division of the microspore into two daughter cells, a vegetative cell and a germ cell. However, approximately half of the population failed to progress through the second mitotic division of the germ cell and result in a production of a single sperm cell instead of two sperm cells (Iwakawa *et al.*, 2006 and Nowak *et al.*, 2006). CDKA;1 also plays a critical role in post-embryonic development. Overexpressing a dominant negative form of Arabidopsis CDKA;1 in tobacco seedlings showed larger and fewer cells (Dissmeyer *et al.*, 2007; Hemerly *et al.*, 1995).

The role of CDKA in controlling microtubule array reorganisation has been dissected through immunolocalization, the use of a CDKA-green fluorescent protein (GFP) fusion and cosedimentation, which has provided detailed information on the intracellullar localization of CDKA during the cell cycle (Colasanti *et al.*, 1993; Stals *et al.*, 1997). During interphase CDKA-GFP is observed in the nucleus and the cytoplasm with nuclear expression tightly associated with chromatin. During late G2 the GFP signal from CDKA-GFP is briefly associated with the cortical portion of the preprophase band. During prophase and metaphase CDKA is detected in association with condensing chromatin, and it is recruited to the metaphase spindle. At anaphase CDKA is localized to the central region of the spindle; during telophase the CDKA accumulates on the midline of the phragmoplast. At later stages of telophase CDKA reassociates with chromatin (Weingartner *et al.*, 2001). This close involvement of CDKA with the rearrangements of the microtubules that accompany mitosis suggests it has a key role in controlling microtubule dynamics and hence mitotic progression (Steinborn *et al.*, 2002).

B-type CDKs are unique to plants, (CDKBs) and have not been described for any other organism. In CDKBs the PSTAIRE hallmark in CDKA is replaced by either PPTALRE or PPTTLRE motifs, reflecting the existence of CDKB1- and CDKB2-classes (Boudolf *et al.*, 2001). Similar to CDKA, these kinases show ability to complement yeast cdc2/cdc28 mutants (Corellou *et al.*, 2005). In addition, the activity of CDKBs is linked with the G2-to-M transition phase, although CDKB1;1 transcripts accumulate mainly from late S phase to late mitosis (Segers *et al.*, 1996). In agreement, the activity of CDKBs is mainly associated with mitosis (Porceddu *et al.*, 2001; Sorrell *et al.*, 2001). CDKB1;1 possibly interacts with the mitotic cyclin, CYCB1;1 at the G2-to-M transition (Criqui *et al.*, 2001) and CDKB1;1 and CYCB1;2 genes also show a coordinated transcriptional up-regulation

during the G2 to M phase (Mironov *et al.*, 1999; Morgan, 1995). Furthermore, accumulation of CDKBs has been shown to be restricted to dividing tissues and is distributed in a nonuniform pattern, indicative of cell cycle phase dependent expression. Similar to CDKA, CDKBs appear to interact with D-type and B-type cyclins in regulating progression through S- and M-phases. Arabidopsis plants overexpressing a dominant negative allele of *CDKB1;1* result in an increase of proportion of cells with a tetraploid DNA content (4C) over that of diploid DNA content (2C) because of a blockage at G2/M transition (Boudolf *et al.*, 2004; Porceddu *et al.*, 2001). In addition, plants carrying the dominant negative form of CDKB1 also posses reduced number of stomata complexes, as substantiated by the increase activity of CDKB1;1 in the progenitor cells of stomata complexes (Boudolf *et al.*, 2004). Immunolocalization of alfalfa CDKB2;1 (*cdc2MsF*) showed that it colocalises to microtubular structures such as the preprophase band, preprophase spindle, metaphase spindle, therefore, these kinases are expected to play a role in cytoskeleton reorganisation through phosphorylation of microtubule associated proteins (MAPs) and kinesin-related proteins (Criqui and Genschik, 2002) (Figure1-4).

In addition to A-type and B-type CDKs, there are other two CDKs involved in the cell cycle, CDKD and CDKF. These kinases are functionally related to the animal CDK-activating kinases (CAKs). CDKF is a plant specific CAK showing a unique enzyme chrateristics (Reviewed by Inze and De Veylder, 2006). Both CDKs posses substrate specificity and unique interactions with the cyclin subunit, and recently CDKF;1 has been shown to phosphorylate and activate CDKDs in Arabidopsis and function as a CAK-activating kinase (CAKAK) (Shimotohno *et al.*, 2004).

Plants also have C-type CDKs that are closely related to the mammalian cholinesterase-related cell-division controller (CDC2L5), that possess a PTAIRE or SPTAIRE motif and shows preferential expression in dividing tissues with no clear role in cell cycle control. In *Medicago truncatula*, CDKC can interact with CYCT and phosphorylate Retinoblastoma related protein (RBR) as well as the C-terminal domain of RNA polymerase II (Reviewed by Inze and De Veylder, 2006). Thus, CDKC might have a putative role in transcription elongation and control of cellular differentiation by repressing RBR activity. Another class of CDKs with a SPTAIRE motif is CDKE. Unlike CDKC, CDKE is strictly restricted to

dividing tissues and is identical to *HUA ENHANCER3* (*HEN3*) (Reviewed by Inze and De Veylder, 2006). In common with CDKC, CDKE has been shown to phosphorylate the C-terminal domain of RNA polymerase II, following analysis of *hen3* mutants, CDKE has been proposed to play role in cell expansion in leaves and cell-fate specification in floral organs (Wang and Chen, 2004). Transcriptome analyses show that all *CDK*s are expressed in pollen (Honys and Twell 2004; Pina *et al*., 2005).

1.3.2 Plant cyclins

The plant cell cycle is regulated by the periodic synthesis and destruction of cyclins that associate with and activate cyclin-dependent kinases. Despite its small genome size, the *A. thaliana* genome contains at least 32 cyclins with a putative role in cell cycle progression. The large number of cyclins highlights the high developmental plasticity of sessile plants essential to respond to both intrinsic developmental signals and environmental mechanisms. Amazingly, each cyclin has a distinctive expression profile during the cell cycle. The arrangement of plant cyclins is based on the functional similarities with mammalian systems as well as complementation of yeasts deficient in the expression of specific cyclins. Arabidopsis gene annotation identified 10 A type, 11 B-type, 10 D-type, and 1 H-type cyclins (Vandepoele *et al*., 2002; Wang *et al*., 2004).

***A*-type cyclins (*CYCAs*)**

Arabidopsis contains at least 10 different genes, which encodes for the A-type cyclins and they are grouped into three subclasses, CYCA1, CYCA2 and CYCA3 classes (Chaubet-Gigot, 2000; Renaudin *et al*., 1996). CYCAs are mainly present from S- phase to mitosis and activate CDKA to regulate S-phase progression primarily. Analysis of cell suspension cultures from tobacco BY2 cells revealed an increased transcript abundance of the CYCA1 subfamily at mid-S phase, whereas CYCA3 subclasses showed maximum expression at G1/S transition (Reichheld *et al*., 1996). In contrast to CYCA1/A3 subclasses, CYCA2 family members showed a wider pattern of expression and display a biphasic kinase activity. Transcript levels were high for CYCA2 during G1 and S-phase, peak at G2 stage, and then drop during M-phase. Whereas protein levels were low at G1 stage, increased during S-phase and remained at a constant level during G2 and M-phase.

This is in contrast with their kinase activity in which high activities were observed at mid S-phase, reduced thereafter, and reach a maximum again at the G2/M transition (Roudier *et al*., 2000). This unique expression pattern of the A-type subfamilies highlights various biological functions among the family members during different cell cycle stages. Furthermore, subcellular localization of CYCA3;1 protein GFP fusion detected GFP localization in the nucleus and nucleolus in cells undergoing S phase which then disappeared in mitotic cells. A similar pattern was also observed for CYCA2 in alfalfa in which GFP was detected in the nucleus until prophase before disappearing during mitosis (reviewed by Dewitte and Murray, 2003).

Ectopic expression of the tobacco CycA3;2 in Arabidopsis, results in promotion of cell division and a delay of cell differentiation, but in tissue culture, ectopic expression of CYCA2;3 prevents regeneration of shoots and roots (Yu *et al*., 2003). Moreover, yeast two hybrid experiments have demonstrated the ability of CYCA2 to interact with a maize retinoblastoma protein in the presence of the cyclin destruction box, highlighting the role of A-type cyclins in S-phase progression (Roudier *et al*., 2000). In contrast to the enhanced expression of CYCA, loss of function of CYCA2;3 results in a slight increase in cell ploidy levels (Imai *et al*., 2006). In the *tardy asynchronous meiosis* (*tam*), mutation of a conserved amino acid in CYCA1;2 results in a delay in cell cycle progression during male meiosis (Magnard *et al*., 2001; Wang *et al*., 2004). Whereas, in the double mutant of *osd1*/*tam* led to failure of male meiocytes before entry into meiosis, whereas female meiocytes progress to meiosis I, but fail to enter meiosis II. The occurrence of a subtle phenotype in both cases suggests that other CYCAs may compensate for the absence of CYCA1;2 (d'Erfurth *et al*., 2010).

_B_-type cyclins (*CYCBs*)

CYCBs were among the first cell-cycle regulators identified and cloned in plants and they were isolated from carrot, soybean and Arabidopsis (Reviewed by Dewitte and Murray, 2003)**.** The CYCB family plays a conserved role during late G2 to M transition and is transcribed during G2. CYCB has 11 members that are classified into three subfamilies CYCB1, CYCB2 and CYCB3. CYCB1 contains 5 members (CYCB1;1- CYCB1;5),

CYCB2 contains 5 members CYCB2;1-CYCB2;5), while CYCB3 has one member (Menges *et al.*, 2005; Vandepoele *et al.*, 2002). CYCBs distinguish themselves from CYCAs by their later expression during the cell cycle. All identified CYCBs were subdivided into two subclasses, CYCB1 and CYCB2, however, CYCB-like protein without the typical B-type destruction box, was assigned to a third class, CYCB3 (Vandepoele *et al.*, 2002). Extensive progress has been made in the description of the mechanism underlying G2/M specific transcriptional regulation. Studies in cell suspensions and in plants has demonstrated that transcripts for the CYCBs are detected as early as S-phase, rising at G2 phase, with enriched detection at G2-M and then rapid degradation as M-phase progresses (Menges *et al.*, 2002). This expression pattern was supported by the analysis of full length AtCYCB1;1 promoter with and without a destruction box motif fused to β-glucuronidase (Colon-Carmona *et al.*, 1999; Shaul *et al.*, 1996). The accumulation of GUS mRNA resembles the kinetics observed in cell suspension suggesting that the kinetics of CYCBs are controlled by transcriptional regulation (Culligan *et al.*, 2006; Ito *et al.*, 1997; Shaul *et al.*, 1996; Trehin *et al.*, 1997).

To understand the regulatory elements that are responsible for the G2/M specific transcriptional enhancement, a promoter deletion analysis of CYCB1;1-Luciferase from *Catharanthus* and *Nicotinana* was performed. This observation led to the identification of M-phase specific activator (MSA), containing a central core pentamer that is closely related to Myb-binding sites as responsible element for the M-phase specific regulation. Moreover, the MSA-like elements have been identified and found to be conserved in a number of cyclin promoters from wide range of plant cyclins (Ito *et al.*, 1997; Trehin *et al.*, 1997). Three Myb proteins have been isolated from tobacco BY2 cells (NtMybA1, NtMybA2, and NtMybAB) using the MSA elements identified previously in *Catharanthus* (Ito *et al.*, 2001). NtMybA1 and NtMybA2 and were found to activate MSA containing promoters, whereas NtMybAB antagonise NtMybA1 and A2 activity. This study suggests that MSA-mediated mechanisms are necessary to drive G2/M specific transcriptional regulation of the CYCBs.

In addition to transcriptional control, the levels of CYCBs in higher plants are regulated by the proteolysis complex, the APC, leads to cylins proteins destruction during the

1998). The accumulation of CYCB protein was observed in tobacco BY2 cells whereby the protein levels were high at S/G2 stage and then dropped during M-phase progression (Crique *et al.*, 2001). Furthermore, analysis of a CYCB1;1-CYCB1;1::GFP fusion construct in tobacco G2 cells showed cytoplasmic and nuclear localization of the protein, the GFP signal was then associated with the condensing chromosomes during prophase and was absent at anaphase and telophase as predicted (Criqui *et al.*, 2001). Similar to mammalian cyclins, microinjection of tobacco CYCB1;1 into *Xenopus oocytes* can overcome their G2/M arrest (Qin *et al.*, 1996). In addition, overexpression of the *CYCB1;2*, but not the *CYCB1;1*, cyclin in the normally endoreduplicating trichomes promotes the G2/M transition and shifts trichome cells into cell divisions and leads to increase root growth (Schnittger *et al.*, 2002). Overexpression of a non-degradable version of CYCB in yeast and animals causes block of mitotic progression. However, a similar experiment using the tobacco CYCB1;1 under the 35S in tobacco BY2 cells did not show severe effect on mitotic progression, instead there was severe growth retardation and few multinucleate cells were observed in endoreduplicated cells (Criqui *et al.*, 2001; Weingartner *et al.*, 2004). Taken together this evidence indicates that plant *CYCB1* is specifically involved in licensing the G2/M transition and its degradation is essential for mitotic exit.

1.3.3 CDK phosphorylation

The activity of CDK is generally regulated by post-transtional modification. This requires the phosphorylation of CDK kinases by Thr160 that results in protein conformational changes to allow greater recognition of the substrates (Holmes and Solomon, 2001; Song *et al.*, 2001). This conformational change may enhance the association between the cyclins and CDKs and that may enhance phosphorylation.

In plants several CAK kinases, that complement *S. cerevisiae* CAK mutations and that phosphorylate CDKs, have been identified (Shimotohno *et al.*, 2004). The first plant CAK was isolated in rice and used as a model to identify another four CAK-encoding genes in Arabidopsis, which fall into two classes, CDKD and CDKF, (Reviewed by Dewitte *et al.*, 2003; Inze *et al.*, 2006). CDKD is preferentially expressed during S-phase and can associate with H-type cyclins for activation and possess kinase activity towards CDK and the C-terminal domain of RNA polymerase II (Fabian-Marwedel *et al.*, 2002). The

Arabidopsis genome encods three CDKD genes, namely, CDK;1-CDK;3 (Vandepoele *et al*, 2002; Shimotohno *et al*, 2004). Whereas CDKF is unique to plants in the sense that it does not phosphorylate RNA polymerase II as other CAKs and requires no association with H-type cyclin for activation, however, it can specifically phosphorylate Arabidopsis CDKDs (Shimotohno *et al*., 2004). The evidence comes from inducible co-suppression using sense and antisense down-regulation of AtCDKF activity, which leads to premature differentiation of the root meristem (Umeda *et al*., 2005). Recently it was shown that *CDKF;1* plays a critical role in post-embryonic events by regulating the protein stability of CDKD;2 (Takatsuka *et al*., 2009).

The major candidate for the Tyr I5 kinase is WEEl, which was originally identified in *S. pombe*. In plant, a WEE1-related kinase has been described for maize (*Zea mais*), tomato (*Solanum lycopersicum*), and Arabidopsis (Gonzalez *et al*., 2007; Sorrell *et al*., 2002; Sun *et al*., 1999). Although the plant WEE1 fails to rescue mutations in its yeast homolog, its overexpression inhibits cell division in fission yeast. In Arabidopsis, WEE1 kinase is able to phosphorylate CDKA;1 at tyr15, and CDKD;1, CDKD;2 and CDKD;3 at tyrosine 23/24 in vitro (Shimotohno *et al*., 2006). In plants, the role of WEE1 cell cycle progression and growth is not well defined. However, in Arabidopsis the loss of function of WEE1 showed no obvious phenotype when grown under normal growth conditions (De Schutter *et al*., 2007). This suggests that unlike in yeast and animals, WEE1 has a function that may be unrelated to cell division in plants. In fission yeast, the progression into M phase is regulated by the activity of Wee1 and Cdc25 and the introduction of mutated Wee1 resulted in premature entry into mitosis. In plant, no Cdc25 homologue has been identified yet. However, the overexpression of yeast Cdc25 gene in tobacco cells showed high activity during different cell cycle stages (McKibbin *et al*., 1998). A small protein Cdc25-like has been reported in Arabidopsis, with structural homology to animal Cdc25 phosphates (Landrieu *et al*., 2004). The Arabidopsis Cdc25 is capable of recognizing CDKs *in vitro* and can activate them, but it lacks N-terminal regulatory motifs (Sorrell *et al*., 2005). However, misexpresssion of Cdc25 in Arabidopsis has no obvious effect under normal plant growth conditions (Bleeker *et al*., 2006). In accordance with its role in CDK regulation, cyclins are also subjected to phosphorylation.

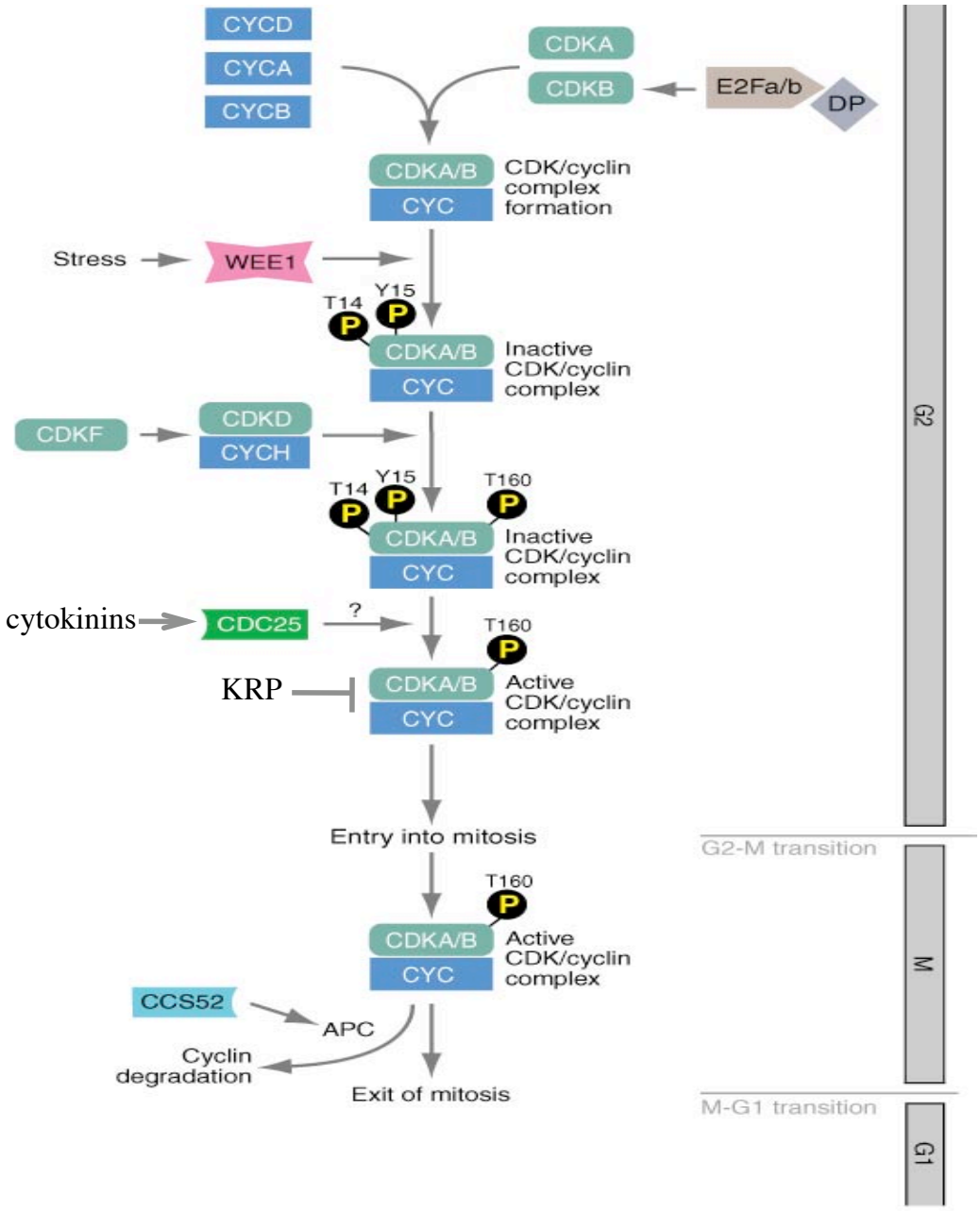

Figure 1.4: Model of cell cycle control in plants during G2-to-M transition. The G2/M transition is regulated by complexes CYCA, CYCB and CYCD associated with both CDKA and CDKB. The E2F pathway regulates the transcription of some CDKBs. he Activation of specific CDK/cyclin complexes is controlled by CDKF, and CDKD associated with CYCH. Phosphorylation of T14 and Y15 by WEE1 inhibits the pathway. Dephosphorylation of T14 and Y15 is thought to be done by a CDC25-related kinase. Exit of mitosis requires targeted of cyclin subunits for degradation by the activity of APC/CCS52 complex. high levels of ICKs/KRPs block CDKA;1 activity at both G1/S and G2/M transitionn (modified after Inze and De Veylder, 2006).

The tobacco CYCD3;3 is phosphorylated on Thr191, and this process is required for nuclear activity to achieve the full kinase activity (Nakagami *et al.*, 1999). In particular, mutational analyses showed that Thr-191 in Nt;CYCD3;3 is likely to be involved in kinase activity in a complex with CDKA and its localization to the nucleus.

In addition to cyclin subunits, CDK activities are also regulated by CYCLIN-DEPENDENT KINASE INHIBITORS (CKIs) through negative phosphorylation. This mechanism of regulating CDK activity is conserved across all species and several CKI encoding genes have been identified. CKIs are a group of low-molecular-weight proteins that have the ability to bind to cyclin-CDK complexes, subsequently, inhibiting the activity of CDKs. CKI complex with CDK or their components and inhibit their activities. This complex appears to regulate cell cycle progression, in response to inhibitory signals. For example, budding yeast contains three CKIs encoding genes; Far1p that inhibits CDK activity at the G1 phase in response to mating signals. In addition Sic1p regulates CDK activity during S-phase entry and Pho81 that negatively phosphorylates the CDK/CYC complex, controls gene expression under low phosphate conditions (Reviewed by Inze *et al.*, 2006).

1.4 The ubiquitin system

In dividing cells, the degradation of cell cycle regulator proteins is necessary to drive the periodic fluctuations in protein levels through different stages of the cell cycle. To cycle in a unidirectional fashion, cells use key regulatory mechanisms to guarantee that the destruction of proteins is turned off at the right time and in the right phase of the cell cycle. Such proteins turnover is operated through the ubiquitin-26S proteasome pathway (UPP) (Pagano, 1997; Scheffner *et al.*, 1995). The ubiquitin/26S proteasome proteolytic pathway is well conserved in eukaryotes and is involved in a wide variety of cellular functions aside from cell cycle progression (Genschik *et al.*, 1998; Hochstrasser, 1995; Nakayama and Nakayama, 2006). The molecular mechanisms that induce these complex processes are poorly understood and many of the target proteins still subject to further studies. Protein ubiquitination is a three-step enzymatic process generated by E1, E2 and E3 proteins. The ubiquitination of target proteins is performed by the combination of E2-ubiquitin carrying enzyme and an E3-ubiquitin protein ligase

that mediate the interaction between E2 and the target protein. This interaction results in decoration of the target substrate by covalent attachment of ubiquitin, but the monoubiquitinated substrates are not recognized by the 26S proteasome complex. Following that the tagged protein is subject to multiple ubiquitination (Pickart, 2004). Protein degradation occurs during two major phases of the cell cycle, DNA synthesis and mitosis, which is mediated by the ubiquitin-protein ligase pathway. The two principal E3 Ub-ligases involved in cell cycle control, namely the SCF (Skp1, Cullin, F-box), complex and the APC/C (anaphase promoting complex/cyclosome), which are evolutionarily related. Both complexes share several conserved domains, suggesting that both proteins may use a similar mechanism for substrate recruiting.

1.4.1 The APC/C is not just important for mitosis.

1.4.1.1 The structure of the APC/C

The APC/C is particularly known for its role in cell division and initiation of chromosome segregation at anaphase stage of mitosis. The APC was identified according to the role that it plays in the multiubiquitination and destruction of cyclin A and cyclin B during mitosis. In vertebrates, the APC is composed of at least 11 subunits, while in yeast APC is composed of more than 13 subunits (Capron *et al*., 2003a; Castro *et al*., 2005; Harper *et al*., 2002), and all orthologous Arabidopsis APC/C components have been found (Capron *et al*., 2003a; Tarayre *et al*., 2004). Remarkably, about 5 % of the proteome, is involved in the ubiquitin/26S proteasome pathway, making it one of the most complicated regulatory mechanisms in plants (Smalle and Vierstra, 2004).

The RING-H2 protein and the cullin homologue together with Apc2 are sufficient to support E2 activity. These domains were most likely to play an important role in ubiquitination of target proteins (Gmachl *et al*., 2000). Analyses of the 3 D-structure of APC showed that the RING subunit associates with the E2 through a hydrophobic cavity, which is important for APC to generate multiubiquitin chains on the target substrate (Zheng *et al*., 2002). The Cdc16, Cdc23 and Cdc27 subunits of the APC each contain 8–10 copies of the 34-amino-acid TPR (tertracopeptide repeat), which is used as

a protein-protein interaction mediator. Another TPR-containing subunit, Apc7, has so far been identified only in vertebrate APC. These TPR motifs are hypothesized to form a scaffold onto which the other subunits will assemble. In addition, Cdc27 and Apc7 interact with several proteins containing an Ile-Arg motif at their C-terminal. This protein-protein interaction motif is present in co-activator proteins in Cdc20 and Cdh1-like protein as well as the Doc- domain subunit/Apc10. Moreover, Apc10/Doc1 could help to maintain the substrate during elongation of ubiquitin chains (Carroll *et al*., 2005; Vodermaier *et al*., 2003). In particular, deletion of Doc1 in yeast inhibits APC activity, while E2 complex formation remains unaffected.

In sharp contrast, Ohi and colleagues (2007) showed that the analysis of Slp1, the Cdc20 ortholog, binds at a position discrete from the TPR domains. Indeed, in yeast the activity of APC/C^{Cdh1} does not depend on Apc3/Cdc27 (Schwab *et al*., 2001). Instead, a domain called the C-box could play a critical role to allow Cdh1 to associate with the APC/C (Ohi *et al*., 2007; Thornton *et al*., 2006).

1.4.1.2 The APC activators and substrates

The degradation of cell cycle regulator proteins is a critical step to maintain the periodic fluctuations in protein levels during the cell cycle, and serves as a means of cell cycle control. This must be achieved through modification of APC activity to generate a stable ubiquitination reaction platform that is controlled by phosphorylation and by dynamic interactions with substrates and so-called activators. These activator substrates participate in target protein recognition by the APC. The C-terminal regions of Cdc20/Fizzy and Cdh1/Hct1/Fizzy-related activators contain a WD40 domain that is critically required to form a propeller-like binding platform that binds APC substrates (Peters, 2006; Yu, 2007). Several APC subunits were phosphorylated, which include Apc1 and the TPR subunits (Harper *et al*., 2002). Patra and Dunphy, 1998 identified multiple phosphorylation sites in the TPR-containing subunits and Cdc kinase subunit (Cks)- mediated phosphorylation was reported as a modulator of the activity of the complex. However, It remains ambiguous how CYCB1-CDK1- dependent phosphorylation contributes to enhanced APC/C^{Cdc20} activity.

The mechanism that leads to APC/C activation and substrate specification by these activators has been the subject of intensive research in the past several years (reviewed in Thornton and Toczyski, 2006). One mechanism of regulation of APC/C activity is through the regulation of these activators through post-transcriptional modification. Each activator binds APC/C in a cell cycle dependent manner to dictate which targeted substrates are degraded as well as the precise timing for their degradation. The Cdc20-dependent APC/C (APC/C^{Cdc20}) functions in mitosis as its activity can be detected from prometaphase until telophase. Cdc20 links the spindle checkpoint to the APC/C through its binding to Mad2. In late mitosis and G1 the APC/C is activated by the other APC/C activator, Cdh1 (also called Hct1), which is present throughout the cell cycle (Kramer *et al.*, 2000). Cdh1, however, shows the ability to bind APC/C only when its inhibitory phosphorylation is removed (Fang *et al.*, 1998; Kramer *et al.*, 2000; Zachariae *et al.*, 1998). Some experiments show that phosphorylation of Cdh1 by the CYC-CDKA complex prevents its interaction with the APC/C in G2 phase and during the first part of mitosis (Lukas *et al.*, 1999).

Several sequence motifs have been identified that required for the degradation of APC substrates. The destruction box composed of the sequence RxxLxxxxN has been found in all known Cdc20-APC substrates, which makes it subject to APC/C^{Cdh1} activity (Glotzer *et al.*, 1991). A second motif that is frequently found in proteins targeted by APC after anaphase and in G1, is the KEN box (KENxxxE/D/N) (Buschhorn and Peters, 2006; Pfleger and Kirschner, 2000). New motifs have been identified recently, namely the A-box (RxLxPSN). This motif has been discovered only in Aurora-A kinse, that directs the proteolysis of these proteins (Crane *et al.*, 2004; Littlepage and Ruderman, 2002). It is notable that the location of functional destruction motifs are often located in the N-terminus region of the APC substrate, and D-boxes in protein regions that are natively unfolded, so that APC recognizes the D-box and binds to it with high specificity and low affinity (Cox *et al.*, 2002). CYCA and CYCB contain D-box sequences, and are susceptible to rapid proteolytic destruction. On the other hand, most CYCD family members possess a PEST motif in their C-terminal regions, which is also a mark of short-lived proteins (Rechsteiner and Rogers, 1996; Wang and Chen, 2004).

In plants, mostly in Arabidopsis, the expression of several APC subunits has been detected in differentiated tissues (Capron *et al.*, 2003b). The Arabidopsis genome encodes five *CDC20* genes, as well as three CDH1-related proteins, named as cell cycle switch CCS52 proteins (CCS52A1, CCS52A2, and CCS52B) that are plant-specific (Tarayre *et al.*, 2004). In *Schizosaccharomyces pombe*, expression of the three Arabidopsis *CCS52* genes generates distinct phenotypes, pointing at a nonredundant function of the CCS52 proteins (Tarayre *et al.*, 2004). In synchronized Arabidopsis cell cultures the CCS52B transcripts were present from G2/M, whereas CCS52A1 and CCS52A2 were detected from late M until early G1, suggesting consecutive actions of these APC activators in the plant cell cycle (Fulop *et al.*, 2005). These two subclasses of CCS52 proteins appear to be highly conserved in plants.

The role of CDC20s in plants remains poorly understood. *CDC20* seems to be expressed specifically in proliferating cells and together with *CCS52* can mediate the degradation of mitotic cyclins at different phases of the cell cycle. CCS52 proteins were first identified in *Medicago* species (Cebolla *et al.*, 1999; Tarayre *et al.*, 2004) as orthologs of the fission yeast *Srw1*/*Ste9*. Overexpression of CCS52A in fission yeast promotes mitotic cyclin degradation and leads to growth inhibition, cell elongation and DNA endoreplication. Functional analysis of the CCS52 proteins in *Mediacgo* led to the identification of another conservative motif (YxxLL(K/R)xxLFC) in the CCS52 proteins, called Cdh1- Specific Motif (CMS) that plays a critical role in APC activation (Tarayre *et al.*, 2004). In addition potential phosphorylation sites were identified in front of a domain called the C-box, which might be critical for CCS52 binding to APC. The role of *CCS52* in promoting endoreplication was first discovered through downregulation of CCS52A and CCS52B in *Medicago* (Cebolla *et al.*, 1999). Moreover, in Arabidopsis loss of function of *CCS52A2* leads to a reduction in cell size and ploidy level (Lammens *et al.*, 2008).

Mutants in APC exhibit defects during female gametophyte development and have been mostly isolated through genetic screens in Arabidopsis. For example, knockout of *APC2* leads to blocked female gametogenesis, as result of cell cycle arrest at the early stages of embryo sac development (Carpon *et al.*, 2003). Whereas a defect in an *APC3*/*CDC27* gene caused by the *hobbit* mutation reduces cell division rate and meristem

differentiation. In accordance with the essential role of APC in female gametophyte development, the *NOMEGA* gene which encodes *APC6*/*CDC16,* was shown to be required for cell cycle progression after one nucleate stage of megasporgenesis (Kwee and Sundaresan, 2003).

1.4.2 The SCF complex regulates cell cycle progression through timely protein destruction

Protein degradation in animals and yeasts is mediated by the SCF ubiquitin ligase complex (Skp1,Cullin , F-box) that plays an important role in DNA replication. The SCF complex is a multisubunit structure with three components: RING-finger protein, cullin1/Cdc53, and Skp 1(adaptor protein). The F-box proteins share a 40 amino acid conserved domain, which is called "F-Box" at the N-terminus (Xu *et al*., 2009). In the C-terminus, the F-Box protein contains a protein domain that binds substrate/target proteins, often in a phosphorylation-dependent manner and represents a critical step in SCF dependent proteolysis. Based on the substrate-specific motifs at the C-terminus, F-Box proteins are classified into three families, the Fbw (or FBXW), LRR (leucine-rich repeat) and WD40 containing F-Box (Trp-Asp)-40 protein families (Andrade *et al*., 2001; Gagne *et al*., 2002; Kuroda *et al*., 2002). Reconstruction of the SCF in yeast and further crystal structure studies have shown that CSF components are assembled in a structure in which the RING-finger subunit functions to bridge the Cullin1 and the E2 enzyme. Whilst Cullin1 functions as the scaffold of this multimeric E3 complex, its N-terminus associates with SKP1 and the C-terminal part is linked to the RING-Box1. The F-box protein is intimately associated with SKP1 (Gagne *et al*., 2002).

Many processes might be regulated through the SCF complex, as a large number of proteins with F-box signatures in different organisms have been discovered (more than 19 in yeast, 50 in vertebrates). By comparison the *A. thaliana* genome contains over 700 F-Box genes, which highlights the importance of SCF E3s in the control of plant protein abundance or might reflect a high level of functional redundancy among them (Gagne *et al*., 2002; Kipreos and Pagano, 2000). In contrast to APC/C, the SCF complex is considered to be active throughout the cell cycle, targeting only phosphorylated proteins (Bachmair *et al*., 2001; Winston *et al*., 1999). In both budding yeast and animals,

degradation of cell cycle regulator proteins is typically performed by the SCF/cdc4 and SCF/Grr1 complexes. In *S. cerevisiae*, S-phase Cdc28/Clb5-6 complexes are kept inactive by the activity of the Sic1/CDKI complex (Siegmund and Nasmyth, 1996). During G1 stage, the accumulation of Cdc28/Cln1-3 results in the phosphorylation of Sic1 which subsequently, directs it to SCF^{Cdc4}. In addition, the increase of Cdc28/Cln1-3 activity results in autophosphorylation on C1n1-2, which the SCF/Grr1 complex will recognize.

In plants, only small fractions of F-box proteins have been investigated to date, and they have been shown to play critical roles in regulating different developmental processes and stress responses (Zhang *et al*., 2010). The role of SCF in the cell cycle is supported by the analysis of loss of function mutant *cul1* that leads to early embryo arrest at the zygote stage (Chew and Hagen, 2007). Moreover, the F-box protein (FBL17) is expressed during the male gametogenesis after microspore division and targets the KRP6 and KRP7, allowing the activation of CDKA /CYCD complex and the germ cell to progress through S-phase (Kim *et al*., 2008). Correspondingly, two RING-finger E3 ligases, RHF1a and RHF2a, target the KRP6 in microspores for proteasome mediated-degradation, allows regular progression through microspore and subsequent germ cell to progress through the mitotic cell cycles (Liu *et al*., 2008).

Despite the rapid progress in understanding cell cycle regulation in plants (Huntley and Murray, 1999; Menges and Murray, 2002; Stals and Inze, 2001), little is known about the role of the cell cycle machinery in the promoting male germ cell division in plants to ensure two sperm cell production. One approach is to screen cell division mutants that specifically disrupt normal development of the germ cell, shedding more light on the molecular-genetic mechanisms with function in male gametophytic regulators of cell cycle progression and differentiation. The work presented in this thesis has explored molecular, genetic and cytological approaches to understand the mechanisms that govern cell cycle progression and cell fate specification in the male gametophyte.

1.5 Aims of this project

Over recent years some effort has been made to identify and characterise mutants that affect germ cell cycle progression. Genetic analysis of male gametophytic mutants is challenging because of the fact that it occupies a relatively short phase in the life cycle. In addition, the male gametophyte is embedded in the sporophytic tissues, making it difficult for direct examination (Page and Grossniklaus, 2002). In order to overcome these challenges, the combination of forward and reverse genetics approaches provides powerful tools. Both genetics approaches were used in this thesis to identify and characterise a new gene involved in gametophyte development. Work on the *duo4* mutant was initiated after the isolation of several *duo pollen* mutants in a morphological screen described in Durbarry (2005). The phenotype of the identified *duo4* mutant affects germ cell division with no obvious other gametophytic (pollen) or sporophytic plant phenotypes. The detailed analysis of the *duo4* mutant and the corresponding casual gene, *CCS52A1*, provides a better understanding of the molecular mechanisms controlling male germline development and fertilisation.

In the third chapter of the thesis the specific aims of the experiments were to characterise *duo4 pollen* mutant, phenotypically. The precise point of development arrest of germ cell mutant in *duo4* was established by measurement of DNA content. Ultrastructure of the *duo4* mutant was analysed by transmission electron microscopy. Cytological analysis such as vital staining, cell fate and cell cycle markers were monitored. In addition, the impact of the *duo4* mutation on double fertilisation and germ cell morphogenesis was investigated.

In the fourth chapter of the thesis, the main efforts of the experiments were to characterise the *duo4* mutant genetically. This involved analysing the genetic transmission through the male and the female gametes to determine the gametophytic nature of the mutation. In addition a map-based approach was undertaken to isolate the *DUO4* gene and elucidate its role in male gametophyte development. The *duo4* mutant gene was investigated further with the possibility that *duo4* phenotype results from a gain of function mutation in *CCS52A1* gene. Thus to examine this possibility reverse

genetics experiments in the form of RNAi (interference) and gene overexpression were carried out in order to change the *CCS52A1* expression level. Collectively, these approaches delivered new insights into the role of *CCS52A1* gene in plant cell cycle control and development, specifically during the male gametophyte development.

In the fifth chapter, the aim was to screen for novel *DUO1* target genes (*DATs*), inducible system in a time-course microarray experiment has been applied in the Twell laboratory (Brownfield *et al*, 2009a). This yielded a cluster of genes that are predicted to be *DUO1* targets. Taking advantage of this, the final aims of this project were to:

- To verify whether these genes are native *DUO1* targets, this was achieved by building promoter-reporter constructs for these genes.
- To determine if *DAT* genes follow the similar expression profile of *DUO1* gene during pollen development.
- To validate if the *DUO3* gene is required for the expression of *DAT* genes.

By achieving the goals described above, this project contributes to the knowledge of male germline development and the mechanisms that control cell cycle progression and cell fate determination. In addition, the present study provides new knowledge about the molecular roles of the APC/C during pollen development and paternal control of seed development.

Chapter Two

Materials and methods

2. Materials and methods

2.1 Materials used for the experiments

Plant materials were grown at the botanic garden of the University of Leicester. Seeds of *qrt1/qrt1* (Ler accession) were provided by D. Preuss. Line of *proCDKA-GUS* used in this study was provided by Moritz K. Nowack. The KS22 enhancer-trap line (C24 accession) expressing the GFP endosperm marker protein was generated in J. Haseloff's laboratory (www.plantsci.cam.ac.uk/Haseloff). Seeds of pCDF marker line were provided by Peter Doerner. The GEX2-GFP marker line was supplied by Sheila McCormick. pMGH3/pLAT52-H2B::GFP were generated in Twell laboratory (Brownfield *et al*., 2009a).

All Chemicals and materials used were purchased from Melford Laboratories, Sigma-Aldrich, Thermo Fisher Scientific, PerkinElmer, BioGene, Calbiochem, Promega, Duchefa Biochemie, DHAI PROCIDA and Lehle seeds. Purification kits were purchased from Qiagen, Sigma-Aldrich and Bioneer. Enzymes and other reagents were obtained from Invitrogen, Finnzymes, New England Biolabs, Novagen, Sigma-Aldrich and Bioline. Companies from which equipment and instruments were purchased are indicated in the materials and methods.

2.2 Preparation of plant materials

2.2.1 Media for plant tissue culture

Arabidopsis seeds were plated on Murashige and Skoog salt media (MS Duchefa Biochemie, Netherlands). 4.3g of MS salt was dissolved in 950ml of deionised water with no added sucrose (MS0) or with 1-3% (w/v) sucrose. The media pH was adjusted to 7.0 with 5N NaOH and the media were then autoclaved for 20 minutes at 120 ºC and 15psi on liquid cycle. To make MS agar for plating, 0.6% (w/v) of Phyto agar (Duchefa Biochemie) was added before autoclaving.

2.2.2 Plant growth conditions

Arabidopsis thaliana plants of ecotype Columbia (*Col-0*) and Nossen (*No-0)* were grown either in soil in a 3:1:1 of compost (Levington$^{(R)}$): vermiculite: sand. Plants were grown with 16 hours light at 22 ºC, with a typical greenhouse conditions or plated onto growth media.

2.2.2.1 Seed surface sterilization

Prior to plating, seeds were surface sterilised with 70 % (v/v) (containing 0.5 % Triton X-100) for 5 minutes followed by 1 minute incubation in 100 % (v/v). Afterward, the seeds left to dry on sterile filter paper in the plant hood. For the primary transformants, ~100 mg of T1 seeds were selected on MS0 media with appropriate selection antibiotics.the associated concentrations are shown in table 1. In the case of BASTA resistance plants on soil, similar amount of seeds were sown with a 30mg/ml BASTA solution. For selection of kanamycin or a hygromycin resistance, seeds were selected on MS0 medium with 35-50 μg/ml kanamycin or 20 μg/ml hygromycin, respectively. Non-transformed seeds were plated on MS0 media without selection.

2.2.3 Concentrations of antibiotics used for selection of transformed plants

Antibiotic name	Working concentration (mg/ml)
Cefotaxime (Melford Lab, UK)	200
Benamyl (Melford Lab, UK)	10
Kanamycin (Melford Lab, UK)	50
Hygromycin (CALBIOCHEM)	20
Glufosinate ammonium [Basta]	30
Gentamicin (Melford Lab, UK)	100

2.2.4 Crossing of plants

When the flowers were closed and the pollen of the anthers was not ripe, the anthers of the acceptor flower were removed completely using fine forceps. The center part of the

inflorescence and remaining older flowers from the same branch were also removed. After two days, the stigma on top of the carpel was pollinated with mature pollen from the donor plant (the cross works best when the papillae cells are nicely erect). Occasionally male sterile *ms1-1* plants were used as female. This plant was pollinated without emasculation.

2.3 Bacterial culture and storage

2.3.1 Media for growth of bacteria

Escherichia coli (*E. coli)* and *Agrobacterium tumefaciens* (*A. tumefaciens*) were grown in Luria Bertani Broth media (LB Broth) consisting of: 10 g/l peptone, 5 g/l yeast extract, 10 g/l NaCl. For bacterial growth on plates, 1.5 % (w/v) bacto-agar was added into the media before autoclaving. The media pH was adjusted to 7.0 with 5N NaOH and autoclaved for 20 minutes at 120 ºC and 15 psi on liquid cycle. When a ready mix media was used (Melford), no pH adjustment was needed.

2.3.2 Bacterial strains

The strains used in this study were DH5α, DB3.1 for *E. coli* and GV3101 for *A. tumefaciens*. The DH5α was used for conventional cloning. DB3.1 strain, which is sensitive to the ccdB gene, which poisons for the DH5α, was used for the Gateway cloning. For plant transformation *A. tumefaciens* contains a binary vector (pSKI15) with the ability to infect plants and incorporate a segment of its helper Ti plasmid, called T-DNA, into the host cell genome.

Escherichia coli (*E. coli*)

- DH5α
- DB3.1

Agrobacterium tumefaciens (*A. tumefaciens*)

- GV3101

Cells were inoculated on plates or in liquid medium with appropriate antibiotics, cultures were placed in an incubator (LEEC Ltd, UK) or constant shaking (SANYO orbital shaker Gallenkamp, UK) at 200 rpm set at 37 ºC for *E. coli* and 28 ºC for *A.*

tumefaciens respectively. Cultures were grown over night until desired optical density was reached.

2.3.3 Concentrations of antibiotics used for bacterial selection

Antibiotic name	Working concentration (mg/ml)	
	E.coli **(DH5α / DB3.1)**	***A.tumefaciens*** **(GV3101)**
Rifampicin (Melford Lab, UK)	n.a	50
Gentamycin (Melford Lab, UK)	n.a	50
Spectinomycin (Melford Lab, UK)	100	100
Kanamycin (Melford Lab, UK)	50	50
Ampicillin (Melford Lab, UK)	30	30
Chloromphenicol (SIGMA)	30	20

2.3.4 Bacterial culture and long term storage

A single colony was used to inoculate 5 ml LB medium. 700 μl aliquot of the overnight bacterial culture was transferred to a cryogenic storage tube and mixed with 300 μl sterile 50% (v/v) glycerol. The cells were flash frozen in liquid nitrogen and stored at -80 ºC. The strains were recovered by streaking a small portion of the frozen culture on agar medium containing appropriate selection and grown as required.

2.3.5 Preparation and transformation of competent *E. coli*

For transformation of *E. coli,* 50 μl aliquot was removed from -80 ºC freezers and thawed on ice for 10 minutes. 1 μl (~125 ng) of plasmid or half of the recombination reaction was added into a 50 μl aliquot and incubated on ice for 30 minutes. The mixture was heat shocked for 40 seconds in a water bath at 42 ºC and then incubated immediately on ice for more 2 minutes. 900 μl of LB medium wsa added and the culture was incubated at 37 ºC for 1 hr with horizontally shaking (200rpm). After that, the bacterial cells were centrifuged at 5,000 rpm for 30 seconds. 100 μl of cells

suspension were plated on LB agar containing appropriate antibiotics. The plates were incubated at 37 ºC overnight to develop colonies.

2.3.6 Preparation and Transformation of *A. tumefaciens*

A single colony of *Agrobacterium* strain GV3101 containing an appropriate helper Ti plasmid (pMP90) was grown overnight in a 5 ml LB medium containing 100µg/ml spectinomycin, 50 mg/ml Rifampicin and 50 mg/ml Gentamycin. 1ml of the overnight culture was subcultured into 50 ml LB medium in a 250 ml flask with the appropriate antibiotics and shaken vigorously (250rpm) at 28 ºC until the culture grew to OD_{600} of 0.5 to 1.0. The culture was chilled on ice and then centrifuged at 3000 g for 5 minutes at 4ºC. Cells were resuspended in 1ml of 20mM ice-cold $CaCl_2$ solution. 0.1 ml aliquots were dispensed into pre-chilled 1.5ml microfuge tubes, flash frozen in liquid nitrogen and stored at -80 ºC.

Transformation of Agrobacterium was carried out using a heat shock variation, 3 μg of plasmid DNA was added directly into the frozen aliquot and incubated at 37 ºC for 5 minutes to heat-shock the cells. 1ml of LB media was added into the mixture, and then the culture was incubated at 28 ºC in 200 rpm shaker for 2 – 4 hrs. Then the cultured cells were centrifuged for 30 seconds at 5Krpm and the supernatant was discarded. Transformed cells were resuspended with the remaining solution and then plated on LB agar plate containing appropriate antibiotics. The plates were incubated for 2-3 days at 28 °C.

2.4 Isolation of nucleic acids

2.4.1 Genomic DNA isolation

2.4.1.1 CTAB-DNA extraction

About 2-3 leaf tissues were collected in a 1.5 ml eppendorf tube containing 200-300 glass beads (Sigma, UK) of size 425-600 micron and were frozen in liquid nitrogen. The leaf tissue was ground for 10 seconds in a silamat amalgam mixer (Ivoclar

Vivadent, UK) at room temperature. 250 µl of DNA extraction buffer (1.4 M NaCl, 3% (w/v) CTAB, 20 mM EDTA, 100 mM Tris-Hcl pH8) was added, vortexed briefly and incubated for 15 minutes at room temperature. An equal volume of chloroform: IAA (24:1) (250 µl) was added and centrifuged for 10 minutes at 13000 rpm. The upper phase (200 µl) was transferred to a fresh eppendorf tube, precipitated with 0.7 volumes (140 µl) of isopropanol, incubated for 5 minutes at room temperature and then centrifuged for 7 minutes at 13000 rpm. The supernatant was discarded and the pellet was washed with 1ml of 70% (v/v) ethanol and centrifuged for 5 minutes at 13000 rpm. Ethanol was poured off and the pellet was vacuum dried for 5 minutes or left at room temperature for 30 minutes to dry. The dried pellet was resuspended in 100 µl of deionized water (DW) and incubated at 55ºC for 5 minutes. The DNA solution was then stored at -20 ºC. 1-2 µl of DNA was used for a PCR reaction.

2.4.1.2 High-throughput isolation of genomic DNA

Isolation of Arabidopsis genomic DNA was carried out following a protocol based on Edwards buffer (Edwards *et al.*, 1991) adapted for high-throughput extraction. This technique involves the crude extraction of DNA from leaf material ground with glass beads. Typically this method is used to extract a large number of tissue samples in a 96 microtiter plate format, using a shaker TissueLyser (Siegen, Germany). Leaf tissue sections of about 0.5 cm^2 were collected into individual 1.2 ml collection microtubes in a 96-tube box resting on ice, with each microtube containing cap. 0.5 cm of 1.5 - 2.5 mm glass beads (BDH, UK). Once all samples were collected, the tissue was flash frozen by placing the tube box in liquid nitrogen. Next, samples were ground by shaking at 30 Hz for 30 seconds using TissueLyser (Siegen, Germany). The previous step was repeated after rotating the rack of tubes so that the tubes nearest to the TissueLyser were now outermost. After disruption, 400 µl of extraction buffer (200 mM Tris 1 M pH 8, 250 mM NaCl 5 M, 25 mM EDTA, 0,5 M SDS 10 %) was added to each microtube using the 300 L multi-channel pipette with 300 L tips, and centrifuged with microplate adaptors at 3000 g for 30 minutes at 4 ºC. Next, 200 µl of supernatant from each sample was transferred into new 1.2 ml collection microtubes in another 96-tube box, and 200 µl of isopropanol was added to each microtube and mixed by inverting 3-4 times. DNA was pelleted by centrifuging with microplate adaptors at 3000 g for 20

minutes at room temperature and the supernatant was discarded. To wash the pellet, 200 µl of 70% ethanol were added and then poured off, leaving the samples to dry in the sterile hood. DNA was resuspended in 60 µl of sterile dH_20, and could then be used immediately or stored at –20ºC.

2.4.2 Isolation of total RNA

Isolation of total RNA was carried out using RNeasy Plant Mini Kit (Qiagen, UK) according to manufacture instructions. Tissue samples were collected and frozen immediately liquid nitrogen and stored at -80 ºC. 50-100 mg of frozen tissues were grounded to a fine powder in liquid nitrogen with 450 μl of buffer RLT containing 10 μl of β-mercaptoethanol. To avoid RNA degradation, the last step should be carried out as quickly and completely as possible. The mixture was left to thaw and ground further to a homogenous lysate. The lysate was transferred onto a QIAshredder spin column and collection tube and centrifuged for 2 minutes at 13000 rpm. The supernatant was then transferred to a new eppendorf tube containing 225 μl of absolute ethanol. The mixture was then transferred to an RNeasy mini column and centrifuged for 15 seconds at 10000 rpm. The flow-through was discarded and 700 μl of buffer RW1 was added to the column and centrifuged for 15 seconds at 10000 rpm. The RNeasy column was transferred to a new collection tube and 500μl of buffer RPE was added. The sample was centrifuged for 15 seconds at 10000 rpm and an additional centrifugation was performed for another 2 minutes at 13000 rpm. The column was centrifuged for another 1 minute to dry off the membrane, and the RNA was eluted with 50 μl RNAse free water into a 1.5 ml eppendorf tube. RNA samples were quantified by spectrophotometer and RNA integrity was verified by gel electrophoresis before storage at -20 ºC.

2.4.3 Quantification of nucleic acids

After the RNA/DNA isolation, 1 μl of the total RNA or genomic DNA was loaded in 1.5% agarose gel to check the quality of the RNA. The concentration of the nucleic acids was determined using absorption of light at 260 (PU-8740 spectrophotometer, Philip), using the following criteria:

Concentration (ng/µl) of RNA = 40 x Abs260 x dilution factor

Concentration (ng/µl) of DNA = 50 x Abs260 x dilution factor

Total amount (ng) = Concentration (ng/µl) x total volume of extraction (µl)

The above criteria are based on the extinction coefficient calculated for RNA in water. RNA samples were diluted 1/50 or 2/100 in RNAse free water and loaded in RNAse free quartz cuvette. A fixed wavelength (260nm) was selected and a blank was set using RNAse free water. The quartz cuvette containing the RNA sample was loaded and placed in the appropriate cell. Then the reading was recorded for each sample. The total concentration of the RNA was calculated with the above criterion using Microsoft excel software. The concentration of the RNA was verified by running fixed amounts of RNA 1.5% agarose gel.

2.4.4 Isolation of plasmid DNA from bacteria cultures

Transformed Plasmid DNA was isolated from *E. coli* and *A. tumefaciens* using QIAprep Spin Miniprep Kit (Qiagen, UK) according to manufacture instructions. Single colonies of transformed bacteria were inoculated in 5ml LB media containing appropriate antibiotics. A 1.5 ml of the overnight culture was transferred into an eppendorf tube and centrifuged for 1 minute at 13000 rpm. The supernatant was discarded and the pelleted cells were resuspended in 250 µl of buffer P1 containing RNase by brief vortexing. Then 250 µl of buffer P2 containing blue lysate dye was added to lyse the cells and the tube was gently inverted to achieve a homogenous blue mixture. Immediately, 350 µl of buffer N3 was added and the suspension was mixed gently to precipitate cell debris and the associated bacterial chromosomal DNA. Lysed bacterial cells were centrifuged for 10 minutes at 13000 rpm and the clear upper phase was transferred into a new QIAprep spin column and centrifuged for 1 minute at 13000 rpm. 500 µl of buffer PB was added to the column and centrifuged for 1 minute at 13000 rpm. The column was washed with 750 µl of buffer PE containing 70% (v/v) ethanol and centrifuge for 1 minute at 13000 rpm. The supernatant was discarded and the column was centrifuged for an additional minute at 13000 rpm. The column was then transferred into a clean 1.5 ml eppendorf tube and 50 µl of buffer EB was added to the middle of the column. The column was

left for 1 minute before being centrifuged at 13000 rpm for 1 minute to elute the plasmid DNA.

2.5 DNA synthesis by polymerase chain reaction (PCR)

2.5.1 Primer design

Different oligonucleotide primer pairs were designed to amplify genomic DNA, cDNA, cloned products and vector sequences (Appendix: Table A1). Primers were designed either manually or using software Primer3 (Rozen and Skaletsky, 2000). Any problems arising with annealing temperatures, such as low yield or incorrect fragment size, were tackled by using a temperature gradient to select the optimal temperature for that specific reaction.

For genomic and cDNA sequence amplification, primers were designed with length ranged between 20 – 25bp and melting temperature (Tm) between 60 – 65 ºC. When possible, a GC clamp was also included at the 3'-OH end, amplifying product with sizes between 250 – 1200 bp for cDNA and genomic DNA sequences. For gateway recombination, primers were designed to create complementary binding sites for att sites for use in MultiSite Gateway® recombination reactions and included 1 or 2 additional nucleotides to keep the sequence in frame. The GC clamp was not always included in these primer sets. The PCR product sizes varied between 600 – 1800 bp with an optimum melting temperature of 60 ºC.

All primers were supplied from Sigma-Aldrich and resuspended in an appropriate volume of Tris buffer or water (10mM Tris-Cl, pH 8.0) to achieve a stock concentration of 100µM. A 5µM working solution of primers was prepared for use in PCR reactions. All primers were stored at -20 ºC.

2.5.2 PCR reactions

PCR reagents including Taq-polymerase, 10xNH_4 buffer and $MgCl_2$ were supplied from Bioline. dNTPs were obtained from either Bioline or Invitrogen, UK. For amplification

of cloning products, proof reading enzymes, Phusion (Finnzymes) DNA polymerases were used instead.

A 20μl PCR reaction using Taq-polymerase was set up as follow;

	Volume	Final conc.
dH2O	13 μl	
2 mM dNTPs	2.0 μl	0.2 mM
10xNH_4 Buffer	2.0 μl	x 1
50 mM $MgCl_2$	0.8 μl	2 mM
20 μM primers forward	0.5 μl	0.5 μM
20 μM primers reverse 0.5 μl	0.5 μM	
DNA template (genomic DNA)	1.0 μl	
Taq polymerase 5U/μL	0.2 μl	1 U

2.5.3 Colony PCR

To test the positive colonies, a small portion of a single colony was picked with a sterile tip and inoculated into a 25 μl PCR reaction. Standard PCR amplification was performed as described in section 2.5.2.

2.5.4 High fidelity PCR for cloning

For Gateway® recombination cloning, PCR products were amplified using Phusion® High-Fidelity Polymerase (Finnzymes). Phusion DNA Polymerases generate PCR products with high efficiency and accuracy of amplification. A first reaction (PCR1) is carried out to generate the required product and a second reaction (PCR2) is carried out with relevant attB adapter primers using the product amplified in PCR1 in order to extend the attB sites prior to Gateway® recombination. The buffers that were used to make master mixes were supplied with the Phusion enzyme. dNTPs were supplied by either Bioline or Invitrogen. The DNA template was diluted 1:100 for plasmid DNA and genomic DNA samples in PCR 1 reactions.

PCR 1: **A 25µl Phusion PCR reaction for PCR1**

PCR1	Volume	Final conc.
dH2O	14.2 µl	
5x HF Buffer	5.0 µl	x1
10mM dNTPs	0.5 µl	0.2 mM
5mM $MgCL_2$	1 µl	0.2 mM
5pmol/µl forward primer	1.5 µl	0.3 µM
5pmol/µl reverse primer	1.5 µl	0.3 µM
Template DNA	1 µl	
DNA	1 µl	
Phusion (2.0U/µL)	0.3 µl	0.6 U

PCR 2: **A 50µl Phusion PCR reaction for PCR2**

	Volume	Final conc.
dH2O	15.4 µl	
5x HF Buffer	10.0 µl	x1
10mM dNTPs	1.0 µl	0.2 mM
$MgCL_2$	2.0 µl	0.2 mM
5pmol/µl F - attB adapter	8.0 µl	0.8 µM
5pmol/µl R - attB adapter	8.0 µl	0.8 µM
Product of PCR1	5 µl	
Phusion (2.0 U/µL)	0.6 µl	0.6 U

2.5.5 DNA amplification

The PCR conditions used varied according to amplify desired fragments, melting temperature of the primers and the type of product. Double stranded DNA was denatured either at 96 ºC(with BioTaq) or 98 ºC (with Phusion). The annealing temperature was normally set up 5 ºC below the melting temperature and were necessary an optimum annealing temperature was determined using gradient PCR. Extension time was set up at 72 ºC for 30 seconds per 1kb of product with BioTaq and 15 seconds per 1kb of product with Phusion. Numbers of cycles were adjusted for

cloning products and diagnostic PCR products.

The amplification steps were carried out on a thermal cycler and the DNA was amplified over 39 cycles. The PCR product was analysed by agarose gel electrophoresis.

2.6 Reverse Transcription PCR (RT-PCR)

The total RNA was isolated from different plant tissues i.e leaves, flowers and mature pollen. The RNA isolated samples were first DNase treated with Amplification Grade DNase I (Sigma-Aldrich) according to manufacturer's procedure. The samples were incubated at room temperature for 15 minutes. After that the same amount of stop solution was added and the whole mixture incubated at 70 ºC for 10 minutes to inactivate the DNase. Samples were incubated in ice in preparation for cDNA syntheis. First strand cDNA was synthesised with a standard amount of total RNA primed with oligo dT primers (Invitrogen, UK). 750 ng to 1μg of total RNA was used for cDNA synthesis. A 1:10 dilution of first strand cDNA was used as a template in general BioTaq PCR reactions using gene-specific primers (Appendix: Table A1) to determine transcript abundance for the gene of interest by PCR reaction.

The following was then added to each tube:

M-MLV 5x Reaction Buffer 5.0µl
10mM dNTPs 1.25µl
M-MLV RT 200U
Nuclease-free water to 25.0µl

The tubes were then mixed gently and incubated at 42 ºC for 1 hour in a thermocycler. The cDNA was stored at -20 ºC or used directly for PCR analysis. The PCR reaction mixture was prepared in a 0.2 ml microfuge tube that was kept on ice, mixed and spun briefly. The expression of the target template was detected by analysing the RT-PCR product using agarose gel electrophoresis.

2.7 DNA modification and agarose gel electrophoresis

2.7.1 Digestion of DNA with restriction endonucleases

Restriction digest of PCR products and plasmid DNA was carried out with varying enzymes according to requirements. Digests were performed in an appropriate buffer in a total volume of 20 µl and incubated at appropriate temperature recommended by manufacturers instructions for 1 hour. In case more than one restriction enzyme was used, an appropriate buffer was selected that gave optimal activity for both enzymes. The digest reaction was done with 1 μg of DNA as follow:

Restriction digest reaction

DNA	1 μg
Buffer	2 μl
10 x BSA (1mg/ml)	0.2 μl
Restriction enzyme (10 U/μl)	0.5 μl
Water (DW)	up to 20 μl

All the reagents used for the DNA digest were purchased from Bioline, UK.

2.7.2 Separation of DNA by agarose gel electrophoresis

Identification and purification of different DNA fragments of different sizes from PCR products, restriction digest and purified plasmids were performed by agarose gel electrophoresis. Similar technique was also used for the visualization of extracted total RNA. Agarose gel was made up with 1x Tris-acetate buffer (TAE) supplemented with 0.5 μg/ml ethidium bromide. According to the size of the DNA fragments, the concentration of agarose gels varied between 1 % (w/v) to 4 % (w/v). Based on a method from Sambrook *et al*., 1989. Samples were mixed with 1x gel loading dye {(10x Gel loading buffer: Orange G 0.5 % (w/v), glycerol 50 % (v/v)} then were loaded into gel wells. The loaded gel was placed in the electrophoresis tank and a voltage of 10 V/cm was applied to separate the fragments for approximately 30 minutes. The DNA / RNA fragments were visualized under UVP transilluminator (BioDoc – It^{TM} System, U.S.A) and the size and quantity of the DNA fragments were determined by comparing with a standard DNA ladder (New England Biolabs).

50 X TAE stock:

242 g Tris-base

57.1 ml Glacial acetic acid

100 ml of 0.5 M EDTA (pH 8.0)

Made up to 1L volume of water

To make a working solution of 1x TAE, 20 % (v/v) of the 50x TAE stock was used to make 10x TAE. 10 % (v/v) of 10x TAE was then used to make a final working solution of 1x TAE.

2.8 Purification of DNA for cloning and sequencing

DNA fragments required for sequencing or cloning were purified from agarose gel using QIAquick gel extraction kits (Qiagen, UK) according to manufacturer instructions. The DNA fragment was excised from the agarose gel with a clean scalpel blade. The gel slice was weighed and three gel volumes (100 mg = 100 μl) of buffer QG were added. The sample was then incubated at 55 ºC for 10 minutes with occasional vortexing every 2 minutes to dissolve the gel. Once the agarose was completely dissolved, one gel volume of isopropanol was added to the mixture. The mixed sample was then pipetted into QIAquick column and centrifuged for 1 minute at 13000 rpm to bind the DNA. The flow-through was discarded and 500 μl aliquot of buffer QG was added to the samples to remove all traces of agarose. The column was centrifuged for 1 minute at 13000 rpm and the flow-through was discarded. To wash the column, 750 μl of buffer PE was added to QIAquick column and centrifuged for another minute at 13,000 rpm. After discarding the flow through, the QIAquick column was centrifuged for an additional minute at 13,000rpm to remove any traces of remaining ethanol. 30µl of elution buffer added to the centre of the column and allowed to stand for 1 minute. The DNA was eluted by centrifugation at 13000 rpm for 1 minute. Eluted DNA was used directly for cloning reactions or stored at -20 ºC.

2.9 Cloning by Gateway® recombination

The Gateway® technology is based on the bacteriophage lambda (λ) site-specific recombination system that facilitates the integration into *E. coli* chromosome. The principle of this recombination system based on the recombination courses between site

specific attachment(*att*) sites *att*B on the E. coli chromosome and *att*P on the lambda chromosome to give rise to *att*L and *att*R (Landy, 1989). Further description of gateway cloning procedure is available on the Invitrogen website: http:// tools. invetrogen.com/content/sfs/manuals/gatewayman.pdf

For high throughput DNA cloning, a gateway recombination technology (Invitrogen, UK) was used instead of a traditional conventional cloning. DNA fragments were first amplified by PCR using primer pairs that incorporate the recombination sites (attB1 and attB2) at the 5' and 3' -OH end of the DNA fragment. Depending on the specificity of the primers, the PCR product was then purified either by QIAquick gel extraction kit or QIAquick PCR purification kit. The concentration of purified product together with the vector was determined by agarose gel electrophoresis using a standard DNA ladder. The PCR product was cloned into the expression vector in two subsequent steps.

2.9.1 Multisite Gateway® Cloning

Multisite Gateway® recombination cloning (Invitrogen, UK) was used to clone the gene(s). DNA fragments were first amplified by PCR using primer pairs with flanking *att* recombination sites (attB1, attB2, attB3 and attB4) at the 5' and 3' ends to amplify the DNA fragment. Then, the PCR product was purified by gel extraction. The fragment of interest was inserted into stable vectors for expression and functional analysis, using two cloning steps;

Step 1: BP reaction

In the first Gateway® recombination reaction, 125 ng of purified gel product was recombined into 75 ng of donor vector to generate entry clones. Following overnight incubation at room temperature. The reaction was terminated with 0.5 μl of proteinase K enzyme by incubating at 37 ºC for 5 minutes to denature the clonase enzymes. 2.5 μl of the total reaction was used for transformation of *E. coli* (DH5α). The transformed cells were grown in 950 µl LB medium for one hour, then plated onto agar plates with spectomycin (100 ug/ml), and incubated at 37 ºC for approximately 16 hours. The colonies were screened by colony PCR using pDONRF/R M13 primer set to identify the presence of the correct plasmid. Positives colonies were used to setup 5 ml overnight

culture and the plasmid was isolated from the bacteria and verified by restriction digest and sequencing before being used for the second step cloning.

BP-reaction (Invitrogen kit)

PCR product	~125 ng
pDONOR vector	~75 ng
TE buffer	X µl
BP Clonase II	1 µl
Total 5.0 µl	

Step 2: LR recombination reaction

Confirmed entry clones were used to recombine the insert into the destination vector in a LR reaction. Approximately 125 ng of the entry clone and 75 ng of the desired destination vector was used in a second ligation reaction catalyzed by the enzyme LR clonase (Invitrogen). The reaction was incubated overnight at room temperature and then terminated with 0.5µl of proteinase K enzyme by incubating at 37 ºC for 10 minutes. 2.5 µl of the total reaction was used to transform E. coli (DH5α) and the colonies were screened by PCR. Positively screened colonies were inoculated in 5ml of LB overnight culture was setup and recombinant plasmid was isolated and used for restriction analysis and sequencing when appropriate. Verified expression vectors were then mobilized into *A. tumefaciens* (GV3101) for transformation of Arabidopsis plants.

LR-reaction (Invitrogen kit)

Destination vector	75 ng
pDONR entry clone	125 ng
LR Clonase II Plus	1.0 µl
TE buffer	up to 5.0µl

Three-site LR reaction

Destination vector	10fmol
pDONR221 entry clone	5fmol
pDONRP4-P1R entry clone	5fmol
pDONRP2R-P3 entry clone	5fmol
LR Clonase II Plus	1.0µl
dH2O	up to 5.0µl

The formula to calculate the ng of plasmid DNA needed to achieve the desired f mols is as follows: ng needed = desired f mol x size of vector (bp) x (660×10^{-6})

2.9.2 Sequencing of PCR product

Purified PCR product and isolated recombinant plasmid were sent to John Innes Centre lab (The Genome Analysis Centre, Norwich, UK) for sequence confirmation. 50ng of PCR product or 150 ng of plasmid DNA in a total of 20 μl was sent for sequencing, According to the submission requirements. Sequencing primers at a 1.5pmol/µl concentration were sent along with plasmid DNA. In the case of entry clones, M13 primers were used to sequence recombined inserts. Depending on the length of sequencing required (maximum of 500bp per reaction), more than one set of primers were sent to provide full coverage of sequenced regions in the event more than 500bp was analysed. Sequencing result in ABI format were downloaded from the JIC website (http://jicgenomelab.co.uk/account.html) and analysed with the *MacVector version 9.5.2* sequence analysis program (MacVector, U.S.A). Sequence pattern was confirmed by analysing alongside chromatogram files and the expected wild type sequence.

2.10 Transformation of *Arabidopsis*

Arabidopsis plants were transformed by floral dipping method in accordance to Clough and Bent (1998) with some modifications. A single transformed *Agrobacterium* colony was selected and inoculated in 5 ml of LB containing appropriate antibiotic, the cells were allowed to grow overnight at 28ºC. A 1ml aliquot of the overnight culture was subcultured into 400 ml of fresh LB media and the cells were grown for another 24 hrs in a shaker at 200 rpm at 28ºC. The cells were centrifuged at 6400 rpm for 20 minutes and the cells were resuspended in standard infiltration medium.

Infiltration medium

Half strength of MS salts (Sigma, UK)	2.165 g/L
Full strength of Gamborg B5 vitamins (Duchefa, Netherlands)	3.16 g/L
2-[N-Morpholino]ethanesulfonic acid (MES) (Sigma, UK)	0.5 g/L
Sucrose (Sigma, UK)	50 g/L
Benzylaminopurine (1mg/ml)(Sigma, UK)	10 μL/L

Immediately prior to dipping, 200ul/L Silwet L-77 was added to the *Agrobacteria* and infiltration medium mix. The *Arabidopsis* buds were submerged into the mix for 42 seconds with gentle shaking. Five plants were transformed for each construct. A plastic dome was used to cover the dipped plants for 24 hours to expose the plants to high humidity. Plants were watered after two days. After all siliques were formed, watering was stopped and the plants were kept in a drying room for 2 weeks. The dry seed was harvested and cleaned by passing through a 425 μm sieve several times to remove most of debris and selected on plates and/or soil containing appropriate selection to identify primary transformants.

2.11 Cytological analysis

2.11.1 Visualization of spores nuclei with 4',6-diamidino-2 phenylindole (DAPI)

Pollen nuclear morphology was visualized by staining with 4',6-diamidino-2 phenylindole (DAPI) as described by Park *et al*. (1998). 4-5 fully open flowers were collected in an appendorf tube containing 300 μl of 10 μg/ml DAPI staining solution (0.1 M sodium phosphate, pH 7; 1 mM EDTA, 0.1% (v/v) Triton X-100, 0.4 mg/ml DAPI; high grade, Sigma). Pollen grains were released into the DAPI solution by brief vortexing and centrifuged for 5 seconds in a picofuge (Stratagene, UK). 4 μl of the pollen pellet was transferred to a microscope slide, gently pressed down with a cover slip, sealed with nail varnish to prevent sample from drying, and viewed under fluorescence microscope (Nikon TE2000-E, Japan). For general screening, mature pollen from 1 – 2 single open flowers were collected into a 96–well microtiter plate containing 100 μl of DAPI solution. Pollen grains were released from the flowers by

gently tapping the microtiter plate and pollen nuclei were visualised under an inverted epifluorescence microscope (Zeiss Axiophot 100).

For analysis of spores at earlier developmental stages, buds were separated and sequentially arranged based on their position on the floral axis with +1 representing a first fully open flower and approximately -12 stage representing early released microspores (Lalanne and Twell, 2002). Flowers buds were dissected on microscope slide into 5 µl of DAPI solution using a dissecting microscope (Zeiss). Anthers were firmly pressed with fine forceps and dissecting needle to release the spores, coverslip was mounted and gently squashed to flatten the samples, sealed with nail varnish and visualised under fluorescence microscope.

DAPI staining solution

DAPI (10µg/ml)	8 µl
GUS buffer (0.1 M $NaPo_4$ pH 7.0, 0.5 M EDTA, 10% (v/v) Triton)	10 ml

2.11.2 Fluorescein diacetate (FDA) staining for pollen viability

Pollen grain viability was determined cytologically by visualising cellular esterase activity with 0.1mg/ml fluorescein diacetate (FDA) in 0.3M mannitol (Eady *et al.*, 1995). 1-2 open flowers were agitated into 96-well microtiter plate containing 100 µl of freshly made FDA stain. After 5 minutes of incubation at room temperature, the pollen was examined with FITC filter set on Zeiss Axiovert 100 at low power (x10/x20 objectives) to prevent photobleaching.

FDA stain

0.3 M Mannitol	990 µl
10 mg/ml FDA (in acetone)	10 µl

2.11.3 In vitro pollen germination assays

For pollen in vitro germination assay, mature pollen at the stage of anther dehiscence was transferred to slides or in the wells of a 24 well plates with germination medium (1mM CaCl2, 0.01% Boric Acid, 18% Agarose, 1mM Ca $(NO_3)_2$, 1mM $MgSo_4$ and 10 % Sucrose in distilled water, pH adjusted to 7). Germination occurred in a moist chamber at 25 °C in constant light overnight. Samples were stained with a mixture of DAPI and GUS buffer for 1 hour and viewed under a fluorescence microscope using an UV-filter.

2.11.4 Whole-mount preparation of seeds

Siliques of different developmental stages were dissected on a slide using fine forceps to split the silique longitudinally along lines of natural dehiscence under a Zeiss STEMI SV8 dissecting microscope and embryos cleared in a drop of clearing solution (240 g chloral hydrate, 30 g glycerol, 90 ml water). The specimens were cleared 1 hour before inspection at room temperature. Light microscopy was performed with a Zeiss Axiophot microscope using Differential Interference Contrast (DIC) optics.

2.11.5 GUS staining

Transgenic plants carrying construct harbouring a GUS marker were analysed by histochemical assay according to Sessions and Yanofsky (Sessions and Yanofsky, 1999). Analysed Tissues were collected in 24 well plates containing 200 μl of GUS buffer (0.1 M sodium phosphate (pH 7), 10 mM EDTA, 0.1% (v/v) Triton X-100) with 0.5 mM / 1 mM potassium ferricyanide and 2 mM 5-bromo-4-chloro-3-indolyl β-D-glucuronic acid (X-gluc; Biosynth). Materials were then vacuum infiltrated for 30 minutes and sealed with nescofilm. To visualise GUS staining, plant tissues were incubated in variable length of time (depending on the promoter activity) at 37 ºC, Clearing was performed in 70 % ethanol at 4 °C over night.

2.11.6 Microscopy and Image Processing

All images were captured using different cameras and objectives depending on the microscope used and type of image to be captured. When using the Nikon ECLIPSE TE2000-E (Nikon, Japan) inverted fluorescence microscope, a mercury lamp was used as an excitation source together with a Plan Fluor 40x/1.3 NA oil immersion objective or a Plan Fluor 60x/1.25 NA oil immersion objective. DIC images were captured with a Micropublisher 3.3 RTV colour CCD camera (QImaging, Canada) and fluorescence images were captured with an ORCA-ER cooled CCD camera (C4742-95-12ERG, Hamamatsu Photonics, Japan). Images were previewed, captured and saved using Openlab 5.0.2 software (Improvision, UK) in TIFF format.

When using the Nikon ECLIPSE 80i (Nikon, Japan), an LED-based excitation source (CoolLED, presicExcite) was used together with a Plan Fluor 40x/1.3 NA oil immersion obejctive or a Plan Apo VC 60x/1.4 oil immersion objective. Fluorescence images were captured with a DS-QiMc cooled CCD camera (Nikon, Japan). Images were previewed, captured and saved using NIS-Elements Basic Research v3.0 software (Nikon, Japan) in JPEG2000 format. For confocal laser scanning microscopy (CLSM), the Nikon ECLIPSE TE2000-E (Nikon, Japan) microscope was employed using the C1 confocal module (Nikon, Japan). A Melles Griot Argon Ion (excitation 488 nm) and Melles Griot Helium- Neon (excitation 543 nm) were used as laser excitation sources. CLSM was operated using the EZ-C1 control unit and associated imaging software. Images of dissected siliques were captured using a 3-CCD colour video camera (JVC, KY-F55B) mounted on a dissecting microscope (Zeiss STEMI SV8). The video camera was linked to a Neotech IGPCI capture card and images previewed, captured and saved using Image Grabber PCI 1.1 software on running on Mac OS 9. All subsequent image processing was undertaken using Adobe Photoshop CS version 8.0.

2.11.7 Fluorescence DNA content measurement and quantification of cell fates

Mature pollen at the stage of anther dehiscence was stained with a DAPI solution. Relative DNA content of mutant germ cell nuclei was measured based on the resulting fluorescence of the DAPI stained nuclei. In a similar way, the mean signal intensity of

fluorescent fusion nuclear proteins was based on the fluorescence of sperm cell nuclei. images were captured with an ORCA-ER cooled CCD camera (C4742-95-12ERG, Hamamatsu Photonics, Japan). The exposure time was determined empirically in order to avoid image saturation and kept constant during image capture of all mutants or trangenic lines analysed. Openlab 5.0.2 software (Nikon, Japan) was used to process the captured images in order to determine the total pixel intensity (TPI) of manually defined regions of interest (ROI) encompassing germ cell and/or sperm cell nuclei. The ROI was defined using the auto-detect feature within the measurements panel. This ROI was then duplicated and used to measure the TPI of the cytoplasmic background within the same pollen grain. The true fluorescence of the germ cell and/or sperm cell nucleus was obtained by subtracting the cytoplasmic background TPI from the nuclear TPI. Each batch of images corresponding to a germ cell division mutant or a certain transgenic line was processed and the mean TPI calculated. The values obtained were normalized against prophase nuclei, which were used to determine C-value of other germ cell division mutants since its TPI is defined as 2 C.

2.12 Statistical analysis

To determine whether the average fluorescence value of sperm nuclei and the germ nuclei and the average fluorescence value from the mutant germ nuclei were statistically significant from each other, one-tailed *t-test* (Microsoft Excel software) was used assuming unequal variance was applied.

Using Microsoft Excel, the Chi-square (χ^2) test was used to compare observed frequencies to expected frequencies if null hypothesis (H_0) is true. The closer the observed frequencies are to the expected frequencies, the more likely the H_0 is true.

Calculation of the chi square statistics is done according to:

$chi-squared = \sum_{All} \frac{(f_o - f_e)^2}{f_e}$ with (r - 1)(c - 1) degrees of freedom where f_e and f_o are

The observed and expected frequencies respectively. r is the number of rows and c the number of columns. Statistically significant outcomes were determined using an α level of 0.05. If P is smaller than 0.05, Ho should be rejected, which means that the observed differences between the expected and observed ratios is significant. If P is larger than 0.05, it is more than 95% probability for the observed difference being random,

meaning that the observed ratio is not significantly different from the expected ratio.

2.13 Ultrastructural analysis

Plants were grown as described in section 2.2.2 and -1 buds were collected in Eppendorf tubes containing 1 ml fixative solution. Buds were placed in 2.5% glutaraldehyde, 2% paraformadehyde in 0.1M HEPES buffer (Ph7.2) at lab vacuum for 1 hour, followed by 4 hours on mixer, followed by 21 hours at 4ºC. The tissues were washed with 0.05M HEPES buffer 3 x 1 hour. Following post-fixation with OsO_4 the tissues were washed with DW three times for 10 minutes each wash. The buds were carefully transferred in graded series of 1 ml ethanol solutions and Propylene oxide as described below:

1. 30% Ethanol - 30 minutes
2. 50% Ethanol - 30 minutes
3. 70% Ethanol - 30 minutes
4. 70% ethanol overnight at 4ºC
5. 90% Ethanol - 30 minutes
6. 100% Absolute ethanol - 30 minutes (x2)
7. Propylene Oxide - 10 minutes (x2)
8. 3 Propylene oxide : 1 Agar low viscosity resin – 90 minutes
9. 1 Propylene oxide : 1 Agar low viscosity resin – 90 minutes
10. 1 Propylene oxide : 3 Agar low viscosity resin – 90 minutes

Embedded samples were sectioned transversely through using a Reichert Ultracut S ultramicrotome.Thin sections of approximately 80nm thickness were cut from each sample and collected onto copper mesh grids. The sections were counterstained with 2% Aqueous Uranyl acetate for 20 minutes, followed by 4 minutes in Reynold's Lead citrate.Samples were viewed on the JEOL 1220 TEM with an accelerating voltage of 80kV. Images were captured using Mageview III digital camera with Analysis software.

Chapter Three

Characterization of the *duo4* mutant

Characterization of the *duo4* mutant

Introduction

Morphological screening of an EMS-mutagenised population has led to the identification of several *duo* pollen mutants (Durbarry *et al*., 2005). *duo4* mutant was selected for comprehensive phenotypic analysis since it shows a discrete phenotype, in which the germ nucleus is frequently elongated. In heterozygous plants about 50 % of *duo4* pollen failed to undergo germ cell mitosis, resulting in bicellular pollen at anthesis, indicating that *duo4* is a fully penetrant mutation. Moreover, genetic analysis shows that *duo4* is a male specific gametophytic mutation (Section 4.1).

In this chapter the cytological and developmental analysis of *duo4* is described. Analysis of the nuclear morphology of the *duo4* mutant pollen grains was carried out using epifluorescence microscopy and ultrastructure was studied using transmission electron microscopy. In addition, vegetative and germ cell fate markers were assessed and viability tests were performed. The developmental analysis data reveals that *duo4* germ cells were arrested at late G2 transition in the cell cycle. This conclusion was supported by measuring the DNA content of *duo4* mutant germ nuclei in mature pollen compared with the wild type prophase and other *duo* mutant germ nuclei. In addition, analysis of the expression of the *CYCB1;1* marker in *duo4* mutant compared to wild type was used to determine in detail at which stage of the cell cycle *duo4* germ cells were arrested. Moreover, germ cell morphogenesis and double fertilisation were compared in + /*duo4* and wild type.

3.1 Phenotypic analysis of *duo4*

3.1.1 *duo4 pollen* mutant contains a single germ-like nucleus and a vegetative nucleus

Mature *duo4* pollen was examined by light and epifluorescence microscopy to determine

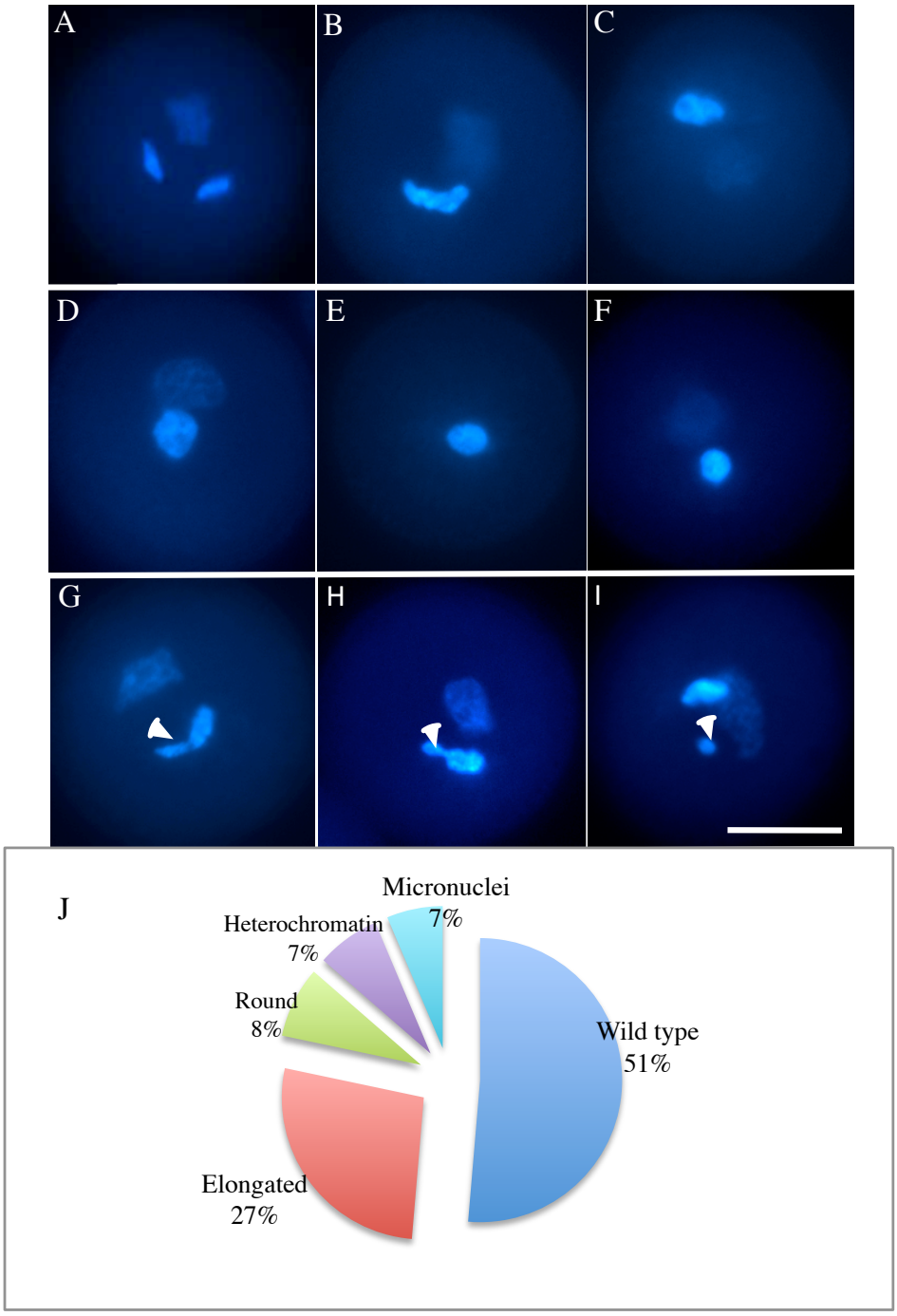

Figure 3.1: Nuclear morphology of wild type and *duo4* pollen. Mature pollen shed from wild type and *duo4* plants was stained with DAPI and screened using fluorescence microscopy. A) Wild type pollen grain with a diffusely stained vegetative nucleus and strongly stained twin sperm cell nuclei. B-C) Elongated *duo4* germ nucleus with perinuclear irregular chromatin condensation. D-F) Round *duo4* germ nuclei. G) Two nuclei that have failed to separate (arrowhead). H) Germ cell nucleus with chromatin projection (arrowhead). I) Pollen showing micronucleus (arrowhead). J) The frequency of pollen phenotypic classes in +/ *duo4* pollen at anthesis. Counts were made from five + /*duo4* individual lines. Data is derived from ~ 816 pollen grains counted from several backcrossed individual lines. Scale bars =15 μm.

pollen morphology and phenotype. In heterozygous plants about 50 % of the population exhibits a mutant phenotype at mature stage, indicating that *duo4* acts gametophytically and is fully penetrant (Section 4.1). Mature pollen carrying *duo4* appeared similar in size and appearance to wild type pollen (Figure 3.1 A), but contained only two nuclei. Mutant pollen possessed one large nucleus with diffuse DAPI staining, typical of the vegetative nucleus, and a small nucleus with highly condensed chromatin similar to the germ nucleus. A number of independent plants were checked to observe the nuclear morphology and frequency of aberrant pollen in the *duo4*. At the binucleate pollen stage, the germ nucleus was frequently elongated compared to wild type (n=816) (Figure 3.1 B-C, J). Detailed examination of mutant pollen phenotype in + /*duo4* shows that the most frequent aberrant phenotypic class scored was elongated germ nuclei with asynchronous chromatin condensation at 27 % (Figure 3.1 B-C, J). Different sizes of roundish germ nuclei were observed at 15 % (Figure 3.1 D-F, J). Another class of abnormal pollen contained germ cell micronuclei and nuclei with chromatin bridges, representing 7 % of the pollen population (Figure 3.1 G-I, J). The percentage of tricellular pollen at anthesis in heterozygous *duo4* pollen population was 51 %.

3.1.2 Ultrastructure analysis shows that *duo4* pollen grains are bicellular

To clarify whether *duo4* pollen grains are binucleate or bicellular, ultrastructural analysis by transmission electron microscopy was carried out on mature undehisced stage (-1 bud stage, which is the next unopened bud from the open flower) from *duo4* plants and compared with wild type. At mature undehisced stage, germ cell division was completed to form the two sperm cells in wild type. Elongated profiles with irregular membrane protrusions defined the sperm cells in the wild type at this stage (Figure 3.2).

In heterozygous *duo4* plants approximately 50 % of the pollen population exhibited mutant phenotypes and the remainder of the population appeared as wild type. In the ultrathin sections (n=53) it was difficult to distinguish between sperm cells and the mutant germ cells as the sperm cells were not always in paired arrangement in wild type (Figure 3.2 A-B). In addition, sections passed through either both or a single sperm cell and some sections did not contain any male gametic cells. Therefore, to distinguish between the sperm cells and the mutant germ cells, all sections that passed through the

Figure 3.2: Transmission electron micrograph of wild type and *duo4* pollen at mature undehisced stage. A) Mature wild type pollen showing a vegetative nucleus (VN) and two sperm cells. B) Two sperm cells in wild type, showing cell membrane (white arrowheads) and single tail-like extension (black arrowhead). C) Mature *duo4* pollen showing undivided germ cell (GN) and single tail-like extension. D) *duo4* germ cell (GC) and germ nucleus (GN), arrowhead indicates the nuclear membrane. E) Elongated *duo4* mutant germ cell with a small nucleate compartment. F) *duo4* germ cell contains a macronucleus and micronucleus, indicating nuclear division without cytokinesis. Note the double tail-like extensions at both ends of the germ cell (black arrowheads). G) A graph showing the distributions of the longest dimension of the nuclei from wild type and *duo4* heterozygous pollen populations. The measurements were obtained from 30 and 50 sections from wild type and *duo4* heterozygous plants, respectively. VN; vegetative nucleus, SC; sperm cell, GC; germ cell, GN; germ nucleus and MN; micronucleus. Scale bar is 5 μm.

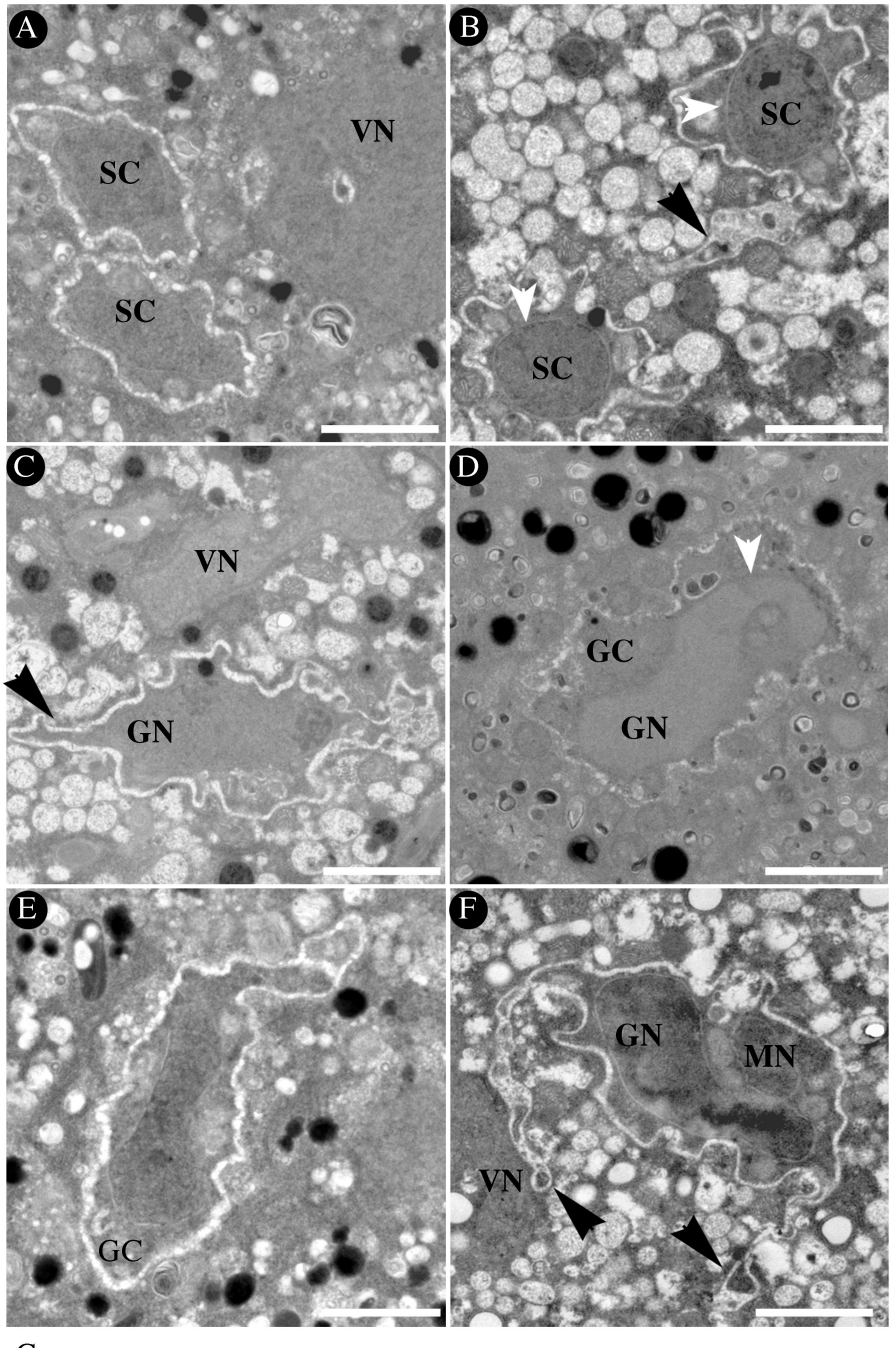
A
VN
SC
SC
B
SC
SC
C
VN
GN
D
GC
GN
E
GC
F
GN
MN
VN

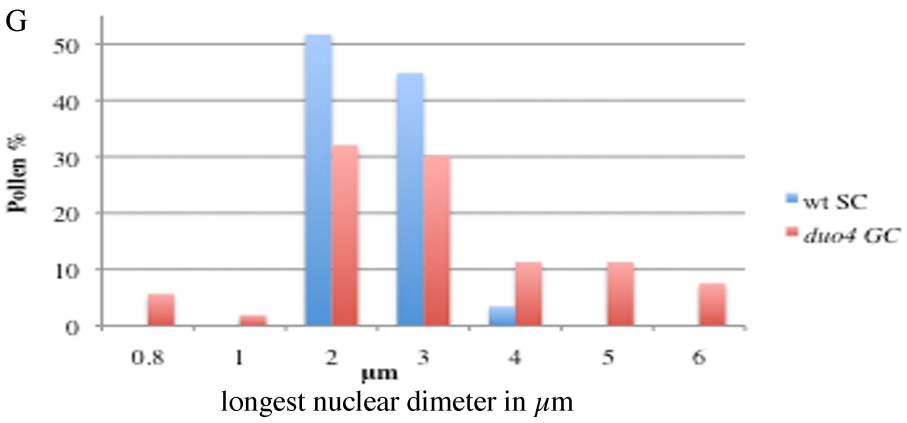
G
Pollen %
50
40
30
20
10
0
0.8
1
2
3
4
5
6
µm
wt SC
duo4 GC
longest nuclear dimeter in µm

nuclei were used to measure the wild type and + /*duo4* cells and that provided a rough estimate of their sizes. These measurements were then used to differentiate between the sperm cells and the germ cells in the sections that the nuclei were not visible.

In the *duo4* mutant two intact membranes surrounded mutant germ cells, confirming that mutant pollen grains are bicellular. Individual nuclei in mutant germ cells were surrounded by an intact nuclear envelope. In all *duo4* mutant ultrastructure sections the vegetative cytoplasm contains many small vacuoles and clusters of starch granules suggesting that maturation of the vegetative cytoplasm occurs as in the wild type (Figure 3.2 C-D).

Another phenotype that was frequently associated with the *duo4* mutant was the formation of micronuclei (7 % of the pollen population). This phenotype is likely corresponds to the presence of binucleated, different in sizes, with or without cell wall was observed (Figure 3.2 E-F). This observation is in agreement with the micronuclei phenotypes observed with DAPI staining. This phenotype further suggests that nuclear division has taken place but cytokinesis failed. The diameters of the nuclei from all the male gametic cells were measured. Compared to the wild type sperm cells, mutant germ cells could be identified based on their larger diameter (4-6 μm) and their distinct regular outline (Figure 3.2 G).

3.1.3 *duo4* pollen is viable

In order to determine *duo4* pollen viability, mature pollen grains from +/*duo4* and wild type plants were stained with the vital stain, fluorescein diacetate (FDA).

FDA is permeable to cell membrane in its native state, and after entry into a living cell the acetate moieties are cleaved by cytoplasmic esterases, producing fluorescein, which is membrane impermeable and brightly fluorescent under blue light. Fluorescein diffuses out of the cells lacking membrane integrity. Hence, viable cells show bright green fluorescence, whereas dead cells are non-fluorescent (Jones and Senft, 1985). Vital staining for plasma membrane integrity showed that the number of fluorescing and thus living pollen grains did not differ between pollen from *duo4* mutants (93%, n=569) and from wild type plants (94%, n=1736)(Table 3.1).

Table 3.1: Percentage of viable pollen in wild type and *duo4*. Pollen viability was tested using the vital stain, fluorescein diacetate (FDA). Viable pollen shows bright green fluorescence whereas non-viable is non-fluorescent under UV fluorescence.

WT	**Viable pollen**	**Non-viable pollen**	**% Viability**	**Totals**
A4	140	13	92	153
B2	106	5	95	111
A1	139	11	93	150
C5	150	5	97	155
Total	535	34	94	569
duo4				
B1	122	7	95	129
C1	169	20	90	189
A3	230	21	91	251
B3	275	15	95	290
A1	210	13	94	223
C2	241	20	92	261
C1	359	34	91	393
Total	1606	130	93	1736

3.1.4 Cell-fate specification is normal in *duo4* pollen

Arabidopsis microspore mitosis is linked with cell-fate specification, resulting in the specific expression of vegetative cell (Twell *et al*., 1998) and germ cell markers (Engel *et al*., 2005; Rotman *et al*., 2005). To further elucidate whether defects in cell division in *duo4* pollen grains are associated with cell fate changes, +/*duo4* (50 % of the pollen population exhibited mutant phenotypes and the remainder of the population appeared as wild type) was crossed to plants expressing different cell fate markers and the F1 progeny was screened for the expression of these markers.

The fate of the vegetative-like cell was monitored with the vegetative nucleus reporter *LAT52*:H2B-RFP (Brownfield *et al.,* 2009a). The *LAT52* promoter has been shown to direct pollen-specific reporter gene expression in *Arabidopsis* and is transcribed in the vegetative cell but not in the germ cell (Eady *et al*., 1994). The expression of the reporter gene was determined by scoring pollen grains with RFP signal in both *duo4* and wild type pollen populations. Expression of *LAT52* in the vegetative cell was observed in approximately 48 % of the *duo4* heterozygous pollen compared to the 52 % in wild type, indicating that vegetative cell function and differentiation is not affected in the absence of germ cell division in *duo4* (Figure 3.3 A).

To examine whether *duo4* mutation affects germ cell fate, +/*duo4* plants were crossed to germline-specific markers. The *Arabidopsis* male germline-specific markers were investigated in the *duo4* mutant, the histone H3 marker *MGH3*:H2B-GFP (Brownfield *et al*., 2009a), and the Generative Cell Expressed 1 and 2 (*GEX1*-GFP and *GEX2*:H2B-GFP) (Engel *et al*., 2005). The proportion of pollen with a single germ cell expressing the germ cell markers is similar to the proportion of wild type pollen, showing that all the *duo4* germ cells express germ cell markers (Figure 3.3 B-D). These results indicate that vegetative and germ cell fates are maintained in *duo4* pollen grains since all the analysed markers show normal expression in both vegetative and germ cells.

3.1.5 *DUO4* is required for male germ cell cycle progression

To pinpoint the step at which *duo4* mutant deviates from the normal pathway of pollen development, DAPI-stained pollen released from single anthers of successive bud stages

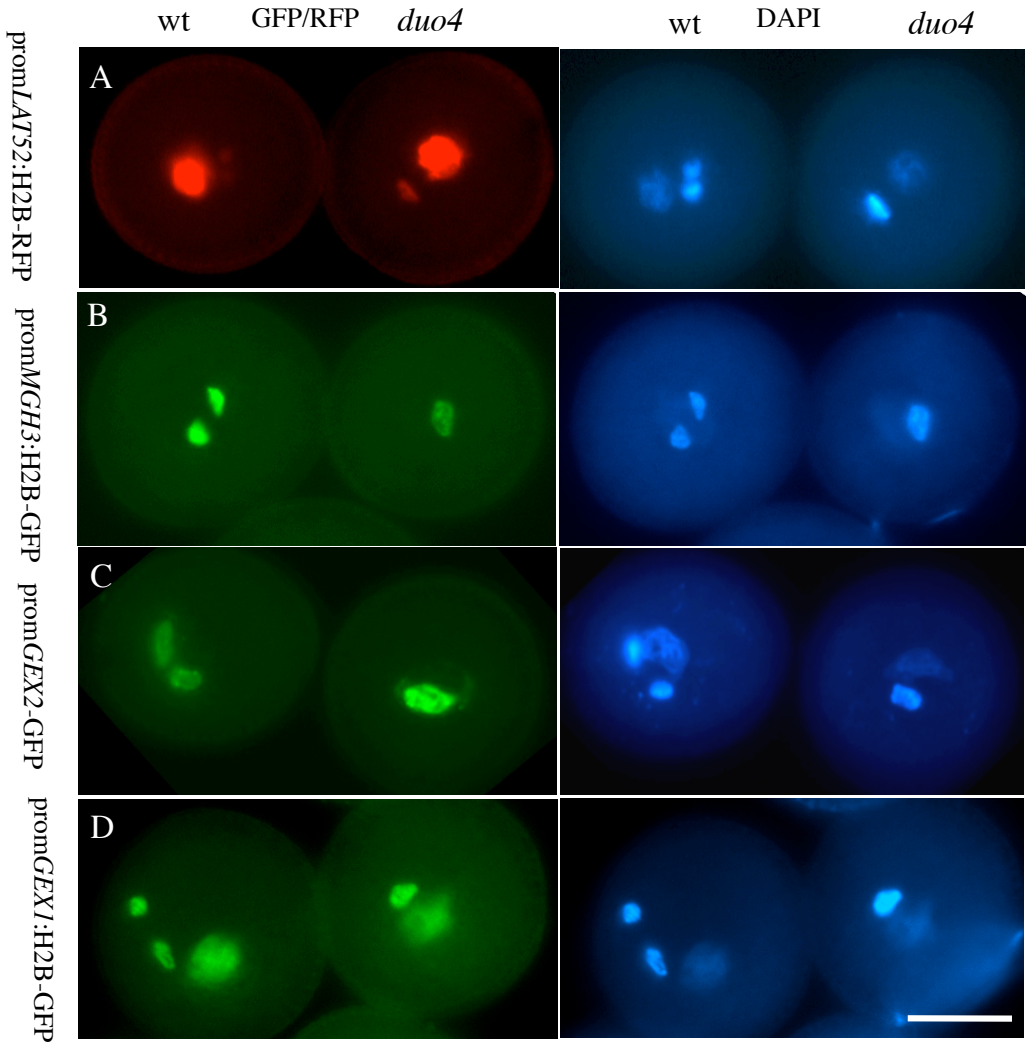

Figure 3.3: Wild type and mutant *duo4* pollen expressing cell fate markers. Mature wild type and *duo4* pollen expressing germ and vegetative cell fate markers. A) prom*LAT52*:H2B-RFP. B) prom*MGH3*:H2B-GFP. C) prom*GEX2*-GFP. D) prom*GEX1*:H2B-GFP. Wild-type pollen is shown to the left and *duo4* pollen to the right in each panel. Corresponding DAPI images are also shown in the right panels. Scale bars =15 μm.

in both wild type and +/*duo4* plants was examined by light and epifluorescence microscopy. Counts were made at several stages of pollen development: late microspore, early bicellular, mid bicellular, late bicellular and tricellular stages. No abnormalities were observed during microspore development in both wild type and *duo4* plants. The pattern of asymmetric microspore division in both wild type and the mutant plants followed the same developmental path, including polarization of the microspore nucleus and its subsequent division. The germ cell thus formed showed the same morphology in both wild type and *duo4* mutant until -6 bud stage as the pollen population was highly synchronous and consisted mostly of bicellular pollen. At -5 and -4 bud stages the pollen population no longer remained synchronous and germ cells at different stages of mitosis were observed along with bicellular and tricellular pollen. The percentage of tricellular pollen at these bud stages was used as a measure of tricellular pollen development. At -5 bud stage about 18 % of the wild type pollen was at the tricellular stage, but a few germ cells had entered mitosis, which corresponded with the appearance of mitotic figures.

In heterozygous *duo4* plants a significant reduction of tricellular pollen at late bicellular (-5 bud) stages was observed compared to the wild type. The percentage of tricellular pollen at -4 and -3 bud stage was not very high, consisting of 10 % and 34 % tricellular pollen respectively. In the later bud stages a maximum of only 52 % of tricellular pollen was observed in heterozygous *duo4* mutant pollen. The results show that pollen development in wild type and *duo4* mutant plants remain similar until the germ cell formation. The deviation from normal pollen development occurs at germ cell division, which appeared at late bicellular (LBC, -5 bud) stage. The bud stages are not completely synchronized between plants which can explain variation in the percentage of tricellular pollen at LBC bud stages. In wild type approximately 20 % and 60 % of tricellular pollen grains were observed at –5 and – 4 stages, respectively, and in the succeeding ontogenic stages 100 % of the pollen population were tricellular

3.1.5.1 Microspore development is normal in *duo4*

Pollen development from uninucleate microspore stage to LBC stage, for both wild type and *duo4* , was released in DAPI solution and examined by epifluorescence microscopy,

after stained with DAPI. In wild type the pollen populations were 100% at the uninucleate microspore stage. At the next stages, about 80 % microspore undergoes an asymmetric cell division, giving rise to early bicellular pollen (EBC) (Figure 3.4 A). After being engulfed by the vegetative cytoplasm, the MBC/LBC germ cell nuclei appeared round and cortical in position, marking the change from MBC to LBC. The later bud stages, MBC and LBC, had variable pollen composition consisting of different stages of bicellular pollen grains i.e. both elongated and round germ cell nuclei were observed. The round germ nuclei underwent morphogenesis to acquire an elongated shape that marked entry into mitosis. The large majority of mitotic figures were observed at -5 and -4 bud stages. Because of the fact that germ cell mitosis is not synchronous in anthers, the proportion of pollen in different mitotic stages in these buds varied in different inflorescences. Similarly, in *duo4* microspores at early and polarized stages until LBC did not differ from those in the wild type, indicating that nuclear migration and division are not affected by *duo4* mutation.

3.1.5.2 *duo4* suppresses entry of germ cells into mitosis

Prior to germ cell mitosis the *duo4* pollen population appeared identical to the wild type. In addition, germ cell division initiates following elongation of the germ nucleus (Figure 3.4 A-C). To establish at which stage *duo4* germ cells are arrested, the sequence of events of germ cell mitosis were evaluated in +/*duo4* plants compared with wild type plants.

To measure the developmental stages, the percentage of tricellular pollen and mitotic stages were counted for *duo4* mutant and for wild type. In wild type, prophase is the first phase of mitosis in which chromatin condenses into thread-like structures that condense further to form five visible chromosomes (Figure 3.4 D-E). Highly condensed chromosomes align on a plane in the metaphase plate (Figure 3.4 F). During anaphase two sets of chromosomes separate and move toward the spindle poles (Figure 3.4 G).

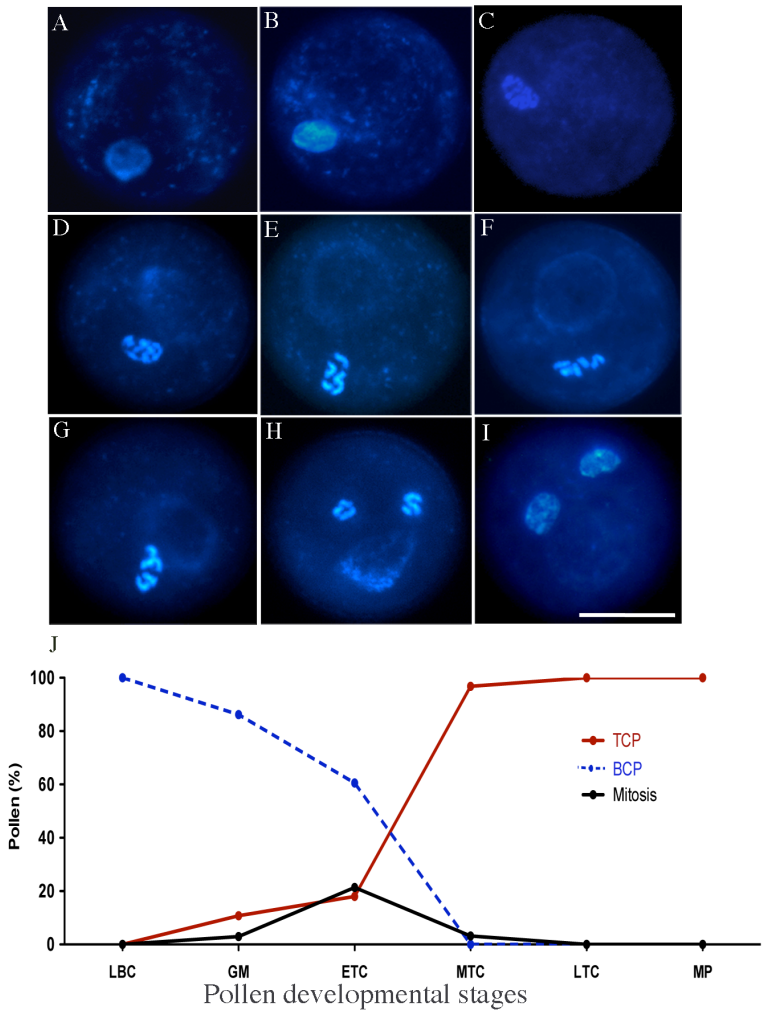

Figure 3.4: Morphology of germ cell nuclei and mitotic progression in wild-type pollen stained with DAPI. A) Round germ nucleus. B) Elongated germ nucleus at late interphase. C-D) Early prophase with thread-like chromosomes. E) Late prophase with four visible condensed chromosomes. F) Metaphase showing condensed five chromosomes arranged on the metaphase plate. G) Anaphase with two sets of chromosomes. H) Telophase, individual chromosomes are still visible. I) Sperm cells at early interphase with heterochromatic regions. J) Analysis of pollen development in wild type. Pollen from individual flower buds was stained with DAPI, and the percentage of tricellular pollen (red line), bicellular pollen (blue line), and pollen showing mitotic figures (black line) was determined. The stages of development are classified as late bicellular (LBC), germ cell mitosis (GM), early (ETC), mid (MTC), and late (LTC) tricellular, and mature pollen (MP). Inflorescences from four wild type plants were analysed (n= 1283). Scale bar is 15 μm.

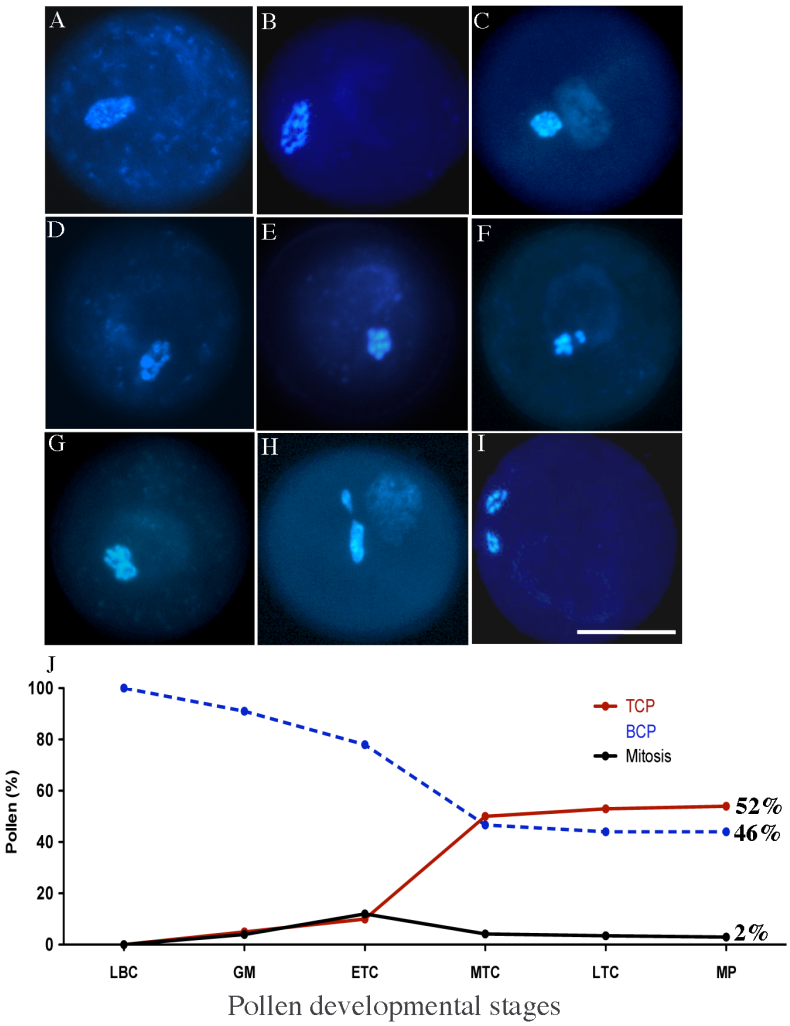

Figure 3.5: Morphology of mitotic progression and male germ cell nuclei in *duo4*. A-B) morphology of DAPI-stained male germ nuclei that elongate normally in *duo4*. C-D) Abnormal chromatin condensation. E) Tightly condensed chromosomes in prophase. F) Prophase with laggards. G) Early anaphase with diffused chromatin. H), I) Teleophase, showing unequal chromosomal segregation. J) Graph showing the percentage of tricellular pollen (red line), bicellular pollen (blue line), or pollen that showed mitotic figures (black line) at different developmental stages in *duo4*. The frequency of bicellular pollen stages close to germ cell mitosis is similar in *duo4* and wild type plants, whereas the frequency of tricellular pollen is reduced by almost half in *duo4* heterozygotes. The stage of development is classified as late bicellular (LBC), germ cell mitosis (GM), early (ETC), mid (MTC), late (LTC) tricellular, and mature pollen (MP). Inflorescences from four + /*duo4* plants were analyzed (n=1215). Scale bar is 15 µm.

Newly formed sperm nuclei are initially round and subsequently become elongated (Figure 3.4 H-I). The overall frequency of mitotic figures was calculated by analyzing about 2000 pollen grains from -5 and -4 bud stages and the wild type anthers was found to be 22 %(Figure 3.4 J).

In *duo4* heterozygous plants prior to germ cell division the pollen population was comparable to that of the wild type. In addition, the round germ cell nucleus (RGN) successively elongated preceding entry into germ cell mitosis, as in wild type (Figure 3.5 A-B).

To further confirm that *duo4* mutant pollen did not enter mitosis, mitotic figures were counted in *duo4* mutant and were compared to the wild type. The mean mitotic index for *duo4* was 12.7 % (n > 1790), almost half that observed in wild type. In addition, the proportions of tricellular pollen increased while the proportion of bicellular pollen decreased, consistent with the reduced frequency of mitotic figures. In *duo4* by early/mid tricellular stages the composition of the pollen population is not significantly different from 50 % bicellular and 50 % tricellular (Figure 3.5 J), whereas all wild type germ cells have divided at the equivalent stage. These results demonstrate that the *duo4* mutant results in germ cell cycle arrest.

3.1.5.3 Progression through germ cell mitosis is disturbed in *duo4* mutant

Despite the fact that the germ cell nuclei in the *duo4* mutant successfully undergo elongation and fail to enter mitosis, observations showed that a small population of cells overcame G2 arrest but remain in mitosis. It is very likely that these cells have difficulty in exiting mitosis, resulting in delay at different mitotic stages. Corresponding data from wild type bud stages did not show delay in mitosis, indicating that these cells might escape G2/M arrest, but delayed to exit mitosis. In *duo4*, approximately 4 % and 3 % of mitotic figures were observed at -2 and -1 respectively, compared to a uniform population of tricellular pollen grains at the same stages in wild type.

In -2 and -1 bud stages, the different types and frequencies of mitotic aberrations were scored. These included prophase with chromosomes abnormally scattered in the cytoplasm, late condensed prophase-like chromosomes with lagging and highly

condensed chromosomes (Figure 3.5 D-F). Surprisingly, some germ cells appeared to exit mitosis, which possibly resulted in abnormal chromosome segregation (Figure 3.5 H-I). This, in turn, might lead to the formation of micronuclei and chromatin bridges that were recorded at frequencies of about 7 % (n=125).

Chromosomal segregation defects during anaphase, represent another mitotic event in *duo4* mutant. Observations revealed anaphase with lagging chromosomes during their migration to the spindle pole. A small proportion of germ nuclei (3%) showed a clear segregation defect during the progression from anaphase. This included chromosomes that stayed attached during anaphase progression, resulting in pollen with two similar nuclei, which were in contact with each other by a long chromatin bridge to form a dumbbell-like structure. In addition, two sperm cell nuclei of different sizes, which were connected together via chromatin bridges, were also recorded at 2.7 %. These connections between two nuclei represent further evidence of disturbed chromosome separation in *duo4* mutant germ cells. The results presented above indicate that the *duo4* mutation leads to a block in male germ cell division. However, some cells escape the arrest and so are delayed in divisions.

3.1.5.4 Undivided germ cell nuclei in *duo4* complete DNA replication

To investigate the consequence of failure of division on cycle progression in *duo4* germ cells, the DNA content of DAPI-stained nuclei was measured and compared to the nuclear DNA content of prophase and telophase nuclei. It was previously demonstrated that germ cell nucleus contains 2 C DNA content before entry into mitosis (Friedman, 1999; Durbarry *et al*., 2005). DNA content of 1 C and 2 C was measured for wild type telophase and prophase nuclei respectively, and used to normalise the DNA content of *duo4* germ cell nuclei, which were also compared to the mean germ cell DNA content in other *duo* mutants (*duo1*, *duo2* and *duo3*). *duo4* male germ nuclei displayed a mean of relative fluorescence values (RFU) of 1800 ±, reflecting a 1.98 C content, which is significantly higher than the 1.4 C of a wild type sperm cell. In contrast, this is not significantly different from 2 C, which is the DNA content of germ cell nuclei at prophase (Figure 3.6) (analysis of variance; P = 0.0019). More precisely, the DNA content of *duo4* was significantly lower than that of *duo1* and *duo3* mutants, which displayed a 2.3 C and 2.2 C, respectively.

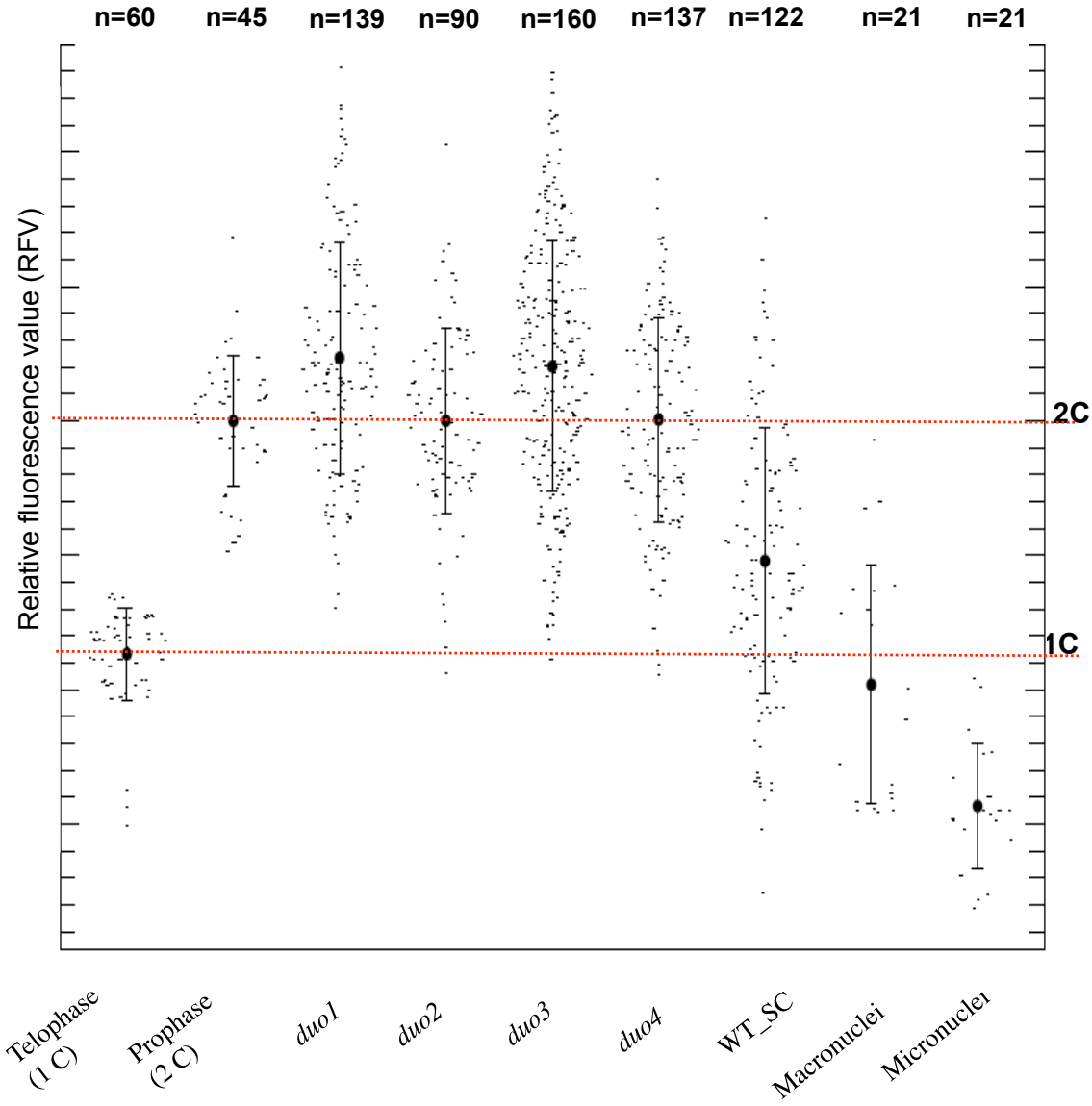

Figure 3.6: Relative DNA content measurement of the *duo4* mutant germ cells. Scatter diagram showing the relative DNA content of the *duo4* mutant germ nuclei (include macronuclei and micronuclei) compared to the DNA content in telophase, prophase, wild type and other *duo* mutants nuclei (*duo1*, *duo2* and *duo3)*. The scatter plot indicates the range of data points, medians (black bold dots) and interquartile ranges (solid black lines). The relative C-values were calculated from DAPI fluorescence values normalized to the mean fluorescence of prophase (2 C) nuclei.

It has been established that both *duo1* and *duo3* germ cells complete S phase without mitosis and continue DNA replication before anthesis, increasing their average DNA content to 2.3 C (Durbarry *et al*., 2005). On the other hand, there was no difference between the average DNA content of *duo4* germ cell nuclei and *duo2* germ nuclei as both of the mutants produced fluorescence values that corresponded to 1.98 C, similar to prophase nuclei. These results indicate that *duo4* has completed DNA replication before mitosis, however, unlike *duo1* mutant germ cells, without reinitiation of DNA replication.

The previous data was consistent with the developmental analysis, confirming that *duo4* mutant leads to arrest of the cell cycle progression at G2/M transition.

3.1.5.4.1 Analysis of DNA content of *duo4* micronuclei (MN)

Analysis of the relative DNA fluorescence of micronuclei, which represent about 7 % of the *duo4* population, may give more detailed information on the action of *duo4* on the cell cycle progression. However, micronuclei DNA content would not verify whether the micronuclei result from fragments or whole chromosomes, because of the fact that *Arabidopsis* chromosomes are small and can have relatively different DNA contents. Relative nuclear fluorescence was determined in both macronuclei and micronuclei. The result showed that macronuclei had a mean DNA content of 1.2 C, which is less than wild type SC (Figure 3.6) while in the micronuclei the mean fluorescence value corresponded to 0.5 C (Figure 3.6).

3.1.5.5 CYCB1;1 is specifically required for germ cell development

It has been described earlier that the *duo4* heterozygote germ cell failed to progress through mitosis, resulting in about 50 % bicellular pollen at maturity. Corroborative results were obtained by measuring DNA content of single germ cells (2 C), indicating that *duo4* germ cells have undergone a single round of replication. Both in plants and animals, entry into mitosis is mediated by a mitosis promoting factor (MPF) that consists minimally of cyclin dependent kinase associated with B-type cyclin. This process requires stringent cell cycle control, in which the level of B-type cyclin peaks in late G2

and M phase, highlighting actively dividing cells and tissues (Colon-Carmona *et al.*, 1999). Afterwards, these proteins are destroyed in anaphase in an APC-dependent manner.

The dynamics of CYCB1;1 expression during male gametogenesis have been examined using the pCDG marker containing the CYCB1;1 promoter region (1148 bp), including the mitotic destruction box, fused to the GUS or GFP reporters. Furthermore, the activity of these constructs was used to visualise the spatial and temporal expression of CYCB1;1 in germline cells and their precursors (Brownfield *et al.*, 2009a).

3.1.5.5.1 CYCB1;1 expression is suppressed in *duo4* germ cells

To monitor the expression of CYCB1;1 in the *duo4* mutant, the *duo4* heterozygous lines were crossed, as a female, to a CYCB1;1-GFP marker line (pCDGFP) (provided by P. Doerner). Bud stages from F2 individual plants in wild type and + /*duo4* plants were analysed based on their arrangement on the floral axis. Pollen grains were released into 0.3 M Mannitol solution and GFP fluorescence was visualized.

First the AtCYCB1;1 marker was analysed in wild type pollen (Figure 3.7 A-G). Individual pollen grains at different stages of development (as determined by DIC images) were analysed for GFP activity. Microspores and bicellular pollen shortly after mitosis showed GFP signal, with the number of pollen grain expressing GFP peaking close to mitosis (Figure 3.7 B-C), indicating that expression of AtCYCB1;1 is linked to the microspore division. GFP signal was then disappeared from bicellular pollen (Figure 3.7 D). Close to germ cell mitosis, GFP signal was detected specifically in germ cells (Figure 3.7 E-F) indicating expression of AtCYCB1;1 in the germ cell before division. The protein is degraded after mitosis and is absent in tricellular pollen (Figure 3.7 G).

In *duo4* heterozygote, microspore division (four plants were analysed) proceeds in a similar fashion to the wild type (four plants were analysed), in which approximately 93 % of the population were microspores, GFP signal was observed in polarized microspores in both wild type and *duo4* heterozygote plants (Figure 3.7 I). At early bicellular stage the proportion of pollen that shows GFP signal was reduced in both wild type (24 %) and *duo4* heterozygote plants (27 %). No GFP signal could be seen in mid-bicellular stage, suggesting that CYCB1;1 protein might be degraded (Figure 3.7 K).

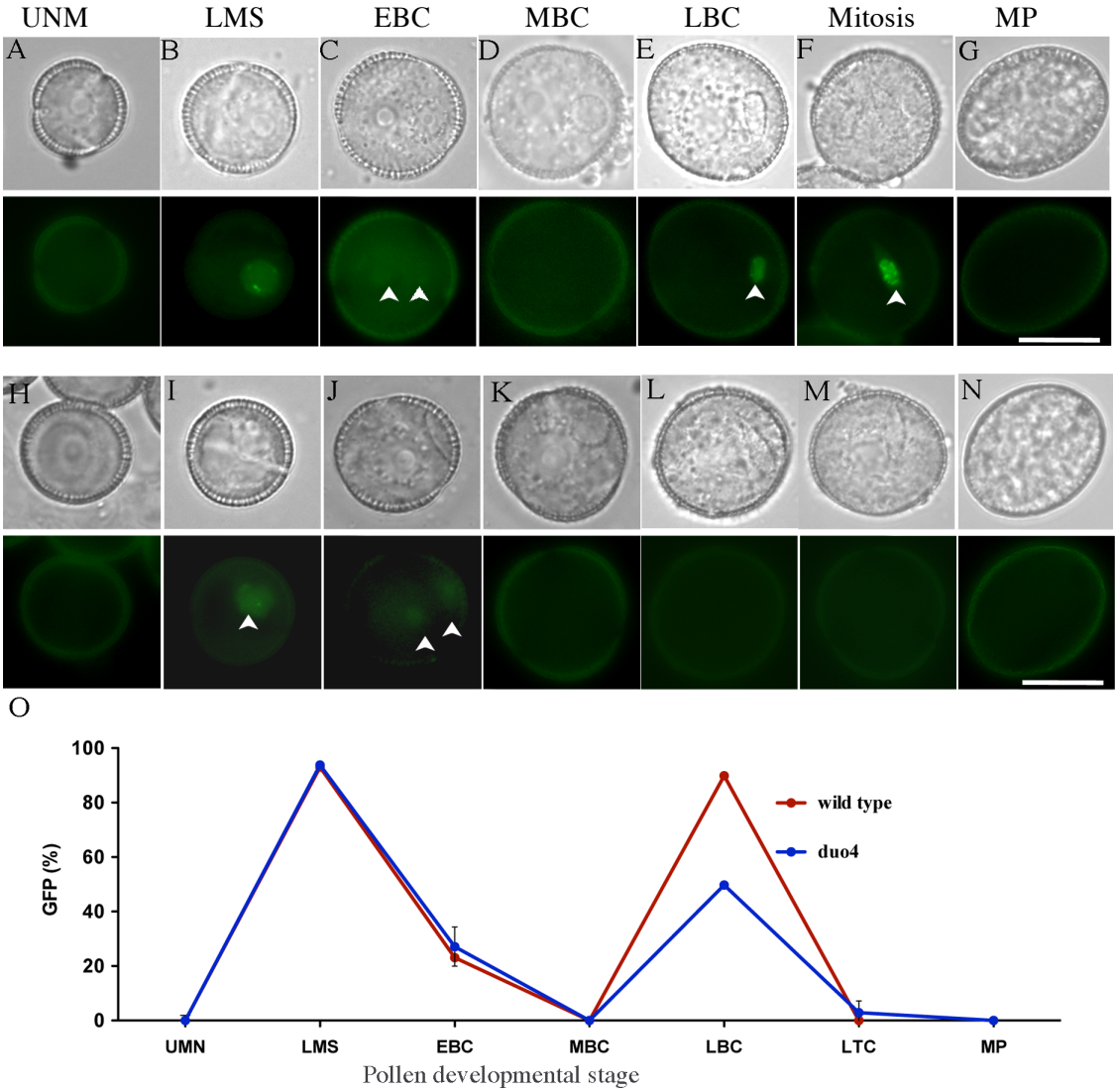

Figure 3.7: Analysis of a *CYCB1;1* marker (pCDGFP) in wild type and *duo4* pollen. The lower panel A-G is a series of fluorescence images illustrating the expression of pCDGFP during microspore mitosis with corresponding DIC images shown in the upper panel. A-B) the microspore undergoes polarisation. C) Expression of *CYCB1;1* peaks at asymmetric microspore division. D) A weak signal is detected in the germ cell after the first mitosis in both germ and vegetative nuclei. E) Complete turnover of GFP at mid bicellular stage. F) Elongated germ cell close to germ cell mitosis showing GFP signal. GFP fluorescence accumulates during mitotic division but GFP signal can not be detected in mature pollen (G) (GFP signal indicated by arrows head). The lower panel H-N is a similar series of figures showing the absence of expression of CYCB1;1 in *duo4* mutant pollen. H-I) shows a similar pattern to wild type where GFP signal can be seen in polarized microspore. K-L) Very weak GFP signal still detectable in both nuclei at early bicellular in pCDGFP is no longer detectable in the next stages of the pollen development (M) or mature pollen (N). The frequency of GFP expressing cells during pollen development is summarised in a line graph (O). GFP signal indicated by arrowheads. Scale bar = 10μm

Generally, there were no differences between wild type and *duo4* in GFP fluorescence patterns during microspore division. During late bicellular stage, which is marked by morphogenesis of male germ cells to an elongated stage (Figure 3.7 L), the number of cells showing GFP signal in the wild type was approximately 90 %, indicating the mitotic activity of the pCDGFP in the germ cell. However, there was a clear reduction in the number of cells showing GFP in the +/*duo4* plants at late bicellular stage to almost half (49 %) compared to wild type (Figure 3.7 O). A gradual decrease in GFP can be seen when cells progress through the next stages and there is a lack of detectable signal at meta/anaphase boundaries. However, some cells with prolonged prophase nuclei still express GFP signal in +/*duo4* plants (2.7 %), when all wild type nuclei have completed mitosis. This result was similar in four F1 and three independent F2 individuals.

Overall, these data are in agreement with the previous developmental analysis. Thus, the expression of CYCB1;1 is inhibited in *duo4* germ cells, providing an explanation for the failure of mitotic entry in *duo4* germ cells.

3.2 Role of *duo4* germ cell in double fertilisation

Seed development in flowering plants is initiated by a double fertilisation event in which two sperm nuclei fuse with egg cell and central cell, resulting in the production of the embryo and endosperm, respectively. The correct cell fate specification, viability of *duo4* pollen and DNA content of 2C, provide the possibility that *duo4* may be able to fertilise and subsequently influence seed development. However, the lack of the second sperm cell required for double fertilisation should result in fertilisation only one of the cells in the embryo sac (egg or central cell).

3.2.1 *duo4* plants possess short siliques compared to wild type

To obtain an insight about the role of *duo4* in seed production, silique length measurements were performed in +/ *duo4* and wild type plants. A significant reduction in silique length and seed set, compared with wild type plants was observed in *duo4* mutant plants, which indicates fertility defects. The mean silique length was reduced to

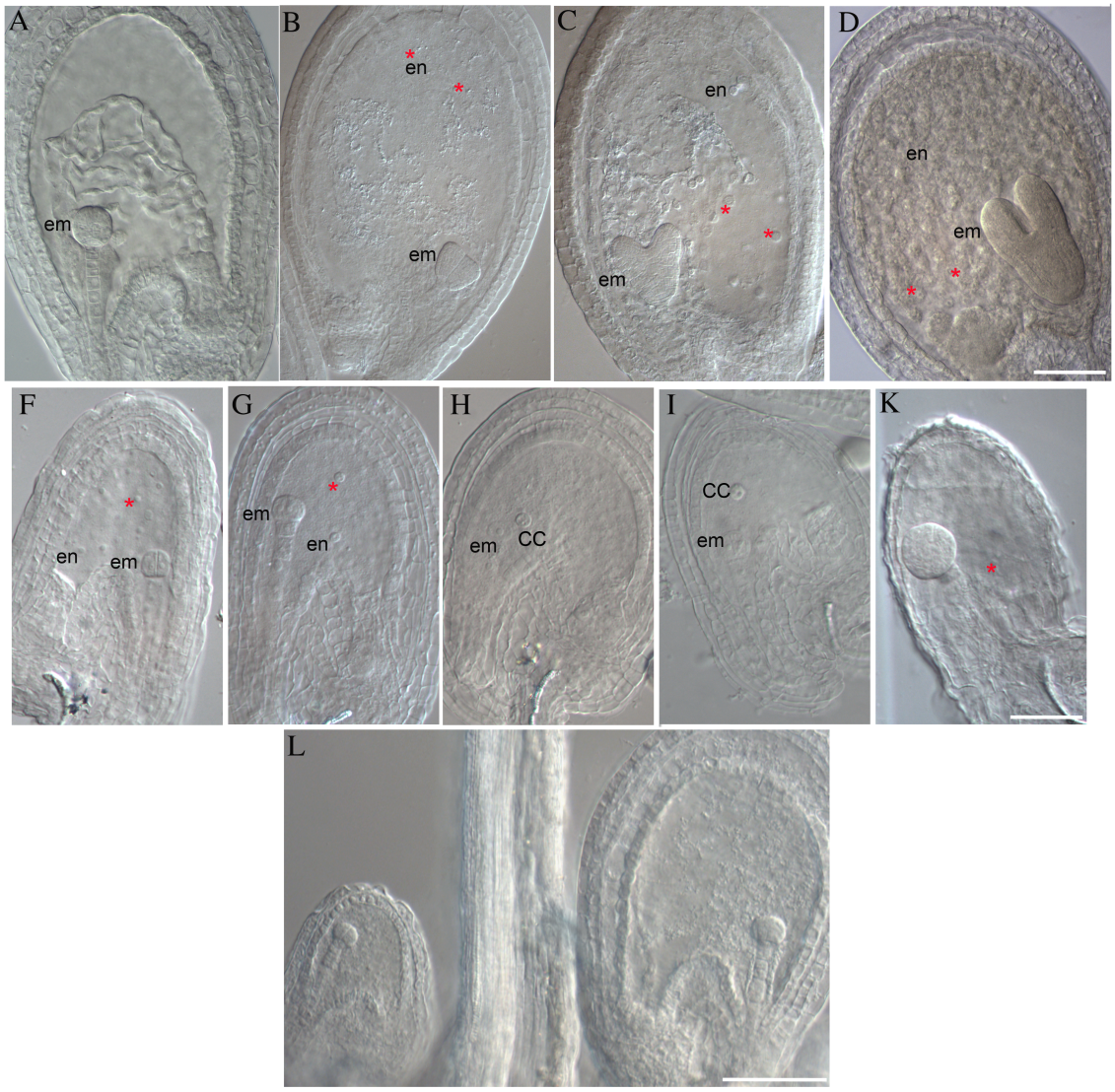

Figure 3. 8: Seed development in wild type and *duo4* heterozygous plants

(A-D) Wild type embryo development. A) Wild type mature seed with a globular embryo and endosperm 3 days after pollination (3 DAP). B) Wild-type seeds with embryo at transition stage (4 DAP). C) Wild type seed with embryo at heart stage (5 DAP). D) Wild type seeds with embryo at late heart stage endosperm nuclei fill the seed. F-G) Four-celled *duo4* embryos with limited endosperm nuclei. H) One-celled embryo and 'unfertilised' nucleus of central cell (cc). I) Two-celled *duo4* embryo where the nucleus central cell remains unfertilised (cc). K) Aborted seed with embryo at globular stage. L) Seeds cleared from a *duo4* heterozygous plant (3 DAP) showing a normally developed seed containing a globular stage embryo (right) and a typical *duo4* seed with an embryo arrested in early globular stage (left). cc, central cell; em, embryo; en, endosperm. Red asterisks mark endosperm nuclei. Scale bars = 200μm.

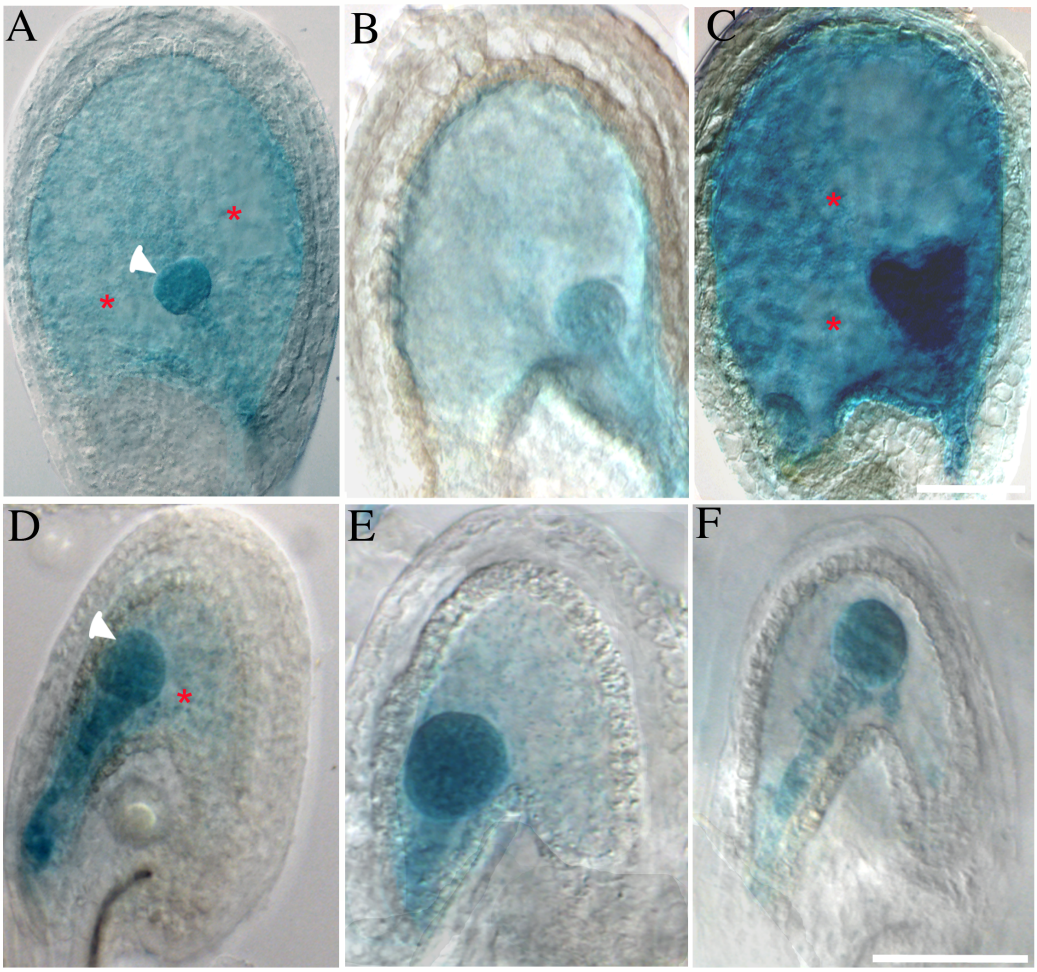

Figure 3.9: The expression of the fertilisation marker prom*CDKA;1*-GUS in wild type and *duo4* seeds. A-B) Wild-type seed 3 DAP from a cross between wild-type pistil and *duo4* heterozygous pollen carrying the GUS marker. Blue GUS-staining is detected in both the embryo (globular stage) and the endosperm. C) Wild-type seed 4 DAP with heart stage embryo. D-F) *duo4* seeds carrying the GUS marker from crosses between wild type pistils and pollen from *duo4* plants carrying the GUS marker, note blue staining is present in both fertilisation products, as found in 40 percent of the *duo4* seeds displaying GUS-staining (n=59). Red asterisks mark endosperm nuclei. Embryo indicated by arrowheads Scale bars = 200μm.

14 mm in the *duo4* (n=20) from 4 individuals, compared with 17.8 mm in wild type (n=20) from 4 individuals (analysis of variance; P = 0.001). The t-test suggests that there is a significant difference between the mean silique length of *duo4* and the mean silique length of wild type plants.

Because silique length is generally correlated with the number of developing seeds, mature siliques collected from heterozygous plants were examined under a microscope. Approximately 40 % of the seeds were aborted and shriveled whereas siliques from control wild-type plants were filled with green and full seeds. The aborted shrunken seeds were non randomly distributed along the silique and did not develop further as the silique matured, however, approximately 35 % of aborted seeds were located in the top quarter of the silique.

Seed abortion is most likely caused by arrival of a *duo4* pollen tube in the micropyle, preventing access by wild type pollen tubes. If *duo4* pollen germ cells were as competent to fertilise as wild type sperm cells, approximately 50 % aborted seeds should be observed. However, about 40 % aborted seeds were observed in *duo4* heterozygote siliques, a significantly reduced portion from the expected 50 %. Thus, about 20 % of the *duo4* pollen tubes clearly do not compete effectively with wild type pollen tubes. These results were consistent when pistils from different ecotypes (No-0, Col-0 and *ms-1*) were pollinated from heterozygous *duo4* plants.

3.2.2 *duo4* germ cells are able to perform fertilisation and lead to aborted seeds

To establish the ability of *duo4* germ cells to fertilise either the egg cell or central cell, *duo4* and wild type plants were crossed, as a male, to *male sterile 1* (*ms-1*) plants. Three days after pollination (3 DAP) ovules were cleared and both wild type and *duo4* embryos were examined by DIC microscopy (Section 2.11.4). The data showed that the majority of wild type fertilised ovules contained globular stage embryos and the seeds showed a completely cellularized endosperm (no=276), filling the whole seed (Figure 3.8 A-D).

In contrast, crossing *duo4* heterozygote plants to *ms-1* resulted in about 38 % seeds that were smaller with embryos arrested at globular stage and with limited endosperm

(Figure 3.8 F-G), while the rest behaves like the wild type. It is noteworthy that in some mutant seeds there were one or two large nuclei, which may represent unfertilised central cell (Figure 3.8 H-I). Later in development, when wild type seeds had reached the late heart stages, all the mutant seeds had shriveled and were eventually aborted with embryos arrested at globular stage (Figure 3.8 K).

In order to further investigate the hypothesis that *duo4* germ cells exclusively fertilise the egg cells in the embryo sac, plants carrying the prom*CDKA;1*-GUS (Nowack *et al.*, 2006) were crossed to + /*duo4* plants. The expression of this marker can be observed immediately in the fertilised products of the seed that received paternal gametes.

Histochemical GUS-assays were performed on dissected siliques 3 DAP (Section 2.11.5). The prom*CDKA;1*-GUS expression was detected in embryo and endosperm of wild type seeds in about 98 % of the population (n= 107, Figure 3.9 A-C). When siliques from +/*duo4* heterozygous for CDKA-GUS were dissected weak GUS staining was present in the limited endosperm surrounding the embryo in the aborted *duo4* seeds in 40 % (n=95) of them (Figure 3.9 D-F). GUS expression was observed in both fertilisation products, embryo and endosperm, indicating that *duo4* germ cells perform double fertilisation.

Another experiment was carried out to investigate if *duo4* germ cell divided during pollen germination. A germination test was performed to monitor the number of sperm cells per pollen tube and measured the proportion of pollen tubes containing two sperm cells. At maturity, *duo4* pollen contains about 50 % of population as bicellular in a heterozygous plant. After 6 hours incubation, a comparable germination rate between pollen from wild type and pollen from *duo4* tubes was observed, indicating *duo4* mutation does not affect pollen germination rates. At 20 hours of germination, about 60 % of pollen tubes contained two sperm cells (Figure 3.10), indicating that about 20 % of *duo4* germ cells undergo the germ cell division in the pollen tube. This result demonstrates that the *duo4* mutation significantly delays the germ cell division instead of blocking the division.

The previous analysis was further investigated by using the endosperm marker KS22 (in the C24 background, Ingouff *et al.*, 2005). In the wild type, the expression of this marker is inactivated immediately when the embryo reaches the heart stage. When *ms-1* plants

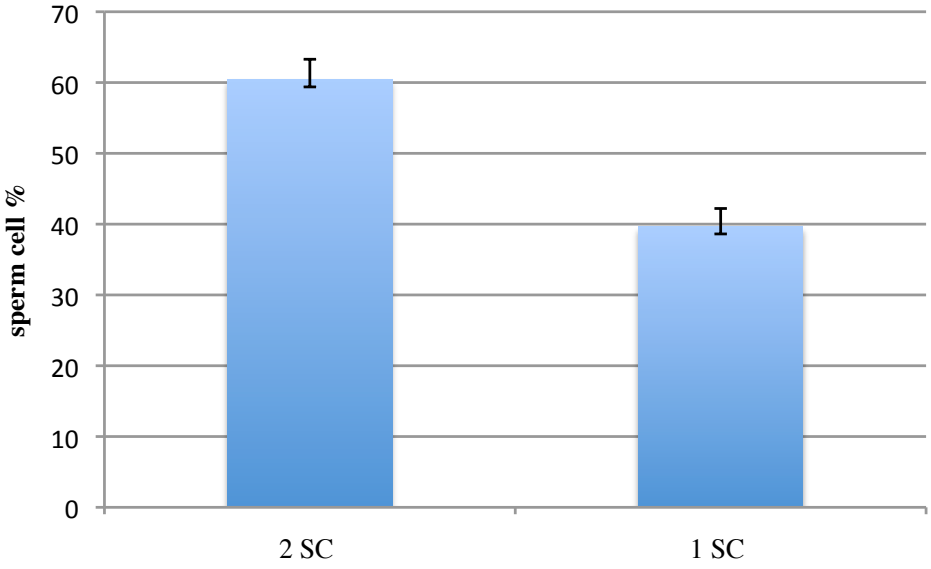

Figure. 3.10: Bar chart representing the percentage of *duo4* pollen tubes containing a single sperm (1 SC) or two sperm cells (2 SC). Mature pollen from +/*duo4* was germinated in vitro and the number of sperm cells was counted in each pollen tube after DAPI staining. The mean values presented consist of pooled data from two independent populations.

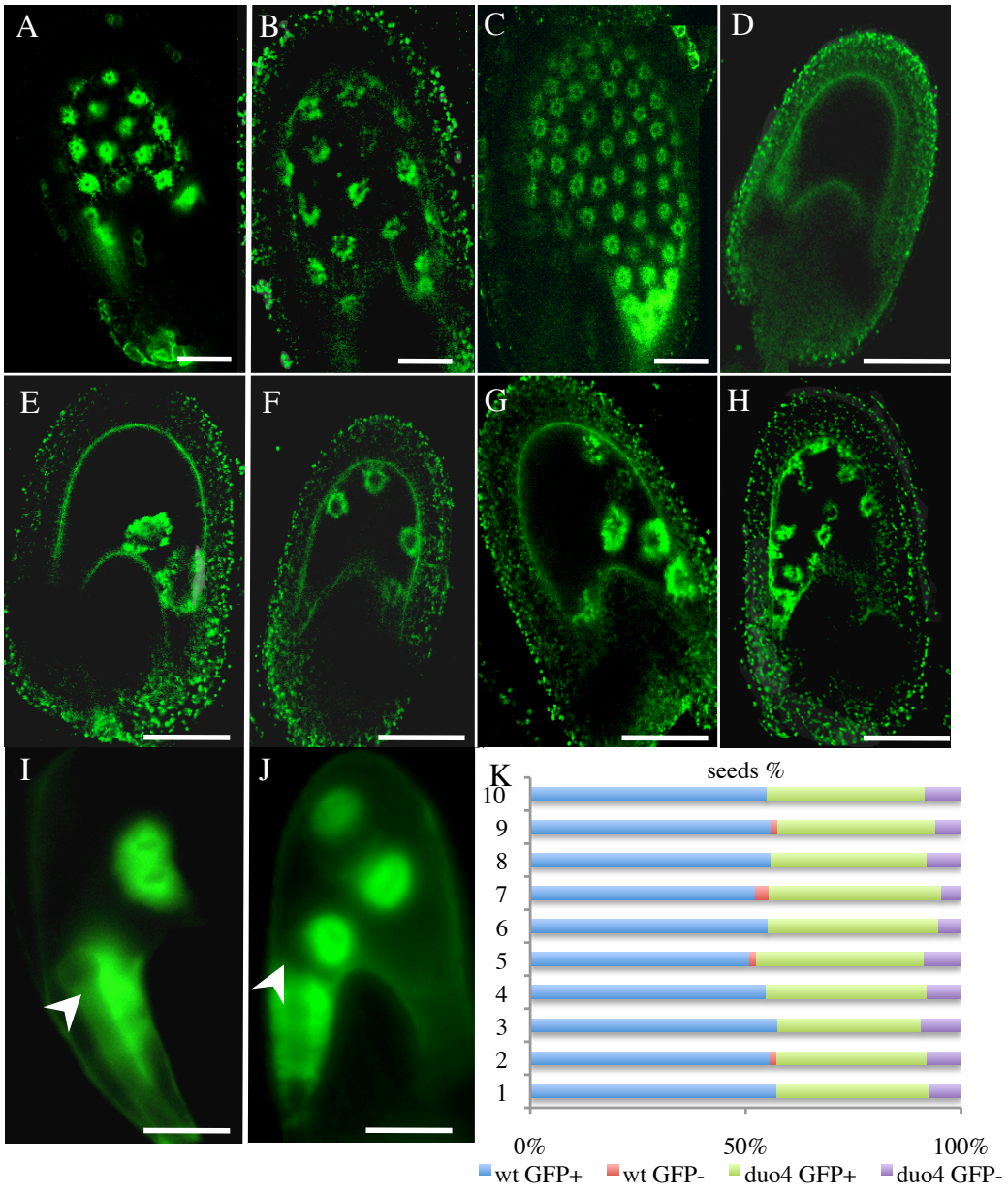

Figure 3.11: *duo4* seeds show the expression of fluorescent KS22 GFP endosperm enhancer trap markers. A-C) Expression of the KS22-GFP endosperm marker in a wild type seed. A) 2 DAP and B-C) 3 DAP where the uniform expression of KS22 could be observed. D) *duo4* mutant seed failed to show the marker expression. E-H) Endosperm nuclei in seeds fertilized with *duo4* mutant pollen express GFP, even in cases where the central cell nucleus has not divided (3 DAP). I-J) Expression of KS22-GFP in a seed containing globular embryo (arrowhead) and endosperm from a cross between wild type ovules and + /*duo4*;KS22/KS22 pollen (3 DAP). The number of endosperm nuclei ranged from 2 to10 with different shape and sizes. Scale bars=200µm. K) Bar chart showing percentage of seeds in ten different siliques originated from crosses between *ms1* and + /*duo4* pollen expressing the KS22-GFP endosperm marker.

were crossed with the KS22-GFP marker line, GFP expression was observed in the endosperm when several rounds of division have occurred (3 DAP) (Figure 3.11 A-C). When similar crosses were carried out using *duo4* as the male parent, results showed that about 80 % of *duo4* seeds, with limited endosperm nuclei, show expression of the paternally derived KS22-GFP reporter. However, in all cases observed the development of endosperm in *duo4* mutant seeds was abnormal compared to the wild type (Figure 3.11 E-G). Only few rounds of nuclear divisions were observed with a range from 2-10 nuclei. In addition, these nuclei showed variability in shape and size with a nonuniform distribution and were associated with globular stage embryos (Figure 3.11 I-J). Counts were carried out using about 10 + /*duo4* siliques (Figure 3.11 K). On the basis of previous observations these seeds do receive the paternally derived endosperm marker gene *KS22*, indicating that two fertilisation events take place in the *duo4*, but central cell fusion fail to promote cell division (Aw et al., 2010).

3.3 Cytoskeleton and germ cell morphogenesis in *duo4*

The general importance of describing the process that results in the production of two sperm cells is related to its critical role in double fertilisation. There has been a remarkable interest focused on the process that results in sperm cell formation from their precursor germ cell. Until recently, a high number of publications about the mechanism of germ cell division in the field of plant reproduction appear somewhat conflicted. Some of these studies point at the role the phragmoplast in sperm cell formation (Charzyńska *et al.*, 1988), while a number of studies refer to a furrowing process that mediates randomly aligned kinetochores followed by cytokinesis (Palevitz and Cresti, 1989). It is clear that the organisation of microtubules (MTs) during male gametophyte development is quite distinct from that in the somatic cells, particularly, the absence of the preprophase band (PPB) that forecasts the division plane and the orientation of an asymmetric spindle and hemispherical phragmoplast MT array (Oh *et al.*. 2010; Terasaka and Niitsu, 1995; Zonia *et al.*, 1999). These gametophytic MT arrays have been observed in live cells, using newly developed markers GFP-TUBULINA6 microtubules (Oh *et al.*, 2010). Therefore, it would be useful to investigate whether the mechanisms of organisation underlying germ cell division are similar among higher plants. In this regard, an important goal is to investigate the germ cell morphogenesis in

A. thaliana prior and during the second mitosis by first looking at some of these events in wild type plants. Then theses observations are followed here by an analysis of the organisation of the microtubular cytoskeleton in the *duo4* germ cells.

3.3.1 Modification of the cytoskeleton marker

In order to achieve a clear overview of the germ cell activities prior and during the period of division, the GFP-Arabidiopsis-α-tubulin 6 (GFPTUA6) expression cassette was chosen as a proven MT-GFP marker. In a previous experiment Cauliflower Mosaic Virus 35S(CaMV35S) promoter driven expression of GFPTUA6, prom35S:GFPTUA6, was used effectively to visualise MT arrays in somatic cells and in MT-defective mutant plants (Ueda *et al.*, 1999). In a recent study, replacing the CaMV 35S promoter with the microspore-specific NTM19 promoter (Custers *et al.*, 1997) allow driving GFPTUA6 expression to male gametophytic cells (Oh *et al.*, 2010), thus, restricting the expression of the modified TUA6 on MT organisation only in the male germline.

In order to localise the GFPTUA6 expression specifically in the germ cell, a pair of primers were designed (smGFP_F and TUA6_R) to amplify the GFP-*Arabidiopsis*-α-tubulin 6 (GFPTUA6) protein fusion from the previous used construct, prom*NTM19*:GFPTUA6. Then the *MGH3* promoter (Okada *et al.*, 2006) was used to drive the expression of GFPTUA6 protein fusion specifically in the germ and sperm cells. +/*duo4* plants were transformed with the prom*MGH3*:GFPTUA6 fusion. About 60 independent plants containing the promMGH3:GFPTUA6 marker were screened. None of the generated lines exhibited any unusual vegetative growth. Wild type and *duo4* lines that showed a strong GFP signal in mature pollen, and which were identified as single locus lines by the presence of approximately 50 % GFP-positive pollen, were kept to perform the analysis.

3.3.2 Cytoskeletal changes during germ cell mitosis and sperm formation in *Arabidopsis thaliana*

Pollen from T1 plants at different developmental stages was released in 0.3 Mannitol and fluorescence microscopy was used to visualise the expression of the GFPTUA6

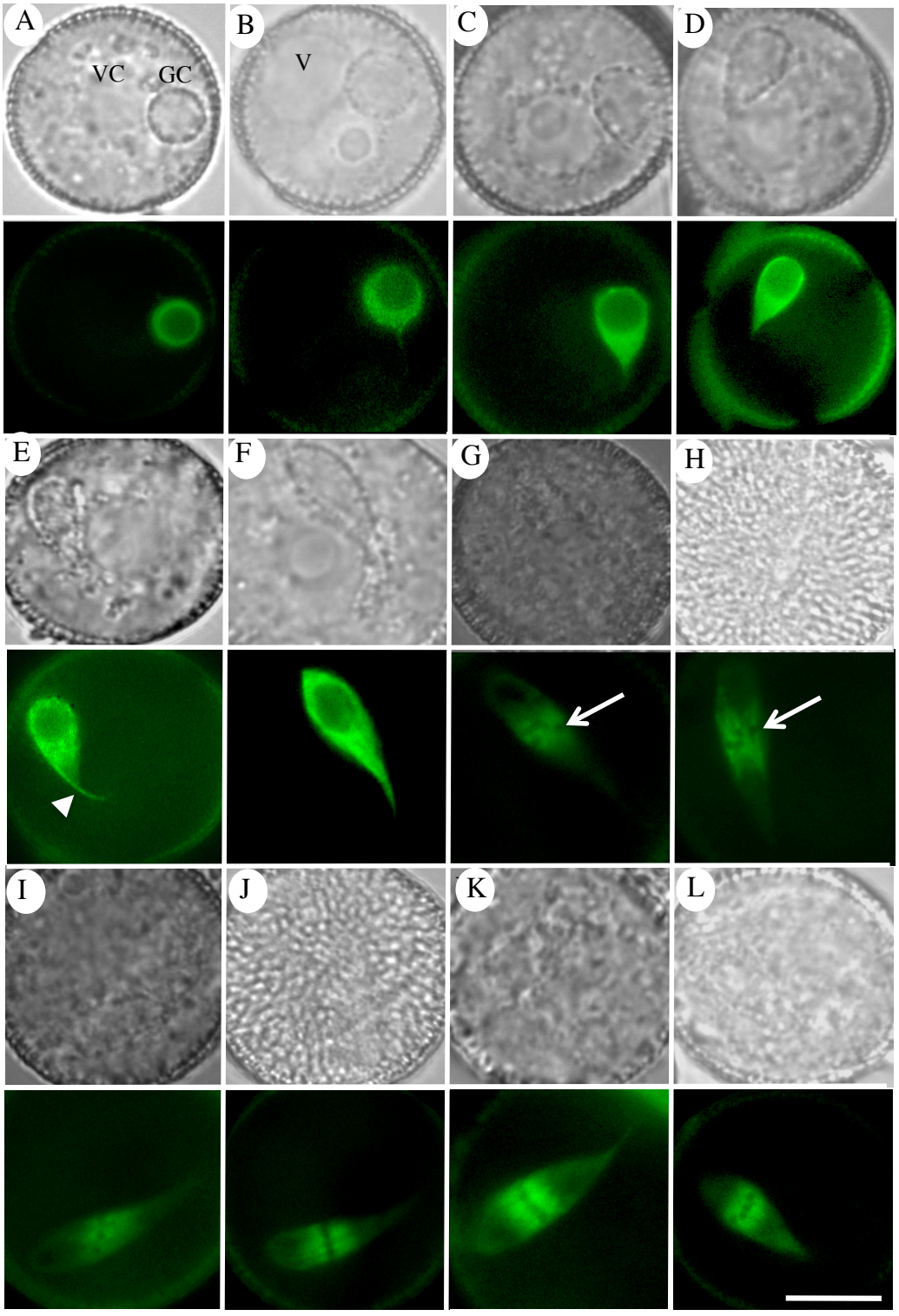
A
VC
GC
B
V
C
D
E
F
G
H
I
J
K
L

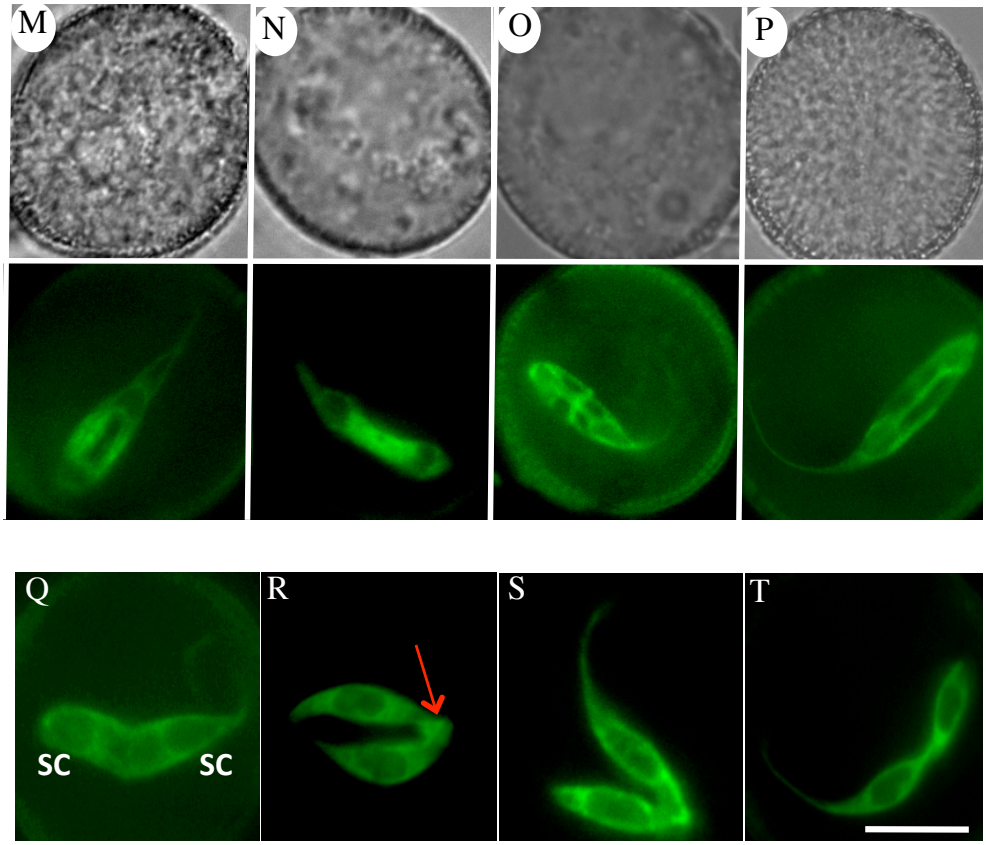

Figure 3.12: Live developing spores and pollen from a promMGH3-GFPTUA6 transgenic line. Fresh spores and pollen viewed with DIC (upper panel) or with GFP (lower panel), A-B) mid-bicellular pollen. C-F) elongated germ cells. Note that the first tail-like extension starts to be visible. G-H) Four interruptions (arrows), corresponding to the kinetochore region of the four chromosomes. I-K) The metaphase half-spindle fibres, where microtubules rearranged into a phragmoplast-like structure can be observed at each side of the newly formed cell. M-T) At early tricellular stage, the twin sperm cells (SC) are arranged in parallel. A microtubule knot (red arrow) becomes clear between the newly formed sperm nuclei. Note that the DIC images for individual spore Q-T were not shown. Microtubule bundles have been formed around and between sperm nuclei. GC; germ cell, V; vacuole, VC; vegetative cell. Bars =15 μm.

construct. Live examination of the same spores using differential interference contrast (DIC) microscopy was used to monitor the shape of both germ and vegetative nuclei.

The expression of GFPTUA6 driven by the *MGH3* promoter is not detectable in early bicellular pollen. A very low level of GFP signal was first detectable in germ cells at mid bicellular stage (-7/6 bud stage) (Figure 3.12 A). As the germ cell progressed to the next stage, early late bicellular (ELBC) stage, bundles of MTs appeared to be broader at one side resulting in the germ cell becoming aspherical.

Usually this reshaping is accompanied with development of the extension of the MT cytoskeleton (Figure 3.12 C), forming a basket-like array enclosing the germ cell in longitudinal orientation. The MT bundles converge at both ends of the germ cell and start to align with each other to form a very short tail-like extension, usually discernible at its distal end (Figure 3.12 D-E).

By late bicellular (LBC) stage, the GC becomes more elongated. The germ cell nucleus subsequently undergoes morphogenesis to a highly elongated pear-shape in mature pollen (Figure 3.12 F). During the next stage (-5 bud stage) where the germ cell undergoes mitosis, a massive change could be observed in the orientation of the MT arrays (Figure 3.12 G). This reorganisation pattern leads to “tangles”, or a network of MTs in which various orientations from both thick and thin bundles take place (Figure 3.12 H). At this stage, kinetochores begin to appear as dark interruptions where the MTs bundles (presumably prophase) directly interact (Figure 3.12 I). These kinetochores remain distributed along the length of the germ cell, in many cases showing oblique or transverse arrangements. Subsequently, the MT superbundles (spindle MTs) became arranged in a uniform structure resulting in the alignment of the kinetochores on the metaphase plate, longitudinally or obliquely with a visible gap (Figure 3.12 J). Kinetochores metaphase chromosome-capturing spindle MTs showed relatively uniform GFP signals along their length (Figure 3.12 K).

In the next stage of pollen development, a noticeable constriction could be observed in the midzone where the kinetochores grouped according to a specific alignment, which apparently highlights the beginning of anaphase stage. As anaphase progresses, a

noticeable constriction in MTs occurs in the midzone where the kinetochore fibres become shorter and more constricted than that in metaphase, this forms what is known as the phragmoplast. The phragmoplast initially appears as a compact round plate filled with fine MTs is positioned in the centre, with the plus end meeting at the midzone of the dividing cell and with a short twin comb-like array arrangement (Figure 3.12 K). Then the phragmoplast changes into a ring-like structure and centrifugally expands, giving the impression that two sperm cells have been formed (Figure 3.12 M-N).

At the end of the telophase the twin sperm nuclei could be seen in parallel orientations, and usually linked together by a thin connecting strand. After that a structure of "a tubuli-knot" was formed at the middle point between the newly formed sperm cells (Figure 3.12 R-S). It is worth mentioning that the knot-like structure was described so far only in maize (Lausser *et al.*, 2010).

Finally, as or soon after two sperm cell nuclei are formed, a localised twist of elongated MT branches appears in the interzone between the two nuclei, connecting the twin sperm cells to each other. The distance between the separated sperm cells is relatively variable with no clear sign of cell plate between the newly formed sperm cell nuclei. In all cases, both sperm cells and their precursor germ cell, showed a bent tail-like extension, mainly at one side, in contact with the vegetative cell nucleus (Figure 3.12 T). At mature pollen stage, the MT bundles show a dramatic increase in the length in one periphery of the GC, which is always distally positioned, highlighting the physical connection of the germ cell to the vegetative cell nucleus by a MT-rich cytoplasmic tail. These observations provide evidence for a physical connection between the vegetative nucleus and one of the sperm cells in *Arabidopsis* in live germ cells.

3.3.3 Effect of *duo4* on germ cell cytoskeleton organisation

The role of *duo4* was shown to prevent entry or completion of mitosis. To further investigate the role of *duo4* in germline MT organisation, the GFPTUA6 cytoskeleton marker was analysed during germ cell development of +/*duo4* plants. About six *duo4* plants were analysed. At mature pollen stage *duo4* plants shed an equal percentage of

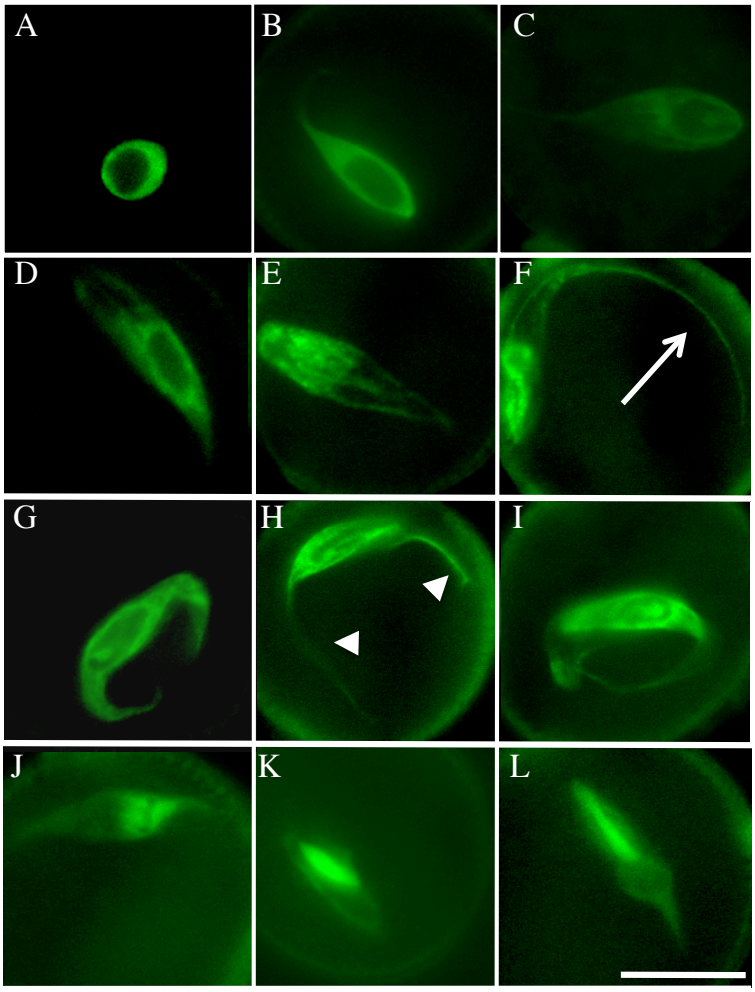

Figure 3.13: Microtubules organisation in the *duo4* germ cell nucleus. A-C) *duo4* germ nucleus elongated prior to germ cells mitosis. D-L) Different examples of shape variation among the *duo4* germ nuclei that failed to enter mitosis with long tail-like extensions (arrow marks a one-tailed-like extension, while arrowheads mark the two tail-like extensions. J) Germ cell at metaphase with the spindle appearing shorter on one side. K-L) *duo4* mutant cells contained bundles of microtubules arranged in disorganized patterns.

bicellular and tricellular pollen grains. Out of the whole population, 6-7 % exhibit a micronuclei phenotype, indicating a disruption of spindles and possibly phragmoplasts in *duo4* germ cells. By imaging MT arrays and germ cell morphogenesis in heterozygous *duo4* population, the *duo4* germ cell was indistinguishable from the wild type until the MBC/LBC stages (Figure 3.13 A-B). In the next developmental stages, when wild type germ cell progressed through mitosis, *duo4* germ cell either arrested at the elongated stage or showed an abnormal spindle structure in about 5 % of the pollen population. However, a closer examination showed that *duo4* GC lacks the closely packed, parallel arrangement of MTs observed in wild type. Instead, the basket-like MT structure was more loosely arranged and highly irregular at this stage, suggesting disorganised MT structures in *duo4* germ cells. In about 3 % of the dividing cells the spindle appeared shorter in one side compared to the opposite one (Figure 3.13 J).

At -3 bud stages, up to 3% of the cells exhibited short remnant MT bundles or rings (Figure 3.13 K-L). Some of these cells were observed in a telophase-like stage, however they never developed an obvious phragmoplast, and the two daughter nuclei remained close to each other (20 cells observed). Thus, in addition to its role in G2/M arrest, the *duo4* mutant also interferes with proper organisation of the MTs during the mitotic stage.

The germ cell at maturity is hugely elongated possess a tail like extension at one end in about 35 % of *duo4* germ cells (Figure 3.13 D-F). However, in about 15 % of the *duo4* germ cells the MT bundles ensheathed the germ cell and fused on both sides, resulting into a long extension at both ends of the *duo4* germ cell axis (Figure 3.13 G-I). The observation might be specific to *duo4* mutation, pointing at another fundamental morphological characteristic of the *duo4* germ cell.

3.4 Discussion

3.4.1 *DUO4* is required for male germline cell cycle progression

duo4 represents a male-specific gametophyte mutant, in which germ cells fail to divide. Developmental analysis revealed that all microspores complete mitosis, giving rise to bicellular pollen grains. Similar to other *duo* mutants, defects in *duo4* are restricted to

progression of the germ cell cycle (Durbarry., *et al* 2005). The ability of *duo4* to progress through asymmetric mitotic division (PMI) and the failure to enter or complete PMII suggested that the germ cell division is regulated in a different way from PMI. Moreover, normal cell cycle progression in microspores indicates that the *duo4* mutation does not affect mitosis processes in microspores.

Developmental analysis revealed that about 43 % of pollen grains in the *duo4* mutant arrested at G2/M transition. In addition, *duo4* mutant displayed a variety of abnormalities at the second pollen mitosis. Similarly to multicellular mammalian systems, the G2/M transition in plants requires mitosis promoting factors (MPF), highly conserved protein kinases, which form mitosis-related CDK-complexes (Porceddu *et al.*, 2001). The expression of CYCB1;1 is restricted to G2/M transition, highlighting actively divided cells (Dube *et al.*, 2005). Whereas cyclin proteolysis is mediated by APC, allowing cells to exit mitosis (Pesin and Orr-Weaver, 2008). In addition, germ cells show a delay in mitosis, evidence of an interruptive of the proper sequence of mitotic events. As a consequence, it is possible that *duo4* germ cells undergo checkpoint arrest and so are delayed until the mitotic defects are repaired. In *Arabidopsis*, ectopic expression of CYCB1;1 accelerated root cell proliferation (Doerner *et al.*, 1996). On the other hand, the ectopic expression of CYCB1;2 can drive cells to overcome G2 checkpoint delay, resulting in abnormal progression during mitosis (Weingartner *et al.*, 2004). The cell cycle in plants is regulated by the interactions of CDK and cyclins. In *duo1* mutant the expression of key regulatory factor, CYCB1;1, controlling progression into mitosis is blocked. As a result of this blockage the germ cells escape pollen mitosis II and enter into a partial endocycle (Brownfield *et al.*, 2009a), suggest that a similar process may occur in *duo4*.

Although, cell cycle arrests at the G2/M transition would account for the most prominent phenotypes observed in *duo4* pollen, it was observed that a minor population escapes into mitosis. This phenomenon may result from checkpoint adaptation, in which the cell cycle arrest can be overcome without complete damage replication (Das *et al.*, 2007). Pollen grains bearing germ cell micronuclei in *duo4* were observed through pollen development. The frequency of micronuclei observed in *duo4* represents about 7 % of the population of arrested cells. A possible explanation that can be proposed for

micronuclei formation is lagging chromosomes and failure to align on the metaphase plate (Fenech, 2007). In the subsequent stages, when the mutant pollen fails to complete chromosome separation, this results in telophase nuclei differing in sizes.

3.4.2 Mutant germ cell nuclei in *duo4* complete DNA replication but fail to enter mitosis

The terminal phenotype of *duo4* indicates that it is very clearly arrested at a late G2 stage, as the *duo4* germ cell is elongated. In addition, relative DNA content measurements of *duo4* mutant germ cell nuclei revealed an average DNA content of 2 C. This demonstrates that cell cycle progression was arrested after completing of S phase but before entry into germ cell mitosis. This indicates *duo4* germ cells do not reinitiate S phase.

In plants, as in animals, the E2F/DP pathway regulates entry into S phase, in which the activity of CYCD/CDKA complexes leads to Rb inhibition, causing transcriptional de-repression of S phase genes (Vandepoele *et al*., 2005). It is evident that molecular events required for DNA replication are functional in *duo4* mutant germ cells. Therefore, *duo4* mutation appears to act specifically at G2/M transition. It is possible that the *duo4* mutant controls the progression into mitosis and G1 or S phase. The hypothesis that *DUO4* controls these events is consistent with the previously reported Chk1-dependent G2 arrest in *Xenopus*, which result from geminin deficiency and leads to the arrest of cells in G2 without shift to second round of DNA replication (McGarry, 2002). Therefore, it can be suggested that DUO4 protein is accumulated prematurely, causing a G2 arrest. Further experiments will be required to evaluate this hypothesis.

Based on the evaluation of DNA content in *duo4* micronuclei and macronuclei, it is not possible to distinguish if the micronucluei result from chromosomal fragmentations or lagging chromosomes. However, the lower but significant amount of the average DNA content of the ‘smaller nuclei’ indicates smaller numbers of chromosomes. Indeed, micronuclei are generally used as an indicator of chromosomal damage (Iarmarcovai *et al*., 2008).

3.4.3 CYCB1;1 fails to accumulate in *duo4* germ cells before entry into mitosis

Unique cell cycle regulation is known to take place in *duo4* male germ cell development in which about 50 % of these cells arrest at G2/M transition of germ cell mitosis. Moreover, the reduced expression of CYCB1;1 in *duo4* germ cells supports the hypothesis that *duo4* plays a role in regulating pollen mitosis II. Downregulation of the CDKA/CYCB1;1 complex activity would lead to the arrest of cell cycle progression at G2/M transition (Corellou *et al.*, 2005) and DUO4 activity could be involved in degradation of CYCB1;1 during cell cycle. These results argue that the *duo4* mutation could result in a failure to synthesize CYCB1;1 prior mitosis entry that correlated with G2 arrest.

Developmental analysis indicates that *duo4* mutant results in germ cells arrest in late G2 phase with 2 C DNA content. However, the presence of the temporally delayed germ cells with mitotic figures, which are not observed in wild type, suggests that *duo4* mutant does not result in a tight regulation of CYCB1;1. The ectopic expression of *cru1*, a fungal Fizzy-related protein in *Ustilago maydis*, also resulted in elongated G2-like state arrest, occurring after APC activation (Castillo-Lluva *et al.*, 2004). Therefore, whether APC is ectopically expressed in *duo4* germ cells or not remains to be tested.

Based on the CYCB1;1::GFP expression pattern in *duo4* compared to wild type, it can be speculated that the *DUO4* gene may be a negative regulator of CYCB1;1 expression during germline development. This conclusion is supported by failure of *duo4* mutant germ cells to accumulate CYCB1;1, which may indicate that *DUO4* belongs to one of the APC activators' subunit. It has been observed that CYCB1;1 is a target for the anaphase promoting complex (APC) and is incompletely degraded at the end of the first meiotic division (MI) in *Xenopus*. Since CYCB is essential for suppression of DNA synthesis and Cdc2 inactivation at MI exit (Iwabuchi *et al.*, 2000; Izutsu *et al.*, 2000).

Similar to *duo4*, the analysis of CYCB1;1 in *duo1* germ cells revealed that *DUO1* regulates the CYCB1;1. Together with CDK-A, CYCB1;1 forms a complex that is essential for the G2/M transition in the cell cycle (Menges *et al.*, 2005). CYCB1;1-GUS fusion containing the native CYCB1;1 mitotic destruction box is targeted for

degradation at anaphase and thus able to act as a G2/M phase-specific marker (Colon-Carmona *et al.*, 1999). This marker was used to examine the dynamic expression of CYCB1;1 during pollen development and it was shown to exhibit GUS activity in both microspores and germ cells, consistent with them entering microspore mitosis and germ cell mitosis, respectively (Brownfield *et al.*, 2009a).

3.4.4 *duo4* germ cells successfully fertilise the egg cell

Cytological characterisation of *duo4* revealed that *duo4* mutant germ cells have the ability to carry out fertilisation. *duo4* germ cells had similar characteristics to the wild type sperm cell, including normal fate marker expression. In addition, the 2 C DNA contents of *duo4* germ cells mimicks the DNA content of wild type sperm cell when the fertilisation takes place. Heterozygous *duo4* plants produce about 50 % bicellular pollen, which is the expected ratio from a fully penetrant gametophytic mutation. However, about 40 % of the seeds were aborted (with embryo at globular stage) when out crossing *duo4* as a male using different ecotypes. This indicates that, even though *duo4* results in a germ cell division defect, the majority of *duo4* germ cells differentiate and develop and are eventually competent to fertilise like wild type sperm cells.

The ability of *duo4* to perform double and single fertilisation is not exceptional since other germ cell division mutants have been identified supporting this hypothesis. The *cdka;1* and *fbl17* mutants both affect the cell cycle regulation (Nowack *et al.*, 2006; Kim *et al.*, 2008). Even though it has been suggested that the *cdka;1,* similar to the *fbl17* in case of delivery one functional sperm cell that preferentially fertilised the egg cell, a recent study has reported that the *cdka;1* pollen can deliver a functional sperm cell with equal ability to fertilise both female gametes (Aw *et al.,* 2010).

Duo mutants result in similar phenotypes in which the germ cell failed to undergo the second mitosis. These mutants deliver a single sperm cell able to enter the female gametophyte, preventing the access of wild type sperm cells. However, the single germ cell in *duo1* and *duo3* mutants is unable to fertilise the female gametes, leading to unfertilised ovules (Rotman *et al.*, 2005). This is possible because *duo1* prevents the expression of sperm specific markers, such as *GCS1*, *GEX1* and *MGH3,* thus showing

incomplete gamete differentiation and function (Brownfield *et al*, 2009a). In contrast, *duo4* germ cells express the *GEX1* and *MGH3* similar to wild type sperm cells, indicating that *duo4* bicellular pollen delivers a fully differentiated single sperm cell able to perform fertilisation. Another possible explanation for the ability of *duo4* to perform fertilisation is based on the stage of the cell cycle that the mutant germ cell is arrested. *duo1* and *duo3* germ cells in mature pollen contain a DNA content of 2.5 and 2.3, respectively, while the *duo4* germ cell failed to enter mitosis with a DNA content about 2 C, the *duo4* germ cells may therefore have the capability to fertilise the egg cell, whilst the higher DNA content of *duo1* and *duo3* make them incompatible with fertilisation.

The expression of the fertilisation markers, CDKA-GUS and KS22-GFP, provides evidence of the ability of *duo4* germ cells to mediate double fertilisation as the expression of the GFP and GUS staining could be seen among *duo4* fertilised endosperm nuclei. The fact that *duo4* fertilised seeds displayed the expression of KS22 is not exceptional since a similar observation has been reported in seeds fertilised with *cdka;1* mutant pollen (Ungru *et al*., 2008). However, the behaviour of the KS22 marker in *cdka*;*1* was described as inconsistent with the authors interpretations. Like in the case of *cdka;1* mutant (Aw *et al*., 2010), the *duo4* germ cell mitosis is either blocked or extensively delayed. Therefore, *duo4* pollen can perform two fertilisation events, fertilising both female gametes, but karyogamy does not take place.

The *duo4* mutant has a gametophytic paternal-effect on embryo and endosperm development, where endosperm development is blocked at a very early stage and embryos develop to the late globular stage. However, it is still largely unclear why the second fusion with the central cell failed to trigger the endosperm nuclei. This series of experiments provide solid evidence that the *duo4* mutant germ cell is able to initiate fertilisation events. However, more experiments, are needed in order to visualise both double fertilisation events in the *duo4* embryo sac.

3.4.5 MT arrangements in elongated GCs

3.4.5.1 Shape changes in the germ cell prior its entry into mitosis

The process of GC division and twin sperm cell formation was analysed, providing a detailed description of the MT cytoskeleton in live germ cells. The aim of this study was to investigate the series of morphological events that occurs in GC during the course of pollen development, which result from MT reorganisations until they separate to form two nuclei. MT bundles were visualised from MBC to mature pollen stages using a male gametophyte specific promoter driving a MT-GFP-reporter, coupled with DIC observations to obtain additional details of each stage of development. The GFPTUA6 marker under the control of *MGH3* promoter was analysed in *duo4* mutant plants. The expression of this marker provides strong fluorescent signals detected only in the germ cell during bicellular stage and in sperm cells in mature pollen in live imaging. In a previous work a newly developed microtubule markers of the prom*NTM19*:GFPTUA6 was used to specifically visualise live MT arrays in microspores and developing pollen (Oh *et al*., 2010). In the present study, using the same protein fusion under the control of the germ cell specific *MGH3* promoter a similar framework configuration and the MT bundles organisation of the GCs were analysed. The clarity of the MTs in the GCs observed was greatly improved by using a germ cell specific promoter that lead to a strong expression in germ cell mitosis but without a high background fluorescence from pollen cytoplasm. This enabled the following of spatial and temporal behavior of the MT cytoskeleton of GCs during different developmental stages, giving extremely comprehensive information.

Basket-like MT arrangements have been described in spindle and GCs (Zhou and Yang, 1991). At the time the GC enters mitosis it undergoes a series of MT organisations, resulting in more MT bundles around the GC, which subsequently becomes elongated. This GC reshaping suggests that MTs have a critical role in the GN morphogenesis (Palevitz and Tiezzi, 1992; Tanaka *et al*., 1989).

The mitotic cytoskeleton of the *Arabidopsis* GC is established via reorganisation of interphase MTs. Preprophase bands (PPB) are critically involved in the determination of the future division plane and the position of the nucleus as it makes the site of cell plate

formation (reviews: Baskin and Cande, 1990; Gunning and Wick, 1985). However, in *Arabidopsis* germ cell no PPB has been observed. A similar observation has been described previously in GCs of other species (Palevitz and Tiezzi, 1992). Obviously, these results indicate that germ cell MTs apply a different mechanism to mark the future division plane. In all cases the sites of attachments of the kinetochores to the chromosomes appear as dark interruptions in the cytoskeleton. At the end of metaphase these dark holes were regrouped at one unique point. The *MGH3*:GFPTUA6 marker enabled the imaging of the kinetochore aligned without using a specific kinetochore reporter because the bipolar spindles are arranged at their opposite sides. Cytokinesis was accompanied by the formation of typical double ring structures that were organised from the spindle mid-zone, and finally they maintained, as a smaller ring at the position of cell plate. The cell plate was not observed, however, more analyses will be required to clarify these observations. Different mitotic stages analyses in *C. majalis* have revealed that no typical cell plate was formed (Del Casino *et al.*, 1999). On the contrary, in the *L. davidii* and *L. macerlatum*, the division of GC is characterised by cell plate formation but the present of phragmoplast was not reported (Zee, 1992). Obviously, the lack of proper metaphase plate appears to be a characteristic of the *Liliaceae* family (Del Casino *et al.*, 1999). At completion of cytokensis, a twisted bundle of MT connects the newly formed sperm cells. During the whole process of mitosis, the germ cell remains connected to the vegetative cell nucleus with a tail-like extension to form the male germ unit (MGU), which has been previously described (Dumas *et al.*, 1998; Lalanne and Twell, 2002).

3.4.5.2 *duo4* shows indirect effect on germ cell mitosis

Predictably, in view of the previous cytological analysis data, *duo4* either blocks or disturbs the germ cell mitosis, resulting in ~50 % of the mature pollen being bicellular. The visualisation of *duo4* germ cell reshaping has revealed that *duo4* germ cells show normal elongation prior to mitosis. However, no typical mitotic figures could be observed. Interestingly, the organisation of microtubules in *duo4 GC* mutant was similar to that in wild type at LBC stage. However, as wild type GCs enter mitosis the *duo4* germ cells fail to properly construct a normal microtubule arrays and spindles, which could explain why *duo4* germ nuclei failed to progress through mitosis

The visualisation of *duo4* germ MTs revealed abnormal mitotic processes that include disruption of spindles and phragmoplasts, which mostly result in micronuclei formation. Generally, the arrangement of the spindle is similar to the wild type, but the opposing half spindles are comparatively shorter in length. In plants, several mutants have been identified that affect cytoskeleton organisation. For example in *Arabidopsis*, mutation in the *TSO1* gene that encodes a protein analogous to the *Drosophila* enhancer of zeste, results in abnormal cell division in floral meristems. It has been reported that the TSO1 protein is able to act as a transcriptional regulator that controls expression of genes encoding some elementary factors that regulate cytoskeleton (Hauser *et al*., 2000; Hauser *et al*., 1998). In the *female gametophyte4* mutant abnormal cellularisation pattern in the embryo sac has observed, which results in organisation defects of the cytoskeleton and nuclear microtubules (review: Otegui and Staehelin, 2000). However, it is difficult to assess precisely whether *duo4* has direct or indirect effect on cytoskeleton organisation.

The most unusual characteristic of *duo4* germ cells is that in about 15 % of germ cells at early and mature stages *duo4* possess two tail like extensions. However, the bundle of MTs that ensheath the GC and fuse to both ends were also reported in other species like *C. majalis* (Del Casino *et al*., 1992). More information is needed to determine the reason for presence of two tails in *duo4* germ cells.

In summary, close examination of *duo4* mutant pollen revealed that the majority of the *duo4* germ cells are arrested at bicellular stage, before entry into mitosis. Moreover, a proportion of mutant *duo4* germ cells that are delayed in cell cycle progression can divide later before pollen shed. Additionally, mutant germ cells in *duo4* displayed chromosomal segregation defects, leading to micronuclei formation which may result of microtubule defects.

Based on previous observations, several hypotheses may help to explain the *duo4* mutant phenotype. It can be proposed that, the ectopic activation of the APC/C during G2 could result in loss of mitotic cyclins before they act to induce mitosis. The premature degradation of CYCB1;1 resulting in G2 arrest has been reported in the *rca1* mutant in

Drosophila. The *Rca1* acts as an Fzr-APC/C inhibitor and in the absence of Rca1 function mitotic cyclins are degraded in G2 of the 16th embryonic cell cycle (Grosskortenhaus and Sprenger, 2002; Zielke *et al*., 2006), resulting G2 arrest. It is clear that *DUO4* is required for the germ cell to progress into mitosis this may involve a mechanism that controls CYCB1;1 expression and CDKA/CYCB activities. Even though the mechanism of regulation of CYCB1;1 through the *DUO4* gene is still unclear, it seems that *DUO4* gene may play a critical role in CYCB1;1 degradation, resulting in late G2 arrest. While there is no data to rule out the first scenario, the data linking the CYCB1;1 degradation at G2/M transition suggests the possibility of the role of an APC component as an attractive hypothesis (see Chapter 4 for misexpression of CCS52A1). Future experiments will be necessary to address these possibilities and it will be an exciting challenge to solve it.

Chapter Four

Isolation and genetic analysis of the *DUO4* gene

Isolation and genetic analysis of the *DUO4* gene

Introduction

In flowering plants, the formation of two sperm cells plays a critical role in double fertilisation and plant fertility. The formation of the sperm cells is achieved following two successive mitotic divisions. In the first mitotic division (microspore mitosis), haploid microspores divide asymmetrically to form two unequal daughter cells, the vegetative and the germ cells. The germ cell represents the male germline and undergoes the second mitotic division (germ cell mitosis) to form twin sperm cells. Despite the importance of sperm cells in plant reproduction, relatively little is known about the molecular mechanisms that govern sperm cell formation. Mutations affecting one of the mitotic divisions during pollen development would disrupt the stereotypical organisation of mature pollen grains. In order to identify such mutants a large-scale morphological screen was undertaken (Park *et al*., 1998). This screening strategy led to the identification of a unique class of mutant, termed *duo pollen* (*duo*) mutants, which specifically affect germ cell division resulting in pollen containing a single germ cell at maturity (Durbarry *et al*., 2005). The *duo* mutants were classified into two main groups based on the shape of the germ cell nucleus. The first group contains *duo1, duo2* and *duo3* that harbour round germ nuclei at anthesis. The second class comprises of *duo4, duo5* and *duo6*, which exhibit elongated germ cell nuclei.

Previous cytological and preliminary mapping data provided an opportunity to further characterise *duo4* mutant phenotype *(*Durbarry, 2004). The first part of this chapter will describe the *duo4* mutation at the genetic and molecular levels, including self and reciprocal crosses. In addition, the previous and newly developed molecular markers applied to identify recombinants in the vicinity of the *DUO4* gene were described. Genetic mapping was used to localise the *duo4* mutation on chromosome IV to a genetic interval of ~15 kb.

The physical mapping localized the *DUO4* gene to a region annotated to contain eight genes and the APC activator *CCS52A1* was predicted to be the best candidate. It was of relevance to investigate what role CCS52A1, a strong cell cycle regulator, and its homologues play in the control of pollen development. For this reason, the final part of this chapter describes experiments to determine whether the *CCS52A1* gene causes the *duo4* phenotype through a gain of function mechanism. These results provide the first insight into the expression and the role of the activities of the *CCS52* gene family during pollen development.

4.1 *duo4* is a gametophytic mutation and is fully penetrant

The *duo4* mutant was backcrossed as female to wild type (Nossen) plants and the phenotype of BC_2 progeny was screened. Fully opened flowers were collected from BC_2 progeny and the pollen was stained with DAPI solution and was viewed under an epifluorescence microscope and nuclear morphology of the pollen grains was scored. Two types of progeny were scored for *duo4* mutant, wild type and *duo4* plants. *duo4* plants from the backcrossed line (BC_2) were allowed to self fertilise and the proportion of wild type to mutant plants was scored. The selfed progeny of *duo4* was screened for pollen phenotype and produced 177 wild type plants to 169 mutant plants and no homozygous plants were found among the screened plants. Chi-squared test (χ^2) showed that these ratios do not differ significantly from 1:1 ratio, ($P = 0.05$ when $\chi^2 = 3.84$). Furthermore, there is no obvious other gametophyte (pollen) or sporophytic phenotypes observed in the heterozygous *duo4* plants. Expression of *duo4* phenotype in the test cross progeny indicated that the *duo4* mutation was originally isolated as heterozygotes and was expected to act gametophytically.

To further confirm that *duo4* is a gametophytic mutation, tetrad analysis was performed using the *quartet1* (*qrt1*) mutant. *qrt1* is a sporophytic recessive mutation, which causes the four microspores produced by meiosis to remain attached for the remainder of pollen

Table 4.1: Tetrad analysis of the *duo4* mutant. The phenotype of pollen grains present within wild type (+/+) and mutant (+/*duo4*). Mature tetrads were analysed by epifluorescent microscopy after DAPI staining. The number of *duo4* in each tetrad is scored.

Genotype	Ratio of wt to mutant phenotype in each tetrad			
	1:3 wt/*duo4*:*duo4*/*duo4*	2:2 wt/wt*: duo4*/*duo4*	3:1 wt/wt: wt/*duo4*	4:0 wt/wt: wt/wt
+/+;qrt/qrt	0	0	0	100 % (n=298)
+/duo4;qrt/qrt	0	90 % (n=359)	7.8 % (n=31)	2.2 % (n=8)

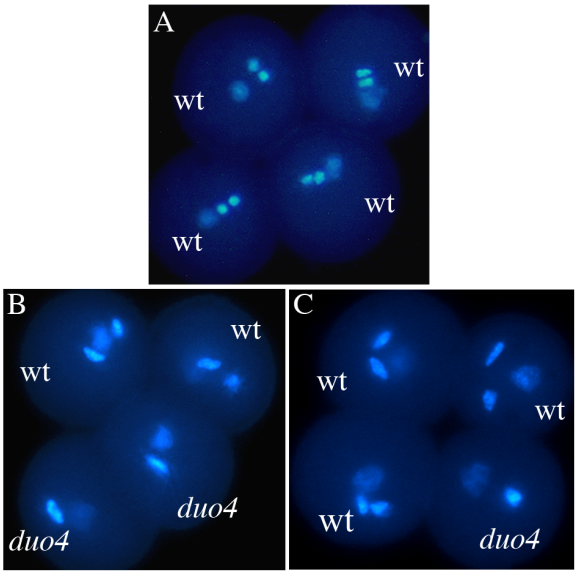

Figure 4.1: The nuclear phenotype of tetrads in the *+/duo4; qrt/qrt* background. A) In +/+:*qrt*/*qrt* all four members of the tetrad show a wild type phenotype B) +/*duo4*:*qrt*/*qrt* two members of the tetrad show a mutant phenotype. C) +/*duo4*: *qrt*/*qrt* example of tetrad showing only one member with a mutant phenotype.

Table 4.2: Genetic transmission of the *duo4* mutation. Number of wild type and mutant plants among test crosses progeny. The reciprocal crosses between the heterozygous mutant and the wild type with the calculated transmission efficiency (TE= number of mutant/number of wild type progeny X 100) through the male (TE^M) and through the female (TE^F). *ms1*; *male sterility1*.

	+/*duo4* X +/+ Female transmission			+/+ X +/*duo4* Male transmission		
Genotype	WT	*duo4*	TE^F	WT	*duo4*	TE^M
No-0	122	118	96.5	272	6	2.2
No-0	185	176	95.8	355	3	1
ms1	204	197	96.6	410	16	4

development as a tetrad (Preuss *et al*., 1994). Heterozygous *duo4* plants (+/+; +/*duo4*) were crossed as female with *qrt* (*qrt*/*qrt*; +/+) plants. Approximately 90 % (n = 359) of the tetrads contained two aberrant members, 7.8 % (n = 31) possessed a single aberrant member and 2 % (n = 8) appeared as wild type whereas 100 % (n = 136) of the tetrads from homozygous *qrt1* plants appear wild type (Table 4.1, Figure 4.1). In addition, tetrads containing one aberrant and one collapsed member were observed at a very low percentage (n = 2). This clearly demonstrates that the *duo4* mutation acts gametophytically and segregates 2: 2 in the tetrads. The absence of tetrads with more than two aberrant pollen grains confirmed the gametophytic role of *duo4* mutation.

4.2 The *duo4* mutation is normally transmitted through the female

Genetic transmission of *duo4* through the male and the female gametes was determined by carrying out reciprocal test crosses in which heterozygous *duo4* mutant plants were crossed to wild type (No-0) plants. Subsequently, the pollen phenotype of the progeny was scored in the offspring. The transmission efficiency (TE) of a mutant allele through both parental gametes describes the ratio of mutant alleles that are normally transmitted to the progeny (Howden *et al*., 1998). If the mutant allele is transmitted with 100 % efficiency, test cross progeny should segregate 1:1 for wild type to mutant plants. When heterozygous *duo4* was used as pollen donor, the transmission of *duo4* relative to the wild type allele was strongly reduced to ~1-4 %, indicating that *duo4* has strongly reduced transmission through the male. However, *duo4* transmission through the female appeared normal, giving rise to an almost equal number of wild type to mutant plants (Table 4.2). These results demonstrate that the *duo4* mutation specifically affects male gametophyte development.

4.3 Positional cloning of the *DUO4* gene

A F2 mapping population was generated by outcrossing heterozygous *duo4* plants as female to Columbia wild type (Col-0) (Figure 4.2A). Initial linkage was established by using a bulk segregant analysis. *DUO4* showed 7.6 % recombinants with the nga1139marker on chromosome IV and 2.1 % recombination with the marker F16G20

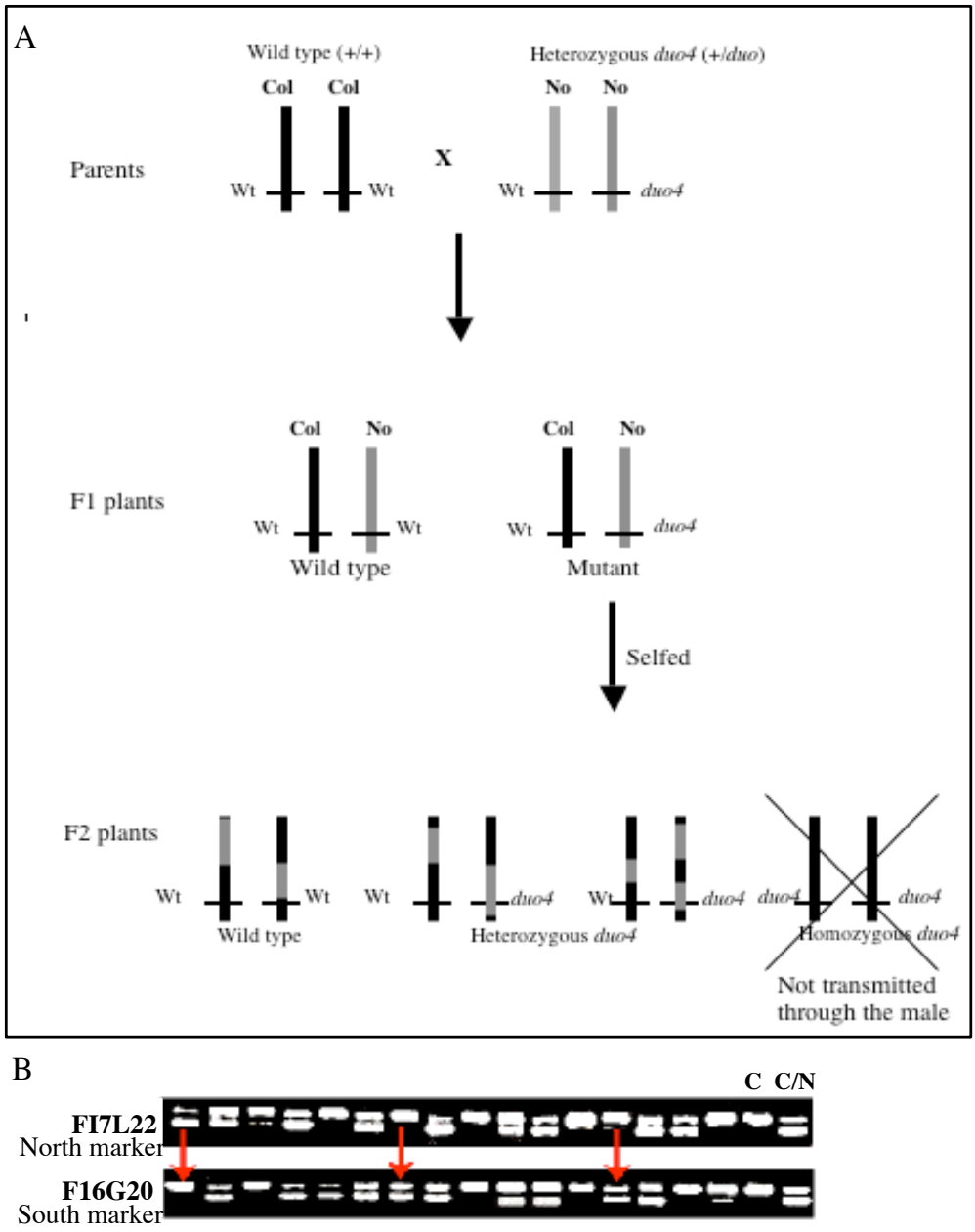

Figure 4.2: A) **Schematic illustration of the crosses that were performed to generate the *duo4* mapping population**. Heterozygous *duo4* plants in the No-0 background were pollinated with Columbia wild type pollen. F1 plants that showed *duo4* phenotype were self-fertilized. F2 progeny was used as the mapping populations. Col-0; Columbia, No-0; Nossen. B) PCR screening of F2 plants *duo4 (No-0 background)* x Col-0 (mapping population) with two flanking genetic markers. F17L22 (the north marker) and F16G20 (the south marker) shown here, to identify recombinants (as indicated by red arrows), based on PCR screening. PCR products visualized by ethidium bromide fluorescence using 4 % agarose gel electrophoresis. Lanes marked C (Col-0) and C/N (F1 parental genomic DNA).

Table 4.3: Molecular markers used to map *duo4* mutation.

Markers	BAC clone	Marker position (bp)	Type	Primer_F	Tm °C	Primer_R	Tm °C	Product size
F17L22	F17L22	11524301	SSLP	GAGCAATTTGGAGATTAGCTGGAATG	55	GATAAGCACAAGGACGTTGATTTCG	55	Col –0 >No-0: 119
T10I14	T10I14	11732701	SSLP	CGTGTGCTTAGCCAGAAACAAAAC	55	CCATCAGATCACATTTTCTCAAACATC	55	Col –0 = No-0: 178
T805	T805	11593701	SSLP	GCTTCTTTAGATTGTCGCCATTCAG	55	TTGAGACGCCGGATAAAATTAC	55	No-0 > Col-0: 109
F7K2	F7K2	11832301	SEQ	TTAGGAGTTTGGGGCTTCAAATCAG	55	TTGCTATCTCTGCAGTTTTATGATTAAC	55	Col-0: 137, No-0: 103
T12H17	T12H17	11966301	SSLP	TCGGCTTCTAAGCAAGTAATTTCAC	55	AGGATCTGTCTTAGCTTGAGGATGG	55	Col-0: >, No-0: 119
810-20	T12H17	12047001	SNP	AGGAGATCACCAGCCATTCTGAGG	64	ATCCGCGTAATATACACGCAAAACC	65	361 Col-0> No-0:T>C
870-80	F7H19	12003101	SSLP	CGACATCATTTGTATCTTGTCCATGC	58	AATGTTTACATTTCTAGTTGTAATTC	58	Col-0: 237, No-0: 207
910	F7H19	12012501	SNP	CCGCTTAACTTCACATGTCGTTTTC	59	CTGGCTGCTGCTGAAGAAATCAAG	59	1635 Col-0 >No-0:G >A
940	F7H19	12023201	dCAPS	GGAATTAGCTGCCTCTGGTTGGCTA	65	GAATGTTCCTCCCCCAATCTGTTGC	64	*Nhe1 cut duo4 199* (No-0)
940_1	F7H19	12023501	SNP	TGGGGTCTCTGTAACGAATAAGTTGG	65	CTGTCTCTGCTCTTGGAATTTGAGG	65	*No-0>duo4 G>C*
940_2	F7H19	12023601	SNP	TGGGGTCTCTGTAACGAATAAGTTGG	62	CTGTCTCTGCTCTTGGAATTTGAGG	60	*No-0>duo4 G>A*
950-60	F7H19	12028401	SSLP	CACGTGTCCATATTAACCGACAACC	68	AGAGAAGCGAAGATCGGACGGTGTG	66	No-0 > Col-0 337
F7H19	F7H19	12028601	SSLP	ATTTAGGGACTCTCTACCGCTGAGG	67	ACCTTCTTAAGGAGTGTATGGTATTC	70	Col –0 > No-0: 180
F16G20	F16G20	12093301	SSLP	GTCCCTTTGACATTGATCACTCAC	55	C ACCTTCTTAAGGAGTGTATGGTATTC	55	No-0 > Col-0: 182
F27G19	F27G19	12273301	SSLP	CCAATCGCCTTAGTCATTTTGACC	55	GCATGCTCGTAAAATGAGACCAGTG	55	No-0 > Col-0 179

that lies north of nga1139 (Durbarry, 2004). Using more precise genetic mapping, the *duo4* mutation was localized between BAC T12H17 (north marker_11524301) and F7H19 (south marker_12273301bp) (Wardle and Twell, unpublished) (Figure 4.3A).

4.3.1 Molecular markers used to map *DUO4*

Three types of molecular markers were localized on chromosome IV used in the mapping experiments: simple sequence length polymorphic markers (SSLPs) (Bell and Ecker, 1994), cleaved amplified polymorphic sequence markers (CAPS) (Konieczny and Ausubel, 1997) and single nucleotide polymorphic markers (SNPs) (Wada and Yamamoto, 1997). An extensive collection of polymorphisms is available between the ecotypes Columbia (Col-0) and Landsberg (Ler), but polymorphisms between Nossen (No-0) and Col-0 are limited in the TAIR database. TAIR (http://www.arabidopsis.org/cgi-bin/maps/Schrom) contains information about all the simple-sequence repeats that are longer than 30 nucleotides in length, along with 200 bp flanking the repeated region (Jander, 2006). These short repetitive sequences are highly conserved and provided a good starting point to develop SSLP markers. In order to find polymorphisms between Col-0 and No-0 new molecular markers were designed using the Col-0 sequence. Fragments of genomic DNA were amplified by PCR and sequenced. The sequence was compared with Col-0 sequence to detect polymorphisms.

The strategy that was used to generate SSLPs markers (F17L22, T805, F7K2, F7H19, F16G20 and AGL19) involved the design of primers across insertions or deletions that are greater than 30 bp in length, allowing the size difference to be detected by PCR amplification and gel electrophoresis. Pairs of PCR primers were designed to detect insertions or deletions, but polymorphisms with size differences less than 5 bp are difficult to detect. In this case the best way was to perform gel electrophoresis for detecting SNP markers (Table 4.3). These include derived CAPS markers; such markers are codominant and can be detected on agarose gel (Michaels and Amasino, 1998).

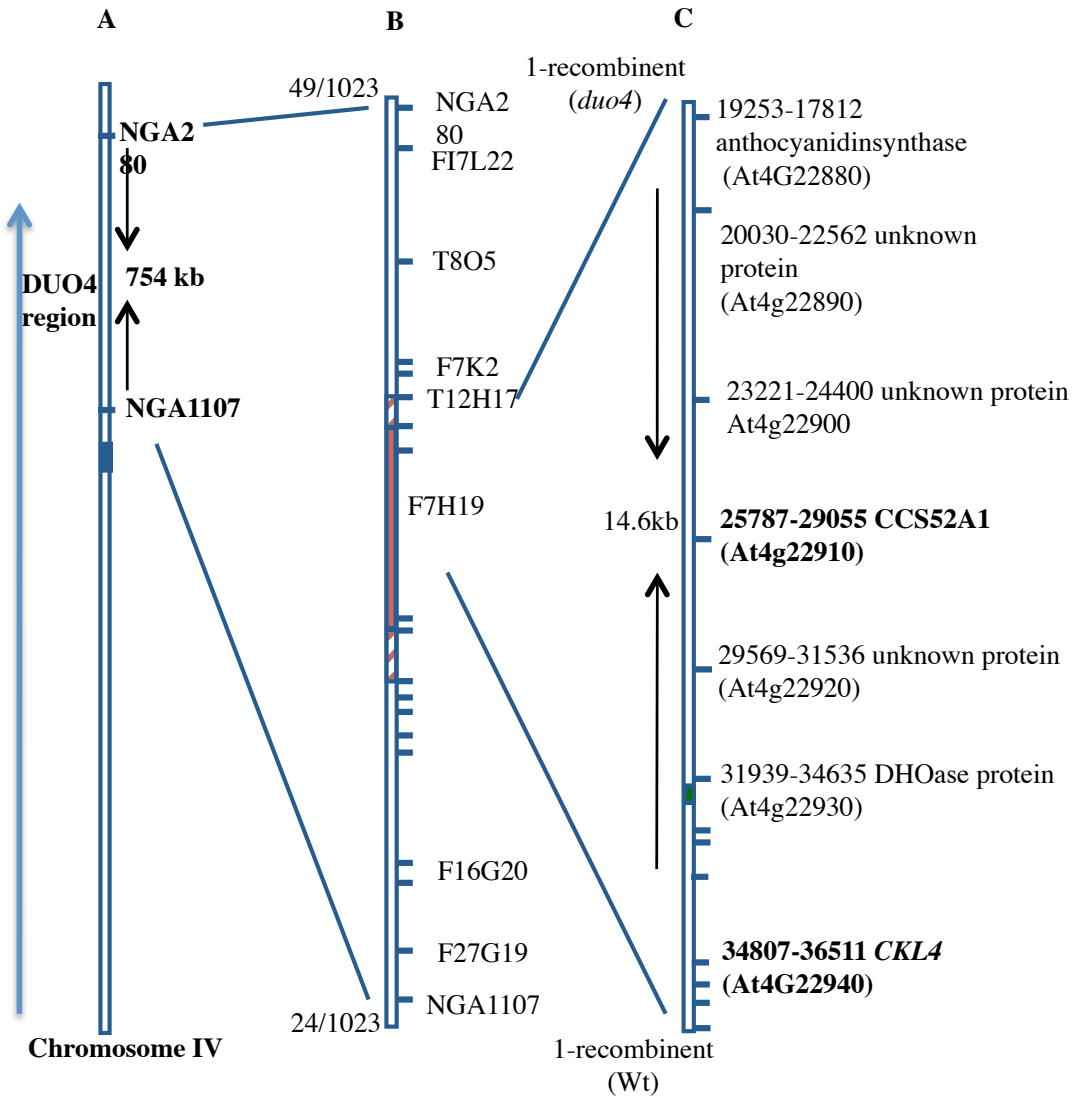

Figure 4.3: Positional cloning of the *DUO4* gene. A schematic representation of important genetic markers used for *duo4* mapping, localized on top of chromosome IV. Blue lines represent the BAC clones on which the respective markers are situated. The number of recombinants identified out of the number of analysed plants for each genetic marker is indicated at both ends. *DUO4* locus was defined between the north marker NGA280 and the south marker NGA1107. Markers were created on the BAC, F7H19 and the *duo4* locus was delineated to a region containing eight genes. In bold, *CCS52A1* and *CKL4* genes both were considered as the best candidate *DUO4* genes.

4.3.2 Genetic mapping of *duo4*

The *duo4* mutation is in the No-0 background and wild type plants in the F2 population homozygous for Col-0 alleles at the *DUO4* locus. In a plant with a wild type phenotype, the presence of the Col-0 and No-0 allele (Col-0/ No-0) would indicate a single crossover event, whereas two No-0 alleles (No-0/ No-0) would represent a double recombination even. Thus, non-recombinant *duo4* plants would have C and N alleles at the *duo4* locus and recombinants would have either Col-0/ Col-0 or No-0/ No-0 alleles.

Fine mapping was carried out by using the F2 seeds from a *duo4* x Col-0 cross. More than 1032 F2 plants were analysed by PCR with different genetic markers. A high throughput assay was used, in which the F2 individuals were grown in 40-compartments trays. Two trays of plant material were harvested for preparation of the DNA from individual plants in a corresponding 96-well plate, and the DNA was used as a template for PCR reactions in a 96-well plate. The PCR products were analysed on high-resolution agarose gels (4 %) to identify the recombinants near the candidate gene. PCR products from 96-well plates were run simultaneously in a large gel chamber and loaded using a multichannel pipette (Figure 4.2 B). Subsequently, recombinants were extracted again using a CTAB-DNA extraction protocol and the genotype investigated with further genetic markers. In this way phenotypic screening of only the recombinant plants is needed to determine the north and south recombinants. This strategy is faster and easier than phenotypically screening the whole population.

A total of 49 north and 24 south recombinants were selected based on PCR screening with two flanking markers, F17L22 (north marker) and F16G20 (south marker). The chosen plants had a signal, either as homozygous or heterozygous, respectively, for the two analyzed markers. Subsequently, the number of recombinants was reduced step by step and the genetic interval of interest was progressively narrowed down using markers closer to the region of interest. In the end, the genetic interval containing the mutation was restricted to 15.2 kb, between At4g22870-80 and At4g22950-60 markers on F7H19 BAC clone (Figure 4.3 C).

4.3.3 Sequencing two candidate *DUO4* genes

The *duo4* locus was localised to a 15.2 kb region containing eight genes according to TAIR (Figure 4.3 C). The region was further examined for genes with potential roles in cell division. According to the annotation provided at TAIR. *At4g22910* and *At4g22940* were considered as the best candidate genes. The *At4g22940* gene was identified as a CDK-related gene (*CKL4)* that forms a tight cluster with 15 related sequences (Guo and Stiller, 2004). However, this gene is one of four genes that are not significantly expressed in cell suspensions (Menges *et al*., 2005). Moreover, this gene structure consists of five exons and four introns, as annotated in TAIR. Sequencing of *CKL4* in *duo4*, revealed two mutations in the first exon that result in amino acid changes. Pairs of primers were designed to amplify the entire *At4g229490* locus. Based on a primer walking strategy, four forward primers and one reverse primer were designed to sequence *CKL4* (Figure 4.4 A). The DNA was sequenced and the chromatogram showed two overlapping peaks both in the first exon. These double peaks represent single nucleotide changes C > G at position 244 bp and G > A at position 281 in the *duo4* mutant. This resulted in a proline to alanine change and a glycine to an aspartic acid change at amino acid positions 82 and 94 respectively (Figure 4.4 A).

In parallel, a study of T-DNA insertions was carried out (Table 4.4). Three different insertion lines were identified in the *CKL4* locus and ordered from the NASC stock centre (Scholl *et al*., 2000) (Figure 4.4 A, Table 4.4). SALK_ 152483 is reported to carry a T-DNA insertion in the 5' UTR. Lines SALK_038725 and SAIL_529 had insertions in the first exon (Figure 4.4 A). About 15 plants from each lines were screened by PCR in order to identify plants hemizygous or homozygous for the T-DNA insertion that later would be screened for *duo4* phenotype. Mature pollen was stained with DAPI to observe possible pollen phenotypes. Genotyping results identified more than one homozygous line from each insertion. However, no visible phenotype was detected in mature pollen.

Since two recombinants remained (one south and one north), DNA from the south recombinant plant was sequenced to look for a recombinant breakpoint. However, the

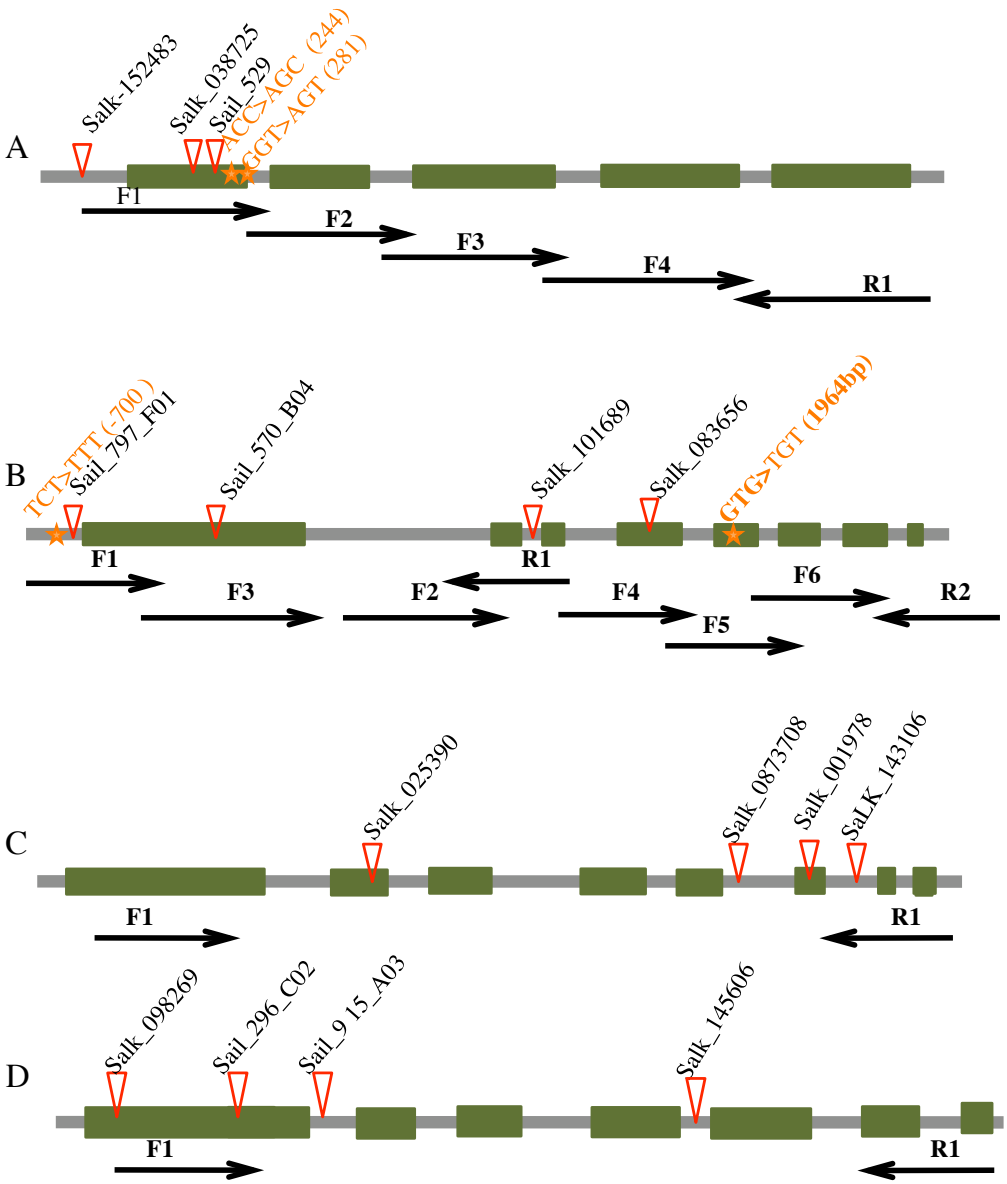

Figure 4.4: Walking sequencing strategy and position of the T-DNA inserts in the *DUO4* candidate genes. Black arrows show the direction of sequencing and primer locations (F1, F2, F3, F4 and R1) that used to amplify and to sequence each gene. The region is split into overlapping fragments. Three to four different insertion lines were ordered for *CKL4* (A) *CCS52A1 (*B) and its homologues *CCS52A2* (C) and *CCS52B* (D). The red triangles indicate the position of the available and analysed T-DNA insertions. Exons are presented as green boxes, introns are in light grey. Single point mutations indicated as orange asterisks.

sequence result revealed that the south recombinant was still recombinant at the position of the determined point mutation. This means that no reversion event occurred in the promising gene, subsequently, *CKL4* gene was excluded. This data indicates that the *CKL4* gene does not correspond to the *duo4* locus.

Since the analysis of *CKL4* gene gave a negative result, *At4g22910* was considered as the best candidate. The *At4g22910* gene encodes a protein similar to the cell cycle switch protein *CCS52A1* (Tarayre *et al*., 2004). This gene has eight exons interrupted by seven introns. Sequencing of this gene, using *duo4* heterozygous plants, revealed two base pair changes but they did not result in any amino acid changes. In addition, sequencing of the promoter region of this gene revealed a possible point mutation (TCT to TTT) occurring at -700 bp position (Figure 4.4 B).

4.3.4 Analysis of T-DNA knockout mutants in *CCS52A1* and its homologues, *CCS52A2* and *CCS52B*

In parallel four T-DNA lines were ordered for the other *DUO4* putative gene (*CCS52A1_At4g22910*) as well as for the two closest homologues, *CCS52A2* (*At4g11920*) and *CCS52B* (*At5g13840*) (Table 4.4).

For the *CCS52A1* gene, four T-DNA lines were obtained: SAIL_797_F01 occurred in the 5'UTR and SAIL_570_B04 in the middle of the first exon. Two SALK lines, 101689, carrying the insertion in the third intron, and 083656, which was located in the first part of the fourth exon, were also studied (Figure 4.4 A, Table 4.4). For *CCS52A2*, SALK_025390 (second exon), SALK_073708C (fifth intron), SALK_001978 (sixth exon) and SALK_143106 (sixth intron) were chosen for analysis. (Figure 4.4 B, Table 4.4). For *CCS52B*, four lines were ordered and analysed. SALK_098269 and SAIL_296_C02 carrying the insertions in different part of the first exon (first and middle part), while SAIL _915_A03 and SALK_145606 were located in the middle part of the first and the fourth introns, respectively (Figure 4.4 D, Table 4.4). DNA was isolated from about 24 plants for each insertion and genotyped, using two different combination of primers to amplify

Table 4.4: Insertion locations relative to the annotated *DUO4* putative genes. The annotation is according to TAIR. The resistance gene tagging the T-DNA insert, and the concentration of antibiotic/herbicide used to select these mutated plants are displayed (kan^{35}_ kanamycin (35 mg/ml) and ppt^{20}_phosphinothricin 20 mg/ml). Gene specific primers were used in combination with LB-insertion primers to confirm the sequences obtained and the size of each fragment which will be generated from each amplification were shown.

Gene	Insertion	Location	Selectable marker	Gene product size (bp)	T-DNA size (bp)
CKL4 (AT4G22940)	SALK_038725	promoter	kan^{35}	1993	600
	SALK_152483	exon_1	kan^{35}	1993	1010
	SAIL_79_C01	exon_1	ppt^{20}	1993	400
CCS52A1 (AT4G22910)	SALK_101689	intron_2	kan^{35}	1635	1417
	SALK_083656	exon_4	kan^{35}	1200	617
	SAIL_570_B40	exon_1	ppt^{20}	1635	1017
	SAIL_797_F01	promoter	ppt^{20}	1635	600
CCS52A2 (AT4G11920)	SALK_073708	exon_2	kan^{35}	3000	700
	SALK_001978	intron_5	kan^{35}	3000	800
	SALK_025390	exon_6	kan^{35}	3000	800
	SALK_143106	intron_6	kan^{35}	3000	700
CCS52B (AT5G13840)	SALK_098269	exon_1	kan^{35}	2000	1000
	SALK_145606	intron_4	kan^{35}	2000	1000
	SAIL_296_C02	exon_1	ppt^{20}	2000	1000
	SAIL_915_A03	intron_1	ppt^{20}	2000	1000

the wild type and the insertion products. This led to the identification of homozygous, heterozygous and wild type plants.

Pollen from all homozygous and heterozygous lines was screened for morphological defects. However, these lines did not differ morphologically from wild-type plants. Therefore, a simple loss of function mutation in CCS52As was not identified. In order to test the possibility that CCS52A1 and CCS52A2 may be functionally redundant, double-mutant will be created by crossing between plants homozygous for an insertion in each *CCS52* locus.

4.3.5 Development of a dCAPS marker for the "*duo4* allele"

In order to positively detect the *duo4* mutant alleles by genotyping, the dCAPs Finder program on the TAIR website was used to develop a dCAPS (derived Cleaved Amplified Polymorphic Sequences) marker. A point mutation that previously was identified in the CKL4 coding region (Section 4.3.3) was used to design primer sets. dCAPS marker, which can recognize single nucleotide changes and result in different restriction pattern for the analysed genotypes. In this way, a marker can be developed that allows a mutant plant to be easily identified by a PCR reaction. A *NheI* restriction site is present in the *duo4* type PCR product (199 bp). This marker was used to detect *duo4* mutant plant in the segregating population without phenotypic analysis. The *duo4* mutant DNA shows a heterozygous pattern when the resulting PCR product is cut with *NheI* enzyme but not in the wild type (Figure 4.5 B).

4.4. CCS52 genes expression analysis

4.4.1 Transcriptional level of *CCS52A1* gene in *duo4* is indistinguishable from the wild type in mature pollen

In order to check the expression level of *CCS52A1* gene in +/*duo4* compared to wild type

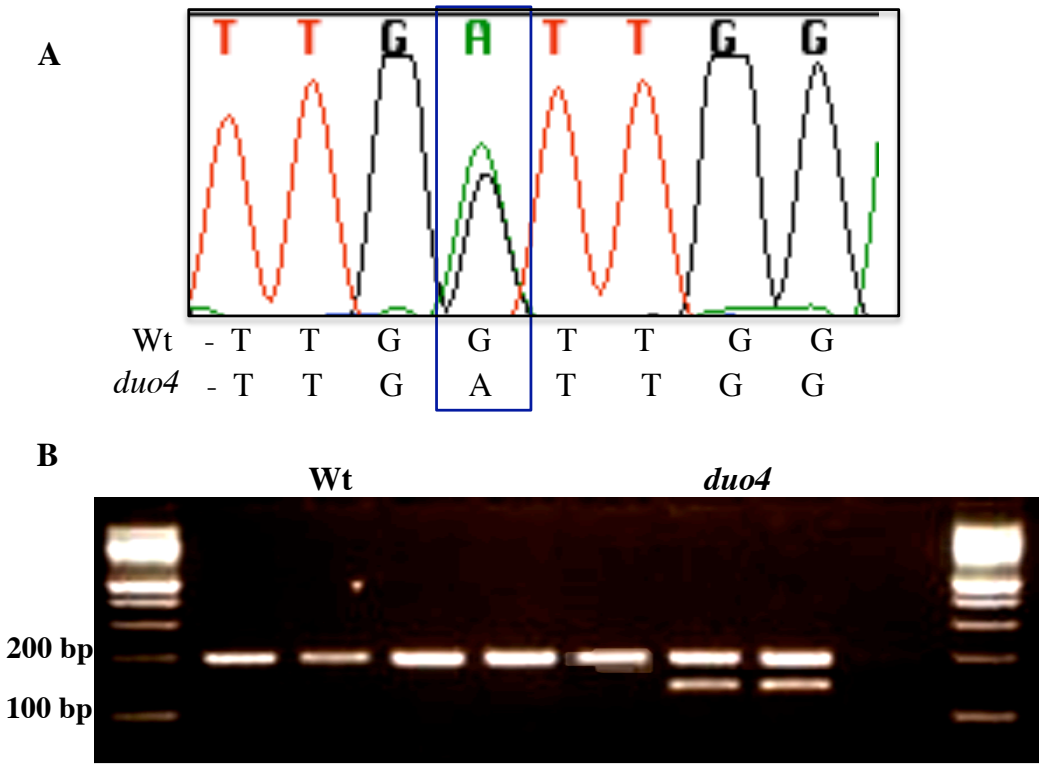

Figure 4.5: Development of a dCAPS marker for the *duo4* allele.
A) Snapshot of the chromatogram sequencing result verifying the presence of point mutation in *duo4* heterozygous plant, resulting in a glycine to aspartic acid change at amino acid 94 in the first exon. B) PCR product amplified with dCAPs primers. PCR products corresponding to wild type and *duo4* mutant DNA restricted with *NheI* and then run on a high resolution agarose gel (4 %). WT plants produced one fragment of 199 bp whereas, heterozygous plants containing *duo4* produced a pattern of two fragments as expected.

(No-0) plants, total RNA was isolated from three independent samples of mature pollen and leaf in wild type and +/*duo4* plants. The cDNA was synthesised and used as a template to check the transcript levels of *CCS52A1*. The result showed that the relative level of *duo4* transcript appeared similar compared to the wild type for any of the investigated samples (Figure 4.6 B). This may be as result of the subtle differences in transcript of the CCS52A1, which makes it hard to detect in mature pollen. However, a further experiment is required in which the relative expression level of CCS52A1 transcripts should be determined by quantitative real time polymerase chain reaction (qRT-PCR).

The sequencing of the *CCS52A1* gene in + /*duo4* reveals that the mutations at locations which do not involve the coding region of the CCS52A1 gene. Theses mutations may affect mRNA splicing sites, in turn, can result in misexpression of CCS52A1. RT-PCR experiment was used to investigate any mRNA splicing defect, which may lead to aberrant transcript, using total RNA extracted from +/*duo4* lines compared to wild type plants. Results of RT-PCR of +/*duo4* using two forward primers in exons 3 and 4 while the reverse primers located in exon 8, flanking the predicted splice sites (Figure 4.6 A). In addition to the expected fragments of 829 bp (splicing 5 exons) and 724 bp (splicing 4 exons), amplification using cDNA of the *duo4* shows a similar fragments, which was observed in wild type. These results confirmed the absence of mutations in the tested splicing sites (Figure 4.6 B).

4.4.2 Verification of expression analysis of *CCS52A1* and two close homologues by RT-PCR analysis

To investigate the expression profile of the *CCS52* genes during pollen development, reverse transcription polymerase chain reaction (RT-PCR) was carried out using four pollen samples of different developmental stages. RT-PCR primers were designed for *CCS52A1* and its two homologues *CCS52A2* and *CCS52B*. PCR amplification was performed using 1 in 10 dilutions of the synthesised cDNA (750 ng) and the transcripts were amplified for 30 cycles with the RT-specific primers. Genomic DNA was also amplified to check primer efficiency and the correct size of amplicon and to detect any genomic contamination.

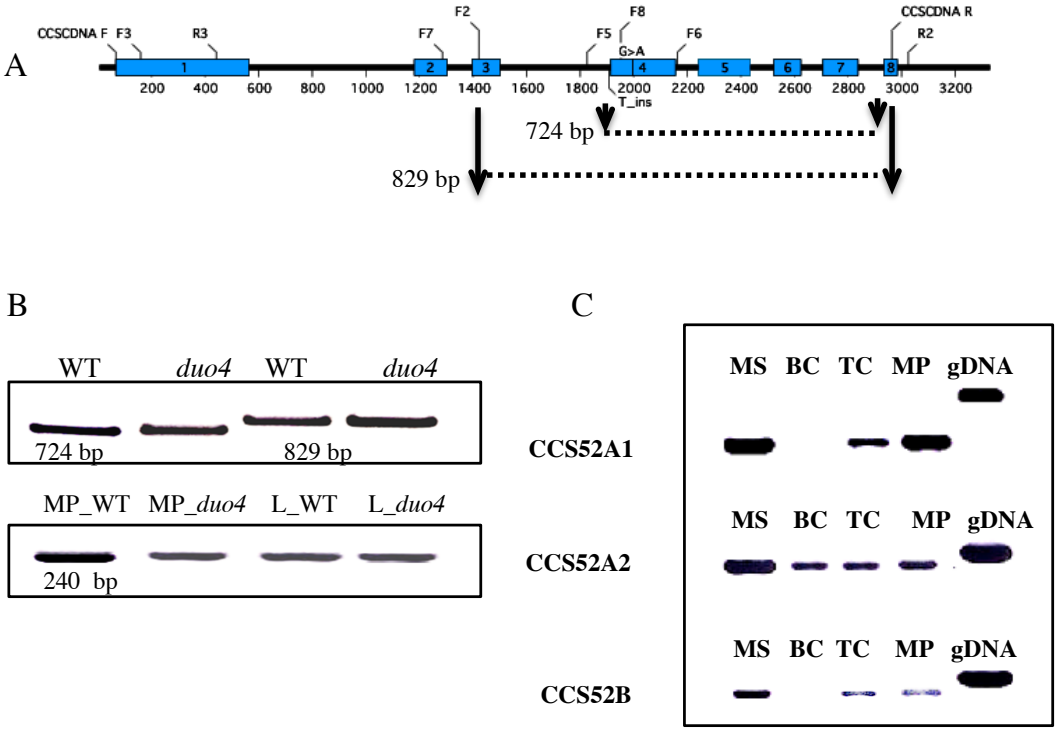

Figure 4.6: Expression of CCS52 in pollen. A) Schematic representation of CCS52A1 showing position of the primers that were used in the RT-PCR analysis along with the position of the exons. B) Results of RT-PCR of +/*duo4* using primers in exons 3, 4 and 8. In addition to the expected fragments of 724 bp and 829 bp, amplification using cDNA of the *duo4* shows a similar fragment of ~240bp, which was observed in wild type. C) Expression profile of the *CCS52* genes during wild type pollen development. RT-PCR was performed from RNAs extracted from mature pollen and leaves from WT and +/*duo4* plants. The stage of development are MS; microspore, BC; bicellular, TC, tricellular and MP; mature pollen, gDNA; genomic DNA.

Histone H3.2 was used as a control, as its expression transcript is stable throughout pollen development (the data is not shown).

The RT-PCR results showed that *CCS52A1*, *CCS52A2* and *CCS52B* are expressed highest in the microspore stage (MS) (Figure 4.6 C). In contrast to the situation in *CCS52A1* and *CCS52B*, were no transcript could be detected at bicellular stage, the CCS52A2 transcript was detected with a slight increase at the same stage (BC) (Figure 4.6 C). For the three analysed genes, it is clear that the expression levels were the lowest throughout tricellular (TC) and mature pollen stages. Interestingly, the expression of *CCS52A1* showed a clear increase at mature pollen compared to the tested homologues *CCS52A2* and *CCS52B* (Figure 4.6 C). The expression levels remained the same in *CCS52A2* (Figure 4.6 C).

4.4.3 CCS52A1 and CCS52A2 are expressed during different stages of pollen development

To explore the expression pattern of the *CCS52A* genes further during male gametogenesis, the *CCS52A1* (1.3 kb) and *CCS52A2* promoters (2.4 kb) were used to drive H2B-GFP. Each of the cloned promoters was used to transform wild type No-0 and *duo4* /+ plants. Transformed plants were selected on BASTA and 24 resistant plants were examined. Mature pollen and buds at different developmental stages, from each construct, were analysed to monitor the spatial expression pattern of each promoter.

Analysing mature pollen from T1 plants showed only a few lines with a detectable GFP signal in wild type sperm cell as well as *duo4* mutant germ cell (n= 4). Moreover, the GFP signal in both sperm and *duo4* germ cells was quite low, which made it very difficult to count pollen with GFP fluorescence at mature pollen stage.

At early developmental stages, a relatively weak GFP signal could be detected in polarized microspores prior to asymmetric division (Figure 4.7 A), indicating that CCS52A1 may be involved in microspore division. In early bicellular pollen, GFP was still detectable in both the germ cell nucleus and the vegetative cell nucleus (Figure 4.7 B). In the next stages, mid

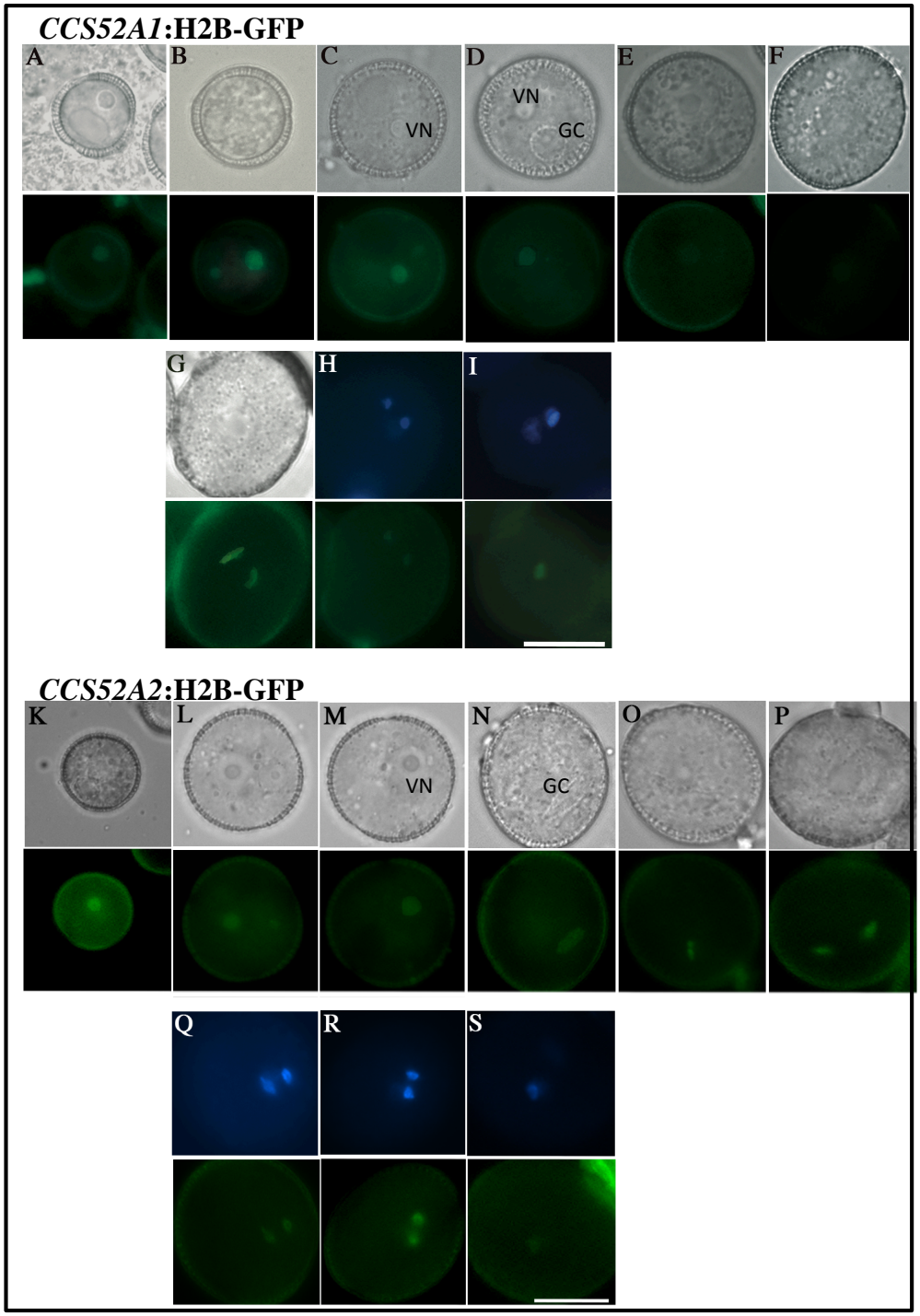

Figure 4.7: Expression profile of *CCS52A1*:H2B-GFP and *CCS52A2*:H2B-GFP promoters. DIC image (upper panel) and GFP fluorescence (lower panel) of different stages of pollen development in plants carrying the Prom*CCS52A1*:H2B-GFP (A-I) and Prom*CCS52A2*:H2B-GFP (K-S). GC; germ cell, VN vegetative nucleus. H-1 and Q-S show mature DAPI stained mature pollen (corresponding DIC images were not included). Scale bars = 15μm.

and late bicellular, the GFP fluorescence it continues to persist in the vegetative nucleus and no obvious GFP signal was observed in the germ cell nucleus (Figure 4.7 C-E). At early tricellular and mature pollen, the fluorescence signal was present only in the sperm cell nuclei, however, the promoter activity appeared to decrease in mature pollen (Figure 4.7 G-H). Similarly, CCS52A2 was clearly detectable at the microspore stage (Figure 4.7 K). While the fluorescence signal in the germ cell appears to decline following microspore division (Figure 4.7 L), it continues to persist in the germ cells during bicellular stage of pollen development. A clear signal was observed in the germ cell during mitosis in the case of *CC52A2*, but not *CCS52A1* (three out of six lines analysed) (Figure 4.7 N-O). In early tricellular and mature pollen, the fluorescence signal was present only in the sperm cell nuclei, however, the promoter activity appeared to decrease in mature pollen (Figure 4.7 Q-S). These results suggest that the activities of *CCS52A1* and *CCS52A2* genes may be required for the cell cycle progression during pollen development. It is also worth noting that the GFP signal of mature pollen was observed only in 2 lines compared with the microspore signal which was observed in all the analysed lines, suggesting that the expression of CCS52A1 together with the analysed homolog, CCS52A2, is not very high at mature pollen stage.

4.5 A point mutation in *DUO4* promoter might be sufficient to induce germ cell division arrest

Fizzy-related proteins regulate the degradation of mitotic cyclins through the APC activation pathway. Therefore, the ectopic expression of APC activators can induce G2-like arrest as a result of the unscheduled degradation of mitotic cyclins (Kitamura *et al*., 1998). It is likely that endogenous overexpression of CCS52A1 may lead to a *duo4* phenotype. Indeed, the lack of *CYCB1;1* expression in *duo4* germ cells provide evidence to support the possibility that DUO4 protein is encoded by a *CCS52* related gene (section 3.1.5.5.1). In addition, the final mapping interval included *CCS52A1*. Furthermore, analysis of the T-DNA insertion lines resulted in no obvious phenotype, indicating the *duo4* mutation may be the result of a gain-of-function or misexpression of the *CCS52A1* gene.

To confirm that misexpression of *CCS52A1 (*CCS52A^{ME}) is the cause of the *duo4* phenotype, C-terminal GFP fusions were generated with the open reading frames of *CCS52A1* and its closely related homologue, *CCS52A2*, in frame with a *GFP* reporter gene. The coding regions of the *CCS52A1* and *CCS52A2* genes were PCR amplified and inserted into GATEWAY entry vector pDONR221 cloning system (Invitrogen). Both stop and nonstop C- protein terminal fusions were made and were specifically expressed in pollen, under the control of a germ cell specific 1.2 kb fragment, *DUO1* promoter (Rotman *et al.*, 2005), whose expression is not affected in *duo4* as *MGH3* appeared to be expressed normally. The insert was then transferred into the GATEWAY destination vectors, pB34GW7 (ppt^{R}). The resulting GFP constructs were transferred into *A. tumefaciens GV3101* and then into wild type No-0 and *duo4* heterozygous plants (Clough and Bent, 1998). The constructs were previously sequenced to check that the GFP coding regions were in the correct reading frame with *CCS52*, and for the absence of any mutations.

4.5.1 Misexpression of *CCS52A1* phenocopied the *duo4* mutant phenotype

4.5.1.1 Analysis of the primary transformants

T1 seed were selected on soil hydrated with 20 mg/L of BASTA and the resistant seedlings were transferred to individual pots and grown until flowering. DAPI stained mature pollen grains from wild type plants were screened for the percentage of bicellular pollen phenotype with a possible scenario that *duo4* pollen phenotype results from misexpression gain of function mutation. In this case it is predicted that 50 % *duo4*-like and 50 % wild type pollen would result in transformant (T1) lines. i.e. the expected distribution between *duo4* and wild type pollen from the T1 plants would be in the case of phenocopy or enhance *duo4* mutation ~1:1 bicellular: tricellular pollen phenotype in the wild type transformed plants. If the transformed plants display a similar phenotype to the original *duo4* mutation, this would support the hypothesis that misexpression of CCS52A1 may be the cause of the *duo4* phenotype.

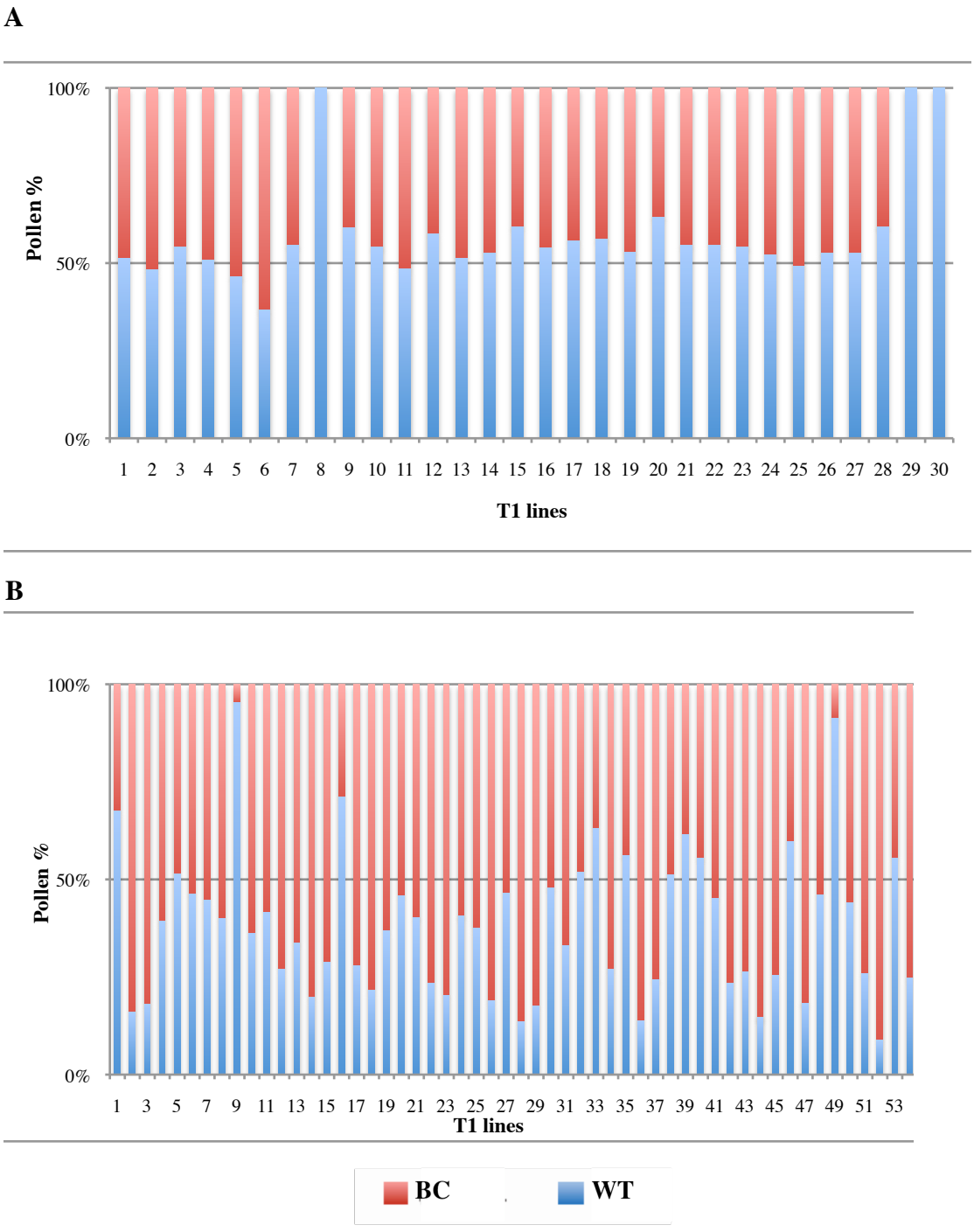

Figure 4.8: Counts of the percentage of bicellular pollen in T1 plants harbouring the construct pDUO1-CCS52A1. Graph shows the segregation of mutant pollen grains (*duo*) in the T1 primary transformants harbouring the construct pDUO1-CCS52A1 in wild type plants (A) and + /*duo4* plants (B) (BC-bicellular; WT-wild type)

Transformants harbouring pDUO1-CCS52A1 (n=30) were classified into three categories based on the proportion of *duo4*-like pollen grains in each transformed line. In 70 % of the primary transformants the proportion of *duo4*-like pollen grains ranged from 43 – 51 %. Three percentages of the transformants showed more than 63 % *duo4*-like pollen grains and the remaining transformants showed less than 40 % mutant pollen grains (Figure 4.8 A).

Chi-square tests showed that the three categories are statistically different from each other ($p>0.05$). This result revealed that 70 % of the transformants phenocopy *duo4* mutation and 25 % of the transformants partially phenocopied *duo4* mutation. In partially phenocopied lines the segregation of *duo4* mutant to wild type pollen was 1:1.5 and in the fully phenocopied penetrant lines the segregation ratio was 1:1, indicating that the construct behaves in a gain of function manner, assuming that the plants carried one T-DNA insertion. In addition, the overall phenotype was comparable to the *duo4* phenotype. In fact, these lines had similar mitotic errors (micronuclei). The non-transformed lines showed no deviation from the wild type phenotype (Figure 4.8 A).

A similar result was observed of the counts of the transformants generated in +/ *duo4* plants (n=53), which showed a significant increase in the proportion of the *duo4*-like phenotype. This screening showed that the majority of plants fell within the normal range of % *duo* that representing fully penetrant, approximately 50 %. Chi-squared test verified that 25 % of the *duo4* transformant lines were significantly different from 1:1, showing a 3:1 *duo* to wild type segregation ratio. While 47 % were significantly similar to the segregation ratio 1:1 and 13 % was partially penetrant with 2:1, *duo* : wild type. None of the plants screened resulted in wild type segregant plants, deviates from the expected 1:1 wild type to mutant plants segregate from heterozygous parents, indicating that the high level of CCS52A1 induces *duo* phenotype in wild type segregant plants (Figure 4.8 B). None of the BASTA resistant plants with the C-protein terminal GFP fusion showed a GFP fluorescence signal when analysed under both the fluorescence and confocal microscope, which made it difficult to identify how many inserts the transformant had.

Overall, screening of the T1 progeny showed that the phenotype observed is likely to be

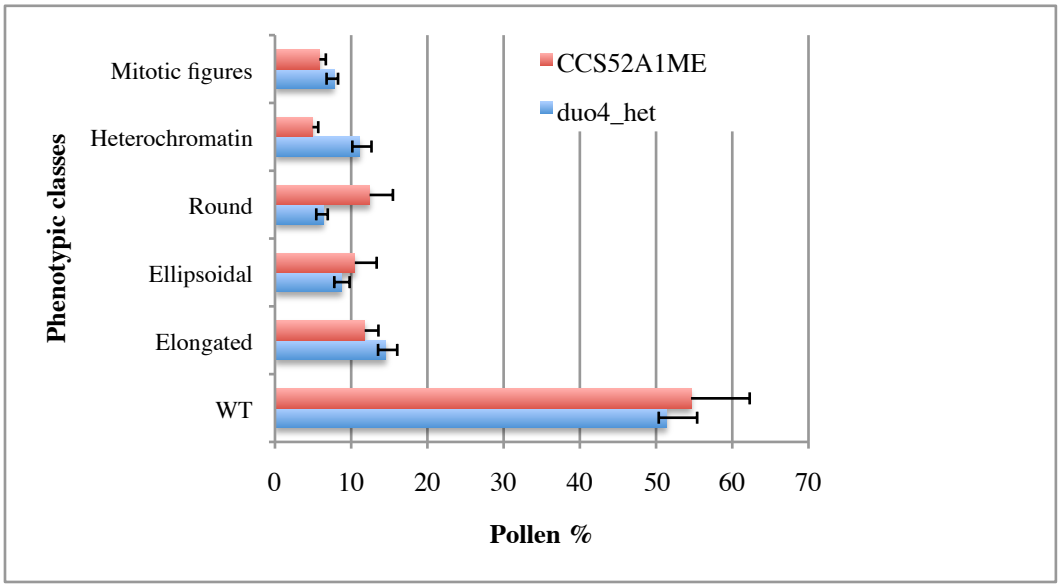

Figure 4.9: The frequency of pollen phenotypic classes in heterozygous *duo4* and transgenic lines harboring the construct promDUO1-CCS52A1. Counts were made on different heterozygous *duo4* and T1 individuals. Data are derived from > 600 pollen grains counted from each line. Pollen was collected at anthesis.

hemizygous for the transgenes insertion and of the overexpressed tested gene resulted in ~39- 48 % *duo4*- like pollen phenotype in the wild type transformed T1 generation. CCS52A2 was also expressed in wild type plants as a CCS52A2-GFP (green fluorescent protein) fusion protein under the control of the *DUO1* promoter. In total, 20 independent lines carrying the pDUO1:CCS52A2-GFP construct were generated. No obvious phenotype was observed in the transgenic plants due to the presence of a stop codon within the coding region in the stop version. Consistent with *CCS52A1*, misexpression of nonstop version *CCS52A2* induces the same *duo4*-like phenotype in the analysed plants. These data can be explained by a functional redundancy of the CCS52 protein family.

4.5.1.2 Phenotypic characterisation of CCS52A1^{ME} compared to *duo4* mutant

To address whether CCS52A1^{ME} shows similar effects to the *duo4* mutation, a comparison was performed on the mature pollen shed from these plants (four lines). The result revealed that 15 % of the germ cells in CCS52A1^{ME} plants exhibit roundish phenotype compared to 8 % in +/ *duo4*. The elongated germ cells include elongated, ellipsoidal and ridged boundary classes, account for 23 % of the transformed population compared to 34 % in +/ *duo4* (Figure 4.9, also see Section 3.1.1). The transformed plants harbouring pDUO1-CCS52A1 show stronger effects compared to *duo4* mutation, which are most likely caused by higher transgene expression levels compared to +/ *duo4* in the transgenic plants. In addition, the nuclear DNA content was measured in several lines. Germ cells of CCS52A1^{ME} lines showed approximately 2.3 C compared to 2 C in *duo4* germ cell, indicating that a new round of endoreduplication had taken place in a proportion of *duo4*-like germ cells.

The biological significance of *duo4*-like germ cell in terms of its ability to perform a single fertilisation was also investigated. To explore this, pollen from the CCS52A1^{ME} was used to fertilise *ms1-1* pistils. Three days after pollination (3 DAP) siliques were dissected and ovules were cleared. The observations showed that *duo4*-like pollen was capable to successfully fertilise the egg cell, and that the embryo in these fertilised seeds did not differ from that in the *duo4* pollen, arguing that pollen tubes from CCS52A1^{MS} plants are able to

guide normally and are able to initiate fertilisation. These results are consistent with the paternal effects of *duo4* mutant pollen on seed development (section 3.2.2).

4.6. RNAi Knockdown of *CCS52A1* was predicted to suppress *duo4* phenotype

An RNAi knockdown approach was used to further demonstrate that inappropriate expression of *CCS52A1* in the germline is the cause of failure of entry of *duo4* germ cells into mitosis. Because the possible function of the redundancy among the CCS52A family members, a strategy was used to design RNAi fragments that would target only CCS52A1 degradation. Based on gene sequence two fragment were selected hairpin 1 and 2 that would target only CCS52A1 (hp1 and hp2, Figure 4.10 A). RNAi Knockdowns of CCS52A1 with two germ cell specific promoters. *DUO1* and *GEX2*, driving hp1 (250 bp) and hp2 (285 bp) constructs were generated. Stable transgenic lines harbouring these constructs were transformed into +/ *duo4* plants. Mature pollen from about 24 T1 lines for each construct was examined by fluorescence microscopy. In order to determine the ability of knockdowns of CCS52A1 to rescue the *duo4* bicellular phenotype, the frequency of *duo4* pollen grains was determined by counting the number of bicellular and tricellular pollen grains after DAPI staining. In DUO1-hp1 the transformants segregated into 17 :7 wild type to *duo4* plants (Figure 4.10 B, appendix: Figure A2). In DUO1-hp2 the transformants segregated into 18 :6 wild type to *duo4* plants (Figure 4.10 D, appendix: Figure A2). For GEX2-hp1 and hp2 the transformants segregated into 10 :10 and 16 :8 wild type to *duo4* plants, respectively (Figure 4.10 C-E, appendix: Figure A2). Pollen phenotype of all the *duo4* transformants were screened to determine if *duo4* phenotype had suppressed for reversion from 1:1 to 3:1 wild type to mutant pollen phenotype. It was found that multiple +/*duo4* individuals showed a reduced percentage of bicellular pollen in *duo4* heterozygous plants resulting in that the transformants were not segregating 1:1 for wild type to *duo* pollen grains. The results revealed that in pDUO1-hp1 12.5 % of the transformants partially complemented *duo4* mutation and 8 % of the transformants fully complemented *duo4* mutation, while the rest of the transformants (75 %) show wild type phenotype (Table 4.5 appendix: Figure A2). In partially complemented lines the segregation of wild type to

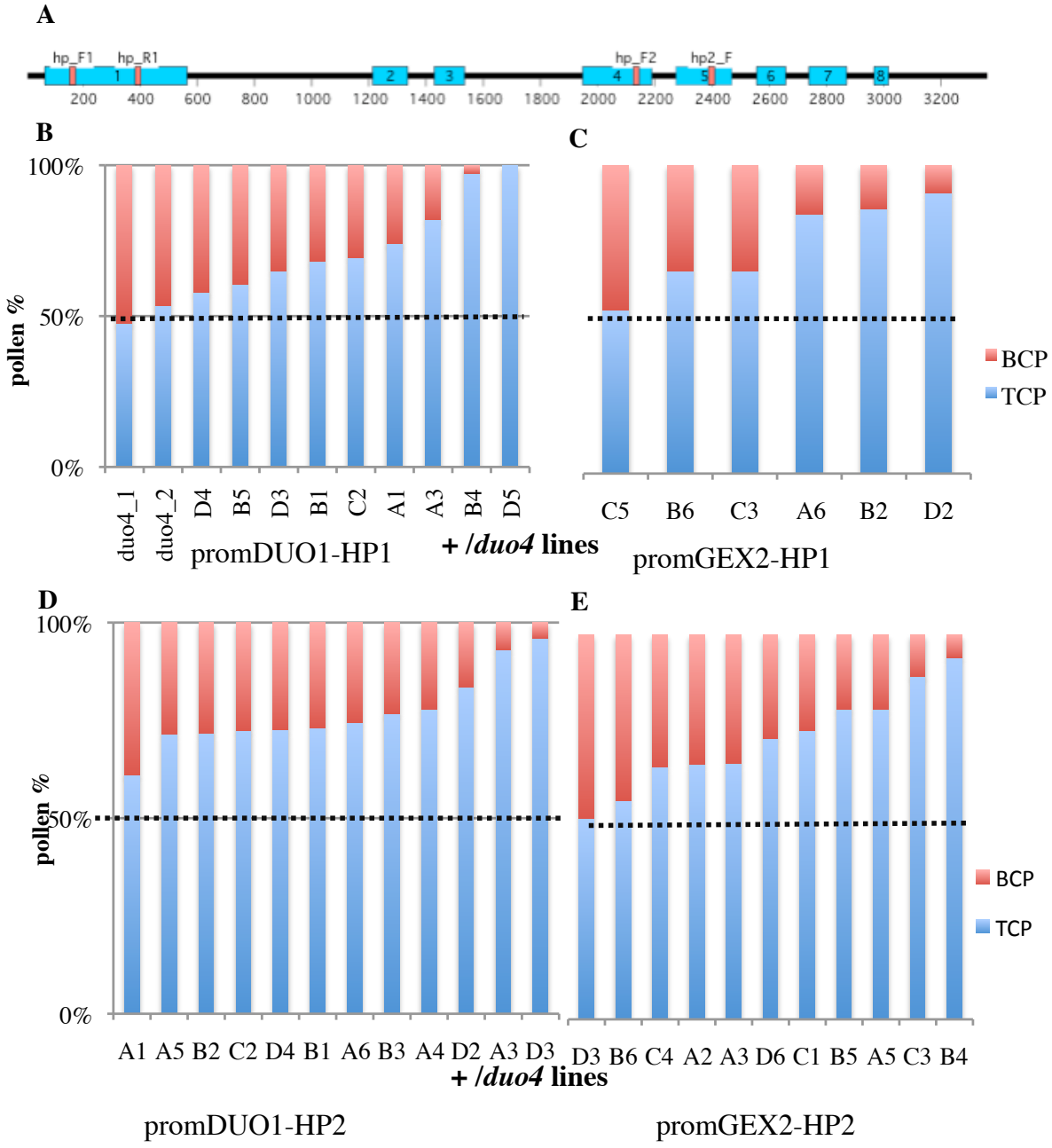

Figure 4.10: Rescue of *duo4* germ cell mitotic defect by RNAi knockdown. A) Diagram of CCS52A1 gene showing the position of hairpin1 (hp1) and hairpin2 (hp2) fragments. B-E) Graph showing the frequency of tricellular and bicellular pollen grains. Four different constructs were used to drive the expression of RNAi Knockdown of CCS52A1 to induce transcripts turnover at G2 stage during germ cell development. Heterozygous *duo4_1* and *duo4_2* were used as control to monitor the percentage of rescue, where 50 % of the pollen is TC (tricellular pollen) and the other 50 % is BC (bicellular pollen), is marked with a dashed lines.

Table 4.5: RNAi knockdowns are able to complement the cell cycle defect in the *duo4* mutant. NS: not significant, * indicate statistically significant differences from an expected 3:1 ratio ($p < 0.05$). TC; Tricellular pollen and BC; Bicellular pollen.

pDUO1-hp1					3:1	
Line	**TC**	**BC**	**Total**	**TC:BC**	**X^2 value**	**Significance**
A1	170	60	230	3:1	0.1	NS
A3	140	31	171	4.5:1	4.3	*
B1	120	56	176	2:1	4.4	*
B5	96	63	159	1.5:1	3.3	NS
C2	120	53	173	2.3:1	4.2	*
D3	106	57	163	2:1	3.3	NS
pDUO1-hp2					3:1	
Line	**TC**	**BC**	**Total**	**TC:BC**	**X^2 value**	**Significance**
B2	109	18	127	6:1	8	*
B6	140	73	213	2:1	10	*
C3	73	38	111	1.9:1	5	*
pGEX2-hp1					3:1	
Line	**TC**	**BC**	**Total**	**TC:BC**	**X^2 value**	**Significance**
A1	75	48	123	1.5:1	12.90	*
A4	140	40	180	3:1	0.74	NS
A5	55	22	77	2.5:1	0.52	NS
A6	116	40	156	3:1	0.03	NS
B1	150	55	205	3:1	0.37	NS
B2	114	45	159	3:1	0.92	NS
B3	112	34	146	3:1	0.23	NS
C2	120	46	166	3:1	0.65	NS
D2	76	15	91	5:1	3.52	NS
D4	95	36	131	3:1	0.43	NS
pGEX2-hp1					3:1	
Line	**TC**	**BC**	**Total**	**TC:BC**	**X^2 value**	**Significance**
A2	75	38	113	2:1	4.49	*
A3	80	40	120	2:1	4.44	*
A5	116	28	144	4:1	2.37	NS
B5	91	22	113	4:1	1.84	NS
B6	79	60	139	1:1	5.89	*
C4	82	43	125	2:1	0.35	NS
D6	136	50	186	3:1	24.46	*

mutant pollen was 1.5: 1 and in fully complemented lines the segregation ratio was > 2.5: 1, while in the non-complemented lines the proportion of *duo* pollen were similar to *duo4* heterozygous parental lines (Figure 4.10 B-C) with four of these lines showing full rescueof germ cell mitotic division. Similarly, pDUO1-hp2 can also fully complemented the *duo4* mutation since the 8% of analysed plants showing about 75% tricellular pollen grains. Statistical analysis of the cell cycle rescue was carried out using chi-square analyses, which tested deviations of the observed ratio of wild type to *duo4* pollen grains from a 3:1 ratio (in fully-rescued single locus line) and a 1:1 ratio (a non-rescued line). As predicted, multiple + /*duo4* individuals showed a reduced percentage of bicellular pollen in *duo4* heterozygous plants while tricellular pollen percentages that was observed in lines rescued with CCS52A1 knockdown showed no difference from a fully rescued line (3:1).

In transgenic lines that fully complemented with the GEX2-hp1 and GEX2-hp2 (Figure 4.10 C-E), the percentage of tricellular pollen in the population was approximately 75 %. Chi-square analysis of the GEX2-hp1 and GEX2-hp2 expression results showed that the ratio of tricellular to bicellualr pollen does not differ significantly from a fully rescued line with a 3:1 ratio (Table 4.5, appendix: Figure A2). This confirms that GEX2-hp1 and GEX2-hp2 are able to fully rescue the *duo4* cell cycle defect. It is worth noting that in some of the T1 lines the difference from a 3:1 ratio was significantly high, which indicates that these plants might have more than a single insertion of the transgene. In addition, the number of insertions and general expression level is expected to differ amongst a T1 population, which reflects a difference in the percentage of tricellular pollen. These experiments provide solid evidence that *duo4* phenotype results from the ectopic expression of CCS52A1. Thus supporting the possibility that inappropriate expression of CCS52A1 in the germline results in the failure of germ cells to entre mitosis, while S-phase proceeds normally, and *duo4* mutant acts specifically during G2.

4.7 Discussion

The aim of this chapter was the identification and the genetic characterisation of genetic components involved in male gametophyte development. Forward and reverse genetics

approaches were employed to identify the molecular nature of the male gametophytic *duo4* mutation. *AtCCS52A1* and *AtCCS52A2*, two genes that encode putatively APC activators were characterised. In the first part of this chapter the main focus was to identify the molecular identity of the *DUO4* gene and to study its role in male gametophyte development. In the second part of this chapter the expression and functional analyses was used to study the *CCS52A1* and *CCS52A2* genes and to describe their putative roles in male gametophyte development.

4.7.1 *duo4* is a male gametophyte specific mutant

Phenotypic analyses showed that *duo4* germ cells are arrested at germ cell division, resulting in about 50 % bicellular pollen at anthesis. The analysis of cross progeny indicating that the *duo4* mutation was originally isolated as heterozygote and specifically impairs male gametophyte transmission while is fully transmitted maternally. Expression of 50 % or less than 50 % mutant pollen grains in + /*duo4* with tetrad analysis confirmed the gametophytic role of *duo4*. The normal female transmission in *duo4* suggests that the development or function of the megagametophyte is unaffected.

4.7.2 *duo4* mutant was isolated through mapping positional cloning approach

Initial linkage was established by using a bulk segregant analysis, flanked by NGA1139 and F16G20 markers in genetic interval about 145 kb (Durbarry, 2004). The outcome of the map based cloning approach resulted in localization of the *DUO4* gene on the lower arm of chromosome IV. It was critical to develop new molecular markers in the vicinity of *DUO4* gene as the mapping progressed. Obviously, this strategy has led to narrowing down the region containing the *DUO4* gene to a genetic interval of 15 kb, with one north and one south recombinants flanking the mutation. F3 seeds from the south recombinant were grown and were confirmed as recombinants in the vicinity of the *DUO4* gene. The final mapping interval included eight genes, two of which, *CKL4* and *CCS52A1,* were selected as candidate DUO4 gene with respect to their role in cell division.

Sequencing of the first gene, *CKL4,* revealed two possible point mutations in the first exon. However, genotyping the south recombinant plant resulted in no reversion of the recombinant genotype at the identified point mutations. Additionally, *CKL4* transcript does not show any expression in sperm cells according to the isolated sperm cell transcriptomic study of Borges *et al*, (2008). Consequently, the *CKL4* gene had to be excluded as the putative *DUO4* locus, and the best candidate remained was *CCS52A1*.

Another strategy to identify the molecular nature of *DUO4* was the screening of T-DNA insertion lines for cell cycle related genes in the identified genetic interval. Although all the insertions resulted in the identification of homozygous lines, none of them displayed any possible defect in pollen. The extensive genomic duplication in Arabidopsis has created a possible functional redundancy (Vision *et al*., 2000), which may explain the lack of visible phenotype in *CCS52A1* gene knockdown. CCS52A1 and CCS52A2 genes show a high amino acid identity (86%) with particularly significant conservation between the APC conservative binding interaction domains, the putative CDK phosphorylation sites as well as the RVL cyclin binding domain (Cebolla *et al*., 1999) all these together suggest that *CCS52A1* and *CCS52A2* may be functionally redundant (Appendix: Figure A1).

The *CCS52A1* (*At4g22910*)/ *CCS52A2* (*At4g11920*) promoter: H2B-GFP fusion constructs were generated in order to investigate the expression pattern of the APC/C activators, throughout pollen development. RT-PCR also assayed the results of the promoter expression patterns. The transcripts of *CCS52A1* and *CCS52A2* were detected at different stages of pollen development; microspore, bicellular, tricellular and mature pollen.

The expression of CCS52A1 is relatively high in the microspore stage and in both the germ and the vegetative cells at the early bicellular. The expression was maintained in the next stages with obvious steady levels but only observed in the vegetative cell. The low level of CCS52A1 might be related to the role of CCS52 in driving the cell to exit mitosis, through mitotic cyclin degradation. Moreover, the disappearance of CCS52A1 from the germ cell, as well as its restricted activity to the vegetative cell, suggest that mitotic cyclins need to be kept at low level in the vegetative cell. This keeps the vegetative nucleus in G1 phase, preventing initiates of division. Fission Yeast *Ste9*, a homologue of CDH1, is involved in

both cell cycle regulation and progression in G1 phase by keeping mitotic cyclin under tight control (Blanco *et al*., 2000). Similarly, in *Arabidopsis* roots the role of *CCS52A2* is to maintain the quiescent center cells (QC) in a prolonged G1 phase by promoting a low mitotic state activity.

In the later stages of pollen development CCS52A1 expression peaks at early tricellular stage and is slightly decreased in mature pollen, with a GFP signal detected only in sperm cell nuclei. Sperm cell transcriptomic data indicates that the transcript accumulates appear two fold higher in the sperm cell compared with mature pollen (Borges *et al*., 2008). Thus, the absence of the GFP signal from the mature pollen vegetative nucleus may be due to the ability to detect the GFP in mature pollen. Moreover, it is likely that CCS52A1 could be required to induce another round of S-phase within the sperm cell nuclei.

The homologue of *CCS52A1*, *CCS52A2* , was also expressed in most of the analysed pollen stages, but at a slightly higher level than *CCS52A1*. It is also notable that the GFP signal from *CCS52A2* was detectable at low level at the germ cell mitosis, which distinguishes *CCS52A2* from *CCS52A1*. The results of the promoter:H2B-GFP experiments were confirmed by RT-PCR. However, there is a notable increase in the *CCS52A1* transcript levels in mature pollen compared to the *CCS52A2* profile that remains relatively uniform through pollen maturation. No obvious expression was detected in the bicellular stage. After that the expression was found to be in the tricellular pollen with obvious increase in mature pollen. This suggests that both *CCS52A1* and *CCS52A2* could show functional redundancy with a transcript profile differences at germ cell mitosis.

4.7.3 Misexpression of *CCS52A1* supports the identification of *duo4* mutation in *DUO4* gene

The main goal of this experiment was to validate the hypothesis that *duo4* phenotype is due to ectopic expression of *CCS52A1*. Since the precise nature of the mutation is not resolved and sequencing of the mutant showed a single point mutation in the promoter of *CCS52A1* gene, pointing at significant difference between the wild type and mutant *duo4* genes. These findings raise the question of whether the *duo4* mutant phenotype is due to the

misregulation of the endogenous *CCS52A1* gene.

Cloning of the *CCS52A1* gene was followed by its introduction into wild type and +/*duo4* plants under the control of the *DUO1* promoter. The statistical and phenotypical analysis of the prom*DUO1*-CCS52A1 plants indicated that *duo4* mutation is a gain-of-function mutation that blocks germ cell mitosis and that may provide the molecular explanation for *duo4* mutant phenotype, as the gain of function mutation can result from a single point mutation, which may lead to a change in protein function or enhanced expression of the mutated gene.

About 13 % of the tranformants partially induced the *duo4* phenotype, which could be due to several reasons. The site of integration in the genome plays an important role in the level of expression. If the gene becomes integrated in the heterochromatin region, expression will be low. Moreover, sub-optimal regulatory signals, promoters and enhancers can also reduce expression. Fully penetrant lines induced the *duo4* mutant phenotype in the wild type plants. A distinct dominant oval to round germ cell morphology was observed in pollen form transgenic plants that display *duo4* phenotype. In addition, the increase in the ploidy level that correlates with the observed phenotype could be simply explained as a result of using a germ cell specific promoter, displaying a higher CCS52A1 transcript in the transgenic lines compared to + /*duo4* plants. Even though, these results support the arguments in favour of the misexpression hypothesis. Another attempt to gather concrete evidence that the overexpression hypothesis is valid, was an experiment using RNAi knockdown lines targeting *CCS52A1* gene in *duo4* background, which helped to restore the germ cell division defects by down regulation of *CCS52A1* expression in *duo4* plants. Beyond discovering the molecular nature of *duo4* mutation, this work pinpoints the role of APC^{CCS52} complex at the gametophyte level, which has not been previously studied.

Collectively, it can be concluded that the misexpression of *CCS52A1* under the control of *DUO1* promoter is able to phenocopy *duo4* phenotype in wild type plants. In addition, these results are consistent with possibility that *duo4* mutation resulted from excess CCS52A1 transcript.

4.7.4 Molecular explanation for the *duo4* phenotype

On a molecular level, *CCS52A1* regulates the level of mitotic cyclins directly through APC ubiquitin ligase activity to promote polyubiquitination and degradation of mitotic cyclins in mitosis and G1. Even though the role of APC in cell cycle regulation is widely investigated, its possible function throughout germline development remains poorly understood. In this chapter, in addition to investigating the role of *CCS52A1* and *CCS52A2* genes during pollen development, biological and genetic methods were employed to describe the nature of gametophytic mutation that lead to delayed germ cell division.

To successfully enter mitosis, cells must accumulate mitotic cyclins and that requires that the APC must be inhibited after the cell completes S-phase. Thus the failure of + /*duo4* germ cells to progress through mitosis could be a result of a loss of CYCB1,1 , which is required to allow G2/M progression. These findings, therefore, leads to the conclusion that the up-regulated CCS52A1 in *duo4*, prevents CYCB1,1 accumulation and hence *duo4* germ cell fails to progress through mitosis.

A model could be applied to explain the *duo4* mutation phenotype in regard of the ectopic expression of the *CCS52A1* and that may provide potential evidence to support the *duo4* gain of function hypothesis. The *CCS52A1* activity is essential in preventing an accumulation of CDKA-CYCB complex, resulting in G2 arrest. Therefore, *duo4* phenotype could be accounted simply for its absent of the *CCS52A1* inhibitor, which would phosphorylate CCS52A1 at the right time/place of the cell cycle, resulting in APC remaining ectopically active in *duo4* mutant germ cells. In fact, in *Drosophila*, *Rca1* (regulator of cyclin A) is required to prevent degradation of mitotic cyclins by keeping APC-Cdh1^{Fzr} activity low in G2. In addition, in *rca1* mutants, a premature degradation of mitotic cyclins was observed in interphase of the 16th cell cycle, which resulted in APC/C remaining constitutively active, thereby blocking entry into mitosis and preventing a build up of CYCB1,1 in G2 (Machida and Dutta, 2007; Grosskortenhaus and Sprenger, 2002).

The expression of Rca1 has been described in its homolog, Emi1 (early mitotic inhibitor). In absent of *Emi1*, *Drosophila* embryos arrest at G2 and fail to enter mitosis as a result of premature degradation of cyclins (Jackson and Reimann, 2007). Consistent with this hypothesis RNAi transgenes were able to rescue the *duo4* mutation and restore wild type phenotype.

The overexpression of Cdh1 (Cdc20 homologue 1) has also been reported to result in a G1 arrest in HeLa cells. This arrest can be overcome in response to overexpression of Emi1, indicating that Emi1 regulates S phase entry via inhibition of APC/CCdh1 (Hsu *et al.*, 2002). In yeast, overexpression of CCS52 triggered mitotic cyclin degradation and cell division arrest, resulting in cells undergoing endoreplication and cell enlargement, providing another intriguing link between APC upregulation and induced G2-arrest.

duo4-like germ nuclei in the CCS52A1^{ME} plants show an average DNA content 2.3 C while no further increase in DNA content was detected in *duo4* germ nuclei (~ 2C), which could be related to the expression level of CCS52A1 is variable between duo4 mutant and CCS52A1^{ME} plants. It is possible that the APC^{CS52A1} activity is not high enough to reinitiate another DNA synthesis in *duo4* germ cell and that leads to a lower mitotic cyclin concentration to be balanced with CCS52A1 levels, preventing any DNA reinitiation.

Studying the level of CCS52 during different stages of the cell cycle in *Medicago sativa* (Tarayre *et al.*, 2004) and synchronized cell suspension cultures of *Arabidopsis* (Fulop *et al.*, 2005) showed that the expression of CCS52 was detected through G1 until the early G2, with a slight enhancement during S phase. Consistent with these results is that fact that the overexpression of *Cru1*, a *Cdh1* homologue, in *Ustilago maydis*, has also resulted in a premature degradation of cyclin B, which was sufficient to cause G2-like cell arrest, (Castillo-Lluva *et al.*, 2004). In addition, *rca1*/*emi1* mutants continue to undergo DNA synthesis cycles without mitosis (Di Fiore and Pines, 2007; Di Fiore and Pines, 2008). Thus, the CCS52A1, which normally is present until the early G2 phase, could be sufficient to induce the degradation of CYCB1;1 if ectopically expressed throughout G2.

Despite this corollary, many questions regarding *duo4* mutant gene remain to be answered, such as, how does *DUO4* expression becomes activated? What kind of mutation in *DUO4* gene renders its protein constitutively active?

Chapter Five

Identification of novel *DUO1* target genes

Identification of novel *DUO1* target genes

Introduction

Sexual reproduction in higher plants involves a relatively short gametophyte stage that has a fundamental role in producing the next generation. The fact that life on earth relies mostly on seed crop plants, the molecular mechanisms responsible for reproductive function represent one of the most important systems to investigate. Despite this, the mechanisms underlying sexual plant reproduction remain poorly understood. Genome wide analysis of transcriptomic datasets is a powerful tool that has been used to characterise different stages of pollen development (Honys and Twell, 2004; Pina *et al*., 2005; Zimmermann *et al*., 2004). Male germ cell specification involves about 6,000 genes, as shown by transcriptome analysis of isolated sperm cells (Borges *et al*., 2008). These datasets, coupled with the discovery of many regulatory proteins with important roles in germ cell division and specification, has led to the construction of models of the regulatory networks governing male germline development (Borg *et al*., 2009; Borg and Twell, 2010).

Genetic analysis of mutants affecting germ cell mitosis and germline differentiation has led to identification of the *DUO1* gene, the first characterized male germline-specific transcription factor (Rotman *et al*., 2005). Subsequent work identified three target genes regulated by *DUO1* (Brownfield *et al*., 2009a). These three target genes have been shown to be expressed in the male germline and include *MGH3* (Okada *et al*., 2005), *GEX2* (Engel *et al*., 2005) and *GCS1* (*HAP2*) (Mori *et al*., 2006). In this respect it is prudent to determine to what extent DUO1 is involved in the regulation of a broad range of biological processes. Thus, the main goal of this chapter was to identify novel downstream target genes that are regulated by DUO1 and hence further elucidate the role of *DUO1* in double fertilisation and male fertility. This has significantly expanded the known genes regulated by DUO1, and has contribute to a deeper understanding of the complexity of germline regulatory networks.

The *DUO1* transcript happens to contain a functional recognition site for the microRNA miR159 (Palatnik *et al*., 2007) and so this was considered as a potential caveat that could affect the sensitivity of the assay. An additional effector vector (35S-mDUO1) was thus

generated containing a DUO1 cDNA sequence in which the miR159 site is silently mutated. That achieved by changing nucleotide sequence at the miR159 binding site. Transgenic seedlings in which the m*DUO1* cDNA was placed under the control of an estradiol inducible promoter showed *mDUO1* induction when exposed to estradiol. This sequence has been shown to exhibit unperturbed ectopic expression in sporophytic tissues as well as activating ectopic expression of known DUO1 target genes (Brownfield *et al.*, 2009a). Isolated RNA from sporophytic tissues was converted into cDNA and subjected to microarray analysis using the *Arabidopsis* ATH1 Genome Array (Affymetrix). This analysis was performed in triplicate, allowing the results to be averaged, and statistically analysed. In order to gain insight into the extent of the *DUO1* regulatory network, a subset of candidate target genes were chosen for further analysis (Borg *et al.*, 2011). These genes were considered as DUO1 targets if, at the 24 h time point, there was at least a three fold difference between the average of the uninduced and induced replicates, (TTEST=0.05) (Figure. 5.1). In addition, a putative target must have a present call (MAS5.0) in at least two of the three induced samples. Using these criteria 63 putative targets were selected as potential *DUO1* targets, and belonged to different protein families (Borg *et al.*, 2011).

During the writing of this chapter, the DUO1 regulatory network paper was published, describing a parallel collaborative effort between Twell laboratory members (Borg *et al.*, 2011). Altogether, this work has revealed a large number of novel putative target genes that show DUO1-dependent male germline-expression. In this chapter the aim was to study five putative target genes (Table 5.1) with several goals in mind: to validate whether or not these genes are truly regulated by *DUO1*, by generating stable H2B-GFP marker lines driven by a native promoter of the candidate target genes and monitoring their expression in the *duo1* background. In parallel, the expression of these targets was explored in *duo3* mutant germ cells to investigate the overlapping regulatory network between *DUO1* and *DUO3* genes. In addition, the activities of these promoters were determined at different stages of pollen development. Finally, the affect of T-DNA knockout alleles of these genes on the transmission through the male was analysed. A further objective was to validate another gene (*At2g24370*) that un-reliably induced during the time course experiments. Some of

Table 5.1: A table to show the average microarray signal obtained from the ATH1 Genome Array analysis. This analysis was performed on seedlings after induction of DUO1 at three time points, 6, 12 and 24. This was done in triplicate, and seedlings with non- induced DUO1 was used for comparison. The 'signal' value is the average difference between the microarray signal value in the induced and non-induced microarray results. The 'fold induction' is the ratio of signal increase when compared to the non-induced signal value for that gene.

Gene	AGI	Protein	Signal (6h)	Fold increase	T-TEST	Signal (12)	Fold increase	T-TEST	Signal (24)	Fold increase	T-TEST
TIP5;1	At3g47440	Tonoplast intrinsic protein	356	60.6	0.01	853.3	133.5	0	856	582.75	0
DAA1	At1g64110	AAA+ type ATPase	26.5	1.28	0.4	86.36	6.7	0.01	154	12.06	0.02
PCR11	At1g68610	Plant cadmium resistance112	10.8	2.4	0.11	40.6	29.9	0	111	34.2	0
VCK	At2g24370	Kinase	4.51	0.88	0.81	6.59	2.21	0.2	4.9	3.31	0.05
IMPa-8	At5g52000	Importin alpha-1 subunit	8.92	9.52	0.01	19.45	7	0.04	14.8	34.53	0.01

these candidate *DUO1* target genes will be referred as *DUO1-Activated Target* (*DAT*) genes (Borg *et al*., 2011).

5.1 *DAT* genes belong to diverse functional categories

The *DAT* genes selected and analysed in this chapter belonged to various gene families with different biological functions (Table 5.2). Several DATs are involved in transport, which include *TIP5;1, PCR11* and *IMPa-8. DAA1* belongs to a large superfamily that has been reported to play roles in various cellular activities such as DNA replication and repair (Snider and Houry, 2008). The involvement of *DUO1* target genes in diverse functions highlights the critical role that *DUO1* plays in diverse cellular processes during sperm cell development.

5.1.1 ***TIP5;1 (At3g47440)*** belongs to a subclass of tonoplast intrinsic protein (TIPs) a member of the plant major intrinsic protein (MIP) plant aquaporins family (Forrest *et al*,. 2007) *TIP5;1* function as specific transporter for water and urea (Soto *et al*., 2008; Vander Willigen *et al*., 2006). A previous result has showed that TIP5;1 and its homolog, TIP3;1, are the highest pollen-expressed aquaporin genes in *Arabidopsis* and thus represent strong candidates for water and urea transport in mature pollen. TIP5;1 localises to mitochondria and mutations in *TIP5;1* gene result in shorter pollen tubes grown in the absence of exogenous nitrogen (Soto *et al*., 2008). *TIP5;1* showed the highest fold induction over the 24 hour time course, with induction increasing 10-fold at 6 hours to 24 hours (Figure.5.1). According to available microarray data at GENEVESTIGATOR (http://www.genevestigator.ethz.ch), *TIP5;1* has a higher expression signal in mature pollen compared to other plant tissues (Honys and Twell, 2004). Male gametophyte data originating from transcriptomic studies have provided the opportunity to infer the expression pattern of this gene in male gametophytes. Strikingly, *AtTIP5;1* is absent in the microspore, with transcripts increasing after germ cell mitosis and peaking in mature pollen (Honys and Twell, 2004) (Figure. 5.2). Furthermore, *TIP5;1* is one of the most highly expressed genes in sperm cell (Borges *et al*., 2008).

5.1.2 ***DAA1/At1g64110*****;** belongs to large protein family of *ATPases* called "ATPases associated with diverse cellular activities", containing ATPases Associated with diverse cellular Activities AAA+ (Erdmann *et al.*, 1991). This family is involved in a variety of cellular activities such as protein unfolding and degradation as well as DNA recombination, replication and repair (Snider and Houry, 2008). Based on the response in the time course array experiment *DAA1* showed the highest fold induction after 24 hours, with induction increasing 10-fold at 12 hours and 24 hours (Figure.5.1). Transcriptomic data were used to investigate the expression level of this gene throughout pollen development. The transcriptomic data shows that DAA1 is assigned absent calls by the MAS5 detection call algorithm in microspore and bicellular stages. *DAA1* shows an increase in expression levels after germ cell mitosis (Figure. 5.2). According to the available microarray data at Genevestigator (Zimmermann *et al.*, 2004), *DAA1* is highly expressed in pollen and it is detectable in sperm cells (Borges *et al.,* 2008).

5.1.3 ***IMPa-8/At5g52000;*** belongs to the Importin α-like family of proteins, which are involved in the export and import of nuclear- proteins (Lange *et al.*, 2007). *IMPa-8* showed a 3-fold increase at 12 and 24 h after induction (Figure.5.1). Analysis of microarray data shows that the *IMPa-8* only had a moderate expression level in tricellular and mature pollen and was undetectable in any other plant tissues (Figure.5.2), suggesting that *IMPa-8* may be specific to the male gametophyte.

5.1.4 ***PCR11/At1g68610;*** is a member of the *PLANT CADMIUM RESISTANCE* family of genes, which encode small plasma membrane proteins that are involved in the transport of heavy metals in *Arabidopsis* (Song *et al.*, 2010). *PCR11* shows the highest fold induction over the 24 hour time course, with induction increasing 10-fold from 12 hours to 24 hours (Figure.5.1). *Arabidopsis* microarray data from aGFP for PCR11 showed increasing transcript abundance after germ cell mitosis (Figure.5.1), reaching maximum in mature pollen.

5.1.5 ***VCK/At2g24370*****;** the last candidate gene was analysed**,** a protein kinase protein. The protein kinase- like family has 610 members, coding approximately 2.5 % of the

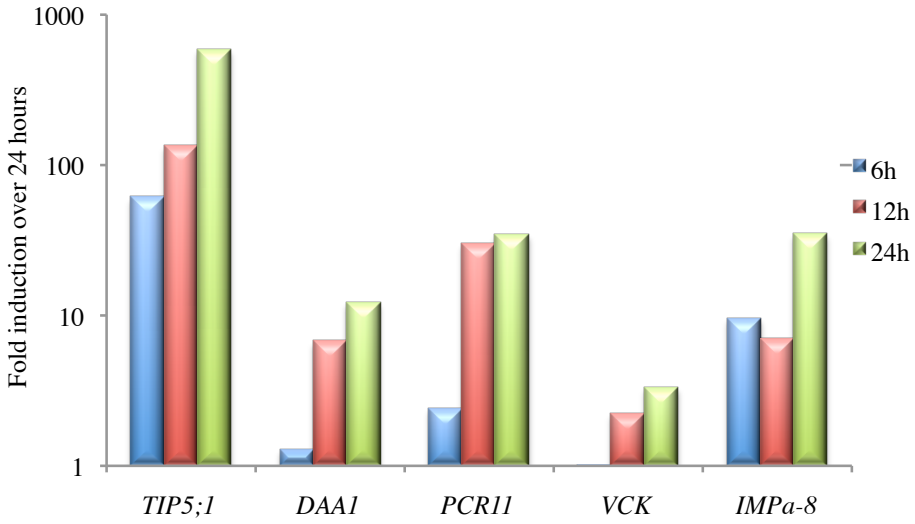

Figure 5.1: Graph showing fold induction of four putative *DAT* genes during the microarray course experiment at three time point, 6,12 and 24 hours after DUO1 induction.

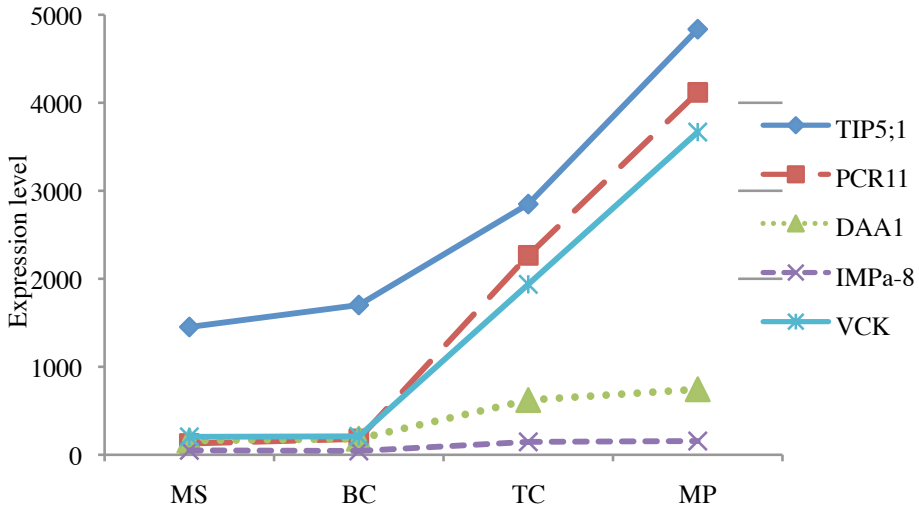

Figure 5.2: Graph showing the expression profile of *DAT* genes during pollen development. The majority of the *DAT* genes are expressed highly at the mature pollen stage. Microarray data from four different stages of pollen development; microspore; MS, bicellular; BC, tricellular; TC, and mature pollen; MP were plotted (Honys and Twell, 2004).

Table 5.2: List of putative functional protein domains that exist in selected *DATs*. The PPDB (The Plant Proteome Database) (Sun, Q et al, 2009; http://ppdb.tc.cornell.edu/) was used to search for motifs.

Gene	Domains	Descriptions	Start	End
TIP5,1	Na^+_H $^+$_antiport_1	Na+/H+ antiporter 1	1	239
	MIP	Major intrinsic protein	15	235
DAP1	PLACE8	PLACE8 family	19	120
	Keratin_B2	keratin, high sulfur B2 protein	20	111
PCR11	Sigma54_activat	sigma54 interaction domain	542	740
	Mg^{+2}-chelatase	Magnesium chelatase, subunit Ch1I	547	692
	SRP54	SRP54-type protein, GTPase domain	549	682
	AAA1,2,3,5	ATPase family associated with various cellular activities	548	685
	ABC	ABC transporter	553	662
IMPa-8	Arm(1-8)	Armadiallo/beta-catenin-like repeat	38	370
	DUF634	protein of unknown function	111	349
	HEAT 1,2,3	HEAT repeats	84	328
Kinase	Usp	Universal stress protein family	16	169
	DUF444	protein of unknown function	210	568
	To1A	To1A protein	278	562
	Pkinase	Protein kinase domian	480	743

Arabidopsis genome. Plant receptor-Like Kinases (RLKs), sharing similar kinase domains. Plant *RLKs* play important roles in a wide range of signalling processes. In agreement with the array results from Borges *et al* (2008), this gene has an absent call in sperm cells. However, kinases are considered to be pollen-enriched, indicating that the kinase is vegetative cell specific**,** and as such will be referred to as VCK (Vegetative Cell Kinase). A recent study has shown that the promoter of *At2G24370* is pollen specific as GFP expression was detected of a promoter marker line only in pollen (Xiao *et al*. 2010).

The putative functional motifs that exist in the predicted protein product of each gene were investigated using the PPDB (The Plant Proteome Database) (Sun *et al*., 2009; http://ppdb.tc.cornell.edu/). Although the main purpose of the present study was to investigate the promoter of these putative target genes in *duo1* germ cells, an overview is given on the main domains for each target gene in terms of their primary structure in Table 5.2.

Strikingly, transcriptomic data for developing *Arabidopsis* pollen obtained from the microarray data collected by Honys and Twell (2004), show that all these genes exhibit transcripts increases after microspore mitosis and peak in mature pollen. This is similar to the expression pattern of DUO1 transcripts. The expression profile of these putative targets are in agreement with those previously published targets, i.e. Germline-specific *DUO1* target genes are expected to be low in microspores and increase in response to DUO1 expression from bicellular through to mature pollen (Brownfield *et al*., 2009a).

5.2 Generation of promoter H2B reporter (GFP) transgenic lines

Current work was focused on the function of these putative targets in *planta*. Germline cell-fate marker constructs have been generated that use each of the native target promoters to drive the expression of a histone H2B-GFP fusion that localises the fluorescence to the nuclei (Figure 5-3). These constructs were created using Multisite Gateway recombination vectors (Invitrogen) (Karimi *et al*., 2002).

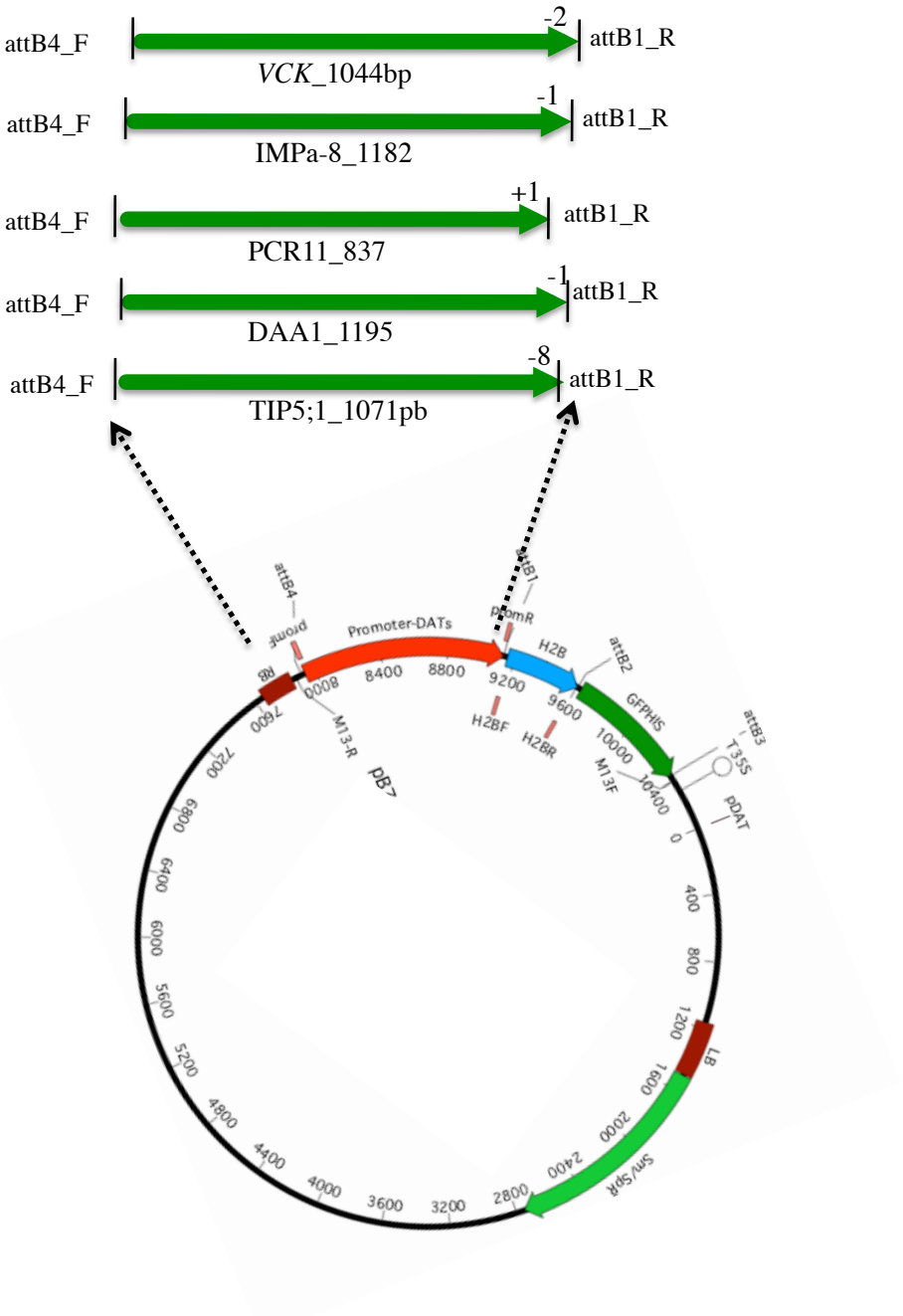

Figure 5.3: Schematic representation of the *DAT* promoter fragments that were used to drive expression of H2B-GFP. Plasmid map of a recombinant pB7m34GW plasmid. This map shows the position and orientation of the gene promoter, H2B and GFPHIS DNA fragments, after recombination. The position of the promoter specific, H2B and GFPHIS primer sites are depicted. Other important features shown are the spectinomycin and BASTA resistance genes. The left and right borders (LB and RB) are also shown flanking the expression construct and the BASTA resistance gene, which is important for selection for transformed seedlings after floral dip transformation.

The T1 + /*duo1* lines (Six independent lines) were transformed for each construct that resistant to BASTA selection. Heterozygous *duo1* plants are expected to produce 50 % *duo1* (bicellular) and 50 % wild type (tricellular) pollen grains (Durbarry *et al*., 2005). Transformed T1 plants, with single locus insert are expected to produce 50 % of pollen grains with the insert that is expressing the marker, and 50 % pollen without the insert or GFP expression that correspond to the wild type portion of the population. If more than 50 % pollen grains are observed with GFP, it can be considered that this plant has two or multiple inserts for the introduced transgene. From these lines, only plants with a single locus were considered for further analysis. The wild type pollen present will display the expression of the construct in the presence of *DUO1*, and were used as a comparison for the expression of the construct within mutant *duo1* pollen. In addition pollen at different developmental stages was examined by counting GFP fluorescing pollen grains.

5.2.1 New *DUO1* target genes identified by ectopic expression of DUO1

The generated constructs were introduced into heterozygous *duo1* plants and GFP expression was scored in T1 plants. For the promoters analysed; *TIP5,1*, *DAA1* and *PCR11* about 50 % of wild type pollen showed a strong GFP signal within twin sperm cells, while no GFP expression could be seen in the single germ cell in *duo1* pollen for all 3 constructs analysed (Figure 5.4 A-C & Figure 5.5 A-C). A weak GFP signal was observed in some *duo1* mutant germ cells for the other construct. This was rarely seen in some T1 individuals from the *IMPa-8* marker line (4.4 %) (Figure. 5.4 E and Figure. 5.5 D). Visual observation of the GFP expression level between wild type sperm cells and the *duo1* germ cells showed that the signal within the sperm cells was much stronger than that of the undivided germ cells. Interestingly, no expression was detectable in the vegetative cells, indicating that the expression of these promoters is restricted to the male germ line. The absence or weak GFP expression in mutant *duo1* germ cells indicates that *DUO1* is necessary for the expression of these genes in the male germline. In contrast, the VCK:H2B reporter construct was expressed only in the vegetative cell nucleus. GFP fluorescence was unaffected in the vegetative cell of *duo1* pollen (Figure 5.4 D), with no difference between the percentages of GFP positive vegetative nuclei in wild type and *duo1* pollen.

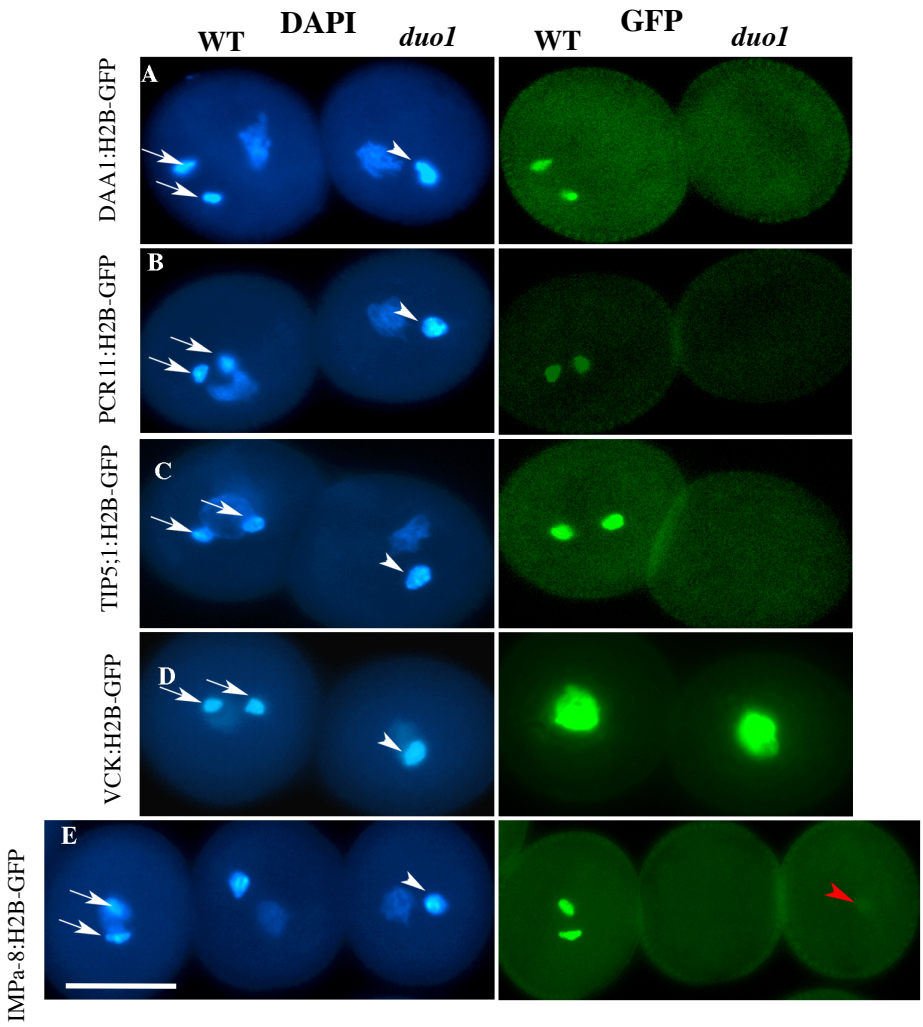

Figure 5.4: Examples of wild type and mutant pollen grains harboring *DAT* promoter:H2B-GFP viewed by fluorescence microscopy. A) DAA1:H2B-GFP. B) *PCR11*:H2B-GFP. C) *TIP5;1*:H2B-GFP. D) *VCK*:H2B-GFP are not expressed in *duo1* pollen while in E) *IMPa*-8:H2B-GFP low GFP signal can be detected in the *duo1* background (red arrow head). Each image has a WT pollen grain to the left (arrow) and a *duo1* mutant grain to the right (arrowhead). The grains are shown under DAPI and GFP fluorescence respectively. Scale bars = 15µm.

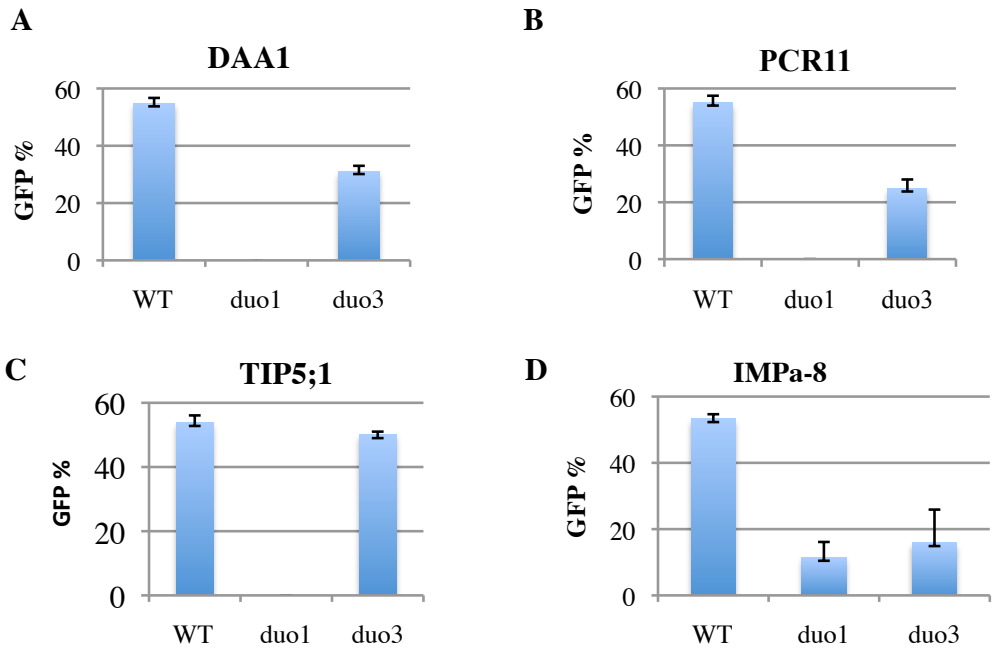

Figure 5.5: The percentage of pollen showing GFP expression in sperm cells of wild type pollen or in the mutant germ cell of *duo1* and *duo3*. Three to four individual heterozygous plants were examined for A) *DAA1*:H2B-GFP. B) *PCR11*:H2B-GFP. C) *TIP1;5*:H2B-GFP. D) *IMPa*-8:H2B-GFP.

5.3 *DUO3* is required for the normal expression of some *DAT* genes

Previously, ectopic expression of *DUO1* allowed the identification of putative target genes. The expression of *GEX2* and *GCS1* was also enhanced in response to the presence *DUO1* and *DUO3* transcript. The expression of *MGH3*, however, exclusively depends upon DUO1 (Brownfield *et al.,* 2009b). Further experiments were employed to find out if DUO3 is also required for the normal expression of these putative *DUO1* target genes. Therefore, the expression of *DATs* was also investigated in +/*duo3* plants. Similar to *duo1*, in heterozygous *duo3* mutant about 50 % from germ cells fail to enter the second pollen mitosis. The four target markers were crossed to heterozygous *duo3* plants and GFP expression was scored in F1 plants. GFP signal from the *DAA1*-H2B: GFP was observed in both mutant and wild-type germ cell from +/*duo3* plants (Figure 5.6 A). However, the *DAA1* expression was detectable only in about 25 % of the mutant germ cells with a relatively weak GFP signal compared with a moderate signal in about 50 % in wild type sperm cells (n=851). Accordingly, quantitative analysis of GFP fluorescence, showed at least a one-fold decrease in *duo3* germ cell expression compared with wild type sperm cells ($*P < 0.05$) (Figure 5.7).

The expression of *PCR11*:H2B-GFP was reduced in *duo3* germ cell compared with wild-type sperm cells (n=814, Figure 5.6 B), with about 60 % of *duo3* mutant germ cells showing no fluorescence and the level of fluorescence in the remaining 40 % was highly variable with up to 2-fold reduction in *duo3* germ cell compared to the sperm cells (Figure 5.7). GFP fluorescence from *IMPa-8*:H2B-GFP was observed in about 11 % of *duo3* germ cells compared with 50 % in wild type sperm cells in the *duo3* mutant background (n=659, Figure 5.6 D). By comparing the GFP expression signal between wild type sperm cells and *duo3* germ cells, it could be seen that the signal within the sperm cells were much stronger than that of the *duo3* germ cells and the brightness of GFP was 3-fold lower than that of wild type sperm cells (Figure. 5.7). As the percentages and the brightness of GFP expression germ cells in *duo3* was less than that in wild type sperm cells it can be concluded that these genes may be direct or indirect targets of *DUO3*. These data indicate that along with *DUO1*, *DUO3* is a germline regulator that shares common targets with *DUO1*.

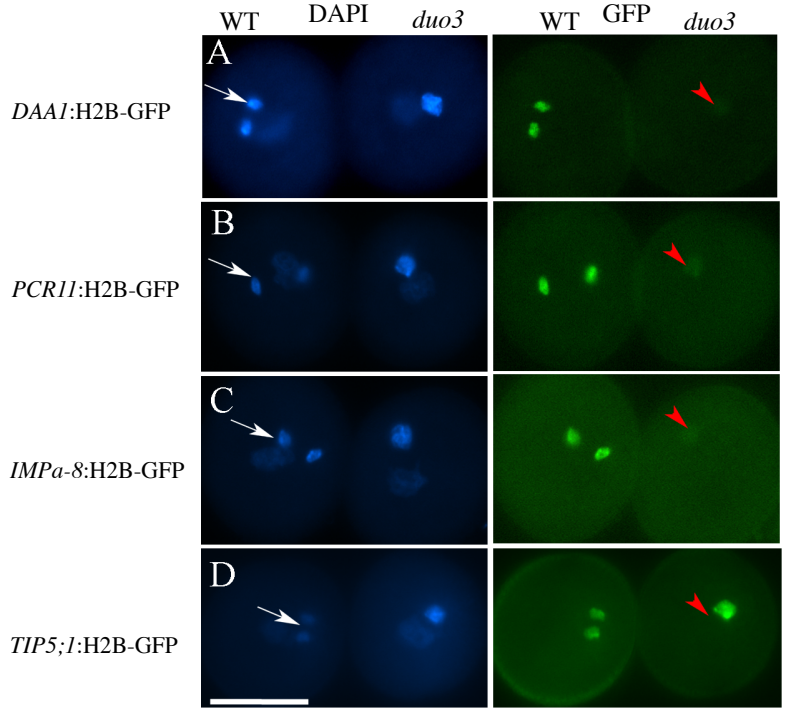

Figure 5.6: Expression of *DAT* promoter :H2B-GFP constructs in pollen grains carrying the *duo3* mutation. A) prom*DAA1*:H2B-GFP. B) *PCR11*:H2B-GFP. C) prom*IMPa-8*:H2B-GFP. D) *TIP5;1*:H2B-GFP. The images show DAPI and GFP fluorescence respectively, low GFP signal can be detected in *duo3* germ cells. Bright fluorescence from the prom*TIP5,1*:H2B-GFP marker was observed in both mutant and wild-type pollen. Each image has a WT pollen grain and a *duo3* mutant grain. Sperm nuclei are indicted by arrow and *duo3* germ nuclei are indicated by red arrow head. Scale bars = 10µm.

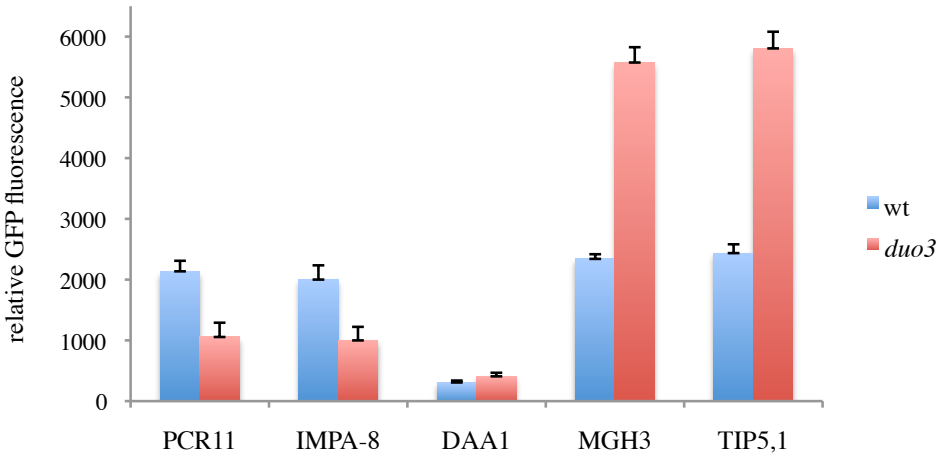

Figure 5.7: Quantification of the GFP signal of prom*DATs*:H2B-GFP in *duo3* germ cells compared with wild type sperm cells. Mature pollen shed from four independent lines for each construct was pooled and imaged randomly under standardised conditions. GFP fluorescence represents the mean total pixel intensity corrected for background in the sperm cells analysed.

In contrast, when *TIP5,1* was crossed to + /*duo3* mutant plants, GFP was observed in *duo3* mutant germ cells as well as in wild type sperm cells in equal proportions and similar brightness (t-test p-value). This observation indicates that *DUO3* does not control *TIP5,1* promoter activity (n=837, Figure. 5.6 D). Promoter:GFP activity was quantified in *duo3* mutant germ cells compared with wild type sperm cells. GFP fluorescence was also quantified in *MGH3* in *duo3* pollen, which was previously demonstrated to be a target for *DUO1,* but not *DUO3*. Interestingly, the data showed that the mean GFP intensity of *TIP5; 1:H2B*-GFP and *MGH3*:H2B-GFP in *duo3* germ cells was not different. Moreover, the data showed that for both promoters, *MGH3* and *TIP5*;*1*, the GFP level in undivided *duo3* germ cells was 2.3 fold higher than that in the wild type sperm cells.

5.4 Expression of the *DAT* genes during pollen development

As shortly described above, different *DAT* gene promoter constructs were confirmed to be under the transcriptional control of *DUO1*. It remained to be elucidated whether the promoter activity of these genes show similar profiles to the previously described *DUO1* target genes *MGH3*, *GEX1* and *GCS1* which was detected soon after the first pollen mitosis (Brownfield *et al*., 2009a).

In order to verify if the identified *DAT* genes showed the same GFP expression patterns during pollen development, each construct was analysed by examining developing pollen from flower buds stained with DAPI and observed by using DAPI and GFP filters. Detailed analysis of the expression of the 1071 bp *TIP5;1*-promoter during pollen development showed that the GFP signal was detectable at EBC only in approximately 10% of the population. Afterwards, the signal could be observed at MBC stage within germ cell. During the next stage of pollen development, GFP expression, as expected, clearly increased (Figure 5.8 A-D). Throughout pollen maturation, no GFP expression was detected within the vegetative nucleus, suggesting that the expression of these targets is restricted to male germline (3 lines were analysed).

In contrast to *TIP5;1*, the expression of the 1182 bp *IMPa-8* promoter was clearly expressed within the nucleus of the microspore (Stage -8) (3 lines analysed). A moderate GFP single was seen at early bicellular, within both vegetative and germ cells. At late bicellular stage, the GFP level seems increased within the germ nucleus, however, the signal in the vegetative nucleus becomes weaker during pollen development. In mature pollen GFP expression could be seen only within the two sperm cells (Figure. 5.8 E-H).

Unlike *IMPa-8,* expression of the 1195 bp *DAA1* promoter was not observed either in non-polarized microspore (Figure. 5.8 I-J) or in bicellular stages. By early tricellular stage a weak GFP signal can be seen in the sperm cells (3 lines). At mature pollen, a much stronger GFP signal could be observed only within the sperm cell nuclei (Figure. 5.8 M-P). Similarly to *DAA1,* activity of the 837 bp PCR11 promoters was not observed in the microspore or bicellular stages. Furthermore, at the tricellular stage of pollen development GFP fluorescence could be seen only in newly formed sperm nuclei. The GFP level seems to be enhanced in the *PCR11* promoter in mature pollen stage. Remarkably, the promoter activities of *DAA1* and *PCR11* were detected only in the sperm cells, while GFP positive signal in vegetative cell was never observed. Overall these observations have provided critical evidence concerning the expression patterns and regulation of male germline-expressed *DAT* genes during pollen development.

The developmental expression of the 1044 bp *VCK* promoter was also studied. Individual pollen grains at different developmental stages (as determined by DIC imaging) were analysed for GFP activity (Figure 5.9 A-B). GFP level was first observed in about 75 % of late bicellular stage pollen (elongated germ cell) in 5 lines (n= 2422). Afterward, the GFP accumulated dramatically in the vegetative nucleus at the later stages of the pollen development and reached a maximum in mature pollen stage.

The expression pattern of the *VCK* promoter was compared with the vegetative cell-specific *LAT52* promoter (Twell *et al*., 1989; Twell, 1992). Unlike *VCK*, the 570 bp *LAT52* promoter driving expression of an H2B-GFP fusion was first detected in about 40-60 % of the non-polarized microspores (three lines were analysis for each fusion) (Figure 5.9 C-F). However,

Figure 5.8: Promoter activities of *DAT* genes during pollen development.

The pollen nuclei were stained with DAPI (lower panel) and observed with GFP filters (upper panel). A-D) In prom*TIP5*;1:H2B-GFP the GFP signal was absent in MSP stage, at the mid- bicellular stage, a weak signal of GFP can be seen within the germ cell nucleus only. Through the mitotic progression and tricellular pollen stages, a much stronger GFP expression level can be seen within the sperm cell nuclei only. E-H) In prom *IMPa*-8:H2B-GFP GFP expression can be seen within the MSP. At the early bicellular stage, a high concentration of GFP expression can be seen within the germ and vegetative cell nucleus. At late bicellular pollen, the GFP expression is noticeably weaker within the vegetataive cell nucleus and much stronger GFP signal was observed within germ cell. At tricellular and mature pollen, GFP expression is seen within the sperm cell nuclei. I-L) In prom*DAA1*:H2B-GFP, the GFP expression can not be seen within the unicellular microspore nucleus or at bicellular stage, a weak GFP signal can be seen only within the sperm cell nuclei at the tricellular and mature pollen stages. Throughout pollen development, no GFP expression can be seen within the vegetative cell nucleus. M-P) prom*PCR11*:H2B-GFP shows a similar pattern to prom*DAA1*:H2B-GFP. The figures display: unicellular microspore ;MSP, early bicellular; EBC, late bicellular; LBC, and mature pollen grain; MPG stages (This figure has been published as figure 3 in Borg *et al.*, 2011). Bars = 10 μm.

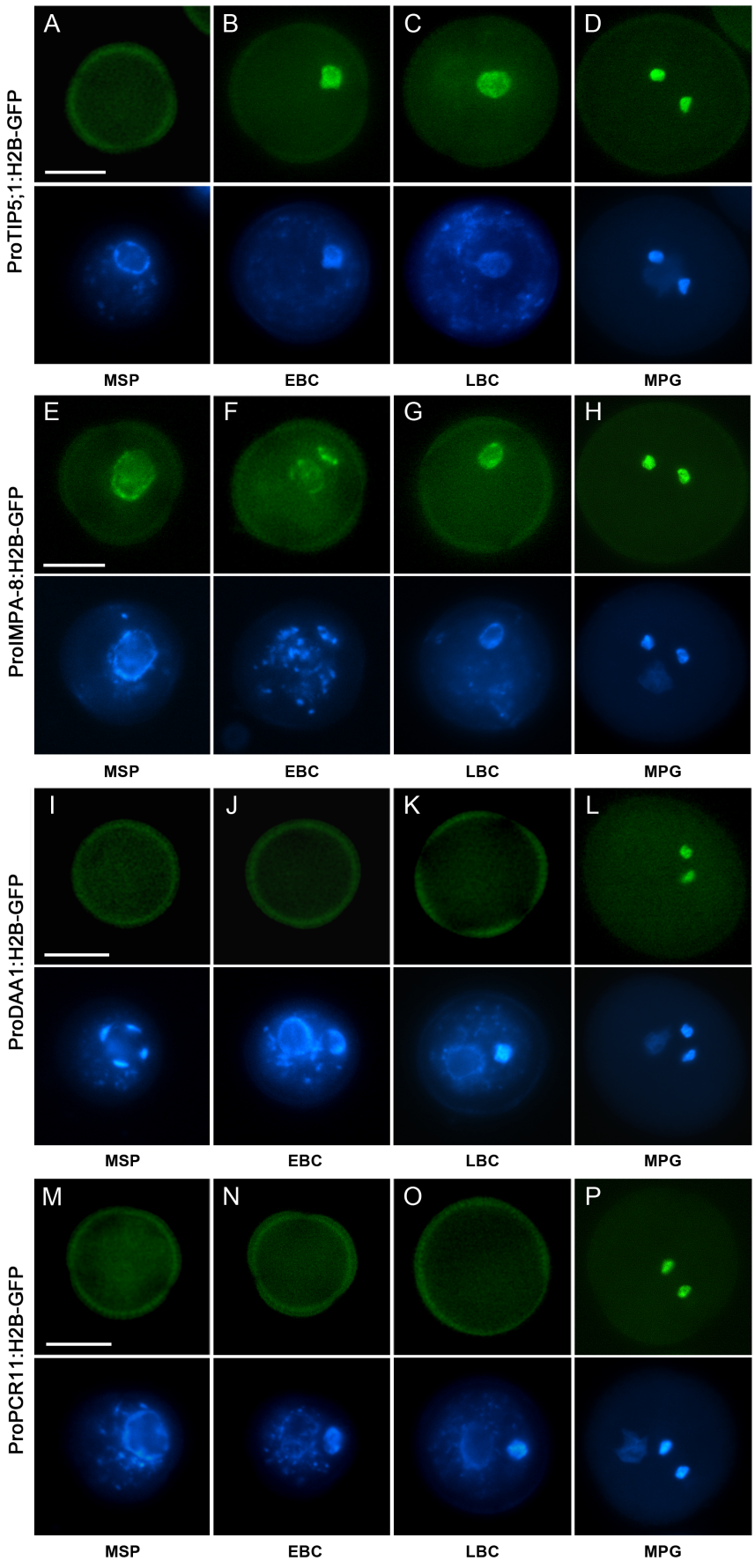
A
B
C
D
ProTIP5;1:H2B-GFP
MSP
EBC
LBC
MPG
E
F
G
H
ProMPA-8:H2B-GFP
MSP
EBC
LBC
MPG
I
J
K
L
ProDAA1:H2B-GFP
MSP
EBC
LBC
MPG
M
N
O
P
ProPCR11:H2B-GFP
MSP
EBC
LBC
MPG

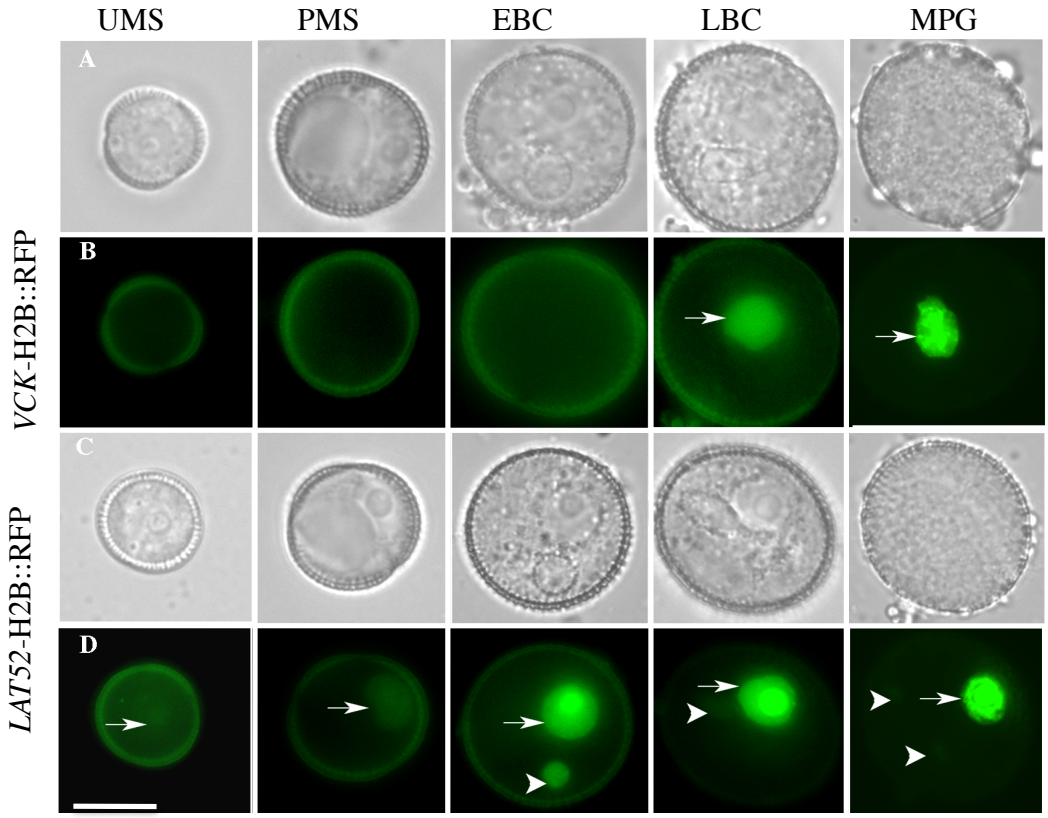

Figure 5.9: Analysis of *VCK and LAT52* promoter activities during pollen development. Expression of prom*VCK*:H2B-GFP (A-B) and prom*LAT52:*H2B-GFP (C-D) throughout wild type pollen development (upper panel DIC image and lower panel GFP fluorescence). In isolated spores, UMS, PMS, MBC, LBC and MPG. For the VCK promoter, weak expression is first detected in the vegetative nucleus at LBC stage. Fluorescence increases during the next stage of development then the GFP level was dramatically accumulates in the vegetative nucleus in mature. C-D) In *LAT52*, GFP is detected in the UMS (arrow) and in both the vegetative (arrow) and germ cell (arrowhead) nuclei at EBC stage. GFP expression was enhanced in the vegetative cell accompanied by a decrease in the germ nucleus at MBC/LBC stages. GFP flourescence increased in vegetative cells at MPG stage . All images were taken using fluorescence microscopy. Unpolarized microspore; UMS, polarized microspore; PMS, early bicellular; EBC, mid bicellular; MBC, late bicellular; LBC and mature pollen; MP. Scale bars = 15μm.

GFP expression can be seen in about 100 % of polarised microspores close to asymmetric division (n = 1122). Afterwards, bright fluorescence can be observed in both nuclei immediately after microspore mitosis and the smaller germ cell showed higher GFP activity. During the next stages of pollen development GFP expression was enhanced in the vegetative cell accompanied by a decrease in the germ nucleus. At the tricellular stage of pollen development, GFP expression reaches maximum in the vegetative cell. While the promoter activity appears to be very weak or absent within the two sperm cells.

5.5 *DAT* genes do not affect genetic transmission

Independent insertion mutants for each of these genes have been identified and have been analysed. Furthermore, genetic transmission of each of these insertion lines has been carried out to test gamete function and data from this experiment was investigated.

Genomic DNA from each of the insertion lines was screened by PCR. The isolated genomic DNA of each T-DNA insertion plant was tested using either a pair of primers amplifying a specific wild type product, or primers designed to yield a product specific for the T-DNA insertion, with the aim of identifying homozygous insertion plants. Pollen phenotypic analysis carried out using DAPI staining was also used to detect germline phenotypes and any other visible alterations in pollen morphology. T-DNA insertion lines available for *TIP5;1, DAA1* and *AtIMPa-8* were studied, excluding *PCR11* where no T-DNA insertions were found. T-DNA insertion lines were ordered from the SALK, GABI and SM collections for each *DUO1* target gene (Figure. 5.10). Performing a chi-square test, with the expected of a 1:2:1 segregation pattern in T1 seeds, for homozygous: heterozygous: wild type. It was observed in the *DAA1*, *TIP5;1* and *IMPa-8*. *TIP5;1* ,GABI_171E08 and the results showed no difference from the expected ratio (Table 5.3). This result suggests that the mutated gene do not affect transmission through the male.

Moreover, transmission analysis through the male germline was carried out in order to determine any possible subtle pollen defects. F1 seeds from self fertilised and crosses onto *ms1-1* pistils were plated on MS0 medium supplemented with kanamycin. The number of

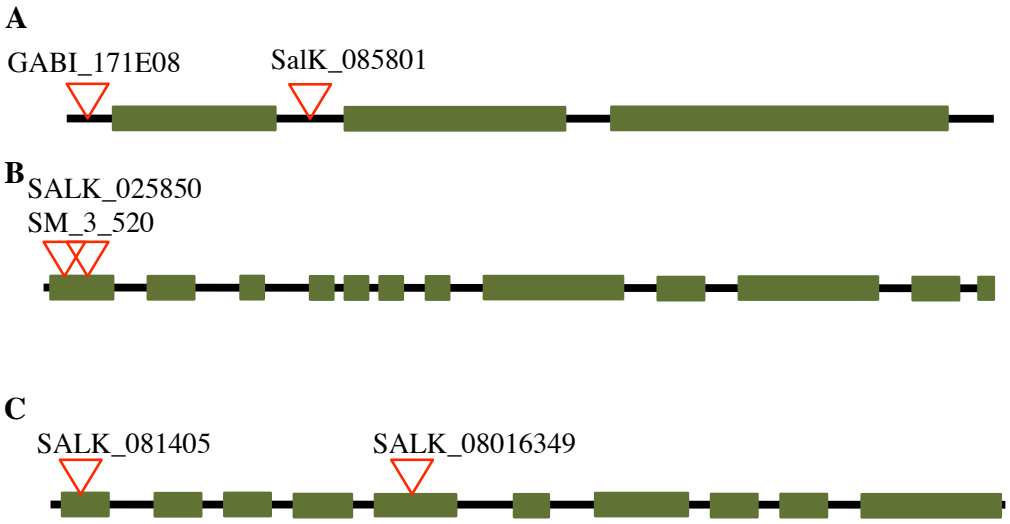

Figure 5.10: the position of the T-DNA insert in the *DUO1* target genes. Two insert lines were ordered for A) *TIP5,1*, B) *DAA1* and C) *IMPa-8*.

Table 5.3. A table to show the number of homozygous, heterozygous and wild type plants found in the T1 generation of the T-DNA lines. The results from performing a chi-square test, to analyse whether the homozygous (Hom.) to heterozygous (Het.) to wild type (Wt) ratio found is statistically significantly different from the expecting 1:2:1 ratio if the T-DNA insertion does not induce a gametophytic mutation. NS: not significant, * indicate statistically significant differences from an expected ratio ($p < 0.05$).

Gene	Insert	Hom.	Het.	Wt	Total	X^2 value	Significance
DAA1 (At1g64110)	SALK_025850	10	7	12	29	5.6	NS
	SM_3_520	5	7	3	15	1.5	NS
IMPa-8 (At5g52000)	SALK_081405	9	13	10	32	1.2	NS
	SALK_016349	9	10	8	27	2.0	NS
TIP5;1 (At3g47440)	SALK_085801	4	6	5	15	0.83	NS
	GK_171E01	2	4	9	15	9.8	S*

Table 5.4: Number of Kan^R:Kan^S seedlings from selfed and F1 crosses found in *+/impa-8* , *+/daa1* and *+/tip5;1* plants. The segregation analysis was verified using chi-square analyses to test deviations from a 3:1 ratio If the T-DNA segregates as a dominant Mendelian if the T-DNA insert causes a recessive mutant, lethal to either of the gametophytes, this will prevent the transmission of the mutant through this germline and will deviate from the expected 1:1 ratio. NS: not significant, * indicate statistically significant differences from an expected ratio ($p < 0.05$).

						Expected 1:1		Expected 3:1	
Genotype	Generation	Total	Kan^R	Kan^S	R:S	χ^2 value	significance	χ^2 value	significance
+/impa-8	Selfed	189	108	81	1:1	3.9	NS	32.1	*
+/daa1	Selfed	229	110	119	0.9:1	0.4	NS	0.4	*
+/tip5;1	Selfed	203	141	62	2.2:1	80.2	*	3.3	NS
ms1-1 x / impa-8	F1	351	211	140	1.5:1	19.5	*	41.5	*
ms1-1 x +/ tip5;1	F1	455	340	115	03:01	111	*	0.0	NS

Kan^R:Kan^S seedling was counted and tested using chi-square as any deviation of this Mendelian ratio would indicate that the gene providing antibiotic resistance is transmitted at a reduced frequency through one or both parents, and that the insertion has disrupted a gene required either for gametophyte or embryo viability. Segregation of T-DNA insertion line derived kanamycin resistance in self-fertilised + /*impa-8* and + /*daa1* plants the ratio of resistant to sensitive (Kan^R:Kan^S) plants close to the expected 1:1 ratio distortion which result from failure to transmit through either female or male gametophyte reversion to 3:1 ratio ($p < 0.05$) (Table 5.4). This suggests that the *impa-8* and +/*daa1* insertions may have a small negative effect on genetic transmission or this may be as a result of the silencing of the selectable marker tagging the T-DNA which is a common phenomenon with many T-DNA lines (O'Malley and Ecker, 2010). Self-fertilised progeny from +/*tip5;1*, showed that the ratio of Kan^R:Kan^S plants is close to the expected 3:1 ratio and differs significantly from a 1:1 ratio ($p < 0.05$) (Table 5.4). In contrast to the data from self-fertilised, + /*impa-8* plants shows that the ratio of resistant to sensitive (R:S) plants showed a significant difference from a 3:1 and from 1:1 ratios. Whereas in +/*tip5;1,* the Kan^R:Kan^S segregation ratio of the F1 progeny was close to 3:1, consistent with the self-fertilised segregation data (Table 5.4), indicating that transmission through the male is normal. For the *tip5;1* the result showed that a 3:1 segregation ratio. This data suggests that disruption of the *DATs* locus have had affect on pollen fitness.

5.6 Discussion

The *duo1* mutant is characterised by the appearance of a single germ cell due to failure of germ cell division (Durbarry *et al*., 2005). *duo1* germ cells also fail to express several germline markers and do not result in fertilization (Brownfield *et al*., 2009a). Moreover, according to previous observations, ectopic expression of DUO1 in seedling is sufficient to up-regulate the expression of known *DUO1* target transcripts *MGH3*, *GEX2*, and *GCS1* (Brownfield *et al*., 2009a).

A time-course microarray experiment using RNA isolated from seedlings grown in the presence and absence of inducer for three independent time points of 6, 12 and 24 hours,

enabled the investigation of the *DUO1* target and led to the discovery of > 60 germline-specific or enriched genes (Borg *et al.*, 2011). This strategy was adopted to identify additional regulatory targets of *DUO1*. Functional analysis showed that the R2R3 MYB transcription factor, DUO1, regulates genes that belong to several functional categories. In this chapter, constructs for a subset of target genes were built, using each of the native target promoters to drive the expression of an H2B-GFP fusion. Their expression was monitored in wild type and in the *duo1* background. Four genes were found to be *DUO1* dependent target within the gametophyte. Among them, a number of transporter related genes, were most clearly expressed in sperm cells. *PCR11*, another target of *DUO1*, is involved in a wide variety of different functions, such as protein unfolding and degradation, peroxisome biogenesis, and DNA replication and recombination (Snider *et al.*, 2008). Thus, *DUO1* target genes are apparently involved in the regulation of a variety of different processes needed for successful double fertilisation. The discovery and characterisation of novel regulatory targets will be great help for establishing the essential *DUO1* regulatory network in the male germline and plant sexual reproduction.

5.6.1 The novel *DAT* genes are germ line specific

In this chapter, *DAT* promoter construct was used to transform *duo1* to monitor the *DAT* promoters. All the wild type pollen showed GFP fluorescence in twin sperm cells while there was no fluorescence in *duo1* germ cells, excluding *IMPa-8* where a weak expression was detected in about 4 % of the *duo1* single germ cells. When these constructs were crossed to *duo3* mutant, a variable GFP level was observed in a small percentage of *duo3* single germ cells. However, when *TIP5;1* was introduced to *duo3*, GFP fluorescence was seen in the single germ cells in the mutant pollen in a similar percentage to that of wild type pollen. A more detailed analysis involving of the GFP quantification showed a reduction in GFP level in *duo3* germ cells compared to wild type sperm cells. This argues that the activity of these promoters is suppressed to some extent in *duo3* mutant germ cells.

A detailed molecular analysis has been carried out to validate whether these genes are directly regulated by *DUO1* gene (Borg *et al.*, 2011). In fact, motif analysis was employed to

investigate the promoter regions of the genes, looking for any putative promoter region may contain common DNA motifs bound by DUO1 in the region of 500 bp upstream of the target sequences. This analysis showed that the sequence core AACCG is highly over-represented in DATs (Borg *et al*., 2011).

Further work revealed that *DUO1* and *DUO3* have overlapping but distinct targets. Both *DUO1* and *DUO3* are required for the expression of *PCRII*, *IMPa-8* and *DAA1*. However, the expression of these markers in *duo3* germ cells is reduced and variable compared with complete suppression in *duo1* germ cell, indicating that the *DUO3* has indirect role in the regulation of *DAT* promoters. In addition the data demonstrated that the expression of *TIP5,1* is totally independent of *DUO3* as it has normal expression in *duo3* germ cell mutant. In fact, the expression of *MGH3* was totally suppressed in *duo1* but not in *duo3* mutant germ cells (Brownfield *et al*., 2009b). In addition *DUO3* is not required for *CYCB1*;*1* expression in the germline. This overlap is not due to *DUO3* being required for the expression of *DUO1*. Similarly, *DUO1* is not required for the expression of *DUO3 (*Brownfield *et al*., 2009b). To date it is still mysterious how *DUO1* and *DUO3* cooperate to activate expression of their common targets. It is possible that *DUO3* and *DUO1* interact, directly or indirectly, in a complex that activates transcription. Expression of *TIP5*,1 in *duo3* germ cells shows, however, that *DUO3* is not always required for *DUO1* to activate the expression of its targets.

The expression of *DAA1* and *PCRI1* is undetectable until at early tricellular stage of the pollen development, arguing that expression of these genes might be germline-specific and some their expression was exclusively was observed in sperm cell nuclei. This is consistent with the fact that both DAA1 and PCR11 were induced above 3-fold only after 12 h of induction mirroring the delayed activation of these promoters in the germline. Whereas, *TIP5,1* was not expressed in pollen microspores, and its expression was only observed soon after PMI within the germ cell many genes, expressed within the microspore, are known to be repressed as the pollen develops (Honys and Twell, 2004). From this, it can be deduced that after PMI, a set of genes are repressed as other genes are expressed. *IMPa-8*, however, was detected in polarized microspore and bicellular pollen shortly after mitosis. Afterward, the promoter activity becomes sperm cell-specific. This might be due to the role of *IMPa-8*

within microspore. This is consistent with *DUO1*-independent *IMPa-8* expression in the microspore, which after that becomes *DUO1*-dependent in the germline, with a declining vegetative cell signal due to turnover of inherited H2B-GFP protein. It appears that such genes are highly expressed early in pollen development but become under *DUO1* control later on. Indeed, a residual level of *IMPa-8* expression was still detectable in *duo1* germ cells, suggesting that *DUO1* is the major factor required for the activation of these DAT genes in the male germline.

Investigation of T-DNA insert lines showed normal phenotype and segregation ratio distortions. Homozygous plants were detected in all T-DNA lines, suggesting that the T-DNA inserts did not cause an embryonic or gametophytic lethal mutation. It can be concluded, from the segregation ratio results, that the genes being assessed are not exclusively vital for male gametophytic development. In addition, the redundancy of gene function may lead to mask any phenotypic affect that result from disrupting these genes.

Another possibility is that genes within *Arabidopsis* are known to be expressed only under certain environmental stresses (Bouche and Bouchez, 2001; Weber *et al*., 2004). It is possible, these genes are not important unless the pollen is exposed to certain environmental stresses, and therefore an affect would not have been observed under the standard growth condition (Hua and Meyerowitz, 1998). To assess this possibility, the T-DNA lines should be grown under different stress conditions.

In summary, the discovery of new target genes in this chapter has made significant progress toward understanding and establishing the regulatory networks involved in germline specification and in sperm cell formation. An identification of new target genes has shed new light on how *DUO1* regulates these biological processes during sperm cell formation. For example a target gene like *DAA1* encoding *ATPases*, confirming and extending the possible role of *DUO1* in diverse pathways, most noticeably metabolism. Also the identification of other targets involved in nitrogen recycling and transport activity, demonstrating the role of *DUO1* to participate in an extensive reprogramming of gene expression in germline formation, either directly or through the action of other

transcriptional regulators. It is likely that these genes are direct targets of *DUO1* as they show a rapid response to the ectopic expression of *DUO1* in seedling. Moreover, the promoters of these genes contain at least one MYB binding site (MBS) motif, suggesting that these genes are regulated directly by *DUO1*. As in *DUO1*, interestingly, *DUO3* is also required for the normal expression of some of these identified targets. However, some *DUO1* targets, such as *TIP1;5* and *MGH3*, do not require *DUO3*, highlighting different pathways of germline-specific activation.

Because of the fact that *DAT* promoters direct gene expressions exclusively in both germ cells and sperm cells, they can thus provide plant researchers with another resource for future studies such as in screening mutants that affect germ cell fate as well as provide a better understanding the male contribution to fertilization. Precisely, the *DAA1* and *PCR11* promoters offer novel molecular tools for targeted manipulation of gene expression in *Arabidopsis* sperm cells.

Chapter Six
General Discussion

Summary

The major aim of this thesis is to understand more about the mechanisms controlling cell division and cell differentiation during male germline development. In Chapters 3 and 4 general cytological and genetic analysis, including forward and reverse genetics approaches were employed to identify the molecular nature of the male gametophytic defects in the *duo4* mutant and further to analyse and characterise the role of *duo4* mutation in double fertilisation and germ cell morphogenesis. During the course of this work it has become clear that *duo4* does not result from a simple loss of function mutation. In particular, the G2 arrest in *duo4* germ cells was shown to occur as result of misexpression of *CCS52A1*. In the second results chapter of this thesis molecular evidence was obtained to support the role of CCS52A family genes during pollen development, indicating that *CCS52A1* is a very strong candidate for the cell cycle arrest in *duo4* germ cells. The analysis of CYCB1;1 expression in wild type and *duo4* germ cells initially suggested that the *duo4* phenotype results from ectopic expression of CCS52A1, specifically in the male germline and this is further supported by RNAi experiments. Effectively, the successful ability of RNAi constructs to rescue the *duo4* division phenotype provides the best evidence for the misexpression hypothesis. However, it remains unclear how CCS52A1 mis-regulation occurs and whether other CCS52A1 deregulation mechanisms operate during G2 in plants.

The identification of several genes regulated directly by DUO1 in chapter 5 has made a significant contribution to our understanding of the regulation of genes associated with sperm cell differentiation. The analysis of these target genes revealed that they are preferentially expressed in the male germline and belong to different functional classes. Stable H2B-GFP marker lines driven by the *PCR11, DAA1, IMPa-8* and *TIP5;1* promoters showed that these promoters are DUO1-dependent in the male germline expression. Thus, DUO1 plays a critical role in regulating sperm cell production through the control of a diverse collection of germline-specific and germline-expressed proteins.

6.1 *duo4* is a gametophytic mutation

The general goal of this thesis was the identification and characterization of a

gametophytic mutant that specifically affects germ cell division. The *duo4* mutation is a novel class of mutation derived from morphological screening using DAPI staining of pollen (Park *et al.*, 1998). The *duo4* mutant represents a distinct class of gametophytic mutant that results in the specific arrest or the delay of germ cell division. Furthermore, a number of male gametophytic mutants such *cdka;1, fbl17, duo1* and *duo3* have been described in Arabidopsis that result in bicellular pollen due to failure of germ cell division (Kim *et al.*, 2008; Durbarry *et al.*, 2005; Rotman., *et al* 2005; Iwakawa *et al.*, 2006; Nowack *et al.*, 2006). Similar to these mutants, the germline is specifically affected and the morphology of pollen in the *duo4* mutant appeared similar to wild type as no collapsed pollen was observed by light microscopy (Section 3.1.1).

Genetic analysis of the *duo4* mutation (Section 4.1) revealed the gametophytic nature of this mutation. *duo4* is almost completely penetrant resulting in ~50 % of pollen with an undivided germ cell indicating a gametophytic effect for the *duo4* mutation. In addition, analysis of genetic transmission by reciprocal crosses showed that *duo4* is transmitted normally through female gametes, but is only rarely transmitted through the male. This indicated that the *duo4* mutation specifically impaired the development of the male gametophyte and does not affect the development or functions of the megagametophyte (Section 4.2).

6.2 *duo4* affects germ cell division

Developmental analysis revealed that in *duo4* asymmetric division at microspore mitosis progresses normally and the earliest defect is only seen at germ cell mitosis. Furthermore, the proportion of pollen with a *duo4* germ cell expressing germ cell markers (MGH3, DUO1 GEX1 and GEX2) is similar to the proportion of pollen with a single sperm cell (Section 3.1.4). These findings indicate that cell fates are not obviously affected in *duo4* pollen grains in which germ cells failed to divide. The asymmetric division at PMI is critical for the correct cell fate of the male gametophyte and the resulting two daughter cells possess distinct structures and cell fates (Twell *et al.*, 1998). The failure to clearly establish germ cell fate in *gem1* (Park *et al.*, 1998) and *tio* mutants (Oh *et al.*, 2005) provides evidence for the role of cell division including a new cell wall for establishing correct germ cell fate. On the other hand, the bicellular

phenotype of *duo4* pollen shows that *DUO4* has a role in germ cell division with no apparent effect on cell fate. In the *duo1, duo3, cdka;1 and fbl17* mutants (Kim *et al*., 2008; Durbarry *et al*., 2005; Brownfield *et al*., 2009b; Iwakawa *et al*., 2006; Nowack *et al*., 2006), asymmetric division occurs normally suggesting that distinct mechanisms exists to prompt germ cell division. The ability of these mutants to undergo normal microspore division, but their failure to enter or complete the second mitotic division suggests that germ cell division is apparently controlled by a different set of genes and by different mechanisms compared with PMI.

The mean mitotic index was determined by scoring the number of germ cells in mitosis from bud stages –5 and –4 in both wild type and the *duo4* mutant (Section 3.1.5.2). The mean mitotic index in *duo4* was almost one-half the mitotic index of that observed in the wild type. Thus, *duo4* prevents entry into mitosis and *DUO4* could therefore represent a direct or indirect regulator of CYCB/CDK activity or a novel component required for germ cell mitosis.

Several other proteins have been shown to be required for male germ cell division, however, the role of *DUO4* is distinct. In *duo1* and *duo3* mutant germ cells, at least one round of S-phase is completed, as mature germ cells have a DNA content of 2 C or more, while in *cdka*;*1* and *fbl17* germ cells are delayed in S-phase (Nowack *et al*., 2006; Kim *et al*., 2008; Aw *et al* 2010). In *duo4* mutant germ cells, at least one round of S-phase is completed, as germ in mature pollen cells have an average DNA content of 2 C and no further increase in DNA content is detected at anthesis (Section 3.1.5.4). Therefore, the timing of S-phase appears to be normal in *duo4* germ cells. Several studies have demonstrated that entry into mitosis in higher eukaryotes is controlled by the activity of CDK/CYCB (reviewed by Inze and Veylder, 2006). Thus, failure of *duo4* germ cells to enter mitosis might result from impairment of essential cell cycle regulators. In plants, the E2F/DEL1 binding is an important inhibitor of the endocycle by inhibiting the transcription of genes that are required for cells to enter S-phase (Vlieghe *et al*., 2005). In addition, the E2F binding sites play a critical role in the regulation of the activities of many genes involved in the transition from G1 to S-phase.

These observations were extended by investigating the expression of *AtCYCB1;1* as a potential downstream target of *DUO4* which revealed that CYCB1;1 (pCDGFP) does

not accumulate in *duo4* germ cells before entry into mitosis (Section3.1.5.5.1). This demonstrate that *duo4* interferes with the expression of CYCB1;1 in male germ cells reflecting their unique arrest in G2. To progress through G2 phase and prepare for mitotic entry, cells must accumulate CYCB1;1 and further require APC to remain inactive after S-phase. The APC/C complex targets most of the crucial mitotic regulators by changing its substrate specificity throughout mitosis. Evidence for the ubiquitination pathway in the germline development was demonstrated by the turnover of the KRP6/7 by the SCF^{FBL17} complex, which is an CDK inhibitor in S-phase (Kim *et al*., 2008). FBL17 is transiently expressed only in the male germ cell after PMI. However, in the vegetative cell *FBL17* is proposed to maintain inhibition of CDKA activity and vegetative cell cycle progression. Germline-specific expression of FBL17 thus enables differential control of the cell cycle in the germ and vegetative cells, effectively licensing germ cells for progression through S-phase (Liu *et al*., 2008a).

Thus *duo4* germ cells have greatly increased activity of APC, which normally degrades CYCB1;1 to promote exit from mitosis and that occurs mainly at the post-translational level (Harper *et al.,* 2002). Similarly, failure of mitotic entry in *duo1* germ cells is caused at least in part by the lack of germline activation of the G2/M regulator CYCB1;1 (Brownfield *et al*., 2009a). However, the specific mechanism by which *DUO1* target the G2/M phase-specific accumulation of CYCB1;1 has remained unclear. Unlike other target genes, CYCB1;1 transcripts are not ectopically induced in seedlings in response to DUO1, which may indicate that *DUO1* regulates CYCB1;1 indirectly or by using a post-transcriptional mechanism (Brownfield *et al*., 2009a).

6.3 The *duo4* mutation delays germ cell mitosis and causes seed abortion.

The paternal effect of the *duo4* mutation leads to seed abortion, which is characterised by an arrest of embryo development at globular stages that is associated with failure of endosperm development (Section 3.2.2). Cell cycle arrest in G2 phase in *duo4* germ cells has major implications for the secondary phenotype of the *duo4* mutant that concerns fertilisation of the female gametophyte. In *duo4* pollen, all germline fate markers analyzed are properly expressed (Section 3.1.4) indicating that germ cell fate was apparently normal and *duo4* may act specifically on the cell cycle (mitotic entry)

but does not affect differentiation, which could explain their capability of fertilisation. In contrast to *duo4* mutant germ cells which are capable of fertilisation, *duo1* germ cells are, however, incompletely differentiated and no fertilisation events are observed (Rotman *et al*., 2005; Brownfield *et al*., 2009a).

Consistent with observations of arrested globular embryo in *duo4*, limited central cell division was also observed, indicating that germ cells are capable of at least fertilisation of the egg cell, but detailed analysis revealed division of *duo4* germ cells in the pollen tube and fertilisation of the central cell. Mutant *duo4* germ cells successfully divided to produce twin sperm cells in growing pollen tubes and were able to perform double fertilisation showing about 60% of pollen tubes contained two sperm cells. The production of two sperm cells in the pollen tube was recently described for the loss of function of *cdka;1* mutation allele (Aw *et al*., 2010). In these studies, similar to the case of *duo4*, it was found that the *cdka;1* germ cells divided later in the pollen tube and could perform double fertilisation.

Crosses of *ms1-1* plants with *duo4* pollen homozygous for promCDKA;1-GUS fertilisation reporter gene demonstrated that *duo4* mutant germ cells can fertilize the female gametophyte (Section 3.2.2). The possibility that *duo4* pollen tubes deliver two sperm cells was considered and this was examined further by using KS22 endosperm markers (Section 3.2.2). GFP signal was only detectable in endosperm in ovules that are fertilised by *KS22* pollen, confirming that these seeds are the products of double fertilisation . Interestingly, while the *cdka;1* mutant shows retarded S-phase, *duo4* germ cells successfully complete S-phase and arrest at G2. The reason for endosperm development failure and seed abortion in *duo4* and *cdka*;1 unclear, but it may as result from the fact that *duo4* and *cdka;1* mutant germ cells are incompletely differentiated. The production of fully differentiated sperm cells is thus critical for double fertilisation and is an important requirement for successful reproduction. Intriguingly, in *duo4* a substantial number of germ cells appeared to successfully fertilise egg cells and while the fusion with the central cells occurs this fail to support substantional endosperm development.

6.4 Genetic mapping identifies *CCS52A1* as a candidate locus for the *duo4* mutation

Map-based cloning procedures resulted in the localization of the *DUO4* gene on the lower arm of chromosome IV *(*Section 4.3.2). The genetic interval of interest was narrowed down to 14.5 kb, and *CCS52A1* was selected as a strong candidate for the *DUO4* gene based on its known role in cell division (Section 4.3.3). However, sequencing of *CCS52A1* alleles from heterozygous mutant plants showed nucleic acid sequence differences from wild type but that were restricted to intron sequences within the transcription unit. In addition analysis of loss of function *CCS52A1* T-DNA insertion alleles showed no effect on germ cell division or transmission, indicates duo4 is not a simple loss of function mutation in *CCS52A1* (Section 4.3.4). These data, together with the failure of the *duo4* germ cells to accumulate CYCB1;1 (Section 3.1.5.5.1), strongly support the idea that *duo4* phenotype results from misexpression of CCS52A1 in the germ cell at G2 phase.

The CCS52A1 promoter fragment was sequenced that revealed a point mutation at -700 (C >T) relative to the start codon. It is possible that a single-base-pair substitution is sufficient to increase the activity of this promoter. In Arabidopsis, deletion of an E2F binding site in the promoter of the *MCM3* gene leads to increase the MCM3 expression slightly higher compared to the wild type promoter (Stevens *et al*., 2002). Thus, *MCM3* promoter activity persisted in G2 as the promoter activity was no longer repressed (Stevens *et al*., 2002). It has been reported that the FBL17 promoters in, *A. thaliana* and rice, carry E2F binding sites (Vandepoele *et al*., 2005). In addition, in Arabidopsis plants when the S-phase transcription factor E2Fa/DPa ectopically expressed, the expression of FBL17 expression is strongly enhanced. Whether *FBL17* activity is a direct target of E2Fs, however, is not established yet. It is worth noting that a possible E2F binding site was identified in the promoter of the *CCS52A1* gene, but no base pair change was discovered in the identified sequence. However, it has been reported that the temporal expression of *CCS52A2* is regulated through E2Fe/DEL1 but not *CCS52A1* (Lammens *et al*., 2008). Moreover, CCS52A1, but not CCS52A2, are implicated in endoreduplication through the targeting of CYCA2;3 for degradation (Boudolf *et al*., 2009). Additional studies will be necessary to investigate the potential role of the E2F

binding site in *CCS52A1* promoter to find out if *CCS52A1* gene is a native target of E2F and to test the possible effect of the -700 (C >T) change on *CCS52A1* prompter.

Based on the analysis of the GFP reporter lines, *CCS52A1* promoter activity is clearly detectable at the microspore stage and at early bicellular. While the GFP signal is no longer detected during mid to late bicellular stage. It will be interesting to evaluate whether the promoter point mutation identified could affect expression of CCS52A1. It is possible, therefore, that the promoter activity is no longer repressed during S-phase, leading to an increase in CCS52A1 activity and CCS52A1 becomes constitutively activated during G2. To investigate this hypothesis, the mutated *CCS52A1* promoter fragment is being cloned to test its expression and the result will be compared with *CCS52A1* promoter expression pattern that was analysed in previous experiments (Section 4.4.3). If the mutated promoter results in a different expression profile compared with wild type *CCS52A1* promoter, this would demonstrate that the ectopic expression of CCS52A1 induce is due to this promoter mutation.

The cell cycle specific phenotype that was observed in *duo4* germ cells, associated with the loss of expression of CYCB1;1 is mostly due to misexpresssion of CCS52A1 and the subsequent activation of APC (Section 3.1.5.5.1 and Section 4.5.1). Interestingly, transgenic plants overexpressing *CCS52A1* under control of the *DUO1* promoter phenocopied the *duo4* phenotype, thus providing further evidence for the hypothesis that the *duo4* phenotype results from CCS52A1 misexpression (Section 4.5.1). In normal cells, APC/C is constitutively active during the cell cycle, but its activity is thought to be specifically restricted to the period from early mitosis until late G1 and is driven by substrate proteins in a highly selective manner. The temporal regulation and substrate specificity of APC/C are attributed to a conserved family of WD40 proteins that includes CDC20 (fizzy) and CDH1 (fizzy related). In Drosophila, loss of function of *Rca1* result in a failure of embryos to exit mitosis as result of ectopic expression of the APC/C in G2 (Grosskortenhaus and Sprenger, 2002) and this arrest can be rescued by Rca1 expression. Similarly, in humans *Emi1* inhibits both APC/C-Cdc20 and APC/C-CDH1 through posttranscriptional regulation, which keeps APC inactive from early G2 until prophase (Hsu *et al.*, 2002; Reimann *et al.*, 2001). However, no homology to *Emi*/*Rca1* has been identified in *Arabidopsis*, therefore is not clear how the APC activity is regulated during G2 stage (Figure 6.1).

Yeast cell expressing a ste9/srw1 allele, that is homologous to *Drosophila* Fizzy-related, triggered a gain-of-function phenotype. This mutant protein is very stable and associates with APC/C in G2 (Blanco *et al.*, 2000). Overexpression of *Mtccs52* in yeast promotes mitotic cyclin degradation and cell division arrest (Cebolla *et al.*, 1999). In addition, these cells show a high frequency of diploidization. Other study shows that the constitutive overexpression of *CCS52A* genes in Arabidopsis can induce endoreplication while blocking mitosis (Larson-Rabin *et al.*, 2009). Such a mechanism possibly could explain the *duo4* phenotype as results from misregulated association of CCS52 with APC/C in G2 (Figure 6.1). Thus, the $APC^{ste9/CCS52}$ complex activity, which normally is active only in G1, may lead to prevent the accumulation of mitotic CDK activity in G2, thereby blocking mitosis. As both Mt*ccs52a* and *srw1* trigger the same phenotype this suggests that AtCCS52A is the closest homologue of the CDH1-type activators in human with similar functions in the cell cycle.

Vertebrate CDH1 carry two RxxL-type destruction boxes that lie at the N-terminus, therefore, these proteins might be targeted for degradation by APC (Listovsky *et al.*, 2004). However, AtCCS52 family have no D-box sequence. Instead a PEST like motif that lies in the terminal part of AtCCS52A1 may lead to instability of the AtCCS52A1 protein. The MtCcs52A-APC complex is negatively regulated via the CYCB dependent CDK1 phosphorylation (Tarayre *et al.*, 2004). A similar regulatory mechanism has been described in AtCCS52A1 as the CCS52 proteins showed interaction with free and CDK-bounded mitotic cyclins (Tarayre *et al.*, 2004). However, it is still questionable whether the PEST motif is involved in the control of CCS52A1 stability during the cell cycle progression.

To gain further support that the observed phenotype is indeed caused by misexpression of CCS52A1, RNAi Knockdown of CCS52A1 with *DUO1* and *GEX2* promoters was performed and was predicted to suppress *duo4* phenotype. Multiple +/*duo4* individuals expressing hp1-CCS52A1 and hp2-CCS52A1 showed a reduced percentage of bicellular pollen in *duo4* heterozygous plants, thus demonstrating that inappropriate expression of CCS52A1 in the germline is the cause of failure of entry of germ cells into mitosis (Section 4.6). S-phase proceeds normally suggesting that *duo4* acts specifically during G2. RNAi is proven as an efficient approach to rescue mutations that

result from gain of function mutations and it has recently been applied in plant. In fact, the *floury* kernels phenotype that result from the dominant mutation of *Mucronate1* (*Mc1*) in maize when crossed to a homozygous *RNAi* line was able to rescue the mutation and restore a normal seed phenotype (Wu and Messing, 2010). Except for displaying higher DNA content, pollen from *CCS52A1*^{ME} plants is phenotypically similar to the *duo4* mutant, suggesting that enhanced *CCS52A1* expression has a direct and specific impact on germ cell division.

So far the misexpression of CCS52A1 that phenocopied *duo4* and RNAi that efficiently down-regulated CCS52A1 expression and rescued *duo4* mutation, together, have provided direct evidence that the inappropriate expression of CCS52A1 is the cause of failure of entry into mitosis in *duo4* germ cells. However, the level of CCS52A1 transcript in +/*duo4* showed no clear differences from the wild type in mature pollen (Figure 4.6 B). To obtain more quantitative results the relative expression level of CCS52A1 transcripts should be determined by quantitative real time polymerase chain reaction (qRT-PCR).

6.5 CCS52A1 and CCS52A2 genes are expressed throughout male germline development

CDH1/CCS52 are substrate recognisation protein, and activators of APC that regulate the cell cycle by targeting and degradation of various cell cycle regulators. Arabidopsis has three *CCS52* gene copies whose functions have not yet been explored in male gametogenesis. Phylogenetic analysis of the plant CCS52A proteins revealed a distinct subclass CCS52B compared to CCS52A proteins in plants (Lima Mde *et al.*, 2010). The *CCS52A1* and *CCS52A2* genes are present on the same chromosome, thus they result probably from a recent genomic duplication event.
The expression pattern of the three *AtCCS52* genes in the four stages of pollen development in Arabidopsis was determined by RT-PCR. The result showed that the expression of the three *CCS52* genes was overlapping and suggested largely redundant functions of these three homologues during pollen development.

The RT-PCR result was further supported by analysis of the expression profile of

CCS52A1 and *CCS52A2* promoters: H2B-GFP fusions (Section 4.4.3). It was shown that CCS52A1 and *CCS52A2* exhibit similar expression patterns during pollen development. In Arabidopsis, both *CCS52A1* and *CCS52A2* are thought to control G1/S transition and keep the level of mitotic cyclins under tight control, preventing cell division. This could explain the absence of GFP activity in germ cells at bicellular stage. The timing of promoter activation of both *CCS52A1* and *CCS52A2* is quite similar and the GFP activities regulated by both promoters were mainly detected in bicellular pollen only in the vegetative cell. It is suggested that CCS52 proteins may play similar roles in the degradation of mitotic cyclins to maintain cells in G1 (Cebolla *et al.*, 1999). However, in synchronised Arabidopsis cell cultures, the three *CCS52* genes are expressed at different times during cell cycle progression. In addition, CCS52 proteins showed different specificity for different Arabidopsis cyclins, strongly indicating that these genes could be tightly regulated to control cell cycle progression by destroying different cyclins at the right phase of the cell cycle (Fülop *et al.*, 2005). In addition, analysis of the promoter activities of *CCS52A1* and *CCS52A2* in Arabidopsis showed that they are expressed at different times during root development (Vanstraelen *et al.*, 2009).

Thus, the cloning of the *DUO4* gene provides us with valuable information concerning the mechanism of timely and specific activity of APC/C in the plant germline as the APC/C critically requires either one of two WD40-domain proteins as activators, CDC20 or CDH1. Recently, the *APC8* subunit of APC/C has been reported to be involved in the regulation of miR159 that targets *DUO1*, a transcriptional regulator of CYCB1;1 during male gametophyte development (Zheng *et al.*, 2011). This, together with the described information on *CCS52A1* and *duo4* may provide a fascinating link between DUO1 and CYCB1;1. As such DUO1 and its downstream target genes are plausible candidates for repression by *CCS52A1*.

The discovery of the role of CCS52A1 is not only a significant contribution to our understanding of male germline proliferation but also to the wider community since it is one of very rare examples of how cell-specific modules co-ordinate cell cycle progression using basic cell cycle machinery. Even though, a number of articles have been published about the role of the APC in plants, describing its role in the sporophyte, limited data has been described for the role of APC in male gametophyte. Detailed

insight about the APC-dependent regulation of DUO1 will almost surely become available in the near future. Whatever pieces are still missing in the puzzle, the *duo4* mutation will no doubt eventually reveal a better understanding of the role of APC in male germline development.

6.6 Ectopic expression of DUO1 in seedlings results in the identification of novel target genes

The discovery of *DUO1* gene, the first germline-specific transcription factor in plants (Rotman *et al.*, 2005), has made a significant contribution to understanding the mechanisms that govern cell cycle progression in male gametophyte development. *DUO1* plays a unique role in cell specification and cell cycle progression that is necessary to control the production of twin sperm cells (Brownfield *et al.*, 2009a). This presented an opportunity to discover new features of the mechanisms that couple cell specification with cell cycle control in plant development.

A steroid inducible system was used in the Twell laboratory in order to discover potential downstream targets of *DUO1,* with the aim of dissecting the pathways regulated by DUO1. This was followed by a collaborative effort between laboratory members that has confirmed that 14 of these putative target genes are native DUO1 targets (Borg *et al.*, 2011). The main aim of the current strategy was to verify which genes, found to be induced by ectopic *DUO1* expression in seedling, represent native targets of DUO1 in the male germline, and to find possible functions of these targets.

The genes analysed in this thesis (*DAA1,PCR11, IMPa-8* and *TIP5*;1) showed DUO1-dependent expression in the male germline and their promoter activities showed similar profiles to the described expression profile *DUO1*(Section5.2.1). *DAA1* and *PCR11* are a novel class of male germline genes that show sperm cell–specific expression (Section 5.4). Interestingly, *DAA1* and *PCR11* were induced above 3-fold only after 12 h of induction, mirroring the delayed activation of these promoters in the germline. The clear delay in activation of these promoters in the germline in response to the enforced expression of *DUO1* could arise from chromatin modifications and/or derepression of promoters in the presence of DUO1 (Borg *et al.*, 2011). In light of these results, the *DAA1* and *PCR11* promoters could be used as novel molecular tools to investigate gene expression specifically in Arabidopsis sperm cells. Interestingly, the *IMPa-8* promoter

shows microspore activity, with expression still detected in both daughter nuclei after the microspore mitosis, which subsequently becomes sperm cell specific (Section 5.4). This indicates that germline-independent mechanisms also regulate the expression of *IMPa-8* in the microspore followed by DUO1-dependent expression in the germline (Borg *et al.*, 2011).

An important feature is that the expression of *DAT* genes is not restricted to the male germline. Unlike *DUO1* which only shows male germline specific expression (Rotman *et al.*, 2005), *DAT* genes appear to be enriched in sperm cells as well as show expression in sporophytic tissues and other cell types of the male gametophyte (Borges *et al.*, 2008; Honys and Twell, 2004; Zimmermann *et al.*, 2004). For example, according to the publicly availably microarray data, the gene *DAA1* is highly expressed in sperm cells, dry seeds, imbibed seeds and mature siliques. This indicates that germline-independent mechanisms regulate the expression of some DUO1 target genes.

The discovery of the target genes that form the *DUO1* regulatory network highlights the wide range of functions that are required for sperm cell formation and double fertilisation. Indeed, target gene like *TIP5;1*, which has a conditional role in pollen tube growth (Soto *et al.*, 2008) and could have an important role in nitrogen recycling within sperm cells, demonstrates the importance of DUO1 regulation in sperm cell development and function. Identification of sperm cell specific promoters provides potential molecular tools to study gene expression in sperm cells. The strong fluorescent signal of *TIP5,1* and *IMPA-8* promoters may allow improved live imaging of the fertilisation process. In plant male germ cells, genes encoding transcriptional regulators are likely to be an important feature in germline development as have a distinct and diverse transcriptome (Engel *et al.*, 2003; Okada *et al.*, 2006; Borges *et al.*, 2008). Despite this, there are currently no well-characterized regulatory networks described in either the male or female plant germline. This work together with Borg *et al* (2011) significantly expands on the current models of male gamete differentiation. Furthermore, analysis of downstream regulatory proteins requirement for individual DUO1 target genes is being used as a criterion for further analysis (Borg and Twell unpublished). Future research will hopefully reveal whether DUO1 can be regulated through *DUO4*, which is very often downregulated in response to high APC activity Zhang *et al.*, 2011). However, the mechanisms that allow this to occur remain largely

unknown, further experiments will be required to uncover the mechanism by which DUO1 is downregulated in response to high APC activity, and will answer to these challenging questions.

6.7 Conclusions

Not surprisingly, the molecular mechanisms underlying double fertilisation still remain unknown. In particular, how they interact with each other to drive the main fertilisation events. With benefit from increasing the accessibility of forward and reverse genetics, it has become easier to dissect the molecular mechanism in vivo. In combination with the annotated Arabidopsis genome sequence, these advances provide the means to identify and determine the molecular mechanisms involved in double fertilisation.

The work presented in this thesis involved the characterisation of a newly isolated mutant, *duo4*, which affects germ cell division with no obvious other gametophytic phenotype. The *duo4* mutant produces pollen with one sperm cell capable of at least fertilisation of the egg cell, but detailed analysis revealed division of *duo4* germ cells in the pollen tube and fertilisation of the central cell. This is consistent with the observation of arrested globular embryos and limited central cell division. After performing fine mapping, it was determined that the *duo4* phenotype arises from the premature activation of CCS52A1 promoting APC/C dependent turnover of mitotic cyclins. This leads to prevent the accumulation of mitotic cyclins during G2, thereby inhibiting entry of germ cells into mitosis (Figure 6.1).

The ubiquitin system (UPS) is strongly involved in the regulation of the plant cell cycle. In particular the role of the APC/C in the regulation of the mitotic and endocycle is now well investigated in Arabidopsis. Future research will, hopefully, reveal whether analogous mechanisms occur during male gametogenesis. In addition, it will be of great interest to identify how APC activity is regulated during S/G2 transition and putative E2Fs- dependent regulation of CCS52A1 during germline development.

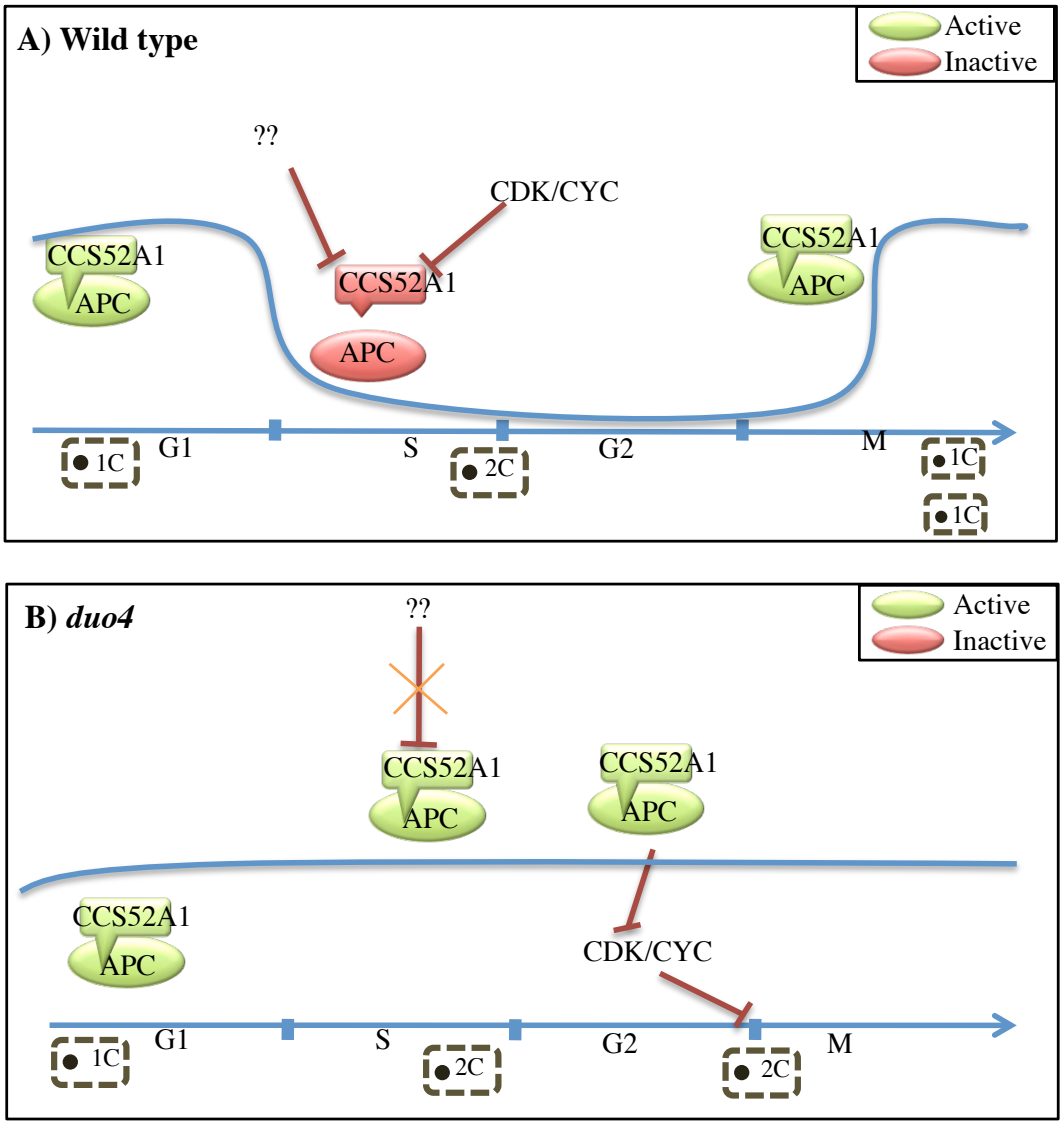

Figure 6.1: Schematic of the CCS52A1 activity throughout the cell cycle progression in the wild type and *duo4* mutant. A) G1 APC is activated by CCS52A1 complex to support maintenance of the G1 phase. Inactivation of APC/C activity at some later point in G1 or during S-phase helps Cyclin stabilization thus establishing S-phase. In G2 phase, an inactive APC/C is a prerequisite to allow the accumulation of CYC-CDK in preparation of mitosis. Cyclins are ubiquitinated, at least during M phase, by APC, and the cell will exit mitosis. B) In *duo4* mutant, the germ cell proceeds normally from G1 to S-phase, however, due to misregulation of APC-CCS52A1 complex CYC-CDK might fail to accumulate and subsequently the germ cell could be arrested at the G2/M transition.

Appendices

Table A1: Sequence of oligonucleotide primers used

Primer	Sequence
At4g11920 F1	CCAAATCTTCAAATCTGGAGGAACG
At4g11920 R2 INT.	GCTCCAACTCTTAGCCGATGACC
At4g11920 F2 INT.	AATAGATATGGGATGTGTTACGATGC
At4g11920 R1	GCAGATCACACAAAACTCATAAAACTTAGG
At4g22910-F1	CCGCTTAACTTCACATGTCGTTTTC
at4g22910-R1	CGGTACTAGTTCCAACAGCCAGATG
at4g22910-F2	GCTGAGGATAGTGTTTGCTCAGTGG
at4g22910-R2	CTGGCTGCTGCTGAAGAAATCAAG
at4g22910-F3	TGGTTTCACTTGAGTCACGAATCAA
at4g22910-R3	CAAAGACCGATGAGTCTCCGTCTTA
at4g22910-F4	GGAGCTGAGGATAGTGTTTGCTCAG
at4g22910-F5	AAAACCTTGGCGGATAAGATTTTCA
At4g22940-F1	TTTGCGTTTGTGTATTGCACTTTCG
At4g22940-R1	CTGTCTCTGCTCTTGGAATTTGAGG
At4g22940-F2	GTAGCTGGTGAAGCCCTTGTTGGTT
At4g22940-F3	TCGGTGTACATTTCTCAGAACCTCAG
At4g22940-F4	GAGCACAGGCTGCGTAATAGGTG
CDS-STARTattF1	ACAAAAAAGCAGGCTCTATGGGTTGTATCATTTCTTATCG
CDS-STOPattR2	ACAAGAAAGCTGGGTCTCAAGAAACCAAGAAACCG
CDS- NSTOPattR2	ACAAGAAAGCTGGGTCGCAAGAAACCAAGAAACCG
5-GENEattF1	ACAAAAAAGCAGGCTCATTGAGGCCATGCAACATTGAG
3-GENEattR2	ACAAGAAAGCTGGGTCCTATGTTTGCTGGAGAAACCCTTC
CKL4 XbaI F	TCTGTAGCTGGTGAAGCCCTTCTAG
CKL4 XbaI R	GAATGTTCCTCCCCCAATCTGTTGC
CKL4 NheI F	GGAATTAGCTGCCTCTGGTTGGCTA
MSGFP f-attb1	ACAAAAAAGCAGGCTCATGAGTAAAGGAGAAGAACTTTTCAC
TUA6 R-attb2	ACAAGAAAGCTGGGTTTAGTATTCCTCTCCTTCATCATCC
At1g64110-F(ATPase)	CTAGCCGAGCCATTCTCTTGTCC
At1g64110-R(ATPase)	AAGAGGTCTGGCCTACGGAGAGG
CCSCDNA F attb1	ACAAAAAAGCAGGCTCAATGGAAGAAGAAGATCCTACAGCA
CCSCDNA R_stop attb2	ACAAGAAAGCTGGGTTCACCGAATTGTTGTTCTACCAA
CCSCDNAR_non stop attb2	ACAAGAAAGCTGGGTGCACCGAATTGTTGTTCTACCAA
prom_seq F1	CAACAAGCATCTTCTCCAGTAAGC
prom_seq F2	TTTCATTGAACCATTTTTGACTAGT
prom_seq R	GAGAAGGAGATAGATCGAAAAGAGC
3' UTR F	TCAGAACACGGATAGTGAAATCG
3' UTR R	GTTTGGTTTGGTGTACATAATGTGG
TIP5 F	GCATCAAAAGTCGTTACCTTCC
TIP5 R	CACAGCTTGGTTCTTAAAGCTTCC
At4g22920 F1	CAAGCTTCGTGAAAGGAGTCTCTC
At4g22920 R	CCAATATTTAGATCCACCAAAAGG
At4g22920 F2	CCCTAGGACTTACACACTCACTCA
IMP F	CGGTTTAGAGTAGACGGTTAAGTAGC

IMP R	CACGTCTTCACTGTTCTTTTCAGC
Ccs52A1 prom att4 F	TGTATAGAAAAGTTGCAACAAGCATCTTCTCCAGTAAGC
Ccs52A1 prom att1 R	TTTTGTACAAACTTGGAGAAGGAGATAGATCGAAAAGAGC
Ccs52A2 prom att4 F	TGTATAGAAAAGTTGGTGATAAAAGTTTTGGAGAGGGACAC
Ccs52A2 prom att1 R	TTTTGTACAAACTTGTCAATCTCTTACTGTTTCGTTCCTC
Ccs52A2CDS F	ACAAAAAAGCAGGCTCTATGGAAGAAGATGAATCAACAACACCG
Ccs52A2CDSR_Stop	ACAAAAAAGCAGGCTCTCACCGGATTGTTGTTCTACCAAAAGAT
Ccs52A2CDSR_nonS	ACAAAAAAGCAGGCTCGCACCGGATTGTTGTTCTACCAAAAGAT
Ccs52A2 prom att4 F	TGTATAGAAAAGTTGGCGTCGACCTGGCAAAACGGGAAAGG
Ccs52A2 prom att1 R	TTTTGTACAAACTTGCCATGTTTGATTTCAATCTCTTAC
RTPCRA_F	GGTCATCGGCTAAGAGTTGGAG
RTPCRA_R	CATCTATCAGCAGTGCCACCAC
RTPCRB_F	GTGTCTTGGCATGGAACTCAAG
RTPCRB_R	ACATGGATGGGTACTTCCAGAG
CCS52A1hp_F1	ACAAAAAAGCAGGCTCGGTGGTTTCACTTGAGTCACGA
CCS52A1hp_R1	ACAAGAAAGCTGGGTGACCACTATGAGAAACACCAGGAG
CCS52A1hp_F2	ACAAAAAAGCAGGCTCCTGGTGGTGGTACTGCTGATAGAT
CCS52A1hp_R2	ACAAGAAAGCTGGGTGTATGTGTGACCGGTTAGAGTAGC
CCS52A2 STOP	ACAAGAAAGCTGGGTTCACCGGATTGTTGTTCTACCAAAAGAT
CCS52A2NS	ACAAGAAAGCTGGGTGCACCGGATTGTTGTTCTACCAAAAGAT
870-80 F1	CGACATCATTTGTATCTTGTCCATGC
870-80 R1	CGGTTGAAAGAGTTGAGAGTCTAGC
870-80 F2	GGAAAACATCGTTGATGCTCTCGAG
870-80 R2	ACTCGGTATAGAGACTCACAGTCC
870-80 F3	GCTCAAACTCAAACTAAAGGTTTCC
870-80 R3	GAGTAGATTGAAGACCAATTCGAACC
870-80 SEQ 1	GAGATAAATATGTACATTGGATCAAG
870-80 SEQ 2	TATGTATGTGTCCCACCAATTAACC
870-80 SEQ 3	CATACCATTTGTTGAGTTCAGTGAC
870-80 SEQ 4	TACTAAGAATCTCCAAAGTATCCCC
870-80 SEQ 5	ACTCGCGTTGTTAGCCAATTTACT
870-80 SEQ 6	ACTATATGGGCTTGGGTCTAGACTC
870-80 SEQ 7	GACGTGGATATTCTGATTATGAGGA
870-80 SEQ 8	GCCTTAGTTTTCTGTTTACAAAGCC
870-80 SEQ 9	GCGATCATGTCTAATGAAGAGTTTG
870-80 SEQ 10	CTTCTTGATCTTGAAGGTAAGAACC
870-80 SEQ 11	ATGAGCACTTCTTCATCTACCTTTG
870-80 F1mod	GCACTTCCTGTATCAAAGGCTACTAC
870-80 R mod	CCGGTAGCTCTACAATGTCTCTTAGT
880F1	ATGGTTGCGGTTGAAAGAGTTGAGAG

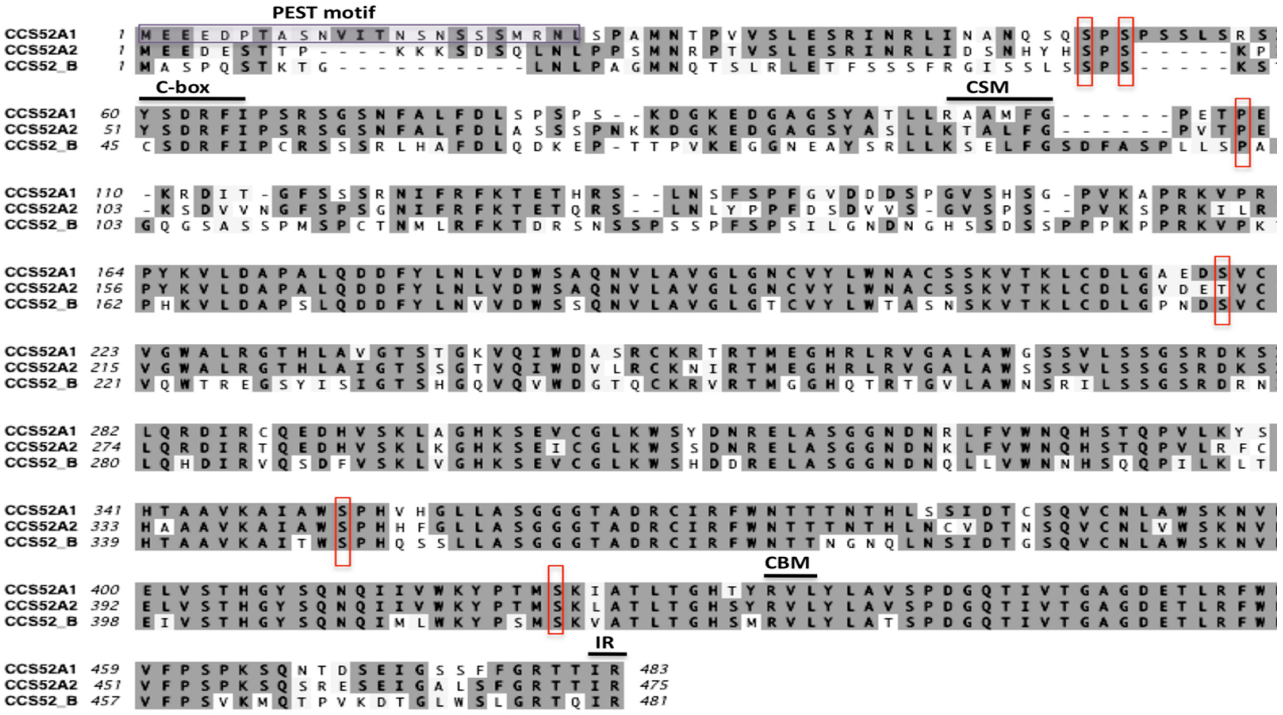

Figure A1: Box shade alignment of the CCS52 proteins. The characteristic CCS52 motifs (KEN, C-box, CBM, IR) are marked with black lines. Red squares mark potential CDK phosphorylation sites. Putative PEST motif at N-terminus of CCS52A1 is highlighted in light gray.

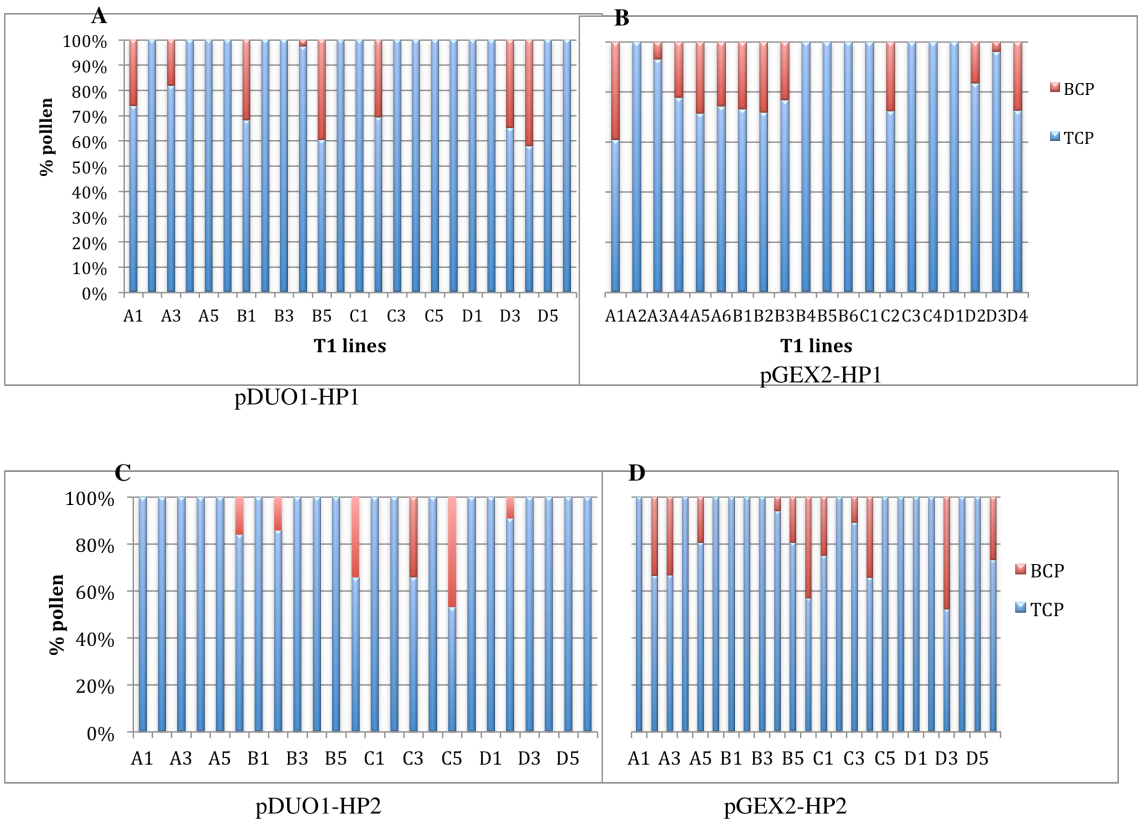

Figure A2: Rescue of *duo4* germ cell mitotic defect by RNAi knockdowns.

Graph showing the frequency of tricellular and bicellualr pollen grains in T1 plants. Four different constructs were used to drive the expression of RNAi Knockdown of CCS52A1 to induce transcripts turnover at G2 stage during germ cell development.

References

Amon, A., Tyers, M., Futcher, B. and Nasmyth, K. (1993). Mechanisms that help the yeast cell cycle clock tick: G2 cyclins transcriptionally activate G2 cyclins and repress G1 cyclins. *Cell* **74**, 993-1007.

Andrade, M. A., Gonzalez-Guzman, M., Serrano, R. and Rodriguez, P. L. (2001). A combination of the F-box motif and kelch repeats defines a large Arabidopsis family of F-box proteins. *Plant Mol Biol* **46**, 603-14.

Aw, S. J., Hamamura, Y., Chen, Z., Schnittger, A. and Berger, F. (2010). Sperm entry is sufficient to trigger division of the central cell but the paternal genome is required for endosperm development in Arabidopsis. *Development* **137**, 2683-90.

Bachmair, A., Novatchkova, M., Potuschak, T. and Eisenhaber, F. (2001). Ubiquitylation in plants: a post-genomic look at a post-translational modification. *Trends Plant Sci* **6**, 463-70.

Baskin, T. I. and Cande, W. Z. (1990). Kinetic analysis of mitotic spindle elongation in vitro. *J Cell Sci* 97 (Pt 1), 79-89.

Bell, C. J. and Ecker, J. R. (1994). Assignment of 30 microsatellite loci to the linkage map of Arabidopsis. *Genomics* **19**, 137-44.

Berger, F. and Twell, D. Germline specification and function in plants. *Annu Rev Plant Biol* **62**, 461-84.

Blanco, M. A., Sanchez-Diaz, A., de Prada, J. M. and Moreno, S. (2000). APC(ste9/srw1) promotes degradation of mitotic cyclins in G(1) and is inhibited by cdc2 phosphorylation. *Embo Journal* **19**, 3945-3955.

Bleeker, P. M., Hakvoort, H. W., Bliek, M., Souer, E. and Schat, H. (2006). Enhanced arsenate reduction by a CDC25-like tyrosine phosphatase explains increased phytochelatin accumulation in arsenate-tolerant Holcus lanatus. *Plant J* **45**, 917-29.

Borg, M., Brownfield, L., Khatab, H., Sidorova, A., Lingaya, M. and Twell, D. (2011). The R2R3 MYB transcription factor DUO1 activates a male germline-specific regulon essential for sperm cell differentiation in Arabidopsis. *Plant Cell* **23**, 534-49.

Borg, M., Brownfield, L. and Twell, D. (2009). Male gametophyte development: a molecular perspective. *Journal of Experimental Botany* **60**, 1465-1478.

Borg, M. and Twell, D. (2010). Life after meiosis: patterning the angiosperm male gannetophyte. *Biochemical Society Transactions* **38**, 577-582.

Borges, F., Gomes, G., Gardner, R., Moreno, N., McCormick, S., Feijo, J. A. and Becker, J. D. (2008). Comparative transcriptomics of Arabidopsis sperm cells. *Plant Physiol* **148**, 1168-81.

Bouche, N. and Bouchez, D. (2001). Arabidopsis gene knockout: phenotypes wanted. *Curr Opin Plant Biol* **4**, 111-7.

Boudolf, V., Barroco, R., Engler Jde, A., Verkest, A., Beeckman, T., Naudts, M., Inze, D. and De Veylder, L. (2004). B1-type cyclin-dependent kinases are essential for the formation of stomatal complexes in Arabidopsis thaliana. *Plant Cell* **16**, 945-55.

Boudolf, V., Lammens, T., Boruc, J., Van Leene, J., Van Den Daele, H., Maes, S., Van Isterdael, G., Russinova, E., Kondorosi, E., Witters, E. et al. (2009). CDKB1;1 forms a functional complex with CYCA2;3 to suppress endocycle onset. *Plant Physiol* **150**, 1482-93.

Boudolf, V., Rombauts, S., Naudts, M., Inze, D. and De Veylder, L. (2001). Identification of novel cyclin-dependent kinases interacting with the CKS1 protein of Arabidopsis. *J Exp Bot* **52**, 1381-2.

Brownfield, L., Hafidh, S., Borg, M., Sidorova, A., Mori, T. and Twell, D. (2009a). A plant germline-specific integrator of sperm specification and cell cycle progression. *PLoS Genet* **5**, e1000430.

Brownfield, L., Hafidh, S., Durbarry, A., Khatab, H., Sidorova, A., Doerner, P. and Twell, D. (2009b). Arabidopsis DUO POLLEN3 is a key regulator of male germline development and embryogenesis. *Plant Cell* **21**, 1940-56.

Brownfield, L. and Twell, D. (2009). A dynamic DUO of regulatory proteins coordinates gamete specification and germ cell mitosis in the angiosperm male germline. *Plant Signal Behav* **4**, 1159-62.

Buschhorn, B. A. and Peters, J. M. (2006). How APC/C orders destruction. *Nat Cell Biol* **8**, 209-11.

Capron, A., Okresz, L. and Genschik, P. (2003a). First glance at the plant APC/C, a highly conserved ubiquitin-protein ligase. *Trends Plant Sci* **8**, 83-9.

Capron, A., Serralbo, O., Fulop, K., Frugier, F., Parmentier, Y., Dong, A., Lecureuil, A., Guerche, P., Kondorosi, E., Scheres, B. et al. (2003b). The Arabidopsis anaphase-promoting complex or cyclosome: molecular and genetic characterization of the APC2 subunit. *Plant Cell* **15**, 2370-82.

Carroll, C. W., Enquist-Newman, M. and Morgan, D. O. (2005). The APC subunit Doc1 promotes recognition of the substrate destruction box. *Curr Biol* **15**, 11-8.

Castillo-Lluva, S., Garcia-Muse, T. and Perez-Martin, J. (2004). A member of the fizzy-related family of APC activators is regulated by cAMP and is required at different stages of plant infection by Ustilago maydis. *Journal of Cell Science* 117, 4143-4156.

Castro, A., Bernis, C., Vigneron, S., Labbe, J. C. and Lorca, T. (2005). The anaphase-promoting complex: a key factor in the regulation of cell cycle. *Oncogene* **24**, 314-25.

Cebolla, A., Vinardell, J. M., Kiss, E., Olah, B., Roudier, F., Kondorosi, A. and Kondorosi, E. (1999). The mitotic inhibitor ccs52 is required for endoreduplication and ploidy-dependent cell enlargement in plants. *EMBO J* **18**, 4476-84.

Charzyńska, M., Ciampolini, F. and Cresti, M. (1988). Generative cell division and sperm cell formation in barley. *Sexual Plant Reproduction* **1**, 240-247.

Chaubet-Gigot, N. (2000). Plant A-type cyclins. *Plant Mol Biol* **43**, 659-75.

Chen, Y. C. and McCormick, S. (1996). sidecar pollen, an Arabidopsis thaliana male gametophytic mutant with aberrant cell divisions during pollen development. *Development* **122**, 3243-53.

Chen, Z., Hafidh, S., Poh, S. H., Twell, D. and Berger, F. (2009). Proliferation and cell fate establishment during Arabidopsis male gametogenesis depends on the Retinoblastoma protein. *Proc Natl Acad Sci U S A* **106**, 7257-62.

Chen, Z., Hui, J. T. L., Ingouff, M., Sundaresan, V. and Berger, F. (2008). Chromatin assembly factor 1 regulates the cell cycle but not cell fate during male gametogenesis in Arabidopsis thaliana. *Development* **135**, 65-73.

Chew, E. H. and Hagen, T. (2007). Substrate-mediated regulation of cullin neddylation. *J Biol Chem* **282**, 17032-40.

Clough, S. J. and Bent, A. F. (1998). Floral dip: a simplified method for Agrobacterium- mediated transformation of Arabidopsis thaliana. *The Plant Journal* **16**, 735–743.

Colasanti, J., Cho, S. O., Wick, S. and Sundaresan, V. (1993). Localization of the Functional p34cdc2 Homolog of Maize in Root Tip and Stomatal Complex Cells: Association with Predicted Division Sites. *Plant Cell* **5**, 1101-1111.

Colon-Carmona, A., You, R., Haimovitch-Gal, T. and Doerner, P. (1999). Technical advance: spatio-temporal analysis of mitotic activity with a labile cyclin-GUS fusion protein. *Plant J* **20**, 503-8.

Corellou, F., Camasses, A., Ligat, L., Peaucellier, G. and Bouget, F. Y. (2005). Atypical regulation of a green lineage-specific B-type cyclin-dependent kinase. *Plant Physiol* 138, 1627-36.

Cox, C. J., Dutta, K., Petri, E. T., Hwang, W. C., Lin, Y., Pascal, S. M. and Basavappa, R. (2002). The regions of securin and cyclin B proteins recognized by the ubiquitination machinery are natively unfolded. *FEBS Lett* **527**, 303-8.

Crane, R., Gadea, B., Littlepage, L., Wu, H. and Ruderman, J. V. (2004). Aurora A, meiosis and mitosis. *Biol Cell* **96**, 215-29.

Cresti, M., Murgia, M. and Theunis, C. H. (1990). Microtubule organization in sperm cells in the pollen tubes of<i>Brassica oleracea</i> L. *Protoplasma* **154**, 151-156.

Criqui, M. C. and Genschik, P. (2002). Mitosis in plants: how far we have come at the molecular level? *Curr Opin Plant Biol* **5**, 487-93.

Criqui, M. C., Weingartner, M., Capron, A., Parmentier, Y., Shen, W. H., Heberle-Bors, E., Bogre, L. and Genschik, P. (2001). Sub-cellular localisation of GFP-tagged tobacco mitotic cyclins during the cell cycle and after spindle checkpoint activation. *Plant J* **28**, 569-81.

Culligan, K. M., Robertson, C. E., Foreman, J., Doerner, P. and Britt, A. B. (2006). ATR and ATM play both distinct and additive roles in response to ionizing radiation. *Plant J* **48**, 947-61.

Custers, J. B. M., Oldenhof, M. T., Schrauwen, J. A. M., Cordewener, J. H. G., Wullems, G. J. and Campagne, M. M. V. (1997). Analysis of microspore-specific promoters in transgenic tobacco. *Plant Molecular Biology* 35, 689-699.

Das, S., Raj, L., Zhao, B., Kimura, Y., Bernstein, A., Aaronson, S. A. and Lee, S. W. (2007). Hzf determines cell survival upon genotoxic stress by modulating p53 transactivation. *Cell* 130, 624-637.

d'Erfurth, I., Cromer, L., Jolivet, S., Girard, C., Horlow, C., Sun, Y., To, J. P., Berchowitz, L. E., Copenhaver, G. P. and Mercier, R. (2010). The cyclin-A CYCA1;2/TAM is required for the meiosis I to meiosis II transition and cooperates with OSD1 for the prophase to first meiotic division transition. *PLoS Genet* **6**, e1000989.

Del Casino, C., Bohdanowicz, J., Lewandowska, B. and Cresti, M. (1999). The organization of microtubules during generative-cell division in<i>Convallaria majalis</i&gt. *Protoplasma* 207, 147-153.

Del Casino, C., Tiezzi, A., Wagner, V. T. and Cresti, M. (1992). The organization of the cytoskeleton in the generative cell and sperms of<i>Hyacinthus orientalis</i&gt. *Protoplasma* 168, 41-50.

De Schutter, K., Joubes, J., Cools, T., Verkest, A., Corellou, F., Babiychuk, E., Van Der Schueren, E., Beeckman, T., Kushnir, S., Inze, D. et al. (2007). Arabidopsis WEE1 kinase controls cell cycle arrest in response to activation of the DNA integrity checkpoint. *Plant Cell* **19**, 211-25.

Dewitte, W. and Murray, J. A. (2003). The plant cell cycle. *Annu Rev Plant Biol* **54**, 235-64.

Di Fiore, B. and Pines, J. (2007). Emi1 is needed to couple DNA replication with mitosis but does not regulate activation of the mitotic APC/C. *Journal of Cell Biology* **177**, 425-437.

Di Fiore, B. and Pines, J. (2008). Defining the role of Emi1 in the DNA replication-segregation cycle. *Chromosoma* **117**, 333-338.

Dissmeyer, N., Nowack, M. K., Pusch, S., Stals, H., Inze, D., Grini, P. E. and Schnittger, A. (2007). T-loop phosphorylation of Arabidopsis CDKA;1 is required for its function and can be partially substituted by an aspartate residue. *Plant Cell* **19**, 972-85.

Doonan, J. H. and Kitsios, G. (2009). Functional evolution of cyclin-dependent kinases. *Mol Biotechnol* **42**, 14-29.

Drews, G. N. and Goldberg, R. B. (1989). Genetic control of flower development. *Trends in Genetics* **5**, 256-261.

Drews, G. N. and Yadegari, R. (2002). Development and function of the angiosperm female gametophyte. *Annual Review of Genetics* **36**, 99-124.

Doerner, P., Jørgensen, J. E., You, R., Steppuhn, J., and Lamb, C. (1996). Control of root growth and development by cyclin expression. *Nature* **380**, 520-523.

Dube, P., Herzog, F., Gieffers, C., Sander, B., Riedel, D., Muller, S. A., Engel, A., Peters, J. M. and Stark, H. (2005). Localization of the coactivator Cdh1 and the cullin subunit Apc2 in a cryo-electron microscopy model of vertebrate APC/C. *Molecular Cell* 20, 867-879.

Dumas, C., Berger, F., Faure, J.-E., Matthys-Rochon, E. and Callow, J. A. (1998). Gametes, Fertilization and Early Embryogenesis in Flowering Plants. In *Advances in Botanical Research*, pp. 231-261: Academic Press.

Durbarry, A. (2004). Genetic analysis of sperm cell formation i n *Arabidopsis.thaliana* L. Heynh.. PhD's thesis (Leicster, UK: University of Leicester).

Durbarry, A., Vizir, I. and Twell, D. (2005). Male germ line development in Arabidopsis. duo pollen mutants reveal gametophytic regulators of generative cell cycle progression. *Plant Physiol* **137**, 297-307.

Dynlacht, B. D. (1997). Regulation of transcription by proteins that control the cell cycle. *Nature* **389**, 149-52.

Eady. C., Lindsey. K., and Twell, D. (1994). Differential activation and conserved vegetative cell-specific activity of a late pollen promoter in species with bi- and tricellular pollen. *Plant J* **5**, 543-550.

Eady, C., Lindsey, K. and Twell, D. (1995). The Significance of Microspore Division and Division Symmetry for Vegetative Cell-Specific Transcription and Generative Cell Differentiation. *Plant Cell* **7**, 65-74.

Edwards, K., Johnstone, C., and Thompson, C. (1991). A simple and rapid method for the preparation of plant genomic DNA for PCR analysis. *Nucl. Acids Res.* **19**, 1349.

Elledge, S. J. (1996). Cell cycle checkpoints: preventing an identity crisis. *Science* **274**, 1664-72.

Engel, M. L., Chaboud, A., Dumas, C. and McCormick, S. (2003). Sperm cells of Zea mays have a complex complement of mRNAs. *Plant Journal* **34**, 697-707.

Engel, M. L., Holmes-Davis, R. and McCormick, S. (2005). Green sperm Identification of male gamete promoters in *Arabidopsis*. *Plant Physiol*. **138**, 2124-213

Erdmann, R., Wiebel, F. F., Flessau, A., Rytka, J., Beyer, A., Frohlich, K. U. and Kunau, W. H. (1991). pas1, a yeast gene required for peroxisome biogenesis, encodes a member of a novel family of putative atpases. *Cell* **64**, 499-510.

Fabian-Marwedel, T., Umeda, M. and Sauter, M. (2002). The rice cyclin-dependent kinase-activating kinase R2 regulates S-phase progression. *Plant Cell* **14**, 197-210.

Fang, G., Yu, H. and Kirschner, M. W. (1998). The checkpoint protein MAD2 and the mitotic regulator CDC20 form a ternary complex with the anaphase-promoting complex to control anaphase initiation. *Genes Dev* **12**, 1871-83.

Fenech, M. (2007). Cytokinesis-block micronucleus cytome assay. *Nature Protocols* **2**, 1084-1104.

Ferreira, P. C., Hemerly, A. S., Villarroel, R., Van Montagu, M. and Inze, D. (1991). The Arabidopsis functional homolog of the p34cdc2 protein kinase. *Plant Cell* **3**, 531-40.

Fobert, P. R., Gaudin, V., Lunness, P., Coen, E. S. and Doonan, J. H. (1996). Distinct classes of cdc2-related genes are differentially expressed during the cell division cycle in plants. *Plant Cell* **8**, 1465-76.

Forrest, K. and Bhave, M. (2007). Major intrinsic proteins (MIPs) in plants: a complex gene family with major impacts on plant phenotype. *Functional & Integrative Genomics* **7**, 263–289.

Friedman, L., Santa Anna-Arriola, S., Hodgkin, J. and Kimble, J. (2000). gon-4, a cell lineage regulator required for gonadogenesis in Caenorhabditis elegans. *Dev Biol* **228**, 350-62.

Friedman, W. E. (1999). Expression of the cell cycle in sperm of Arabidopsis: implications for understanding patterns of gametogenesis and fertilization in plants and other eukaryotes. *Development* **126**, 1065-75.

Fulop, K., Tarayre, S., Kelemen, Z., Horvath, G., Kevei, Z., Nikovics, K., Bako, L., Brown, S., Kondorosi, A. and Kondorosi, E. (2005). Arabidopsis anaphase-promoting complexes: multiple activators and wide range of substrates might keep APC perpetually busy. *Cell Cycle* **4**, 1084-92.

Gagne, J. M., Downes, B. P., Shiu, S. H., Durski, A. M. and Vierstra, R. D. (2002). The F-box subunit of the SCF E3 complex is encoded by a diverse superfamily of genes in Arabidopsis. *Proc Natl Acad Sci U S A* **99**, 11519-24.

Genschik, P., Criqui, M. C., Parmentier, Y., Derevier, A. and Fleck, J. (1998). Cell cycle -dependent proteolysis in plants. Identification Of the destruction box pathway and metaphase arrest produced by the proteasome inhibitor mg132. *Plant Cell* **10**, 2063-76.

Glotzer, M., Murray, A. W. and Kirschner, M. W. (1991). Cyclin is degraded by the ubiquitin pathway. *Nature* **349**, 132-8.

Gmachl, M., Gieffers, C., Podtelejnikov, A. V., Mann, M. and Peters, J. M. (2000). The RING-H2 finger protein APC11 and the E2 enzyme UBC4 are sufficient to ubiquitinate substrates of the anaphase-promoting complex. *Proc Natl Acad Sci U S A* **97**, 8973-8.

Gonzalez, N., Gevaudant, F., Hernould, M., Chevalier, C. and Mouras, A. (2007). The cell cycle-associated protein kinase WEE1 regulates cell size in relation to endoreduplication in developing tomato fruit. *Plant J* **51**, 642-55.

Grosskortenhaus, R. and Sprenger, F. (2002). Rca1 inhibits APC-Cdh1(Fzr) and is required to prevent cyclin degradation in G2. *Dev Cell* 2, 29-40.

Gunning, B. E. and Wick, S. M. (1985). Preprophase bands, phragmoplasts, and spatial control of cytokinesis. *J Cell Sci Suppl* 2, 157-79.

Guo, Z. and Stiller, J. W. (2004). Comparative genomics of cyclin-dependent kinases suggest co-evolution of the RNAP II C-terminal domain and CTD-directed CDKs. *BMC Genomics* **5**, 69.

Gusti, A., Baumberger, N., Nowack, M., Pusch, S., Eisler, H., Potuschak, T., De Veylder, L., Schnittger, A. and Genschik, P. (2009). The Arabidopsis thaliana F-box protein FBL17 is essential for progression through the second mitosis during pollen development. *PLoS One* **4**, e4780.

Haerizadeh, F., Singh, M. B. and Bhalla, P. L. (2006). Transcriptional repression distinguishes somatic from germ cell lineages in a plant. *Science* **313**, 496-9.

Harper, J. W., Burton, J. L. and Solomon, M. J. (2002). The anaphase-promoting complex: it's not just for mitosis any more. *Genes Dev* **16**, 2179-206.

Hauser, B. A., He, J. Q., Park, S. O. and Gasser, C. S. (2000). TSO1 is a novel protein that modulates cytokinesis and cell expansion in Arabidopsis. *Development* 127, 2219-2226.

Hauser, B. A., Villanueva, J. M. and Gasser, C. S. (1998). Arabidopsis TSO1 regulates directional processes in cells during floral organogenesis. *Genetics* **150**, 411-423.

Hemerly, A., Engler Jde, A., Bergounioux, C., Van Montagu, M., Engler, G., Inze, D. and Ferreira, P. (1995). Dominant negative mutants of the Cdc2 kinase uncouple cell division from iterative plant development. *EMBO J* **14**, 3925-36.

Hirayama, T., Imajuku, Y., Anai, T., Matsui, M. and Oka, A. (1991). Identification of two cell-cycle-controlling cdc2 gene homologs in Arabidopsis thaliana. *Gene* **105**, 159-65.

Hochstrasser, M. (1995). Ubiquitin, proteasomes, and the regulation of intracellular protein degradation. *Curr Opin Cell Biol* **7**, 215-23.

Holmes, J. K. and Solomon, M. J. (2001). The role of Thr160 phosphorylation of Cdk2 in substrate recognition. *Eur J Biochem* **268**, 4647-52.

Honys, D. and Twell, D. (2004). Transcriptome analysis of haploid male gametophyte development in Arabidopsis. *Genome Biol* **5**, R85.

Howden, R., Park, S. K., Moore, J. M., Orme, J., Grossniklaus, U. and Twell, D. (1998). Selection of T-DNA-tagged male and female gametophytic mutants by segregation distortion in Arabidopsis. *Genetics* **149**, 621-31.

Hsu, J. Y., Reimann, J. D. R., Sorensen, C. S., Lukas, J. and Jackson, P. K. (2002). E2F-dependent accumulation of hEmi1 regulates S phase entry by inhibiting APC(Cdh1). *Nature Cell Biology* **4**, 358-366.

Hua, J. and Meyerowitz, E. M. (1998). Ethylene responses are negatively regulated by a receptor gene family in Arabidopsis thaliana. *Cell* **94**, 261-271.

Hauser, B. A., He, J. Q., Park, S. O. and Gasser, C. S. (2000). TSO1 is a novel protein that modulates cytokinesis and cell expansion in Arabidopsis. *Development* **127**, 2219-2226.

Hauser, B. A., Villanueva, J. M. and Gasser, C. S. (1998). Arabidopsis TSO1 regulates directional processes in cells during floral organogenesis. *Genetics* **150**, 411-423.

Iarmarcovai, G., Ceppi, M., Botta, A., Orsiere, T. and Bonassi, S. (2008).

Huntley, R. P. and Murray, J. A. (1999). The plant cell cycle. *Curr Opin Plant Biol* **2**, 440-6.

Iarmarcovai, G., Ceppi, M., Botta, A., Orsiere, T. and Bonassi, S. (2008). Micronuclei frequency in peripheral blood lymphocytes of cancer patients: A meta-analysis. *Mutation Research-Reviews in Mutation Research* **659**, 274-283.

Imai, K. K., Ohashi, Y., Tsuge, T., Yoshizumi, T., Matsui, M., Oka, A. and Aoyama, T. (2006). The A-type cyclin CYCA2;3 is a key regulator of ploidy levels in Arabidopsis endoreduplication. *Plant Cell* **18**, 382-96.

Ingouff, M., Haseloff, J. and Berger, F. (2005). Polycomb group genes control developmental timing of endosperm. *Plant Journal* **42**, 663-674.

Inze, D. and De Veylder, L. (2006). Cell cycle regulation in plant development. *Annu Rev Genet* **40**, 77-105.

Ito, M. (2005). Conservation and diversification of three-repeat Myb transcription factors in plants. *J Plant Res* **118**, 61-9.

Ito, M., Araki, S., Matsunaga, S., Itoh, T., Nishihama, R., Machida, Y., Doonan, J. H. and Watanabe, A. (2001). G2/M-phase-specific transcription during the plant cell cycle is mediated by c-Myb-like transcription factors. *Plant Cell* **13**, 1891-905.

Ito, M., Marie-Claire, C., Sakabe, M., Ohno, T., Hata, S., Kouchi, H., Hashimoto, J., Fukuda, H., Komamine, A. and Watanabe, A. (1997). Cell-cycle-regulated transcription of A- and B-type plant cyclin genes in synchronous cultures. *Plant J* **11**, 983-92.

Iwabuchi, M., Ohsumi, K., Yamamoto, T. M., Sawada, W. and Kishimoto, T. (2000). Residual Cdc2 activity remaining at meiosis I exit is essential for meiotic M-M transition in Xenopus oocyte extracts. *Embo Journal* **19**, 4513-4523.

Iwakawa, H., Shinmyo, A. and Sekine, M. (2006). Arabidopsis CDKA;1, a cdc2 homologue, controls proliferation of generative cells in male gametogenesis. *Plant J* **45**, 819-31.

Izutsu, Y., Tochinai, S., Iwabuchi, K. and Onoe, K. (2000). Larval antigen molecules recognized by adult immune cells of inbred Xenopus laevis: Two pathways for recognition by adult splenic T cells. *Developmental Biology* 221, 365-374.

Jackson, P. K. and Reimann, J. R. (2007). Modulation of cell division by an early mitotic inhibitor protein: The Board of Trustees of the Leland Stanford Junior University.

Jander, G. (2006). Gene identification and cloning by molecular marker mapping. *Methods Mol Biol* **323**, 115-26.

Jiang, C., Gu, X. and Peterson, T. (2004). Identification of conserved gene structures and carboxy-terminal motifs in the Myb gene family of Arabidopsis and Oryza sativa L. ssp. indica. *Genome Biol* **5**, R46.

Jones, K. H. and Senft, J. A. (1985). An improved method to determine cell viability by simultaneous staining with fluorescein diacetate propidium iodide. *Journal of Histochemistry & Cytochemistry* 33, 77-79.

Joubes, J., Chevalier, C., Dudits, D., Heberle-Bors, E., Inze, D., Umeda, M. and Renaudin, J. P. (2000). CDK-related protein kinases in plants. *Plant Mol Biol* **43**, 607-20.

Joubes, J., De Schutter, K., Verkest, A., Inze, D. and De Veylder, L. (2004). Conditional, recombinase-mediated expression of genes in plant cell cultures. *Plant J* **37**, 889-96.

Karimi, M., Inze, D. and Depicker, A. (2002). GATEWAY((TM)) vectors for Agrobacterium-mediated plant transformation. *Trends in Plant Science* **7**, 193-195.

Kim, H. J., Oh, S. A., Brownfield, L., Hong, S. H., Ryu, H., Hwang, I., Twell, D. and Nam, H. G. (2008). Control of plant germline proliferation by SCF(FBL17) degradation of cell cycle inhibitors. *Nature* **455**, 1134-7.

Kipreos, E. T. and Pagano, M. (2000). The F-box protein family. *Genome Biol* **1**, REVIEWS3002.

Kitamura K, Maekawa H and Shimoda C. (1998). Fission yeast Ste9, a homolog of Hct1/Cdh1 and fizzy-related, is a novel negative regulator of cell cycle progression during G_1-phase. Mol Biol Cell **9**, 1065–1080.

Klempnauer, K. H., Gonda, T. J. and Bishop, J. M. (1982). Nucleotide sequence of the retroviral leukemia gene v-myb and its cellular progenitor c-myb: the architecture of a transduced oncogene. *Cell* **31**, 453-63.

Konieczny, A. and Ausubel, F. M. (1993). A procedure for mapping Arabidopsis mutations using co-dominant ecotype-specific PCR-based markers. *Plant J* **4**, 403-10.

Kost, B., Bao, Y. Q. and Chua, N. H. (2002). Cytoskeleton and plant organogenesis. *Philos Trans R Soc Lond B Biol Sci* **357**, 777-89.

Kramer, E. R., Scheuringer, N., Podtelejnikov, A. V., Mann, M. and Peters, J. M. (2000). Mitotic regulation of the APC activator proteins CDC20 and CDH1. *Mol Biol Cell* **11**, 1555-69.

Kuroda, H., Takahashi, N., Shimada, H., Seki, M., Shinozaki, K. and Matsui, M. (2002). Classification and expression analysis of Arabidopsis F-box-containing protein genes. *Plant Cell Physiol* **43**, 1073-85.

Kwee, H. S. and Sundaresan, V. (2003). The NOMEGA gene required for female gametophyte development encodes the putative APC6/CDC16 component of the Anaphase Promoting Complex in Arabidopsis. *Plant J* **36**, 853-66.

Lalanne, E. and Twell, D. (2002). Genetic control of male germ unit organization in Arabidopsis. *Plant Physiol* **129**, 865-75.

Lammens, T., Boudolf, V., Kheibarshekan, L., Zalmas, L. P., Gaamouche, T., Maes, S., Vanstraelen, M., Kondorosi, E., La Thangue, N. B., Govaerts, W. et al. (2008). Atypical E2F activity restrains APC/CCCS52A2 function obligatory for endocycle onset. *Proc Natl Acad Sci U S A* **105**, 14721-6.

Landrieu, I., da Costa, M., De Veylder, L., Dewitte, F., Vandepoele, K., Hassan, S., Wieruszeski, J. M., Corellou, F., Faure, J. D., Van Montagu, M. et al. (2004). A small CDC25 dual-specificity tyrosine-phosphatase isoform in Arabidopsis thaliana. *Proc Natl Acad Sci U S A* **101**, 13380-5.

Lange, A., Mills, R. E., Lange, C. J., Stewart, M., Devine, S. E. and Corbett, A. H. (2007). Classical nuclear localization signals: definition, function, and interaction with importin alpha. *J Biol Chem* **282**, 5101-5.

Larson-Rabin Z, Li Z, Masson PH and Day CD. (2009). FZR2/CCS52A1 expression is a determinant of endoreduplication and cell expansion in Arabidopsis. *Plant physiology* **149**, 874–884.

Lee, Y. R., Li, Y. and Liu, B. (2007). Two Arabidopsis phragmoplast-associated kinesins play a critical role in cytokinesis during male gametogenesis. *Plant Cell* **19**, 2595-605.

Lima Mde, F., Eloy, N. B., Pegoraro, C., Sagit, R., Rojas, C., Bretz, T., Vargas, L., Elofsson, A., de Oliveira, A. C., Hemerly, A. S. et al. (2010). Genomic evolution and complexity of the Anaphase-promoting Complex (APC) in land plants. *BMC Plant Biol* **10**, 254.

Listovsky, T., Oren, Y. S., Yudkovsky, Y., Mahbubani, H. M., Weiss, A. M., Lebendiker, M. and Brandeis, M. (2004). Mammalian Cdh1/Fzr mediates its own degradation. *Embo Journal* **23**, 1619-1626.

Littlepage, L. E. and Ruderman, J. V. (2002). Identification of a new APC/C recognition domain, the A box, which is required for the Cdh1-dependent destruction of the kinase Aurora-A during mitotic exit. *Genes Dev* **16**, 2274-85.

Liu, J., Zhang, Y., Qin, G., Tsuge, T., Sakaguchi, N., Luo, G., Sun, K., Shi, D., Aki, S., Zheng, N. et al. (2008). Targeted degradation of the cyclin-dependent kinase inhibitor ICK4/KRP6 by RING-type E3 ligases is essential for mitotic cell cycle progression during Arabidopsis gametogenesis. *Plant Cell* **20**, 1538-54.

Liu, Y., Du, L., Osato, M., Teo, E. H., Qian, F., Jin, H., Zhen, F., Xu, J., Guo, L., Huang, H. et al. (2007). The zebrafish udu gene encodes a novel nuclear factor and is essential for primitive erythroid cell development. *Blood* **110**, 99-106.

Lucas, J. R., Nadeau, J. A. and Sack, F. D. (2006). Microtubule arrays and Arabidopsis stomatal development. *J Exp Bot* **57**, 71-9.

Lukas, C., Sorensen, C. S., Kramer, E., Santoni-Rugiu, E., Lindeneg, C., Peters, J. M., Bartek, J. and Lukas, J. (1999). Accumulation of cyclin B1 requires E2F and cyclin-A-dependent rearrangement of the anaphase-promoting complex. *Nature* **401**, 815-8.

Lausser, A., Kliwer, I., Srilunchang, K. O. and Dresselhaus, T. (2010)**.** Sporophytic control of pollen tube growth and guidance in maize. *Journal of Experimental Botany* **61**, 673-682.

Machida, Y. J. and Dutta, A. (2007). The APC/C inhibitor, Emi1, is essential for prevention of rereplication. *Genes & Development* **21**, 184-194.

Magnard, J. L., Yang, M., Chen, Y. C., Leary, M. and McCormick, S. (2001). The Arabidopsis gene tardy asynchronous meiosis is required for the normal pace and synchrony of cell division during male meiosis. *Plant Physiol* **127**, 1157-66.

Malhó, R., Twell, D., Oh, S.-A. and Honys, D. (2006). Pollen Development, a Genetic and Transcriptomic View. In *The Pollen Tube*, pp. 15-45: Springer Berlin / Heidelberg.

McGarry, T. J. (2002). Geminin deficiency causes a Chk1-dependent G2 arrest in Xenopus. *Molecular Biology of the Cell* **13**, 3662-3671.

McKibbin, R. S., Halford, N. G. and Francis, D. (1998). Expression of fission yeast cdc25 alters the frequency of lateral root formation in transgenic tobacco. *Plant Mol Biol* **36**, 601-12.

Menges, M., de Jager, S. M., Gruissem, W. and Murray, J. A. (2005). Global analysis of the core cell cycle regulators of Arabidopsis identifies novel genes, reveals multiple and highly specific profiles of expression and provides a coherent model for plant cell cycle control. *Plant J* **41**, 546-66.

Menges, M. and Murray, J. A. (2002). Synchronous Arabidopsis suspension cultures for analysis of cell-cycle gene activity. *Plant J* **30**, 203-12.

Michaels, S. D. and Amasino, R. M. (1998). A robust method for detecting single-nucleotide changes as polymorphic markers by PCR. *Plant J* **14**, 381-5.

Mironov, V., Van Montagu, M. and Inze, D. (1997). Regulation of cell division in plants: an Arabidopsis perspective. *Prog Cell Cycle Res* **3**, 29-41.

Mironov, V. V., De Veylder, L., Van Montagu, M. and Inze, D. (1999). Cyclin-dependent kinases and cell division in plants- the nexus. *Plant Cell* **11**, 509-22.

Morgan, D. O. (1995). Principles of CDK regulation. *Nature* **374**, 131-4.

Morgan, D. O. (1997). Cyclin-dependent kinases: engines, clocks, and microprocessors. *Annu Rev Cell Dev Biol* **13**, 261-91.

Mori, T., Kuroiwa, H., Higashiyama, T. and Kuroiwa, T. (2006). GENERATIVE CELL SPECIFIC 1 is essential for angiosperm fertilization. *Nat Cell Biol* **8**, 64-71.

Nakagami, H., Sekine, M., Murakami, H. and Shinmyo, A. (1999). Tobacco retinoblastoma-related protein phosphorylated by a distinct cyclin-dependent kinase complex with Cdc2/cyclin D in vitro. *Plant J* **18**, 243-52.

Nakayama, K. I. and Nakayama, K. (2006). Ubiquitin ligases: cell-cycle control and cancer. *Nat Rev Cancer* **6**, 369-81.

Nowack, M. K., Grini, P. E., Jakoby, M. J., Lafos, M., Koncz, C. and Schnittger, A. (2006). A positive signal from the fertilization of the egg cell sets off endosperm proliferation in angiosperm embryogenesis. *Nat Genet* **38**, 63-7.

Oh, S. A., Bourdon, V., Das 'Pal, M., Dickinson, H. and Twell, D. (2008). Arabidopsis kinesins HINKEL and TETRASPORE act redundantly to control cell plate expansion during cytokinesis in the male gametophyte. *Mol Plant* **1**, 794-9.

Oh, S. A., Johnson, A., Smertenko, A., Rahman, D., Park, S. K., Hussey, P. J. and Twell, D. (2005). A Divergent Cellular Role for the FUSED Kinase Family in the Plant-Specific Cytokinetic Phragmoplast. *Current Biology* **15**, 2107-2111.

Oh, S. A., Park, K. S., Twell, D. and Park, S. K. (2010a). The SIDECAR POLLEN gene encodes a microspore-specific LOB/AS2 domain protein required for the correct timing and orientation of asymmetric cell division. *Plant J* **64**, 839-50.

Oh, S. A., Pal, M. D., Park, S. K., Johnson, J. A. and Twell, D. (2010b). The tobacco MAP215/Dis1-family protein TMBP200 is required for the functional organization of microtubule arrays during male germline establishment. *J Exp Bot* **61**, 969-81.

Ohi, M. D., Feoktistova, A., Ren, L., Yip, C., Cheng, Y., Chen, J. S., Yoon, H. J., Wall, J. S., Huang, Z., Penczek, P. A. et al. (2007). Structural organization of the anaphase-promoting complex bound to the mitotic activator Slp1. *Mol Cell* **28**, 871-85.

Okada, T., Bhalla, P. L. and Singh, M. B. (2005). Transcriptional activity of male gamete-specific histone gcH3 promoter in sperm cells of Lilium longiflorum. *Plant and Cell Physiology* **46**, 797-802.

Okada, T., Bhalla, P. L. and Singh, M. B. (2006). Expressed sequence tag analysis of Lilium longiflorum generative cells. *Plant Cell Physiol* **47**, 698-705.

Otegui, M. and Staehelin, L. A. (2000). Cytokinesis in flowering plants: more than one way to divide a cell. *Current Opinion in Plant Biology* **3**, 493-502.

O'Malley, R. C. and Ecker, J. R. (2010). Linking genotype to phenotype using the Arabidopsis unimutant collection. *The Plant Journal* **61**, 928–940.

Owen, H. A. and Makaroff, C. A. (1995). Ultrastructure of microsporogenesis and microgametogenesis in<i>Arabidopsis thaliana</i> (L.) Heynh. ecotype Wassilewskija (Brassicaceae). *Protoplasma* **185**, 7-21.

Pagano, M. (1997). Cell cycle regulation by the ubiquitin pathway. *FASEB J* **11**, 1067-75.

Page, D. R. and Grossniklaus, U. (2002). The art and design of genetic screens: Arabidopsis thaliana. *Nat Rev Genet* **3**, 124-36.

Palatnik, J. F., Wollmann, H., Schommer, C., Schwab, R., Boisbouvier, J., Rodriguez, R., Warthmann, N., Allen, E., Dezulian, T., Huson, D. et al. (2007). Sequence and expression differences underlie functional specialization of Arabidopsis MicroRNAs miR159 and miR319. *Developmental Cell* **13**, 115-125.

Palevitz, B. A. and Cresti, M. (1989). Cytoskeletal changes during generative cell division and sperm formation in<i>Tradescantia virginiana</i>. *Protoplasma* **150**, 54-71.

Palevitz, B. A. and Tiezzi, A. (1992). organization, composition, and function of the generative cell and sperm cytoskeleton. *International Review of Cytology-a Survey of Cell Biology* **140**, 149-185.

Park, S. K., Howden, R. and Twell, D. (1998). The Arabidopsis thaliana gametophytic mutation gemini pollen1 disrupts microspore polarity, division asymmetry and pollen cell fate. *Development* **125**, 3789-99.

Park, S. K., Rahman, D., Oh, S. A. and Twell, D. (2004). gemini pollen 2, a male and female gametophytic cytokinesis defective mutation. *Sex Plant Reprod* **17**, 63-70.

Patra, D. and Dunphy, W. G. (1998). Xe-p9, a Xenopus Suc1/Cks protein, is essential for the Cdc2-dependent phosphorylation of the anaphase- promoting complex at mitosis. *Genes Dev* **12**, 2549-59.

Pesin, J. A. and Orr-Weaver, T. L. (2008). Regulation of APC/C activators in mitosis and meiosis. *Annu Rev Cell Dev Biol* **24,** 475-99.

Peters, J. M. (2006). The anaphase promoting complex/cyclosome: a machine designed to destroy. *Nat Rev Mol Cell Biol* **7**, 644-56.

Pfleger, C. M. and Kirschner, M. W. (2000). The KEN box: an APC recognition signal distinct from the D box targeted by Cdh1. *Genes Dev* **14**, 655-65.

Pickart, C. M. (2004). Back to the future with ubiquitin. *Cell* **116**, 181-90.

Pina, C., Pinto, F., Feijo, J. A. and Becker, J. D. (2005). Gene family analysis of the Arabidopsis pollen transcriptome reveals biological implications for cell growth, division control, and gene expression regulation. *Plant Physiol* **138**, 744-56.

Porceddu, A., Stals, H., Reichheld, J. P., Segers, G., De Veylder, L., Barroco, R. P., Casteels, P., Van Montagu, M., Inze, D. and Mironov, V. (2001). A plant-specific cyclin-dependent kinase is involved in the control of G2/M progression in plants. *J Biol Chem* **276**, 36354-60.

Preuss, D., Rhee, S. Y. and Davis, R. W. (1994). Tetrad analysis possible in Arabidopsis with mutation of the QUARTET (QRT) genes. *Science* **264**, 1458-60.

Qin, L. X., Perennes, C., Richard, L., Bouvier-Durand, M., Trehin, C., Inze, D. and Bergounioux, C. (1996). G2-and early-M-specific expression of the NTCYC1 cyclin gene in Nicotiana tabacum cells. *Plant Mol Biol* **32**, 1093-101.

Rechsteiner, M. and Rogers, S. W. (1996). PEST sequences and regulation by proteolysis. *Trends Biochem Sci* **21**, 267-71.

Reichheld, J. P., Chaubet, N., Shen, W. H., Renaudin, J. P. and Gigot, C. (1996). Multiple A-type cyclins express sequentially during the cell cycle in Nicotiana tabacum BY2 cells. *Proc Natl Acad Sci U S A* **93**, 13819-24.

Reimann, J. D. R., Gardner, B. E., Margottin-Goguet, F. and Jackson, P. K. (2001). Emi1 regulates the anaphase-promoting complex by a different mechanism than Mad2 proteins. *Genes & Development* **15**, 3278-3285.

Renaudin, J. P., Doonan, J. H., Freeman, D., Hashimoto, J., Hirt, H., Inze, D., Jacobs, T., Kouchi, H., Rouze, P., Sauter, M. et al. (1996). Plant cyclins: a unified nomenclature for plant A-, B- and D-type cyclins based on sequence organization. *Plant Mol Biol* **32**, 1003-18.

Romero, I., Fuertes, A., Benito, M. J., Malpica, J. M., Leyva, A. and Paz-Ares, J. (1998). More than 80R2R3-MYB regulatory genes in the genome of Arabidopsis thaliana. *Plant J* **14**, 273-84.

Rotman, N., Durbarry, A., Wardle, A., Yang, W. C., Chaboud, A., Faure, J.-E., Berger, F. and Twell, D. (2005). A Novel Class of MYB Factors Controls Sperm-Cell Formation in Plants. *Current Biology* **15**, 244-248.

Roudier, F., Fedorova, E., Gyorgyey, J., Feher, A., Brown, S., Kondorosi, A. and Kondorosi, E. (2000). Cell cycle function of a Medicago sativa A2-type cyclin interacting with a PSTAIRE-type cyclin-dependent kinase and a retinoblastoma protein. *Plant J* **23**, 73-83.

Sambrook, J., Fritsch, E.F. and Maniatis, T. (1989). Gel electrophoresis of DNA. In: Sambrook, J., Fritsch, E.F. and Maniatis, T. (Eds.) Molecular Cloning: a Laboratory Manual. New York: Cold Spring Harbor Laboratory Press, Cold Spring Harbor, NY, USA, chapter 6.

Scheffner, M., Nuber, U. and Huibregtse, J. M. (1995). Protein ubiquitination involving an E1-E2-E3 enzyme ubiquitin thioester cascade. *Nature* **373**, 81-3.

Schnittger, A., Schobinger, U., Stierhof, Y. D. and Hulskamp, M. (2002). Ectopic B-type cyclin expression induces mitotic cycles in endoreduplicating Arabidopsis trichomes. *Curr Biol* **12**, 415-20.

Scholl, R. L., May, S. T. and Ware, D. H. (2000). Seed and molecular resources for Arabidopsis. *Plant Physiol* **124**, 1477-80.

Schwab, M., Neutzner, M., Mocker, D. and Seufert, W. (2001). Yeast Hct1 recognizes the mitotic cyclin Clb2 and other substrates of the ubiquitin ligase APC. *EMBO J* **20**, 5165-75.

Scott, R. J., Spielman, M. and Dickinson, H. G. (2004). Stamen structure and function. *Plant Cell* **16, Suppl**, S46-60.

Segers G, Gadisseur I, Bergounioux C, de Almeida Engler J, Jacqmard A, Van Montagu M, Inzé D. (1996). The *Arabidopsis* cyclin-dependent kinase gene

cdc2bAt is preferentially expressed during S and G2 phases of the cell cycle. *Plant J* **10,** 601–612

Sessions, A. and M. F. Yanofsky. (1999). "Dorsoventral patterning in plants." *Genes Dev* **13**, 1051-4.

Shaul, O., Mironov, V., Burssens, S., Van Montagu, M. and Inze, D. (1996). Two Arabidopsis cyclin promoters mediate distinctive transcriptional oscillation in synchronized tobacco BY-2 cells. *Proc Natl Acad Sci U S A* **93**, 4868-72.

Shimotohno, A., Ohno, R., Bisova, K., Sakaguchi, N., Huang, J., Koncz, C., Uchimiya, H. and Umeda, M. (2006). Diverse phosphoregulatory mechanisms controlling cyclin-dependent kinase-activating kinases in Arabidopsis. *Plant J* **47**, 701-10.

Shimotohno, A., Umeda-Hara, C., Bisova, K., Uchimiya, H. and Umeda, M. (2004). The plant-specific kinase CDKF;1 is involved in activating phosphorylation of cyclin-dependent kinase-activating kinases in Arabidopsis. *Plant Cell* **16**, 2954-66.

Siegmund, R. F. and Nasmyth, K. A. (1996). The Saccharomyces cerevisiae Start-specific transcription factor Swi4 interacts through the ankyrin repeats with the mitotic Clb2/Cdc28 kinase and through its conserved carboxy terminus with Swi6. *Mol Cell Biol* **16**, 2647-55.

Smalle, J. and Vierstra, R. D. (2004). The ubiquitin 26S proteasome proteolytic pathway. *Annu Rev Plant Biol* **55**, 555-90.

Snider, J. and Houry, W. A. (2008). AAA+ proteins: diversity in function, similarity in structure. *Biochemical Society Transactions* **36**, 72-77.

Song, H., Hanlon, N., Brown, N. R., Noble, M. E., Johnson, L. N. and Barford, D. (2001). Phosphoprotein-protein interactions revealed by the crystal structure of kinase-associated phosphatase in complex with phosphoCDK2. *Mol Cell* **7**, 615-26.

Song, W.Y., Choi, K. S., Kim, D. Y., Geisler, M., Park, J., Vincenzetti, V., Schellenberg, M., Kim, S. H., Lim, Y. P., Noh, E. W. et al. (2010). Arabidopsis PCR2 Is a Zinc Exporter Involved in Both Zinc Extrusion and Long-Distance Zinc Transport. *Plant Cell* **22**, 2237-2252.

Sorrell, D. A., Chrimes, D., Dickinson, J. R., Rogers, H. J. and Francis, D. (2005). The Arabidopsis CDC25 induces a short cell length when overexpressed in fission yeast: evidence for cell cycle function. *New Phytol* **165**, 425-8.

Sorrell, D. A., Marchbank, A., McMahon, K., Dickinson, J. R., Rogers, H. J. and Francis, D. (2002). A WEE1 homologue from Arabidopsis thaliana. *Planta* **215**, 518-22.

Sorrell, D. A., Menges, M., Healy, J. M., Deveaux, Y., Amano, C., Su, Y., Nakagami, H., Shinmyo, A., Doonan, J. H., Sekine, M. et al. (2001). Cell cycle regulation of cyclin-dependent kinases in tobacco cultivar Bright Yellow-2 cells. *Plant Physiol* **126**, 1214-23.

Soto, G., Alleva, K., Mazzella, M. A., Amodeo, G. and Muschietti, J. P. (2008). AtTIP1;3 and AtTIP5;1, the only highly expressed Arabidopsis pollen-specific aquaporins, transport water and urea. *Febs Letters* **582**, 4077-4082.

Stals, H., Bauwens, S., Traas, J., Van Montagu, M., Engler, G. and Inze, D. (1997). Plant CDC2 is not only targeted to the pre-prophase band, but also co-localizes with the spindle, phragmoplast, and chromosomes. *FEBS Lett* **418**, 229-34.

Stals, H. and Inze, D. (2001). When plant cells decide to divide. *Trends Plant Sci* **6**, 359-64.

Steinborn, K., Maulbetsch, C., Priester, B., Trautmann, S., Pacher, T., Geiges, B., Kuttner, F., Lepiniec, L., Stierhof, Y. D., Schwarz, H. et al. (2002). The Arabidopsis PILZ group genes encode tubulin-folding cofactor orthologs required for cell division but not cell growth. *Genes Dev* **16**, 959-71.

Stevens R, Mariconti L, Rossignol P, Perennes C, Cella R, Bergounioux C. (2002). Two E2F sites in the Arabidopsis MCM3 promoter have diff erent roles in cell cycle activation and meristematic expression. *J Biol Chem* **277**, 32978–32984.

Sun, Q., Zybailov, B., Majeran, W., Friso, G., Olinares, P. D. and van Wijk, K. J. (2009). PPDB, the Plant Proteomics Database at Cornell. *Nucleic Acids Res* **37**, D969-74.

Sun, Y., Dilkes, B. P., Zhang, C., Dante, R. A., Carneiro, N. P., Lowe, K. S., Jung, R., Gordon-Kamm, W. J. and Larkins, B. A. (1999). Characterization of maize (Zea mays L.) Wee1 and its activity in developing endosperm. *Proc Natl Acad Sci U S A* **96**, 4180-5.

Takatsuka, H., Ohno, R. and Umeda, M. (2009). The Arabidopsis cyclin-dependent kinase-activating kinase CDKF;1 is a major regulator of cell proliferation and cell expansion but is dispensable for CDKA activation. *Plant J* **59**, 475-87.

Tanaka, I., Nakamura, S. and Miki-Hirosige, H. (1989). Structural features of isolated generative cells and their protoplasts from pollen of some liliaceous plants. *Gamete research* **24**, 361-74.

Tarayre, S., Vinardell, J. M., Cebolla, A., Kondorosi, A. and Kondorosi, E. (2004). Two classes of the CDh1-type activators of the anaphase-promoting complex in plants: novel functional domains and distinct regulation. *Plant Cell* **16**, 422-34.

Terasaka, O. and Niitsu, T. (1995). The mitotic apparatus during unequal microspore division observed by a confocal laser scanning microscope. *Protoplasma* **189**, 187-193.

Thornton, B. R., Ng, T. M., Matyskiela, M. E., Carroll, C. W., Morgan, D. O. and Toczyski, D. P. (2006). An architectural map of the anaphase-promoting complex. *Genes Dev* **20**, 449-60.

Thornton, B. R. and Toczyski, D. P. (2006). Precise destruction: an emerging picture of the APC. *Genes Dev* **20**, 3069-78.

Trehin, C., Ahn, I. O., Perennes, C., Couteau, F., Lalanne, E. and Bergounioux, C. (1997). Cloning of upstream sequences responsible for cell cycle regulation of the Nicotiana sylvestris CycB1;1 gene. *Plant Mol Biol* **35**, 667-72.

Twell, D. (1995). Diphtheria toxin-mediated cell ablation in developing pollen: Vegetative cell ablation blocks generative cell migration. *Protoplasma* **187**, 144-154.

Twell, D. (2011). Male gametogenesis and germline specification in flowering plants. *Sexual Plant Reproduction* **24**, 149-160.

Twell, D., Park, S. K. and Lalanne, E. (1998). Asymmetric division and cell-fate determination in developing pollen. *Trends in Plant Science* **3**, 305-310.

Twell, D., Park, S. K., Hawkins, T. J., Schubert, D., Schmidt, R., Smertenko, A. and Hussey, P. J. (2002). MOR1/GEM1 has an essential role in the plant-specific cytokinetic phragmoplast. *Nat Cell Biol* **4**, 711-4.

Ueda, K., Matsuyama, T. and Hashimoto, T. (1999). Visualization of microtubules in living cells of transgenic Arabidopsis thaliana. *Protoplasma* **206**, 201-206.

Umeda, M., Shimotohno, A. and Yamaguchi, M. (2005). Control of cell division and transcription by cyclin-dependent kinase-activating kinases in plants. *Plant Cell Physiol* **46**, 1437-42.

Ungru, A., Nowack, M. K., Reymond, M., Shirzadi, R., Kumar, M., Biewers, S., Grini, P. E. and Schnittger, A. (2008). Natural variation in the degree of autonomous endosperm formation reveals independence and constraints of embryo growth during seed development in Arabidopsis thaliana. *Genetics* **179**, 829-41.

Vandepoele, K., Vlieghe, K., Florquin, K., Hennig, L., Beemster, G. T. S., Gruissem, W., Van De Peer, Y., Inze, D. and De Veylder, L. (2005). Genome-wide identification of potential plant E2F target genes. *Plant Physiology* **139**, 316-328.

Vandepoele, K., Raes, J., De Veylder, L., Rouze, P., Rombauts, S. and Inze, D. (2002). Genome-wide analysis of core cell cycle genes in Arabidopsis. *Plant Cell* **14**, 903-16.

Vander Willigen, C., Postaire, O., Tournaire-Roux, C., Boursiac, Y. and Maurel, C. (2006). Expression and inhibition of aquaporins in germinating Arabidopsis seeds. *Plant and Cell Physiology* **47**, 1241-1250.

Vanstraelen, M., Baloban, M., Da Ines, O., Cultrone, A., Lammens, T., Boudolf, V., Brown, S. C., De Veylder, L., Mergaert, P. and Kondorosi, E. (2009). APC/C-CCS52A complexes control meristem maintenance in the Arabidopsis root. *Proc Natl Acad Sci U S A* **106**, 11806-11.

Vision, T. J., Brown, D. G. and Tanksley, S. D. (2000). The origins of genomic duplications in Arabidopsis. *Science* **290**, 2114-2117.

Vlieghe, K., Boudolf, V., Beemster, G. T. S., Maes, S., Magyar, Z., Atanassova, A., Engler, J. D., De Groodt, R., Inze, D. and De Veylder, L. (2005). The DP-E2F-like gene DEL1 controls the endocycle in Arabidopsis thaliana. *Current Biology* **15**, 59-63.

Vodermaier, H. C., Gieffers, C., Maurer-Stroh, S., Eisenhaber, F. and Peters, J. M. (2003). TPR subunits of the anaphase-promoting complex mediate binding to the activator protein CDH1. *Curr Biol* **13**, 1459-68.

von Besser, K., Frank, A. C., Johnson, M. A. and Preuss, D. (2006). Arabidopsis HAP2 (GCS1) is a sperm-specific gene required for pollen tube guidance and fertilization. *Development* **133**, 4761-9.

Wada Y, Yamamoto M. (1997). Detection of single nucleotide mutations including substitutions and deletions by matrix-assisted laser desorption/ionization time-of-flight mass spectrometry. Rapid Commun Mass *Spectrom* **11**, 1657–1660.

Wang, G., Kong, H., Sun, Y., Zhang, X., Zhang, W., Altman, N., DePamphilis, C. W. and Ma, H. (2004). Genome-wide analysis of the cyclin family in Arabidopsis and comparative phylogenetic analysis of plant cyclin-like proteins. *Plant Physiol* **135**, 1084-99.

Wang, W. and Chen, X. (2004). HUA ENHANCER3 reveals a role for a cyclin-dependent protein kinase in the specification of floral organ identity in Arabidopsis. *Development* **131**, 3147-56.

Weber, H., Chetelat, A., Reymond, P. and Farmer, E. E. (2004). Selective and powerful stress gene expression in Arabidopsis in response to malondialdehyde. *Plant J* **37**, 877-88.

Weingartner, M., Binarova, P., Drykova, D., Schweighofer, A., David, J. P., Heberle-Bors, E., Doonan, J. and Bogre, L. (2001). Dynamic recruitment of Cdc2 to specific microtubule structures during mitosis. *Plant Cell* **13**, 1929-43.

Weingartner, M., Criqui, M. C., Meszaros, T., Binarova, P., Schmit, A. C., Helfer, A., Derevier, A., Erhardt, M., Bogre, L. and Genschik, P. (2004). Expression of a nondegradable cyclin B1 affects plant development and leads to endomitosis by inhibiting the formation of a phragmoplast. *Plant Cell* **16**, 643-57.

Weston, K. (1998). Myb proteins in life, death and differentiation. *Curr Opin Genet Dev* **8**, 76-81.

Whittington, A. T., Vugrek, O., Wei, K. J., Hasenbein, N. G., Sugimoto, K., Rashbrooke, M. C. and Wasteneys, G. O. (2001). MOR1 is essential for organizing cortical microtubules in plants. *Nature* **411**, 610-3.

Winston, J. T., Strack, P., Beer-Romero, P., Chu, C. Y., Elledge, S. J. and Harper, J. W. (1999). The SCFbeta-TRCP-ubiquitin ligase complex associates specifically with phosphorylated destruction motifs in IkappaBalpha and beta-catenin and stimulates IkappaBalpha ubiquitination in vitro. *Genes Dev* **13**, 270-83.

Wu, Y. and Messing, J. (2010). Rescue of a Dominant Mutant With RNA Interference. *Genetics* **186**, 1493-1496.

Xiao, Y. L., Redman, J. C., Monaghan, E. L., Zhuang, J., Underwood, B. A., Moskal, W. A., Wang, W., Wu, H. C. and Town, C. D. (2010). High throughput generation of promoter reporter (GFP) transgenic lines of low expressing genes in Arabidopsis and analysis of their expression patterns. *Plant Methods* **6**, 18.

Xu, G., Ma, H., Nei, M. and Kong, H. (2009). Evolution of F-box genes in plants: different modes of sequence divergence and their relationships with functional diversification. *Proc Natl Acad Sci U S A* **106**, 835-40.

Yu, H. (2007). Cdc20: a WD40 activator for a cell cycle degradation machine. *Mol Cell* **27**, 3-16.

Yu, Y., Steinmetz, A., Meyer, D., Brown, S. and Shen, W. H. (2003). The tobacco A-type cyclin, Nicta;CYCA3;2, at the nexus of cell division and differentiation. *Plant Cell* **15**, 2763-77.

Zachariae, W., Schwab, M., Nasmyth, K. and Seufert, W. (1998). Control of cyclin ubiquitination by CDK-regulated binding of Hct1 to the anaphase promoting complex. *Science* **282**, 1721-4.

Žárský, V., Garrido, D., Říhová, L., Tupý, J., Vicente, O. and Heberle-Bors, E. (1992). Derepression of the cell cycle by starvation is involved in the induction of tobacco pollen embryogenesis. *Sexual Plant Reproduction* **5**, 189-194.

Zee, S. Y. (1992). confocal laser scanning microscopy of microtubule organizational changes in isolated generative cells of allemanda-neriifolia during mitosis. *Sexual Plant Reproduction* **5**, 182-188.

Zhang, D. M., He, T., Katusic, Z. S., Lee, H. C. and Lu, T. (2010). Muscle-specific f-box only proteins facilitate bk channel beta(1) subunit downregulation in vascular smooth muscle cells of diabetes mellitus. *Circ Res* **107**, 1454-9.

Zheng, B., Chen, X. and McCormick, S. (2011). The anaphase-promoting complex is a dual integrator that regulates both MicroRNA-mediated transcriptional regulation of cyclin B1 and degradation of Cyclin B1 during Arabidopsis male gametophyte development. *Plant Cell* **23**, 1033-46.

Zheng, N., Schulman, B. A., Song, L., Miller, J. J., Jeffrey, P. D., Wang, P., Chu, C., Koepp, D. M., Elledge, S. J., Pagano, M. et al. (2002). Structure of the Cul1-Rbx1-Skp1-F boxSkp2 SCF ubiquitin ligase complex. *Nature* **416**, 703-9.

Zhou, C. and Yang, H. Y. (1991). Microtubule changes during the development of generative cells in <i>Hippeastrum vittatum</i> pollen. *Sexual Plant Reproduction* **4**, 293-297.

Zielke, N., Querings, S., Grosskortenhaus, R., Reis, T. and Sprenger, F. (2006). Molecular dissection of the APC/C inhibitor Rca1 shows a novel F-box-dependent function. *EMBO Rep* **7**, 1266-72.

Zimmermann, P., Hirsch-Hoffmann, M., Hennig, L. and Gruissem, W. (2004). GENEVESTIGATOR. Arabidopsis microarray database and analysis toolbox. *Plant Physiology* **136**, 2621-2632.

Zonia, L., Tupy, J. and Staiger, C. J. (1999). Unique actin and microtubule arrays co-ordinate the differentiation of microspores to mature pollen in Nicotiana tabacum. *Journal of Experimental Botany* **50**, 581-594.